The influence of fouling and cleaning upon the ultrafiltration of a black tea solution

Wu, Dan

Award date:
2007

Awarding institution:
University of Bath

The Influence of fouling and cleaning upon the ultrafiltration of a black tea solution

Submitted by Dan Wu

For the degree of Ph.D.

At the University of Bath

2007-01-25

Dan Wu

ProQuest LLC
789 East Eisenhower Parkway
P.O. Box 1346
Ann Arbor, MI 48106-1346

Acknowledgements

I would like to give my sincere thanks to my supervisor, Dr. Michael Bird who has provided me with strong academic support, great motivation, enthusiasm, and a lot of chance for my personal development throughout my time in Bath. I could not make such progress without your help.

I wish to thank Department of Chemical Engineering as a whole. Thank Mr. Fernando Acosta, Mr. Robert Brain, Mr. John Bishop, Mr. Richard Bull, Mrs Anne O'Reilly and Mr. Merv Newnes for all the technical support. Thank Dr. Rongsheng Zhang, Dr. Fan Zhang, Mr. Liang Chen, Mr. Chin Chih Tai, Mr. Phil Evans and Mrs Bengu Bozkaya for giving me a lot of help and advice.

My acknowledgements are also extended to the support from Dr Jacek Obuchowicz, Dr Francois Xavier Pierre, Dr Paul D A Pudney and Ms Debbie Samuel from *Unilever Research Colworth*, UK. Thanks for all the help and the supply of tea powder, TF standards, HPLC and ATR-FTIR equipments.

I am also grateful to Professor Marianne Nyström and Dr. Arto Pihlajamäki of Lappeenranta University of Technology for the help on zeta-potential measurements. Thanks go to Dr. Frank Lipnizki of DSS (*Alfa Laval*) for supplying some of the membranes used in this project.

In addition, I would like to give my biggest thanks to my parents and my lovely twin sister for their love, understanding and endless support.

Last but not least, the financial support of the ORs Award and University of Bath are gratefully acknowledged.

Abstract

This study contains pioneering investigations concerning the influence of membrane fouling and cleaning upon black tea ultrafiltration and the interactions between membrane and polyphenol / protein based system. The work described in this thesis can be divided into three parts. The first part concerns the fouling and cleaning performance of three different UF membranes for the processing of cold black tea. The effect of fouling conditions upon the subsequent cleanability was investigated. Both sodium hydroxide and *Ultrasil 11* cleaning agents were tested under a range of operating conditions. From this part of work, polysulphone (PSF) membrane (MWCO 30 kD) was finally chosen for the rest of the studies. NaOH of the optimal concentration 0.2 wt% was also determined to be the cleaning agent in the subsequent cleaning experiments.

In the second part of the research work, tea protein and tea polyphenol have been separated successfully. An advanced technique called Isothermal Titration Microcalorimetry (ITC) was used to study the interactions of (i) tea protein and mixed theaflavin (TF), (ii) tea protein and total tea polyphenol. Gel filtration chromatography, SDS-PAGE, CBB assay and FTIR have been used to characterize protein isolate quantitatively and qualitatively. The molecular mass of tea protein was determined to be approximately 11 kD at pH 5.0. The purity of this protein isolate was 51.4 wt% and FTIR spectrum implied the possible secondary structure – β-sheet when protein is in solid state. The total phenols in the tea polyphenol isolate obtained via Zn^{2+} precipitation was increased to be approximately 65 wt% of the sample tested. The binding mechanism of tea protein and theaflavin and that of tea protein and total tea polyphenol were both fitted into a sequential sites binding model.

Following the separation and purification of tea protein and the study of protein / phenol interactions, the last part of experiments concentrated on membrane fouling by tea model solutions consisting of different tea components such as tea proteins, theaflavins (TFs), thearubigins (TRs) and caffeine. There were clear but varied permeate flux declines for filtrations of single components and mixtures due to different fouling. Unexpected increased protein transmissions were recorded during filtrations of binary mixtures. This is probably due to a modification of membrane selectivity towards

polyphenols and a subsequent charge reduction in the mixed system, allowing more protein-based deposits to pass through the membrane. This explanation was supported by the results from contact angle and zeta-potential measurements of selected membrane samples. The visualization of fouled membrane surfaces by SEM revealed different foulant morphologies.

The corresponding membrane cleanabilities were also subsequently investigated. Membrane cleaning with 0.2 wt% sodium hydroxide was generally found to be effective according to the recoveries of membrane permeability, the inspection of cleaned membranes by SEM and the comparison of IR spectrum of fouled and cleaned membranes by ATR-FTIR. Contact angle and Zeta-potential measurements also showed the recovery of membrane hydrophobicity and surface charge after cleaning.

Contents

List of Figures

List of Tables

Nomenclature

Symbol	Description	Units
A_0	The initial active filter membrane surface area	m^2
a^*	Redness	-
b^*	Yellowness	-
c	The volume of solid particles retained per unit filtrate volume	-
C_b	Concentration in bulk solution	$mg\ L^{-1}$
C_m	Concentration at membrane surface	$mg\ L^{-1}$
C_p	Concentration in permeate	$mg\ L^{-1}$
D	Diffusion constant	$m^2\ s^{-1}$
E	Total colour difference	-
ΔE	The streaming potential	V
ΔH	Enthalpy change	$J\ mol^{-1}$ (0.24 $cal\ mol^{-1}$)
J	Permeate flux	$L\ m^{-2}\ hr^{-1}$
J_c	Cleaning flux	$L\ m^{-2}\ hr^{-1}$
J_f	Fouling flux	$L\ m^{-2}\ hr^{-1}$
J_m	Mass flux	$kg\ m^{-2}\ hr^{-1}$
J_n	The normalized permeate flux	-
$J_{(phenol)}$	Mass flux of total polyphenol	$mg\ m^{-2}\ min^{-1}$
$J_{(protein)}$	Mass flux of tea protein	$mg\ m^{-2}\ min^{-1}$
$J_{(TFs)}$	Mass flux of TFs	$mg\ m^{-2}min^{-1}$
J_w	Pure water flux	$L\ m^{-2}\ hr^{-1}$
J_{wc}	Pure water flux of cleaned membrane	$L\ m^{-2}\ hr^{-1}$
J_{wf}	Pure water flux of fouled membrane	$L\ m^{-2}\ hr^{-1}$
J_{wm}	Pure water flux of conditioned membrane	$L\ m^{-2}\ hr^{-1}$
K	Binding constant	mol^{-1}
L	Membrane thickness	m
L^*	Lightness	-

m	Mass ratio of wet to dry cake	-
P	Pressure	bar (10^5 Pa)
ΔP	Pressure difference	bar (10^5 Pa)
Δp	Pressure difference	bar (10^5 Pa)
Q_0	The initial flow rate	$m^3 s^{-1}$
R	Rejection coefficient	-
R_c	The resistance of cleaned membrane	m^{-1}
R_{bl}	The boundary layer resistance	m^{-1}
R_f	The resistance of fouled membrane	m^{-1}
R_{if}	The total irreversible fouling resistance	m^{-1}
R_m	Membrane resistance	m^{-1}
R_{rf}	The residual fouling resistance left after cleaning	m^{-1}
R_{tot}	The total resistance	m^{-1}
s	The mass fraction of solids in slurry	-
u_0	The initial filtrate linear velocity	$m s^{-1}$

Greek

α	The cake specific resistance	$m kg^{-1}$
β	Surface tension of the liquid	$N m^{-1}$
ρ	Filtrate density	$kg m^{-3}$
γ	Membrane pore size	m
ε_0	Permittivity of a vacuum	$F m^{-1}$
ε_r	Relative dielectric constant of the electrolyte	-
ζ	Zeta-potential	V
η	Kinematic viscosity	$m^2 s^{-1}$
θ	Contact angle	degree (°)
κ	Conductivity of the electrolyte solution	$S m^{-1}$
λ	Wave length	nm
μ	Filtrate viscosity	cP ($g m^{-1} s^{-1}$)

$\Delta\pi$	Osmotic pressure difference	bar (10^5 Pa)
σ	The blocked area per unit filtrate volume	m^{-1}

Abbreviation

Abbreviation	Description
Ag	Silver
AgCl	Silver chloride
ATR-FTIR	Attenuated Total Reflection Fourier Transform Infrared Spectroscopy
BSA	Bovine Serum Albumin
CBB	Coomassie Brillant Blue G
CFV	Cross flow velocity
CIP	Cleaning in – place
dH_2O	Deionized water
Da	Dalton
DNA	Deoxyribonucleic acid
DSS	Danish Separation Systems
EC	(-)-Epicatechin
ECG	(-)-Epicatechin gallate
EDTA	Ethylene diamine tetraacetic acid
EGC	(-)-Epigallocatechin
EGCG	(-)-Epigallocatechin gallate
ETFE	Ethylene Tetrafluoroethylene
FAO	The UN Food and Agriculture Organization
FEP	Fluorinated ethylene propylene
FS	Fluoropolymer
FTIR	Fourier Transform Infrared Spectroscopy
HAP	Haze – active protein
HCl	Hydrochloric acid
HPLC	High Performance Liquid Chromatography
IgG	Immunoglobulin
IR	Infrared Spectroscopy
IRE	Internal reflection element

ITC	Isothermal Titration Microcalorimetry
KCl	Potassium chloride
kD	Kilo Dalton
LMH	L m^{-2} hr^{-1}
MF	Microfiltration
MWCO	Molecular weight cut off
$NaHCO_3$	Sodium bicarbonate
Na_2CO_3	Sodium carbonate
NaCl	Sodium chloride
NaOH	Sodium hydroxide
NF	Nanofiltration
$(NH_4)_2SO_4$	Ammonium Sulfate
NMR	Nuclear Magnetic Resonance
PEG-blue	Polyethylene glycol - blue
PES	polyethersulphone
pI	Isoelectric point
PSF	Polysulphone
PTFE	Polytetrafluoroethylene
PVDF	Polyvinylidene fluoride
PVP	Polyvinylpyrrolidone
PWF	Pure water flux
Rf	Relative mobility
RNA	Ribonucleic acid
RO	Reverse Osmosis
RTD	Ready – to – drink
SDS	Sodium dodecyl sulphate
SDS-PAGE	Sodium dodecyl sulphate-Polyacrylamide Gel Electrophoresis
SEC	Size Exclusive Chromatography
SEM	Scanning Electron Microscopy
TEM	Transmission Electron Microscope
TEMED	N,N,N',N'- tetramethylethylene - diamine
TF	Theaflavin
TF-3-G	Theaflavin-3-gallate

TF-3'-G	Theaflavin-3'-gallate
TF-3,3'-G	Theaflavin-3,3'-gallate
TFs	Theaflavins
TMP	Transmembrane pressure
TRs	Thearubigins
UF	Ultrafiltration
$ZnCl_2$	Zinc chloride
ZP	Zeta potential

Chapter 1 Introduction

1.1 Introduction

Tea is one of the most widely consumed beverages in the world because of its attractive aroma, taste, and health-promoting effects. It is estimated that about 18 to 20 billion cups of tea are consumed in the world every day (Marcos *et al.*, 1998). According to the reports from the UN Food and Agriculture Organization (FAO), the consumption of black tea in the world increased from 1.97 million tonnes in 1993-1995 to 2.67 million tonnes by 2005. The annual growth rate is approximately 2.8% (www.fao.org/waicent/ois/press_ne/PRESSENG/1999/pren9955.htm). Tea's high economic and social importance can clearly be seen.

Due to the high acceptability of tea beverage, tea plants are now widely cultivated in more than 30 countries (Grahan, 1992), which are mainly located in Southeast Asia and central Africa. According to the different activity of tea enzymes in the course of raw tea treatment, commercial teas can be generally divided into three major categories: the non-fermented green tea, partially fermented oolong tea, and fully fermented black tea (Lin *et al.*, 1998). While black tea is considered to be one of the most popular types for its special flavor and thirst quenching properties, especially in western countries. In both US (http:en.wikipedia.org/wiki/Tea) and Italy (Todisco *et al.*, 2002), the consumption of Ready-to-drink (RTD) or Iced tea accounts for approximately 80% of consumption.

1.1.1 Current production processes of the black and cold tea

The production of black tea generally consists of three steps. During the pretreatment, the freshly harvested leaves are subjected to a series of processing conditions including withering, rolling and sorting. After that, an almost complete fermentation is carried out to develop much of the characteristic colour, flavour as well as the aroma of black tea. After a suitable period of time, the last step called firing, which inactivate the enzymes, is performed to obtain the final product (Sanderson *et al.*, 1977).

The manufacture of cold tea starts with the extraction of the tea liquor from black tea, followed by concentration, evaporation and spray drying of the tea extracts. Then the powder is reconstituted and sweetened before packaging and selling. Figure 1.1 shows the flowsheet of current tea manufacturing.

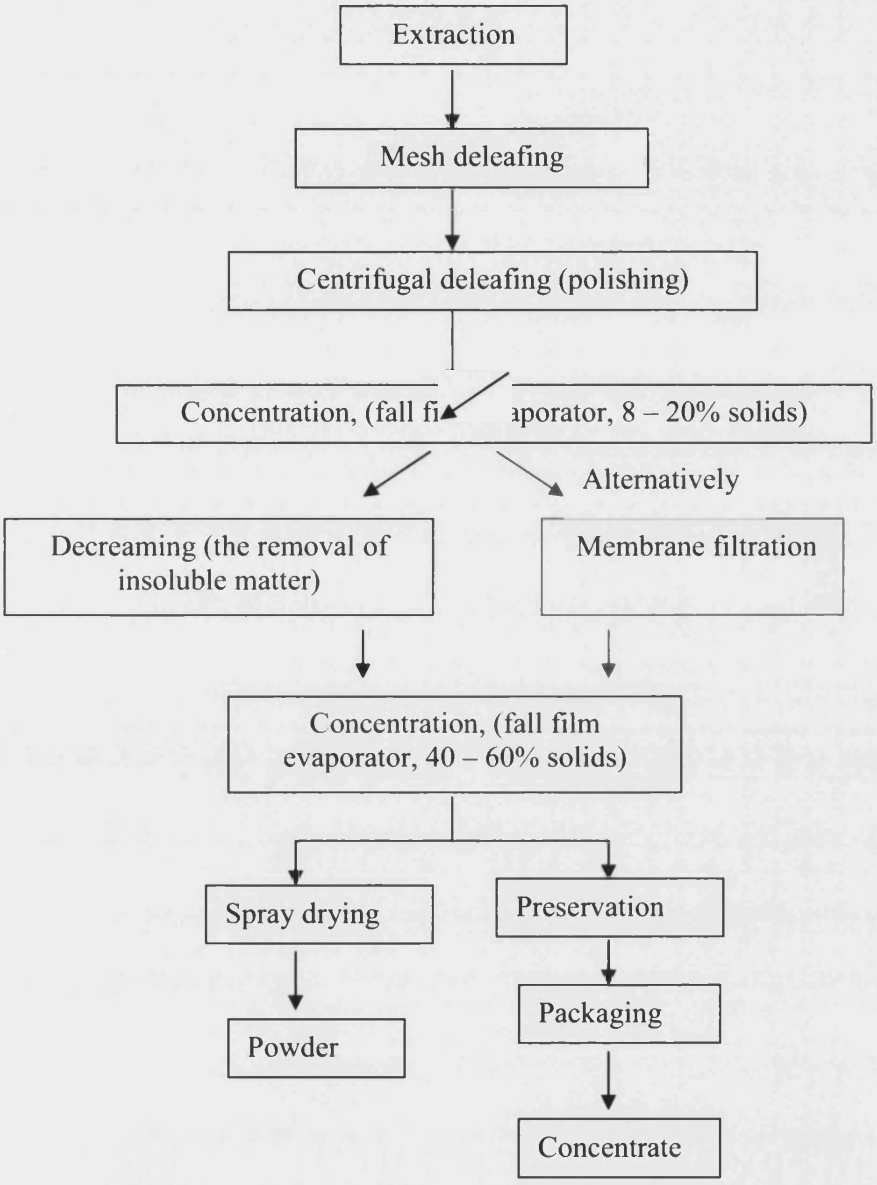

Figure 1.1 The flowsheet of current tea production process

1.1.2 Current problems of Ice tea product

Being an important contributor to a healthy life style for people all over the world, black tea contains a comparatively high percentage of polyphenols together with amino acids,

proteins, fiber, ash, carbohydrates and caffeine. These polyphenols can interact with proteins or other molecular types to form some molecular complexes, which are considered as tea haze and tea cream, when the beverage or the tea extract is allowed to cool to room temperature or lower. Generally, tea haze is considered to be formed by the reaction of polyphenol and protein, while tea cream is relative to the aggregation of polyphenol and caffeine. Both tea haze and tea cream appear to be insoluble materials which are detrimental to the look and the taste of ice-tea product. It is essential to remove haze and tea cream to produce a clear product that is attractive to the consumer. The formation of either tea haze or tea cream is determined by the concentration, pH value and temperature / time history of the liquor (Tolstoguzov, 2002).

1.1.3 The possible application of membrane ultrafiltration

Membrane ultrafiltration offers the possibility of eliminating haze, reducing the thermal treatment of the liquor, whilst allowing relatively low molecular weight polyphenols that impart flavour, colour and acidity, to pass through the membrane in the permeate (Todisco *et al.*, 2002). However, along with the application of membrane ultrafiltration, the problem of membrane fouling can not be neglected. The subsequent chemical cleaning is therefore necessary to maintain the permeability and selectivity of the membrane process.

1.2 Project aims and objectives

To improve the quality, stability and consistency of ice tea product by using membrane ultrafiltration.

To retain membrane permeability and selectivity to prolong membrane life time by optimizing both the production conditions and the cleaning regime of the process.

To improve understanding of the interaction between tea species during filtration.

To understand the interaction between the membrane and tea species through the use of model and reconstituted spray dried tea solutions.

1.3 The outline of the thesis

Chapter 2 gives a literature review regarding tea chemistry, membrane process and techniques used for membrane characterization in this study. Chapter 3 presents the results concerning black tea ultrafiltration on two different membranes and the corresponding cleaning by two cleaning reagents. The experiments involving in the analysis of product qualities as well as relevant tea haze characterization were described in Chapter 4. In Chapter 5, the methods for separating tea protein and polyphenol, and the studies on their interactions have been explained in detail. Chapter 6 and Chapter 7 focus on the results from model solution work, which was aimed to understand the interaction between membranes and polyphenol/protein based systems. Chapter 6 mainly involves the experiments concerning various fouling phenomenon, while the effects of corresponding membrane cleaning have been clarified in Chapter 7. Final conclusions of the work mentioned in this thesis have been drawn in Chapter 8, and the future work is also considered in this chapter.

1.4 List of publications arising from this thesis

1) Wu, D. and Bird, MR, 2007, 'The fouling and cleaning of UF membranes during the filtration of model tea component solutions', *Journal of Food Process Engineering*. In press. (will appear in March 2007)

2) Wu, D. and Bird, MR, 2006, 'The fouling of ultrafiltration membranes using model tea component solutions', *Fouling, Cleaning and Disinfection* 2006, Jesus College Cambridge, 20 – 22nd March 2006, pp 122-129. ISBN 0-9542483-1-7.

3) Wu. D, Sutton, K and Bird, MR. 2004, 'Influence of fouling and cleaning conditions upon the performance of ultrafilters for the processing of black tea liquor', presented in the form of poster on an international conference titled "Fouling and Critical Flux Theory and Applications" held in Lappeenranta University of Technology in Finland from June 16th to June 18th, 2004.

4) Wu, D. and Bird, MR, 'Separation and purification of tea protein and tea polyphenol species and the study of their interaction by ITC'. (Manuscript completed)

Chapter 2 Literature review

2.1 Tea chemistry

2.1.1 The composition of tea

Tea is one of the most popular beverages in the world. The composition of the tea can be influenced by many factors, such as species, season, ages of the leaves, climate, and horticultural conditions (Lin *et al.*, 1996). Generally, the constituents of fresh green tea shoot are polyphenols, caffeine, amino acids, proteins, carbohydrates, organic acids, lignin, lipids, chlorophylls, and ash (Todisco *et al.*, 2002). The percentage of each composition varies slightly from different source of research (See Table 2.1).

Table 2.1 Composition of fresh green tea leaf

Component	% of dry weight (a)	% of dry weight (b)	% of dry weight (c)	% of dry weight (d)
Total polyphenols	25 – 30	30 – 40	39	25 – 40
Amino acids	4 – 5	4	4	4
Organic acids	0.5 – 0.6	0.5	1.5	N/A
Carbohydrates	18 – 27	4	25	7
Protein	14 – 17	15	15	15
Lignin	5 – 6	6	6.5	N/A
Lipids	3 – 5	3	2	N/A
Chlorophyll	0.5 – 0.6	N/A	0.5	N/A
Ash	5 – 6	5	5	5
Caffeine	3 – 4	3 – 4	4	4
Note: a - www.fmltea.com/Teainfo/tea-chemistry%20.htm; b - *Unilever*, Colworth, UK; c - Balentine and Thomas, 1992; d – Lunder, 1992; N/A – not mentioned				

In green tea, the phenolic contents that constitute approximately 30% of the dry weight of the tea leaf include flavanols, flavandiols, flavonoids, and phenolic acids (Hertog *et al.*, 1993). Among them, 90% are flavonols, which are commonly known as catechins

(Krishnan and Maru, 2006). The major green tea catechins are (-)-epicatechin (EC), (-)-epicatechin gallate (ECG), (-)-epigallocatechin (EGC), (-)-epigallocatechin gallate (EGCG), (+)-gallocatechin, and (+)-catechin (http://www.teatalk.com/science/chemistry.htm). The content of these compounds and their chemical structures are shown in Table 2.2 and Figure 2.1 respectively. (Sanderson, 1972).

Table 2.2 Green tea flavan-3-ols (catechins)

Component	% of dry weight (a)	% of dry weight (b)
(-)-epicatechin (EC)	1 – 3	1 – 3
(-)-epicatechin gallate (ECG)	3 – 6	3 – 6
(-)-epigallocatechin (EGC)	3 – 6	3 – 6
(-)-epigallocatechin gallate (EGCG)	8 – 12	9 – 13
(+)-gallocatechin	3 – 4	1 – 2
(+)-catechin	1 – 2	1 – 2
Note: a – www.fmltea.com/Teainfo/tea-chemistry%20.htm; b – *Unilever*, Colworth, UK		

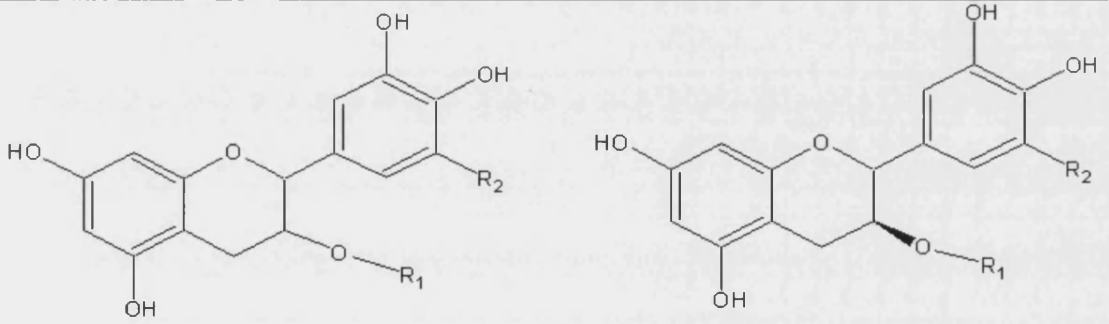

1 2

Structure 1

Catechin: R1, R2 = H

Gallocatechin: R1 = H, R2 = OH

Structure 2

Epicatechin: R1, R2 = H

Epigallocatechin: R1 = H, R2 = OH

Epicatechin gallate: R1 = gallate, R2 = H

Epigallocatechin gallate: R1 = gallate, R2 = OH

Figure 2.1 The chemical structure of green tea flavan-3-ols (catechins)

As to the black tea, the monomeric flavan-3-ols undergo polyphenol oxidase-dependent oxidative polymerization, which leads to the formation of bisflavanols, theaflavins, thearubigins, and other oligomers in the process of the fermentation. Therefore, black tea is low in catechins and has significant quantities of complex polyphenols, compared with green tea. The general composition of black tea leaves is presented in Table 2.3 (Lunder, 1992). Table 2.4 compares the compositions of beverages prepared from green and black tea (Balentine and Thomas, 1992).

Table 2.3 Composition of black tea leaves

Component		% of dry weight
Polyphenols	Thearubigins	15 – 20
	Bisflavanols	2 – 4
	Phenolic acids	4
	Unchanged flavanols	1 - 3
	Flavonols and Flavonol glycosides	2 – 3
Total polyphenols		30 – 40
Carbohydrates (monosaccharide & polysaccharide)		7
Amino acid (theanine, aspartic, glutamic, *et al.*)		4
Proteins		15
Fiber		30
Pigments		5
Caffeine		4
Mineral salts (Na, K, Mg, Ca, Mn, Sr, Fe, Cu, Zn, P, *et al.*)		5

Table 2.4 Composition of green and black tea beverages

Component	Green tea (% of dry extract solid)	Black tea (% of dry extract solid)
Catechins	34.0	4.2
Theaflavins	-	1.8
Thearubigens	-	17.0
Flavonols	0.4	-
Flavonol glycosides	4.4	1.4
Protein	7.6	10.7
Amino acids	5.3	4.8
Caffeine	6.9	7.1
Carbohydrates	12.5	13.5
Organic Acids	9.5	11.0

According to the results shown above, theaflavins and thearubigins are the most important polyphenols contained in black tea. Both of them contribute significantly to the color and the taste of black tea.

2.1.2 Major chemical components in black tea

2.1.2.1 Theaflavins (TFs)

Theaflavins (TFs) are considered to be mainly responsible for the yellowish brown or orange-red colour and astringent/brisk taste of tea brews (Haslam, 2003; Lee *et al.*, 2000; www.fmltea.com/Teainfo/tea-chemistry%20.htm). The major theaflavins (TFs) in black tea are theaflavin (TF), theaflavin-3-gallate (TF-3-G), theaflavin-3'-gallate (TF-3'-G) and theaflavin-3,3'-gallate (TF-3,3'-G). The mechanism of theaflavins formation from catechins has been studied and delineated in Figure 2.2 (Balentine and Thomas, 1992). The reaction involves the oxidative coupling of the aromatic B rings of two flavan-3-ol molecules, namely catechin and gallocatechins. In the structure of theaflavin monomer, two flavan rings are approximately orthogonal to the planar benzotropolone system and stacked against each other. TFs are reported to be able to self associate into dimers via $\pi - \pi$ interactions or intermolecular hydrogen bonds between two anti-parallel benzotropolone rings (See Figure 2.3). The interaction between caffeine and TF was proposed to occur at the flavan rings with a two sequential sites binding model. However, the structure in TF monomer directly relating to the interaction between TFs and protein is not clear yet. Hydrogen and / or hydrophobic bonding were reported to be involved in polyphenol – protein interactions. The formation of π – bonded complexes was also suggested (Siebert, 1999). Charlton *et al.*, (2002) reported that exposed hydrophobic and approximately planar sides chains appeared to be responsible for the polyphenol / peptide binding. This indicates that the stacking of the polyphenolic rings against hydrophobic surface dominates binding interactions. Although only about 1 – 2% of the dry weight of black tea is due to TFs, they are considered to play an important role in the brightness of black tea infusions, which is a key sign for tea quality (Degenhardt, *et al.*, 2000). This is confirmed by Liang, *et al.*, (2003) according to their research on colour analysis of tea infusions. In their study, all TFs presented positive correlation with a^* (redness), b^* (yellowness) and total colour differences E, while negative correlation with L^* (lightness). This indicates the higher the total TFs content in black tea, the higher values of a^*, b^*, E, but lower L^* will be observed, which leads to a tea product of high quality.

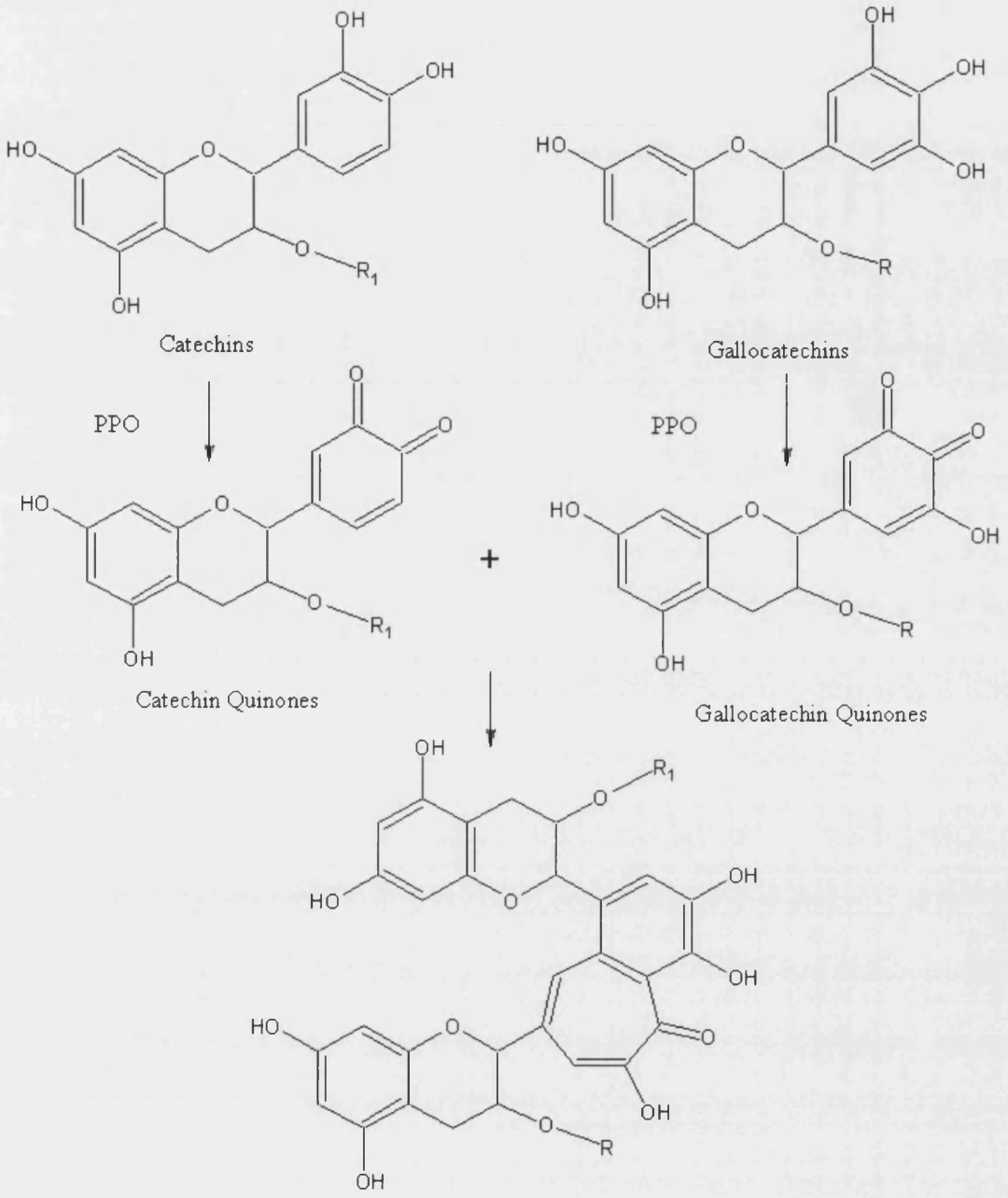

Theaflavin: R = R1 = H

Theaflavin gallate A: R = gallate and R1 = H

Theaflavin gallate B: R = H and R1 = gallate

Theaflavin digallate: R = R1 = gallate

Figure 2.2 The mechanism of the formation of theaflavins (Adapted from Balentine and Thomas, 1992)

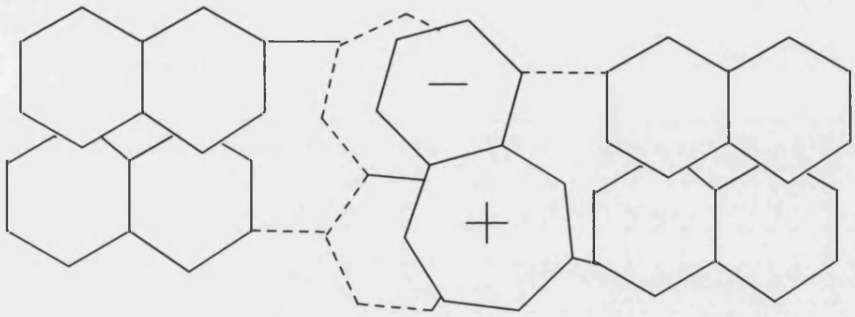

Figure 2.3 A low-energy conformation of the theaflavin dimer (Adapted from Charlton, *et al.*, 2000)

According to the studies on the stability of tea theaflavins and catechins by Su, *et al.*, (2003), TFs are susceptible to degradation when either temperature or the pH of incubation media was increased. Four theaflavins derivatives, namely TF, TF-3-G, TF-3'-G and TF-3,3'-G demonstrated differences in both thermal stabilities and pH-dependent stabilities. Generally, TF and TF-3-G appeared to be less stable than TF-3'-G and TF-3,3'-G in both boiling water and alkaline sodium phosphate solution. Short-term stability of TFs as a whole was observed in the tea drinks with pH 5 or less.

2.1.2.2 Thearubigins (TRs)

Compared with theaflavins (TFs), thearubigins (TRs) are even more complex substances whose molecular weights range from 700 to 40000 Da (Todisco *et al.*, 2002). Taking up approximately 47% of the total polyphenol content in black tea (with 13% from TFs), thearubigins (TRs) are considered to be one of the most important characteristic polyphenols in black tea (Krishnan and Maru, 2006). These extensively oxidized polymers are reported to make more contribution to red-brown colour of black tea infusion, and have an ashy and slight astringent taste (Haslam, 2003; www.fmltea.com/Teainfo/tea-chemistry%20.htm). The literature reports little understanding of the chemistry of thearubigins. They are reported to be acidic and highly water soluble, making up the majority of the water soluble phenolic constituents of black tea (Obanda *et al.*, 2004; Degenhardt *et al.*, 2000). HCl hydrolysis of thearubigins showed the presence of following free amino acid: alanine, arginine, aspartic acid, glutamic acid, glycine, isoleucine, leucine, lysince, phenylalanine, proline, serine, threonine, tyrosine, and valine. This implied that TRs might contain either

substances relative to humic acid or proteins to which quinonoid species are covalently attached (Haslam, 2003; Vuataz and Branderberger, 1961).

Although the chemical structure of thearubigins is not clear yet, they were suggested to be polymeric proanthocyanidins (Obanda *et al.*, 2004). Recent review by Haslam (2003) has mentioned the possible pathways of thearubigins formation (See Figure 2.4). The major substrates, namely EGC and EGCG, were initially oxidized by tea polyphenoloxidase to be the corresponding orthoquinone derivatives. These quinines are highly reactive and are able to produce theaflavins, theasinensins or even thearubigins via oxidative coupling. Theasinensins have been identified as a kind of bisflavanols formed by direct oxidative coupling from polyphenolic flavan-3-ols. They have been certified to be key intermediates during the early stage of fermentation. Both theaflavins and theasinensins are supposed to be able to transform into thearubigins via further oxidation and oligomerisation.

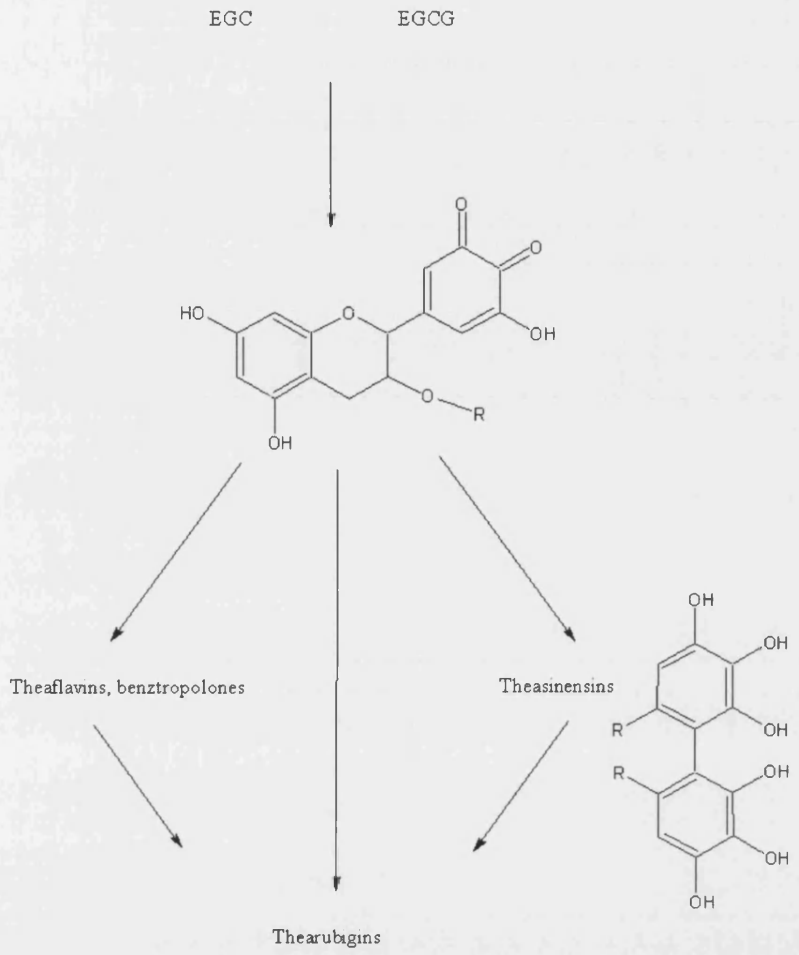

Figure 2.4 The possible passway of thearubigins formation. (Adapted from Haslam, 2003)

A mechanistic model of the brown pigments formation from pyrogallol in alkaline solution has been extended and proposed to explain the possible structure of thearubigins in black tea (Haslam, 2003). From Figure 2.5, the hydroxyquinone (a) in pyrogallol, which is also the characteristic structure of quinines derived from different polyphenolic flavan-3-ols, has the ability to produce an oligomeric structure (b) by self-condensation. Highly conjugated cationic structures (c) could be formed by further intro-molecular oxidation. Although there have not been any specific experimental data to date to support this proposal, it appears to be realistic as it can be used to explain the chemical nature of thearubigins very well (Haslam, 2003).

Firstly, as shown in (b) and (c) in Figure 2.5, a series of conjugated structure such as dimeric, trimeric, tetrameric or even greater structures, could account for the wide range of molecular weight from 700 to 40000 Da for thearubigins.

Secondly, the brown colour of thearubigins can be derived from the chromophoric group resulted from the formation of highly conjugated planar structure due to the oxidative oligomerisation.

Thirdly, the marked acidity of thearubigins could be induced by either the ionization of phenolic protons or the oxidative ring fission of one or more aromatic rings in the highly conjugated planar structure.

Last but not least, the suggested planar structure for the pigmented thearubigins in this model shows the potential to complex with caffeine, theaflavins or other components like protein so as to be involved in the process of tea haze or cream formation.

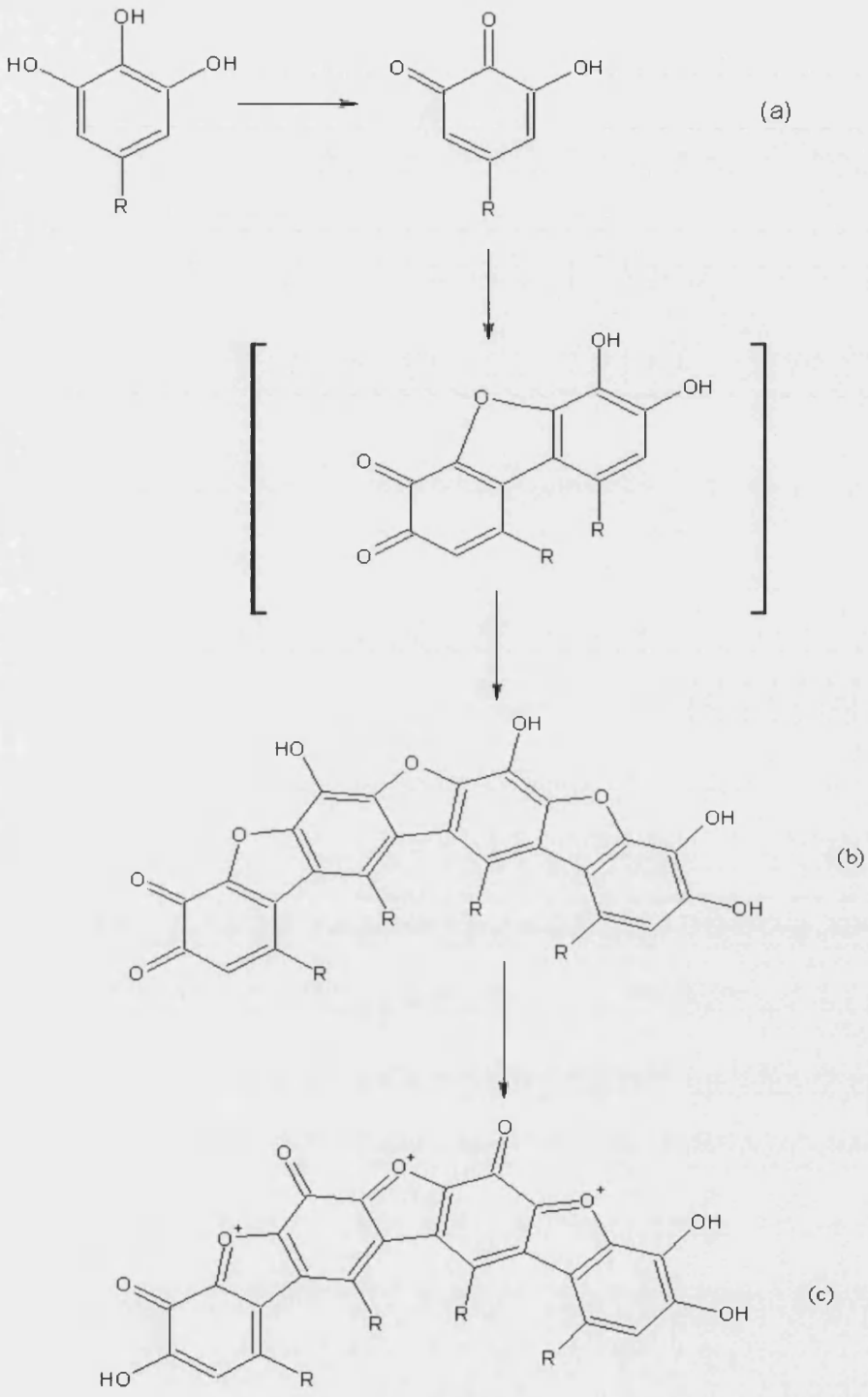

Figure 2.5 The mechanistic model explaining the formation of brown pigment from pyrogallor in alkaline conditions. (Adapted from Haslam, 2003)

2.1.2.3 Caffeine

Caffeine is another important constituent in black tea due to its stimulating properties. It is a purine derivative, which is 1,3,7- tri-methyl xanthine (See Figure 2.6). Despite of the fact that caffeine content is less than 4% of the dry weight in black tea, it makes great contribution to black tea quality such as briskness and bitter taste (Yao *et al.*, 2006). It is reported that caffeine is able to complex with tea polyphenols, for example theaflavins (TFs) and thearubigins (TRs), to produce "tea cream" which is a precipitate formed when tea infusion cools down. According to the study on the binding of caffeine to theaflavins by Charlton *et al.*, (2000), a sequential binding with the ratio of two molecules of caffeine vs one molecule of theaflavin was observed.

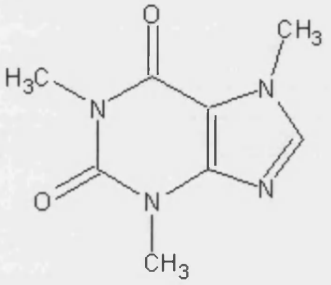

caffeine

Figure 2.6 The chemical structure of caffeine

2.1.3 Tea cream

As mentioned above, tea cream is associated with the interactions occurring between polyphenols and caffeine. The presence of tea cream will give tea a hazy or muddy appearance that is not consumer friendly. Therefore, it is not favored in Ready-to-Drink tea products. Tea creaming being such a critical issue in cold tea product, many researchers have paid their attention to the studies on physical, chemical properties of tea cream as well as the factors influencing tea cream formation.

The predominant constituents of black tea cream are found to be thearubigins (TRs), theaflavins (TFs) and caffeine. The composition of tea infusion rather than their solid concentration exerts great impact on the amount of tea cream formed. The loss of

theaflavins was considered to be the main reason for the decrease of the cream level after a certain period of fermentation.

A decreasing tendency of the average particle size of tea cream was observed during the fermentation process. It is reported that the peak of particle size distribution curve shifted from 0.78 μm to 0.48 μm after fermentation being conducted for four hours (Liang *et al.*, 2002).

The extraction temperature was found to be a parameter influencing cream formation. During the research carried out by Liang and Xu (2003), the dry weight of tea cream, tea cream particle volume concentration, and the amount of haze were increased sharply as the extraction temperature jumped from 50 to 60 °C. Therefore, lower extraction temperatures might be preferred in cold tea production in terms of less tea cream formation.

pH value of the tea infusion also had an effect upon tea cream formation. Acidic conditions were reported to be beneficial to the instant tea yield. Nevertheless, A low pH also encouraged the formation of tea cream by either releasing more solids into the infusion or stimulating polyphenols to interact with polysaccharides and nucleuphilic groups on protein in tea infusion (Liang and Xu, 2001).

2.1.4 Tea haze

In addition to tea cream, tea haze is another serious issue in the preparation of a stable commercial tea concentrate and the acceptance by the consumer of soluble instant tea powders, particularly of instant ice tea products.

In general, tea haze is considered to be associated with the aggregation of polyphenol and tea protein. The amount of tea haze formed in tea infusions was observed to increase simultaneously with the increase of both protein and polyphenol concentrations. However, if either of them was kept constant, a plateau was obtained in the end (Siebert *et al.*, 1996). This indicates that the haze formation depends upon the chemical composition of the infusion and the ratio of protein and polyphenol.

2.1.5 Haze – active protein

Many studies have been reported concerning haze-active proteins, polyphenols and their reactions in beverages such as beers, fruit juices and wines. Nevertheless, the literature contains limited information on tea haze and the role of proteins in this process.

Proteins in grape juice contributing to haze formation were reported to have relative low molecular weight of 12.6 and 20-30 kD with pI 4.1–5.8 (Hsu and Heatherbell, 1987). Two proteins involved in heat haze formation in wine were characterized to be 24 and 32 kD respectively (Waters *et al*, 1992). Wu and Siebert (2002) suggested that three haze-active proteins, namely HAP I, HAP II, HAP III, were extracted from apple and were of different molecular weights of 28, 15 and 12 kD respectively. The rankings of their haze forming activity were gliadin > HAP III > HAP II > HAP I > BSA (Wu and Siebert, 2002). Luck *et al.*, 1994 report that proteins combined with polyphenols contain high level of proline. This results in a conformationally open and flexible structure for protein with a correspondingly greater potential for complexation. Hydrolysis and amino acid analysis of apple juice haze indicated that the percentage of proline contained ranged from 15.9 wt% to 31.7 wt% (Johnson, *et al.*, 1968). However, an even larger amount of proline (from 21.8% to 39.8% depending upon growing conditions) was found in green tea protein by Hu *et al.* (2001) during their study on the effects of selenium on green tea preservation.

2.1.6 Haze – active polyphenols

Haze-active polyphenols are considered to be members of proanthocyanidins, which are monomer, dimers, trimers and higher polymers of catechin, epicatechin and gallocatechin in beer, wine, grape juice and apple juice. The presence of o-dihydroxybenzene groups is reported to be of great importance in haze formation (Siebert *et al.*, 1996). At least two or three hydroxy groups on an aromatic ring are required regarding the binding sites of haze-forming polyphenols. In the case of beer haze, procyanidin B3 (catechin-catechin) and prodelphinidin B3 (gallocatechin-catechin) are strongly associated with haze formation (Siebert, 1999). As for black tea, the fermentation process gives rise to the formation of bisflavanols, theaflavins, thearubigins, and other oligomers. Therefore, black tea contains less catechins and is

rich in complex polyphenols. This indicates a higher precipitating activity of black tea polyphenols compared with those present in green tea, as the degree of polymerization of polyphenols exerts stronger effects on polyphenol binding than does the number of OH groups on an aromatic ring (Siebert, 1999).

2.1.7 The interactions between protein and polyphenols

Luck *et al.* (1994) considered protein – polyphenol reactions to be non-covalent bonding, at least initially, because of the fact that haze can be dissolved to some extent with the warming of beverages. This hypothesis was supported by the observation of non-covalent complexes for a tannin-protein model by electrospray ionization mass spectroscopy (Verge *et al.*, 2002). Hydrogen and/or hydrophobic bonding were more associated according to the results from X-ray crystallography and NMR spectroscopy. However, hydrophilic forces were mentioned to be the main driving force during BSA-tannin aggregation by De Freitas *et al.*, 2003, as they observed a decrease in the amount of protein/tannin aggregation as the ionic strength increased by NaCl addition. The ratio of polyphenol to protein was reported to be a critical factor influencing the amount of haze produced. When the number of polyphenol binding sites is nearly equal to the number of protein binding sites, the largest amount of haze is observed (Siebert, 1999). The different pH values of beverages might also influence the process of polyphenol-protein precipitation. A stronger affinity between one kind of flavonoids – quercetin and BSA was observed at a relatively higher pH in the range tested of 5 - 7.4 (Papadopoulou *et al.*, 2005). However, few studies have been carried out to investigate binding reactions at the pH of the beverages of interest (generally pH 3 for grape juice and wine, pH 4 for apple juice and beer, pH 5 for tea extract). As to the possible structure of haze, in the study of apple juice haze by Beveridge *et al.* (1998), a branched chain-like structure was observed in haze of globular particles of variable size using electron microscopy after negative staining with uranyl acetate. In another study of protein-polyphenol complexation in the mixture of tea and milk, a structure of spherical and porous submicelles (~ 10-15 nm in diameter) of polyphenol and casein was assumed (Luck *et al.*, 1994).

Recently, Isothermal Titration Microcalorimetry (ITC) has been applied to the study of protein and tannin interactions by Frazier *et al.*, (2003). In their study, the interaction

between protein and tannin depended upon the nature of the protein involved. The mechanism of tannin binding to the random coil protein gelatin was a two-stage process, where the first stage was cooperative binding, and the second one was gradual saturation of binding sites.

2.2 Membrane Separation Process

2.2.1 The wide application of membrane separation

Membrane processes have been considered to be a promising method of separation in recent years. Compared with traditional separation processes, membranes have significant advantages from both economic and technical points of view (Mulder, 1996).

Firstly, as there is no change of phase, and ambient operation is possible, the consumption of energy is generally low. Therefore, operating costs are often lower during membrane process. Secondly, it becomes possible to perform a continuous separation under mild conditions. Thirdly, it is feasible to change the conditions or the selectivity of separation due to the variability of membranes. Finally, scale up is also easy as membranes operate in modular structures.

In view of the benefits mentioned above, it is hardly surprising that membrane processes are currently used in nearly all industrial areas, such as food and beverages, metallurgy, pulp and paper, textile, pharmaceutical, biotechnology and so on. Particularly, membrane processes are of special interest for food and beverage processing, because low temperature operation is possible and are economical even for small plant. Many studies have been carried out on the concentration of protein, solutions and the clarification of beverages, such as fruit juice, beer and green tea. Membrane microfiltration has been applied for milk pasteurisation and separation of lipoproteins and whey protein in dairy industry. Fruit juice, wine and beer industry have used membrane ultrafiltration/microfiltration for clarification and sterilization to improve product quality and to prolong product shelf-life time (Mangas *et al.*, 1997;

Vernhet and Moutounet, 2002; Gan *et al.*, 2001). Table 2.5 lists the reviewed papers, which are relevant to the application of membrane filtration in food industry.

Table 2.5 Reviewed papers involving the applications of membrane filtration in food industry

Reference	Objective	Membrane Class	Membranes used
Hsu *et al.*, 1987	Grape juice and wine	Ultrafiltration	Romicon and Millipore systems membranes of MWCO 10 kD – 100 kD
Main findings: UF of wine and grape juice by using membranes of MWCO 10 – 30 kD can be an effective bentonite substitute. Protein retention increased with MWCO decreased. More than 90% of protein in wine was removed by UF with membranes of MWCO 10 kD.			
Mangas *et al.*, 1997	Apple juice	Microfiltration & Ultrafiltration	Inorganic UF membranes of MWCO 50 kD, MF membranes of 0.14 μm mean pore size
Main findings: UF at 20 °C was able to clarify apple juice with an adequate level stability. Membrane type, temperature, and process time had significant influence on the content of phenolic compounds and the colour of the apple juice.			
Riedl *et al.*, 1998	Apple juice	Microfiltration	Polysulphone membrane of 0.2 μm pore size; Polyethersulfone membranes
Main findings: The interaction of tannin and gelation is critical to the formation of fouling layer during MF of apple juice model solution. The addition of excessive tannin into unclarified apple juice did not increase the fouling resistance, while pectin addition significantly increased the fouling resistance.			
Vernhet and Moutounet, 2002	Wine	Microfiltration	Polyethersulfone membranes of 0.08 μm mean pore size; Polyvinylpyrrolidone membranes of 0.09 μm mean pore size; Polyvinylchloride membranes of 0.09 μm mean pore size
Main findings: Membrane surface properties have significant effect in the building of fouling deposit. A pore constriction model was proposed for fouling mechanism. Membrane fouling began with the interactions between membrane and wine constituents, followed by the interactions between molecules resulting into the formation of organic deposits on the membrane feed side.			
Gan *et al.*, 2001	Beer	Microfiltration	Ceramic membranes of 0.2, 0.5, 1.3 μm mean pore size
Main findings: Flux decline and selectivity change mainly due to in pore membrane fouling. Backflush at reversed membrane morphology was useful to improve flux and maintain selectivity.			
Gan, 2001	Beer	Microfiltration	Ceramic membranes with nominal pore diameters of 0.5 μm mean pore size
Main findings: Enhancing surface hydrodynamic conditions by superimposed helical flow pattern and the two way reversing flow pulsation had little effect in increasing flux.			
Eagles and Wakeman, 2002	Model beer solution	Microfiltration	Cellulose nitrate membranes of 0.2 μm mean pore size

Main findings: Starch and casein induced dramatic flux decline due to the formation of deposits on the membrane surface. The rejection levels of both maltose and catechin were mainly determined by the presence of casein because of polyphenol – protein interaction.			
Czekaj *et al.*, 2000	White wine and beer	Microfiltration & Ultrafiltration	Cellulose acetate membranes of 0.45 μm mean pore size and those with MWCO 100 kD
Main findings: Membrane fouling was significantly affected by the initial macromolecular contents and turbidity of the wine and beer. Membrane morphology is important for controlling fouling			
Bird and Bartlett, 2002	Whey protein concentrate	Microfiltration	Sintered stainless steel flat sheet membrane of 2 μm mean pore size
Main findings: 50 °C and 0.2 wt% NaOH appeared to be optimal during cleaning. Both the maximum and steady – state flux recovery values increased with increasing CFV. A mathematic model based on simultaneous removal and swelling processes occurring within the surface and in-pore deposits was developed.			
Kawakatsu *et al.*, 1995	Green tea extract	Microfiltration & Ultrafiltration	Various membranes
Main findings: Small flux reduction rate was observed in dead-end UF. Fluxes were relatively high in cross flow mode, and 30 – 50% pectin was rejected.			
Todisco *et al.*, 2002	Black tea	Ultrafiltration	Ceramic membrane of NMWCO 40 kD
Main findings: Colour and polyphenol stability of black tea was achieved after membrane UF. A relationship between the mass transport coefficient and cross-flow velocity was identified. An in-series resistance model was modified by introducing concentration polarisation.			

2.2.2 The principle and mechanism of membrane separation and category of membrane separation process

Membrane has been identified as "a selective barrier between two phase" by Cheryan (1986). Phase one is usually denoted as the 'feed' on the upstream side of the membrane. While phase two is permeate on the downstream side of the membrane. Because of the differences in physical and/or chemical properties between the membrane and the permeating components, the ability of transport of different components in the feed varies with each other. Therefore, the separation can be achieved as a result of driving force, which is generally generated by concentration differences, pressure differences, electrical potential differences and temperature differences. A schematic illustration of membrane separation is shown in Figure 2.7 (Mulder, 1996).

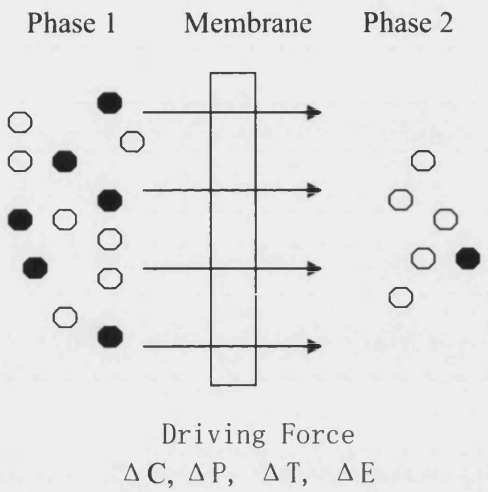

Figure 2.7 Schematic representation of a two-phase system separated by a membrane

According to the driving forces acting on the feed, the currently identified membrane processes can be divided into four groups. (See Table 2.6)

Table 2.6 The classification of membrane processes according to driving forces (Mulder, 1996)

Driving force	Hydrostatic pressure	Concentration difference	Temperature difference	Electrical potential gradient
Membrane Processes	Microfiltration, Ultrafiltration, Nanofiltration, Reverse Osmosis, Piezodialysis	Dialysis, Controlled release pervaporation, Liquid membrane, Carrier impregnated membrane, Gas separation	Thermo-osmosis membrane distillation	Electrodialysis, Electro-osmosis, Electrophoresis, Transport depletion

2.2.3 Pressure-Driven Process

As listed in Table 2.6, there are five membrane processes driven by pressure. As piezodialysis involves the permeation of the ionic solute rather than a solvent, it is of little more than laboratory interest. While, the other four processes, namely microfiltration, ultrafiltration, nanofiltration and reverse osmosis, are the most common industrial membrane processes used today.

Microfiltration and ultrafiltration are conceptually similar processes and are supposed to operate on the basis of sieving mechanism, which means the separation is determined

mainly by the size and the shape of the solutes relative to the membrane pore diameters. However, hydrophobicity, charge and roughness will all determine the membranes performance (Kilduff, *et al.*, 2005; Kang *et al.*, 2006). Generally, microfiltration is used to retain suspensions and emulsions. Whilst ultrafiltration is more suitable for retaining macromolecules and colloids from a solution with respect to its smaller membrane pore size.

Compared with MF and UF, nanofiltration and reverse osmosis are quite different. They are used to separate low molecular weight solutions or small organic molecules. The membranes of NF and RO can be considered as being intermediate between open porous types of membrane (MF or UF) and dense nonporous membranes (pervaporation/ gas separation).

Mulder (1996) has summarized the differences of four major pressure driven membrane processes, namely microfiltration, ultrafiltration, nanofiltration and reverse osmosis from several angles. The results are shown in Table 2.7.

Table 2.7 Comparison of various pressure driven membrane processes

Microfiltration	**Ultrafiltration**	**Nanofiltration/reverse osmosis**
Separation of particles	Separation of Macromolecules (bacteria, yeasts)	Separation of low MW solutes (salts, glucose, lactose, micropollutents)
Osmotic pressure negligible	Osmotic pressure negligible	Osmotic pressure high (about 1-25 bar)
Applied pressure low (<2 bar)	Applied pressure low (about 1-10 bar)	Applied pressure high (about 10-60 bar)
Symmetric structure Asymmetric structure	Asymmetric structure	Asymmetric structure
Thickness of separating layer Symmetric ≈10-150 μm Asymmetric ≈ 1 μm	Thickness of actual separating layer ≈ 0.1 – 1.0 μm	Thickness of actual separating layer ≈ 0.1- 1.0 μm
Separation based on particle size	Separation based on particle size	Separation based on differences in solubility and diffusivity

As the objective of this study is to remove tea haze or cream which are colloidal suspensions, membrane ultrafiltration is considered to be suitable. Mangas *et al.*, (1997)

mentioned that higher level of procyanidin B1 and chlorogenic acid was obtained when apple juices were clarified by ultrafiltration than that by microfiltration. Ultrafiltration at low temperature was good enough to produce an apple juice with adequate stability. The study of clarification of green tea extract by microfiltration and ultrafiltration by Kawakatsu *et al.*, (1995) also confirmed the effectiveness of ultrafiltration and its advantages over microfiltration by observing the retardation of secondary sedimentation and partial rejection of both catechin and caffeine due to the removal of tea haze or cream.

2.2.4 Ultrafiltration

For the purpose of this project, ultrafiltration is described in detail in the following paragraphs.

Ultrafiltration is an effective separation process whose nature lies between nanofiltration and microfiltration. It always involves the retention of substances with low molecular weights of more than a few thousand Daltons (Mulder, 1996).

Membrane ultrafiltration process is becoming widely used in a number of diverse industries and the number of its application is still increasing. For instance, it has been applied in food and dairy industry, pharmaceutical industry, chemical industry, paper industry, leather industry, waste water, pollution control and even medical therapeutics (Eykamp, 1995; Zeman and Zydney, 1996; Kulkarni *et al.*; Cheryan, 1986; Li, *et al.*, 2003).

In the food and dairy industry, various applications have been focused on the concentration of milk and cheese making, the recovery of potato starch and whey proteins, the concentration of egg white, as well as the clarification of fruit juices and alcoholic beverages.

2.2.4.1 Ultrafiltration membranes

Most pressure-driven filtration membranes can be classified as microporous membranes with different morphologies. Many microporous membranes are symmetric in structure. However, most ultrafiltration membranes have an asymmetric structure consisting of a

top layer and a porous sublayer. Generally, the thickness of top layer is only 0.1-1 μm. This thin skin layer is so dense that it determines the major membrane resistance to mass transfer.

The materials used for ultrafiltration membrane preparation are always polymeric materials, such as polysulphone, poly(vinylidene fluoride), polyacrylonitrile, cellulosics, polyimide, aliphatic polyamides and polyetherketone (Mulder, 1996).

Cellulose

Cellulose is a long chain polymer with a very regular structure. The chemical structure of the repeating D-glucopyranose unit in cellulose is as follows (Nunes and Peinemann, 2001; Mulder, 1996):

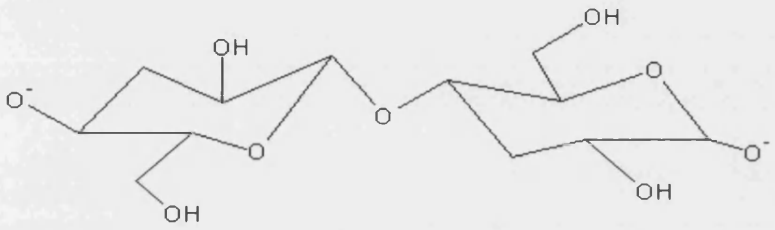

cellulose

Figure 2.8 The chemical structure of cellulose

The hydroxyl groups on the cellulose chain not only facilitate the formation of intermolecular hydrogen-bonds, but also allow the polymer binds to other molecules, such as water, via hydrogen-bonds. Therefore, most cellulose structures are highly hydrophilic. The preparation of cellulose membranes basically involves precipitation from a solution of chemically modified native cellulose. In terms of the capital cost of the membrane per unit area, cellulose acetate membranes are relatively cheap, compared to other membranes. However, the life time of this membrane appear to be shorter if the temperature is higher than 30 °C and the pH is lower than 3. Moreover, the membrane cleaning process based on the alkali solutions will further reduce the lifetime of cellulose membranes. Consequently, the usage of this kind of membrane does not seem to be a preferable choice in industry, especially high temperature or extreme pH is required.

Polysulfone and polyethersulfone

Polysulfone (PSF) and polyethersulphone (PES) are the most widely used polymers for preparing UF membranes. Since the development of PSF / PES membranes, they have been alternatives to cellulose membranes because of their resistance of extreme pH conditions, as well as their thermal stability. However, it can not be denied that they also have several shortcomings. For example, they are comparatively expensive, whose price is nearly three times than that of cellulose membranes. Besides, as a result of their comparatively hydrophobic character, the membrane must be prevented from drying completely. Consequently, most commercial PSF or PES membranes are coated with a hydrophilic agent, such as glycerin before drying, which might have some influence on the nature of membrane. This preservative needs to be removed before the membrane is used if an accurate measure of membrane performance is to be achieved.

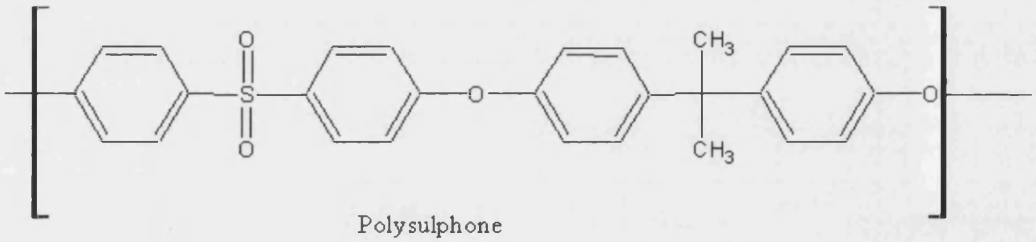

Polysulphone

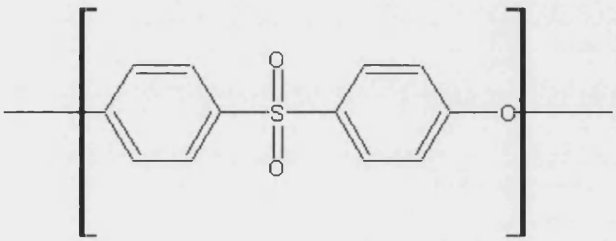

Poly(ether sulfone)

Figure 2.9 The structure of polysulphone and polyethersulphone. (Mulder, 1996; Popescu, *et al.*, 1994)

Fluoropolymer membrane

Fluoropolymers are polymers containing fluorine. They are considered to be another group of outstanding materials for membrane manufacture due to their attractive properties such as the ability to withstand solvents, corrosive chemicals, and high temperature, low pressure drop, insulating properties, non-adhesiveness, and resistance to damage (www.freshpatents.com/Fluoropolymer-membrane-dt20060216ptan20060032813.php). There are various types of fluoropolymers available, for instance, polytetrafluoroethylene (PTFE – known as Teflon), fluorinated ethylene-propylene (FEP), ethylene tetrafluoroEthylene (ETFE), polyvinylidene fluoride (PVDF) and so on. It is difficult to give the exact chemical structures of the fluoropolymers used for membrane production because of their complexity and versatility. Nevertheless, for the fluoropolymer membrane (FS50PP) used in this study, it is reported to be the polymer derived from fluoride and polypropylene (Palmisano, 2006).

2.2.4.2 The selection of membrane molecular weight cut off (MWCO)

A molecular-weight cut-off is defined as the molecular weight at which the membrane rejects 90% of solute molecules. It is very important to choose a membrane of an appropriate MWCO in order to obtain the best separation. Hsu and Heatherbell (1987) have investigated the effects of ultrafiltrate membrane MWCO on retention and stabilities of proteins in wine and grape juice. In their study, wines and grape juices were ultrafiltered with membranes of MWCO ranging from 10 kD to 100 kD. According to their results, there were generally increased tendencies for protein retention with the decrease of MWCO during the ultrafiltration of both wine and juice. However, when wine was ultrafiltered by a membrane of MWCO 30 kD. 99% retention of protein was obtained, which was the same as that for 10 kD – MWCO membrane, indicating that proteins contained in wine are probably larger than 30 kD. Proteins were detected to be stable with the usage of membranes of MWCO of 10 kD and 30 kD.

2.2.5 Membrane modules

With respect to the efficiency of membrane separation, ease of operation, ease of cleaning, and possibility of membrane replacement, the design of membrane module should be very careful and is always a compromise.

There are four major membrane module designs available commercially, namely: plate-and-frame modules, spiral wound modules, hollow fiber modules and tubular ceramics. The first two types are based on flat membrane configurations, whereas, the other two types involve tubular membranes.

2.2.5.1 Plate-and-frame module

A plate-and-frame module whose configuration is relatively simple is designed for housing one or several pieces of flat sheet membranes within sets of sealed plates. This module has some advantages over others, such as lower fouling tendency, good cleanability, together with easy membrane replacement. However, in terms of the limitation of the number of membrane sheets placed in every module, it is commonly used in laboratory scale rather than industrial cases (Mulder 1991). Another drawback is the lack of mechanical strength so that it is unable to adopt back-flushing which is a popular in situ cleaning method.

2.2.5.2 Spiral Wound Modules

The spiral wound module provides another flat membrane configuration in the form of "swiss roll". In fact, it can be obtained by wrapping a plate-and-frame system around a central collection pipe. This cylindrical module poses a higher packing density compared with plate-and-frame module. However, it also has the disadvantages of a higher fouling potential and the impossibility of membrane replacement.

2.2.5.3 Hollow Fiber Modules

The hollow fiber modules consist of a number of fine fibers with diameters 0.1 to 2 mm assembled together in a module. It is the configuration with the highest packing density, as well as the highest fouling tendency. As it is also unable to replace the membrane,

this module is always used when the feed is comparatively clean, as in the case of gas separation and pervaporation.

2.2.5.4 Tubular Module

Tubular module configurations are used to assemble tubular membranes that are not self-supporting. The number of the tubes contained in the module normally varies from 4 to 18. Ceramic membranes are the most common tubular membranes placed in this module. Tubular ceramics can be back flushed. "Inside – out" and "outside – in" configurations are possible. They are chemically and thermally stable. However, ceramics are expensive compared with polymer membranes. The packing density of tubular module is generally low. It also has higher potential of membrane fouling.

2.2.6 Module operations

In addition to the importance of the selection of module configuration, the arrangement of module is also very crucial to achieve an optimal design. Dead-end and cross-flow modes are two conventional module operations used today.

2.2.6.1 Dead-end Operation

As showed in Figure 2.10, the feed flows towards the surface of membrane, and is forced to pass through the membrane perpendicularly in the dead-end operation. This indicates that the quality of the permeate will probably decrease with time as a result of the increase in the concentration of rejected components in the feed (Mulder, 1996). In this case, it might be easier to form a layer of cake on the top of membrane, which will lead to the flux decline of the product.

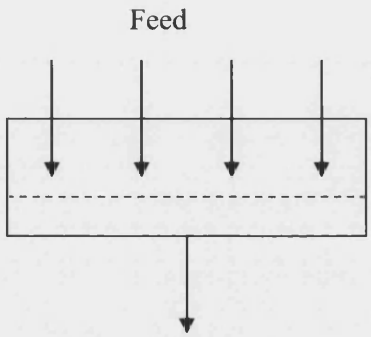

Figure 2.10 The schematic description of dead-end mode

2.2.6.2 Cross flow operation

In contrast to dead-end operation, the feed flows parallel to the membrane surface with the inlet feed stream entering the membrane module at a certain position. Then the stream is separated into permeate and retentate streams. The composition of the feed inside the module varies as a function of distance in the module. With the applicable cross-flow operation, higher rates of mass transfer can be obtained because of the availability of the high shear rate and / or turbulence in the immediate vicinity of the membrane (Mulder 1991; Shorrock and Bird, 1998). Moreover, membrane fouling tends to be less and flux decline is also found to be relatively smaller. Therefore, the operation in cross-flow mode is preferred for industrial applications.

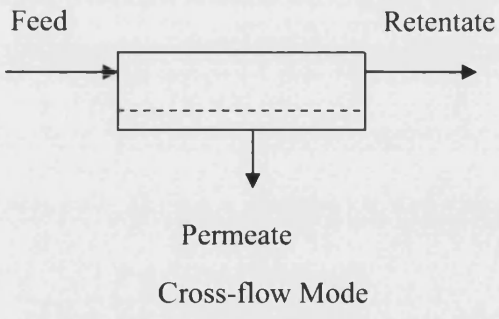

Figure 2.11 The schematic description of cross-flow mode

In the study of monitoring of membrane fouling and cleaning during ultrafiltration by using ultrasonic technique by Li *et al.*, (2003), the different fouling occurred on dead-

end and cross-flow filtration had been investigated. During the ultrafiltration of paper mill effluents of the same concentration, a faster decline of permeate flux was observed in dead-end filtration (0 cm s^{-1}) than cross flow (12.5 cm s^{-1}) until steady state flux was obtained after two hours of filtration. Although both membrane surfaces were found to be covered by dense fouling layers of the same thickness after two hours of fouling operation, the grow rate of the thickness of the fouling layer in dead-end was larger than that in cross-flow. In addition, the compressibility of the fouling cake also varied with the operation mode.

The more severe reduction of permeate flux taking place in dead-end filtration rather than cross-flow was also visualized by Arnot, *et al.*, (2000) during their study on microfiltration of oily-water emulsions. Two membranes, namely Millipore membrane (0.45 μm) and Ceramesh membrane (0.1 μm) were used in their study. For the Millipore membrane the flux declined by 100% for dead-end and 95% for cross-flow. While the corresponding numbers for the Ceramesh membrane were 84% and 66%.

2.3 Membrane fouling and polarisation phenomena

2.3.1 Introduction

In a membrane filtration process, the convective flux through the membrane can be written as:

$$\text{Flux} = \frac{\text{Driving force}}{\text{Viscosity} \times \text{Resistance}} \tag{2.1}$$

As far as the pressure driven process is concerned, the equation becomes:

$$J = \frac{\Delta P}{\mu R_{tot}} \tag{2.2}$$

Where μ is the viscosity of the permeate fluid, and R_{tot} is the total resistance.

In the ideal case, as the R_{tot} should be the hydrodynamic resistance of membrane (R_m) itself, which is unchangeable during the separation as long as the membrane is not compressible, the permeate flux will be directly proportional to the driving force ΔP. However, in a realistic operation, a severe flux decline can be observed when the transmembrane pressure is kept constant. This phenomenon can mainly result from two factors. One is concentration polarisation, and the other is fouling of membrane. Figure 2.12 shows the influence of concentration polarisation and fouling on flux decline.

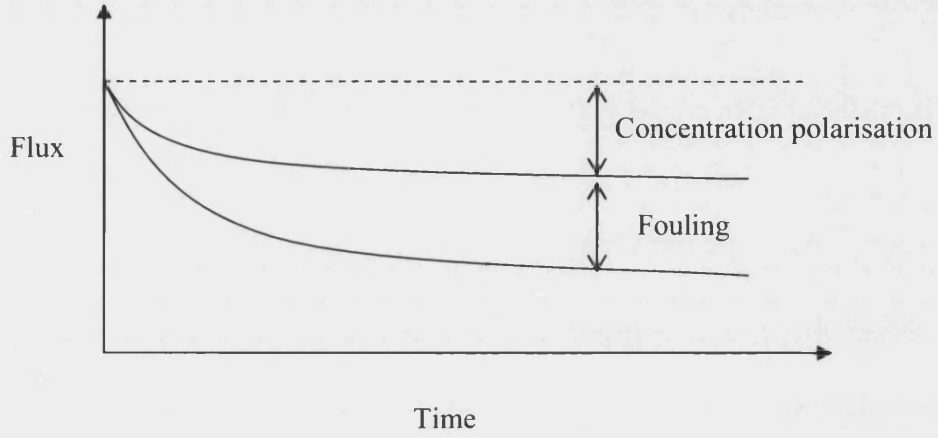

Figure 2.12 Influence of concentration polarization and fouling on flux decline

2.3.2 Concentration polarisation

Concentration polarisation is an inevitable phenomenon caused by the accumulation of the retained solute near the membrane-solution interface. Because of this accumulation at the membrane surface, the local concentration at the membrane surface increases gradually, and reaches a maximum value after a certain period of time. However, such a concentration build-up will also generate a diffusive flow back to the bulk of the feed. Finally, a steady state of transport will be arrived. This is shown in Figure 2.13.

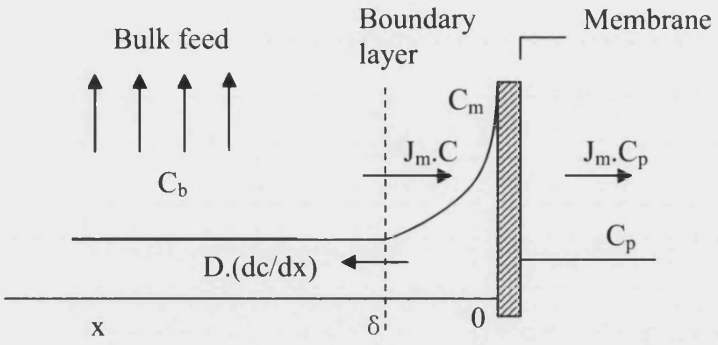

Figure 2.13 Concentration profile under steady-state conditions during concentration polarisation

The presence of concentration polarisation leads to the reduction of permeate flux. However, this decline resulted from concentration polarisation is reversible, which is different from that induced by fouling. Miller *et al.* (1993) reported that concentration polarisation can be reduced by increased shear rate.

To certify the presence of concentration polarisation, the experiment can be stopped and restarted immediately during the operation of membrane fouling. The changes of the values of permeate fluxes can be recorded by the computer. If it is the concentration polarisation which plays a major role in the decline of permeate flux, an increase of permeate flux can be observed after restarting the filtration. However, if the flux remains the same or even reduces after restarting the filtration, it is fouling rather than concentration polarisation inducing the permeate flux decline.

Referring to the current studies, three models have been put forward to explain the flux phenomenon in the process of membrane ultrafiltration (Mulder, 1996).

2.3.2.1 Gel layer model

Concentration polarisation in ultrafiltration can be very severe due to the low macromolecules diffusivity and high retention. In these cases, the solute concentration may reach up to the gel concentration, at which a gel layer is formed. From then on, when pressure driven force grows up, no further increase of concentration can be found. Instead, the gel layer becomes thicker or more compact. This results in an increase in the hydrodynamic resistance, and thus a decrease in the permeate flux.

2.3.2.2 Osmotic pressure model

Osmotic pressure model is developed according to the consideration of the osmotic pressure generated by the retained macromolecules. Generally, the main contribution to the osmotic pressure of a solution arises from the low molecular weight solutions. However, when operating with high flux values, high rejection and low mass transfer, the concentration of solute at the membrane surface can become very high, and hence the osmotic pressure can not be neglected. The flux equation becomes:

$$J = \frac{\Delta P - \Delta \pi}{\mu R_m} \tag{2.3}$$

Where $\Delta\pi$ is the osmotic pressure difference across the membrane. The decrease of the driven force (Δ P-$\Delta\pi$) is therefore the reason for the decline in the flux.

2.3.2.3 Boundary layer resistance model

During the concentration polarisation, the formation of a boundary layer with higher solute concentration exerts a hydrodynamic resistance on the permeating solvent molecules. Thus, the resistance becomes the total of the membrane resistance (R_m) and the boundary layer resistance (R_{bl}). The flux equation can be described as:

$$J = \frac{\Delta P}{\mu(R_m + R_{bl})} \tag{2.4}$$

2.3.3 Membrane fouling

In addition to the reversible concentration polarisation, membrane fouling is another major reason for the continuous decline of permeate flux. The phenomenon of fouling is very common, especially in pressure-driven process, such as microfiltration and ultrafiltration.

According to the categories of fouling materials, there are four types of membrane fouling, namely inorganic fouling, particulate fouling, microbiological fouling and organic fouling. It should be noticed that particulate fouling here stands for the fouling

caused by biologically inert particles and inorganic colloids in order to distinguish from organic fouling (Goosen *et al.*, 2004; Liu *et al.*)

Inorganic precipitate such as metal hydroxide can accumulate scale on membrane surface or within pore structure so as to induce membrane fouling. This kind of fouling was reported to be profound in reverse osmosis (RO) and nanofiltration (NF), while less important in microfiltration (MF) and ultrafiltration (UF) (Liu *et al.*).

The accumulation of particles on membrane surface will lead to flux decline during filtration process. However, this phenomenon is generally reversible by hydraulic cleaning such as backwashing or air scrubbing (Liu *et al.*).

Microbial fouling is considered to be mainly associated with bacterial adhesion and the formation of biofilm. Apart from the quality of feed solution itself, membrane materials also play an important role in microbial fouling potential due to different affinity towards bacterial. It is reported that the biological affinity of polyetherurea is significantly lower than those of polyamide, PSF and PES (Goosen *et al.*, 2004).

Organic fouling is an important issue as most of the feed solutions processed in industrial membrane filtration are abundant in organic matters. Thearubigins might contain substances relative to humic acid, which is a mixture of complex molecules possessing polymeric phenolic structures. It had great tendency towards membrane fouling. Being able to bind to the multivalent ions, humic acid could produce a gel-like layer of foulant on membrane surface. Its fouling potential was considered to relate to the binding capability. As to protein, for example BSA, a similar fouling process was observed during microfiltration. Proteins firstly aggregate on the membrane surface, then the native protein will attach to the existing ones by intermolecular linkages (Goosen *et al.*, 2004).

To better understand the flux behavior, several fouling mechanisms have to be observed (Bowen *et al.*, 1995; Suki *et al.*, 1984; De Barros *et al.*, 2003)

2.3.3.1 Complete blocking (pore-blocking)

In this mechanism, particulates of sizes similar to or larger than that of membrane pores may well block the pore completely. Therefore, no further material can pass through the pore any more.

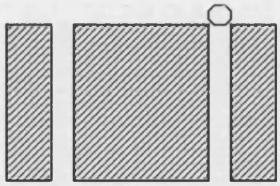

Figure 2.14 Schematic graph of complete blocking (After Bowen *et al.*, 1995 and De Barros *et al.*, 2003)

2.3.3.2 Standard Blocking

The standard blocking mechanism is based on the direct absorption of particles on the internal surface of membrane pores. This leads to the reduction of pore volume, and eventually the block of membrane pores.

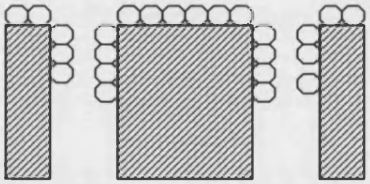

Figure 2.15 Schematic graph of standard blocking (After Bowen *et al.*, 1995 and De Barros *et al.*, 2003)

2.3.3.3 Intermediate blocking

This mechanism is a transition between complete blocking and cake filtration. In this case, any particles reaching the membrane surface are considered to be able to join to those already blocking pores. As a result, the membrane area will be block off and the permeate flux will decrease.

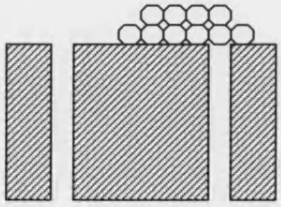

Figure 2.16 Schematic graph of intermediate blocking (After Bowen *et al.*, 1995 and De Barros *et al.*, 2003)

2.3.3.4 Cake formation

With the accumulation and agglomeration of particles absorbed onto membrane surface, a layer of cake filter is formed on the top of membrane. Although the quality of filtration may be improved because of this "secondary membrane", the permeability of membrane is definitely decreased.

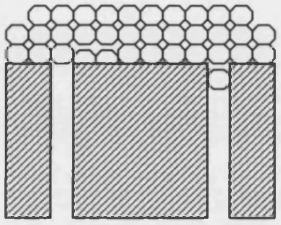

Figure 2.17 Schematic graph of cake formation (After Bowen *et al.*, 1995 and De Barros *et al.*, 2003)

Hermia (1982) has suggested mathematic equations for these four fouling mechanisms in constant pressure dead-end filtration based on the blocking filtration laws. The characteristic form is

$$\frac{d^2t}{dV^2} = K\left(\frac{dt}{dV}\right)^n \quad (2.5)$$

where t is filtration time, V is the filtrate volume. k and n are constants varying with different fouling mechanisms as shown as follows:

Complete blocking: $K_b = u_0\sigma$; n = 2

Standard blocking: $K_s' = \frac{2c}{LA_0}Q_0^{1/2}$; n = 1.5

Intermediate blocking: $K_i = \frac{\sigma}{A_0}$; n = 1

Cake formation: $K_c = \frac{\alpha \rho s}{A R_m Q_0 (1 - ms)}$; n = 0

α is the cake specific resistance (m kg^{-1}). ρ is filtrate density (kg m^{-3}). σ is the blocked area per unit filtrate volume (m^{-1}). A_0 is the initial active filter membrane surface area (m^2). c is the volume of solid particles retained per unit filtrate volume. L is the membrane thickness (m). m is the mass ratio of wet to dry cake. Q_0 is the initial flow rate ($m^3 s^{-1}$). R_m is membrane resistance (m^{-1}). s is the mass fraction of solids in slurry. u_0 is the initial filtrate linear velocity (ms^{-1}).

As the power " n " is a constant only depending on the type of fouling, it could be possible to determine the fouling mechanism by fitting the plot of $\frac{d^2t}{dV^2}$ against $\frac{dt}{dV}$ with mathematic equation. The power parameter obtained from the equation could indicate the possible fouling mechanisms. However, the fitting of the filtration data needs to be carried out with care.

2.3.4 The influence of fouling conditions upon permeate flux

2.3.4.1 Influence of fouling temperature

Temperature has effects on the mass transfer coefficient value as well as the viscosity of solution. With the increase of temperature, the diffusivity of the feed solution will increase, and the viscosity will decrease, all of which are beneficial to the permeate flux (Marshall *et al.*, 1993).

2.3.4.2 Influence of Transmembrane Pressure during fouling

As the driven force of membrane filtration, the influence of transmembrane pressure has been observed by many researchers. Jonsson and Tragardh (1990) reported that as the operating pressure is increased, an initial linear increase of permeate flux can be found. However, after a certain period of time, the permeate flux will level off at a higher pressure. This can be explained by the principle of cake formation mentioned above.

2.3.4.3 Influence of cross flow velocity

During the process of membrane ultrafiltration, cross flow is effective in reducing concentration polarisation at membrane surface. Generally, turbulent flow is used in industry as the total quantity of deposits and their stability within the stagnant boundary layer of the fluid are reported to be dependent on the cross flow velocity and fluid turbulence patterns (Gan and Allen, 1999).

2.3.4.4 Influence of foulant concentration

The composition of the foulant is an important factor in determing the type, as well as the extent of fouling. As a general trend, the flux declines as the bulk concentration is increased. It has been concluded by Marshall *et al.* (1993) that for surface fouling, an increase of foulant concentration has a great effect upon the amount of reversible fouling rather than irreversible fouling. Whereas, when in-pore fouling is the more dominant mechanism of membrane fouling, an increase in fouling concentration will speed up the rate of fouling.

2.3.4.5 Influence of pH

The pH value of the feed solution could have great impact on membrane permeation rate when some bio-macromolecules such as proteins are involved in the filtration. The overall charges of proteins are directly related to the pH value of the surroundings. When a pH is below the protein's isoelectric point, the protein will carry a net positive charge. While at pH above pI, it will be negatively charged. The different surface charge of proteins will influence the transmission behavior due to the interactions between the molecules and membrane. Burns and Zydney (1999) reported that a maximum protein transmission through UF membranes was observed at the protein isoelectric point for most cases they studied. A second maximum in protein transmission was also obtained at a certain pH between the isoelectric points of the protein and membrane. This is presumably due to an attractive electrostatic interactions between protein and membrane when they carried opposite charges at a large difference. Bowen and Gan (1991) have mentioned that pH 7 was preferable in terms of flux decline during the microfiltration of Bovine Serum Albumin (BSA).

2.4 Membrane cleaning

2.4.1 Introduction

Despite the success of the applications of membrane ultrafiltration in chemical engineering, fouling has been one of the major restrictions in the wider application of the technology. From either economic or product's quality perspective, it is necessary to maintain the membrane's permeability, as well as the selectivity. Therefore, it is crucial to clean the membranes without damage as much as possible. Trägårdh (1989) has given the definition of membrane cleaning as follows:

Membrane cleaning is " A process where the membrane is relieved of materials which are not an integral part of the membrane".

2.4.2 Classification

According to the energies used for membrane cleaning, possible methods of cleaning available can be divided into four types, which are hydraulic cleaning, mechanical cleaning, chemical cleaning and electric cleaning (Mulder, 1996).

2.4.2.1 Hydraulic cleaning

Hydraulic cleaning methods are operated on the basis of turbulence or reversal of transmembrane pressure. They contain back-flushing, cross-flushing, membrane rotation and secondary vortex flows. Particularly, back flushing is one of the most effective ones. However, it depends upon the module design, and it can only be applicable to microfiltration and open ultrafiltration membranes.

2.4.2.2 Mechanical cleaning

Mechanical cleaning is a method involving the usage of abrasive materials to scour a fouled membrane surface. Because of the requirement of high mechanical strength and the accessibility of membrane surface, mechanical cleaning can only be applied in tubular system using oversized sponge balls.

2.4.2.3 Chemical cleaning

Chemical cleaning relies upon the usage of chemicals either separately or in combination to clean the fouled membranes. Compared with other three types of cleaning, it is the most important method and probably the most widely used. (Scott 1995; Sandu *et al.*, 1985)

2.4.2.4 Electric cleaning

The principle of electric cleaning is that charged particles or molecules will migrate in a certain direction with the application of electric field across the membrane. This method is applicable during the process, which means continuous membrane filtration process is possible to realize. However, membranes must be sufficiently conductive, and special module designs are always required.

In terms of four kinds of fouling mentioned in the section of membrane fouling above, chemical cleaning is an effective solution for all types of fouling. It is also the only feasible control for majority of ultrafiltration systems (Bartlett *et al.*, 1995)

2.4.3 Chemical Cleaning

For the purpose of this project, much concern has been given to chemical cleaning in the following paragraphs.

Nowadays, cleaning in-place (CIP) is considered to be the major performance of chemical cleaning. It is operated by filling the retentate with a cleaning solution from a separate tank (Romney, 1990). According to NDA chemical safety code (1985), the definition of CIP is "The cleaning of complete items of plant or pipeline circuits without dismantling or opening of the equipment and with little or no manual involvement on the part of the operator."

Although the understanding of cleaning mechanisms is not as great as that for fouling mechanisms, several models have been developed. Gallott-Lavalle and Lalande (1985) have developed a model for the cleaning of proteins from stainless steel by sodium hydroxide. It is assumed that a reaction took place between the deposit and the hydroxyl ions of sodium hydroxide to reach an intermediate state before the removal. This model

was further developed by Bird and Fryer (1991) according to their study on stainless steel surfaces fouled by whey proteins, and subsequently cleaned with sodium hydroxide. Contacting with cleaning solution, the protein deposit was observed to swell and become translucent first. Then the deposit surface was broken down into discrete aggregates by the shear forces of cleaning flow. Finally, aggregates were removed from the surface. Figure 2.14 gives the schematic diagram of cleaning mechanism described above. Although this model was built based on the chemical cleaning of hard surface without porous structure, the interaction between NaOH and proteinaceous deposits remaining on the surface might be similar to that during membrane cleaning.

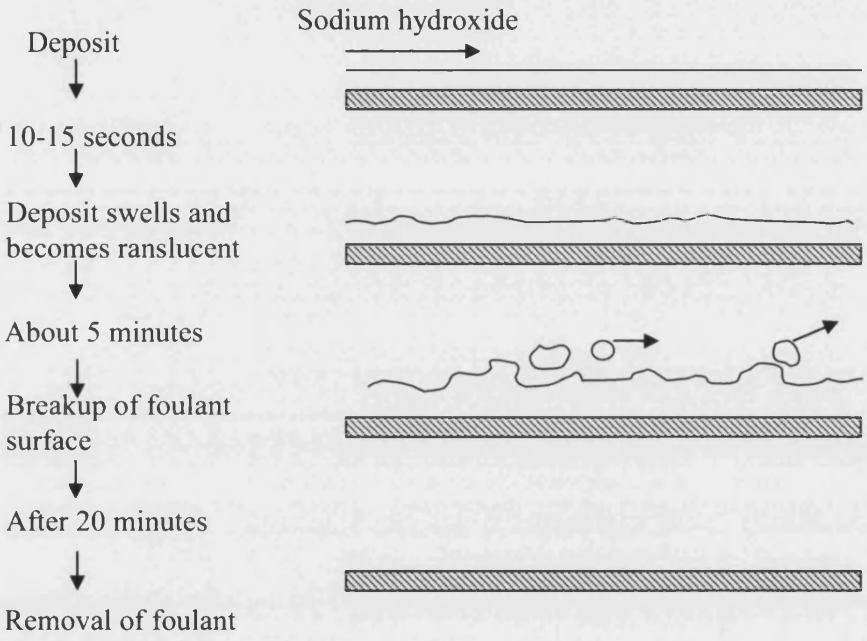

Figure 2.18 Schematic diagram of cleaning mechanism of sodium hydroxide

2.4.3.1 Cleaning agents

In terms of the different characterizations of membranes and foulant, as well as the standard of cleaning, it is crucial to choose appropriate cleaning agents. There are a wide range of cleaner products in use today. However, they are formulated from several major raw materials, such as alkali, acid, chelating agents, surfactants and enzyme cleaner.

Alkali

Alkali is generally used to remove foulants based on protein or fats by regarding its functions of either hydrolysis or solubilization. It can also increase the negative charge of humic substances, which is helpful to remove them from membrane (Nyström *et al.*, 1996). According to the desired degrees of alkalinity, many kinds of inorganic alkalis can be chosen. The most widely used are sodium hydroxide, sodium orthosilicate, sodium metasilicate, trisodium phosphate, sodium carbonate and sodium hydrogen carbonate.

Sodium hydroxide is a cheap and effective alkaline cleaner. It has a good ability of saponificating fats and solubilising proteins (Wright 1990). Therefore, it is considered to be one of the most common used alkali materials formulating many commercial products.

Sodium orthosilicate, sodium metasilicate and trisodium phosplate have better powers of removing heavy soil.

Acids

Acids are effective cleaners for the removal of mineral deposits. Both inorganic and organic acids can be applied in membrane cleaning. In particular, two types of inorganic acids, namely nitric acid and phosphoric acid, are more commonly used (Trägårdh, 1989). Citric acid is also used in certain food industry applications.

Chelating Agents

Chelating agents (or sequestering agents) are contained in detergents to prevent inorganic scale and redeposition. They are water soluble because of the presence of metal cations, such as Ca^{2+} and Mg^{2+}. Typical examples of these materials include sodium polyphosphates; ethylene diamine tetraacetic acid (EDTA) and its salts; and gluconic acid and its salts. EDTA was found to be effective in the removal of divalent cations, which consequently improved the membrane cleaning (Hong and Elimelech, 1997).

Surfactants

Surfactants have the functions of wetting, emulsifying, dispersing and cleaning. In some membrane cleaning cases, the contact angle between foultants and cleaning solution can be increased by resorting to the addition of some surface active agents. They can penetrate into the soil particle that is an aggregate of small particles. Subsequently, the large particle is disintegrated into small ones, which are easier to disperse.

Surfactants are generally classified as anionic, cationic, amphoteric or nonionic, depending on how they disassociate in aqueous solutions (Wright, 1990).

Enzyme cleaner

Enzymatic cleaners are of great interest due to their substrate specificity and environmental / membrane friendliness. Applying enzymatic agents can not only improve the cleaning efficiency, but also minimize membrane damage and energy cost as enzyme works under mild conditions (Maartens, *et al.*, 1996). Several studies have been reported on enzymatic cleaning of UF membranes fouled by proteinous solutions. The proteolytic enzymes provided high cleaning efficiencies in short operating times (20 mins) during cleaning of inorganic membranes fouled by whey protein solutions (Argüello, *et al.*, 2003). Commercially available lipases and proteases were also found to be effective in cleaning polysulphone membranes fouled by abattoir effluent (Allie, *et al.*, 2003).

2.4.3.2 Cleaning process

There are usually a series of discrete cycles in cleaning processes. Generally, one cleaning process begins with a pre-rinse cycle with the aim to remove any loosely adherent residuals from the plant surface, followed by a detergent cycle where the chemical cleaning takes place, ended by a final rinse to ensure there are not any traces of detergents remaining on the membrane.

Industry uses either two-stage cleaning, which is based on the usage of acid and alkali in varying order, or single stage cleaning by means of only one type of cleaning agents, for example, low concentration sodium hydroxide solution. The sequence of cleaning in

two-stage cleaning depends on the nature of foultants (Romney, 1990). In practice, single stage cleaning is more realistic due to its relatively simple process, which offers the chance to reduce the down time and to lower the total cost of cleaning, including chemicals, waste water and labor (Bird and Fryer, 1991).

2.4.3.3 The influence of cleaning conditions

Cleaning concentration

During cleaning operations, both equilibrium and the rate of reactions between cleaning chemicals and fouling materials will be influenced by the concentration of cleaning reagents. The concentration of cleaning chemicals also exerts great impact on the concentration profile of cleaning chemicals within the fouling layer. As a result, a proper concentration of cleaning reagent must be applied with the aim of maintaining the reasonable reaction rate, as well as to overcome mass transfer barrier imposed by the fouling layer.

According to the possible mechanism described by Bird and Fryer (1991) when investigating the removal of whey protein, the cleaning fluid, namely sodium hydroxide, will force a swelling in the foulants, which will lead to a higher voidage in the fouling cake owing to gel swelling. The greatest voidage was found to be associated with the optimum concentration of the cleaning agent. Bird and Bartlett (1995, 2002) found similar optima in the cleaning of whey protein fouled membranes. They identified optimal concentrations of sodium hydroxide of 0.5 wt% and 0.3-0.5 wt% respectively for the removal of whole milk soils and whey proteins from a 0.2 μm sintered stainless flat-sheet membrane.

Vaisanen *et al.,* (2002) did not develop an optimum cleaning concentration during their research of the effect of cleaning agent composition upon ultrafiltration membranes fouled with whey proteins. However, they found that sodium hydroxide with a very high concentration might have an adverse effect on the cleaning efficiency due to the sensitivity of membranes towards alkalinity. In addition, Gan *et al.* (1999) showed that excessive concentrations of *Ultrasil 11*, which is a complex detergent consisting of sodium hydroxide and surfactants, are detrimental to the cleaning process.

Cleaning temperature

Temperature used during cleaning can not only affect the equilibrium and kinetics of the chemical reaction, but also change the solubility of fouling material and / or reaction products. Therefore, cleaning temperature should be taken into account to be an important factor affecting cleaning efficiency.

Bartlett *et al.,* (1995) studied the removal of whey protein deposits from micro and ultra membranes. They identified an optimum temperature of 50 °C at which a maximum of the percentage flux recovery was obtained. The increase of cleaning temperature beginning from a relatively low level will definitely speed up reaction rate, increase the Reynolds number, and decrease viscosity, all of which will result in increases in the kinetics of deposit breakdown chemistry, as well as dissolution. However, the deposit was observed to be resistant to sodium hydroxide breakdown when increasing the temperature after the optimum value. This was possibly due to the inverse solubility that calcium phosphate displays with increasing temperature. This was also demonstrated by the study from Kim *et al.,* (1993) when investigating the cleaning of ultrafiltration membranes fouled by protein.

Nevertheless, the optimal temperature theory does not apply to every case. Nyström and Zhu (1997) observed a direct proportion between the cleaning temperatures and flux recoveries. The highest temperature 80 °C was used. However, this operation at such a high temperature might not be realistic in industry if the membrane can not withstand high temperature.

Cleaning transmembrane pressure

Transmembrane pressure is very important in both the fouling and cleaning cycles. The pressure during the fouling must be high enough so that the feed solution can pass through the membrane. Whereas, the pressure used during cleaning should be lower than that of the fouling so as to prevent from driving the particulates further into the membrane pores rather than allowing the cake to expand and swell (Bird and Bartlett, 1995). The improvement of membrane cleaning performance was observed with the increase of transmembrane pressure during cleaning by Bowen *et al.* (1995). Bowen

showed that in his system, during cleaning the optimum operating pressure for microfiltration was between 1.5 and 2.0 bar.

Cross-flow velocity

The influence of cross-flow velocity upon membrane cleaning efficiency was considered to be negligible according to the conflicting results obtained in several studies by Kim *et al.* (1993), Bird and Bartlett (1995). However, it is recommended to use a high cross flow rate to ensure good mechanical cleaning and to promote high rates of mass transfer.

2.4.4 Ultrasonic cleaning

In recent years, ultrasonic technique has been discovered to be a potential method in the field of membrane cleaning. Duriyabunleng *et al.,* (2001) found that there was a retrieval of membrane permeability after using ultrasonic cleaning and the filtration performance of microfiltration membranes was improved to some extent. Experiments carried out by Chai *et al.* (1998) also obtained similar results.

Ultrasound affects membrane cleaning in various ways. Major mechanisms are considered to be increased turbulence and acoustic cavitation. Turbulence promotes the dispersion of particles while acoustic cavitation can lead to the suspension of particles in the liquid medium. Therefore, ultrasound can assist the cleaning of membranes and is helpful to restore the membranes to their initial permeability.

However, Masselin *et al.* (2001) described the detrimental effects of ultrasonic cleaning on polymeric materials although it has been proven that membranes will stand up to ultrasonic irradiation in a chemical bath. The damage probably arose from the great mechanical stresses at the extremities. As a result, ultrasonic cleaning techniques should be used with great care to avoid damage to the membrane.

2.5 Major techniques for membrane characterization

The major techniques used for membrane characterization in this study are Scanning Electron Microscope (SEM), Transmission Electron Microscope (TEM), Attenuated Total Reflection – Fourier Transform Infrared Spectroscopy (ATF-FTIR), contact angle and zeta-potential measurement. The detailed information of these techniques is given in the Appendix 9.1-9.5.

Chapter 3 The influence of fouling and cleaning conditions upon the performance of ultrafilters for the processing of black tea liquor

3.1 Introduction

As membrane ultrafiltration provides possibility to remove tea haze, it can be applied in the production of cold tea. Therefore, the influence of fouling and cleaning regimes upon the quality of ultrafiltered black tea is of great interest. This part of study is therefore undertaken to determine the effects of fouling and cleaning by using polysulphone (PSF) and fluoropolymer (FS50PP) ultrafiltration membranes, cleaned with two different cleaning reagents, sodium hydroxide and *P3 Ultrasil 11*. Both PSF and FS membranes have relatively higher resistance to solvents, corrosive chemicals, temperature and pressure drop. They are therefore commonly used in industry. The membranes after conditioning, fouling and cleaning were examined using TEM.

3.2 Experimental

3.2.1 Materials and Chemicals

Membranes:

Three different UF membranes used in this part of experiments are described as follows:

1) Polysulphone (PSF GR61PP) ultrafiltration flatsheet membrane, MWCO 20 kD from *Danish Separation Systems (DSS).*

2) Polysulphone (PSF) ultrafiltration flatsheet membrane, MWCO 30kD from *Osmonics.*

3) Fluoropolymer (FS50PP) ultrafiltration flatsheet membrane, MWCO 30kD from *DSS.*

The recommended operation limits for these membranes are shown in Table 3.1.

Table 3.1 The recommended conditions of membranes

Polysulphone membranes	Production		Cleaning	
	pH range	1 - 13	pH range	1 - 13
	Pressure, bar	1 - 10	Pressure, bar	1 - 5
	Temperature, °C	0 - 75	Temperature, °C	0 - 75
Fluoropolymer membranes	pH range	1 - 11	pH range	1 - 11.5
	Pressure, bar	1 - 10	Pressure, bar	1 - 5
	Temperature, °C	0 - 60	Temperature, °C	0 - 65

Foulants:

The black tea has been the fouling liquor used all throughout this investigation. The tea solutions were prepared by dissolving *Lipton*'s spray dried instant tea powder in Reverse Osmosis water at temperature 50 °C. The tea powder is produced in Sri Lanka, manufactured and shipped by *Unilever Bestfoods*, UK.

Cleaning agents:

As the foulant is likely to contain protein deposition, two alkali based cleaning agents, namely Sodium hydroxide and *P3 Ultrasil 11 (Henkel Ecolab)*, were chosen in the experiments carried out in the initial stage of this investigation.

P3 Ultrasil 11 is a powder consisting of sodium hydroxide (>40 wt%), EDTA (>30 wt%), anionic surfactants (5 wt%), and non-ionic surfactants (5 wt%) (Shorrock and Bird, 1998).

3.2.2 The construction of membrane modules

Membrane fouling and cleaning experiments began with the ultrafiltration of black tea solutions on polysulphone membrane (PSF GR61PP) in a rig of small scale. A plastic DSS module consisting of four flat sheet membrane holders was used in this small rig. The larger pilot scale rig with a capacity of 50 litres was used to simulate industrial conditions when membrane fouling and cleaning were carried out on the other two types

of membranes afterwards. A stainless steel membrane module holding one flat sheet membrane was combined with this system so as to withstand the high pressure and high temperature, which are normally required under industrial conditions.

3.2.2.1 Single-flat sheet membrane module

Figure 3.1 shows the side elevation of the assembling parts of the single-flat sheet membrane module. This module consists of a top plate, a replaceable Perspex channel mould, a backstop and a bottom plate. A flat sheet membrane of 10 cm x 20 cm can be housed between these two plates.

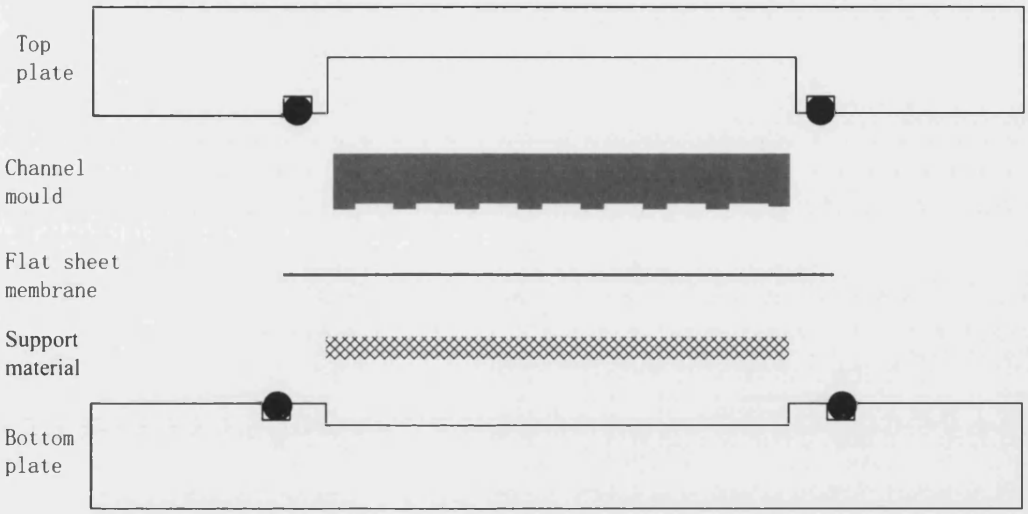

Figure 3.1 The composition of the single flat-sheet membrane module

The replaceable channel mould is designed for the control of cross flow velocity upon the membrane surface. Figure 3.2 illustrates the geometry of the channels. The mould provides seven channels of 190 mm length, 7 mm width, and 1 mm height. Therefore, the filtration area, namely the total areas of seven channels, equals to 93.1 cm^2. The total cross section area of the channels is 0.49 cm^2.

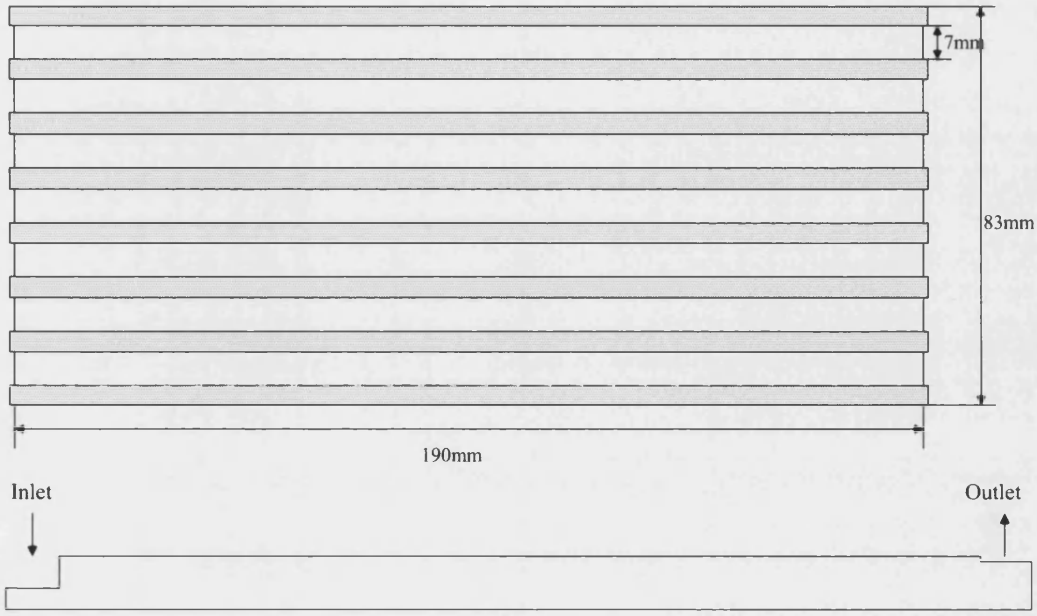

Figure 3.2 The schematic graph of perspex channel mould

A polypropylene backstop with the pores of 1 μm allows for the support of the membrane. The sealing of the module is resorted to a double O-ring system, which is circled in the Figure 3.3. Figure 3.4 and Figure 3.5 demonstrated the graphs of the top and bottom stainless steel plates of the single flatsheet module respectively.

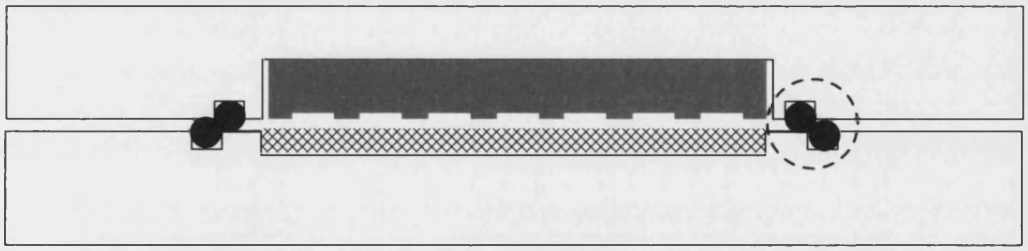

Figure 3.3 The side elevation of the single flatsheet membrane module

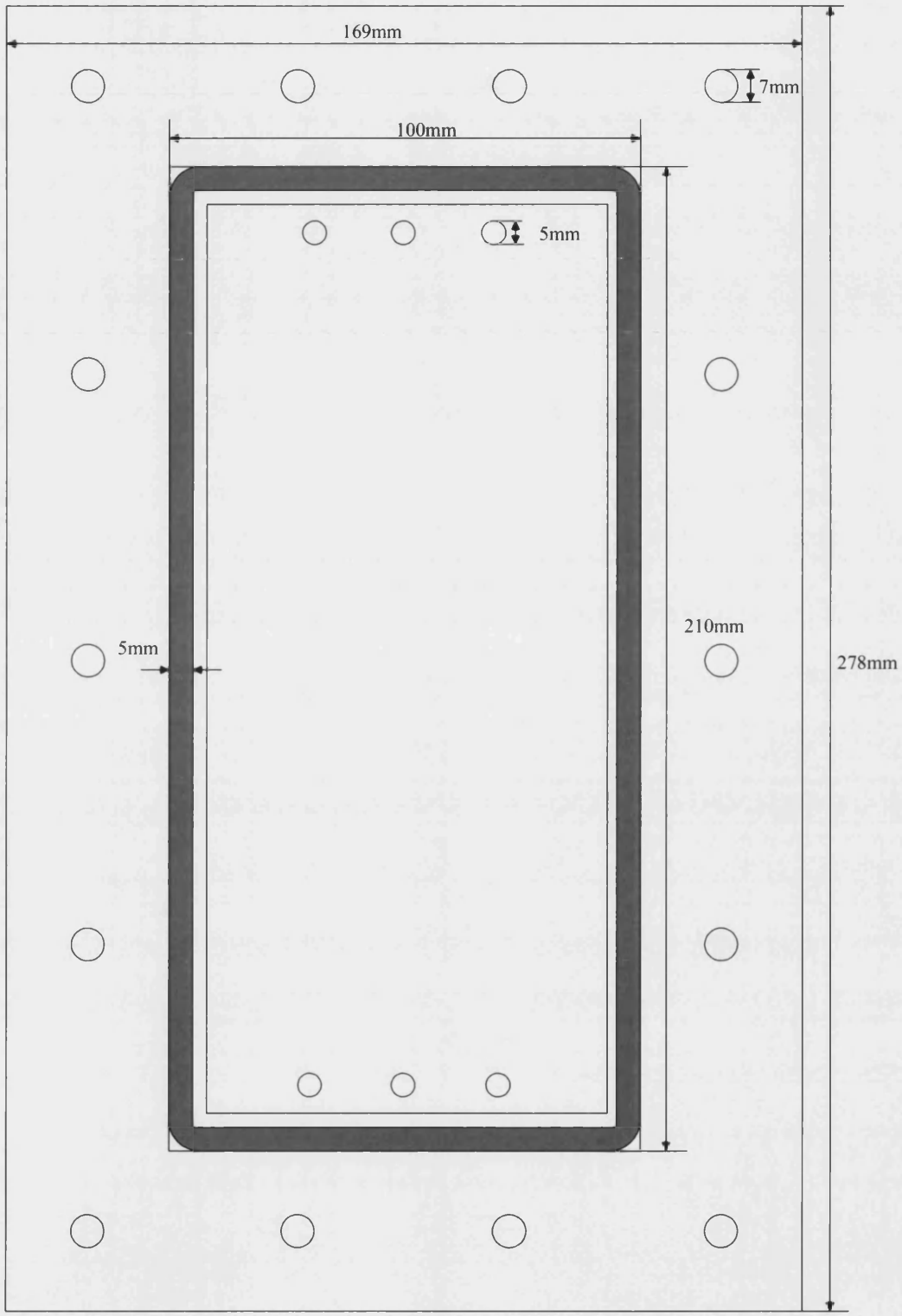

Figure 3.4 The graph of top stainless steel plate of single flatsheet module (shown at actual size)

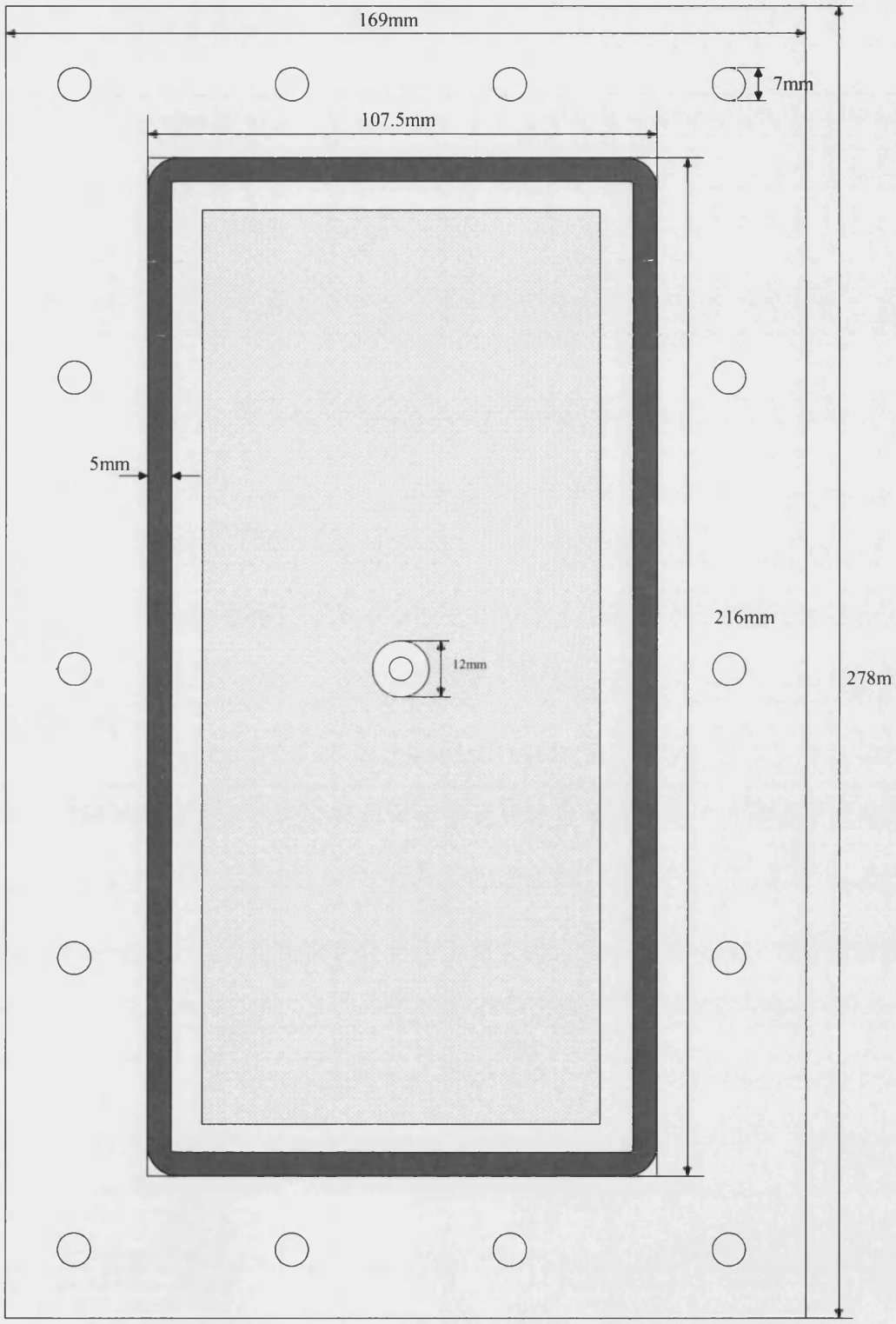

Figure 3.5 The graph of bottom stainless steel plate of single flatsheet module (shown at actual size)

3.2.2.2 Four-flat sheet membrane module (DSS)

The DSS membrane module contains four pieces of transparent plastic plate. Each plate can house a piece of flat-sheet membrane. In terms of the convenience of filtration area calculation, four channels of irregular shapes are considered as rectangles. Therefore, every plate provides a filtration area of 97 cm^2.

Figure 3.6 shows a schematic graph of a plate, and illustrates the direction of flow inside a membrane cell. When the filtration starts, the stream of solution enters the first plate of the module from the inlet, and flows into the membrane cell via four small holes at one end of the channels. Then the solution flows along the channels where it is separated into the permeate and retentate by membrane ultrafiltration. The permeate is collected from a tube in the middle of the plate, while the retentate goes into the outlet which leads to the inlet of the next plate.

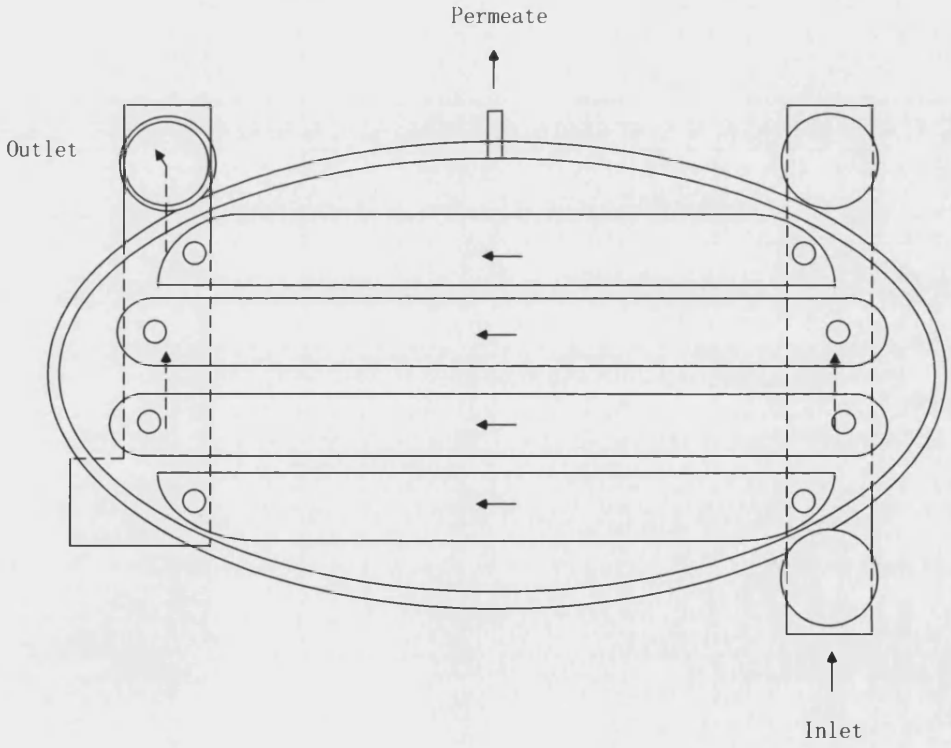

Figure 3.6 The top elevation of DSS membrane module plate

3.2.3 Schematic Diagram of experimental apparatus

3.2.3.1 The flowsheet of small rig with DSS module

As mentioned above, a small rig has been used in the initial membrane fouling and cleaning experiments. The schematic diagram of this rig is presented in Figure 3.7.

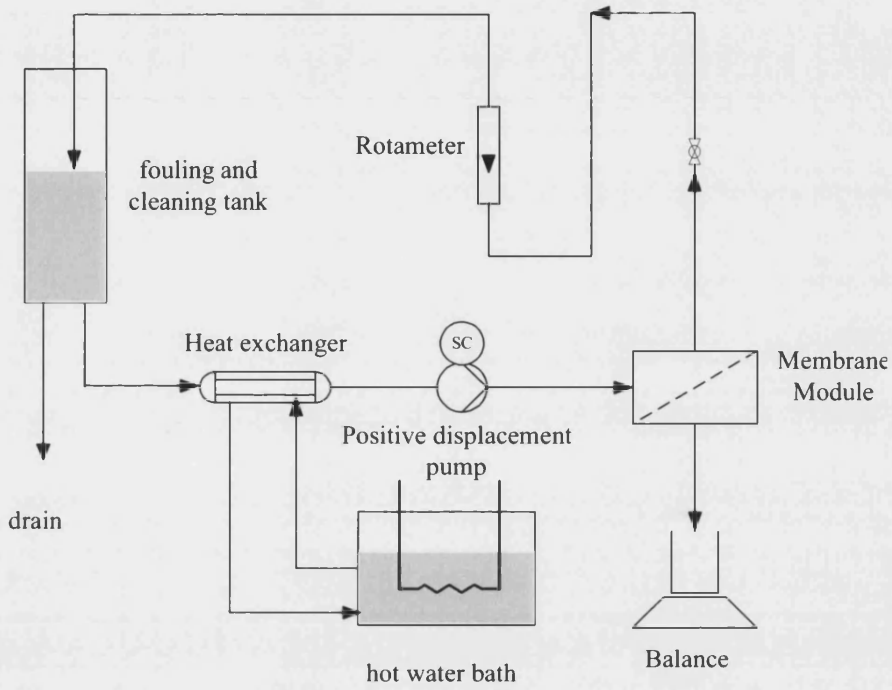

Figure 3.7 Schematic diagram of the small fouling and cleaning rig

A 10 L perspex storage tank is used in this system for the feeding of the pump and then the rest of the system. The pump is a positive displacement pump. This system is capable of delivering a flow of approximate 4 L min^{-1} against a pressure of 4 bar.

3.2.3.2 The flowsheet of the larger pilot scale rig with single-flat sheet membrane module

Figure 3.8 shows the schematic diagram of the larger pilot scale rig. Three calibrated polyethylene holding tanks of small sizes (50 liters) are used to contain the fouling solution, cleaning reagent and Reversed Osmosis water respectively. The desired liquid is pumped by a six stage centrifugal pump from Lowara (Type: SV2-11T15M), which can achieve the flow rate up to 16 L min^{-1}. The pipes and valves between tanks and

pump are made of 1'' (25. 4 mm) UPVC from Durapipe^{TM}. All the pipes and hoses after the pump are constructed of 0.5 (12, 27mm) O.D. 316 stainless steel. The connectors and valves (Swagelok Ltd) are of 316 stainless steel. The desired temperature of the solution is achieved from the heat transfer of a counter-current of hot oil. The heat exchanger used in these experiments is a plate heat exchanger, providing the exchange area of 0.3 m^2. The heat-transfer oil is pumped from an external "Conair" oil heater.

After passing through the heat exchanger, the solution is divided into two parts. According to the volumetric flow rate required, one part of the solution goes through the main pipe, while the surplus of flow goes back to the tank via a flexible hose. The flow rate can be controlled by the needle valves, and be shown on the magnetic flow meter. On the pipes from the Magflo meter to the membrane module, a two way ball valve is fitted to supply the option of recycling without passing the module during the heating process. The flow entering the module is separated by the membrane into permeate and retentate. The permeate is collected in the beaker, and is weighed by a balance, where the change of the weight is signaled to a computer. To maintain the feed concentration, the retentate is recycled to the feed tank directly. Whereas, the permeate is recycled back to the tank every several minutes. Two needle valves on the lines of retentate and the permeate are used to adjust the transmembrane pressure during the operation. The temperatures as well as the pressures are recorded by a computer. A software "GENIE, Application builder for data, Acquisition and Control, Version 3.0, ADVANTECH, Copyright 1993-95 American advantech corp" is used to translating the signal into data output.

To relieve the adverse influence of extra heat produced by the pump, a cooling system is included. A flexible cooling coil can be placed in the tank. The balance of the heat transfer can be obtained by the adjustment of the flowrate of the cold water.

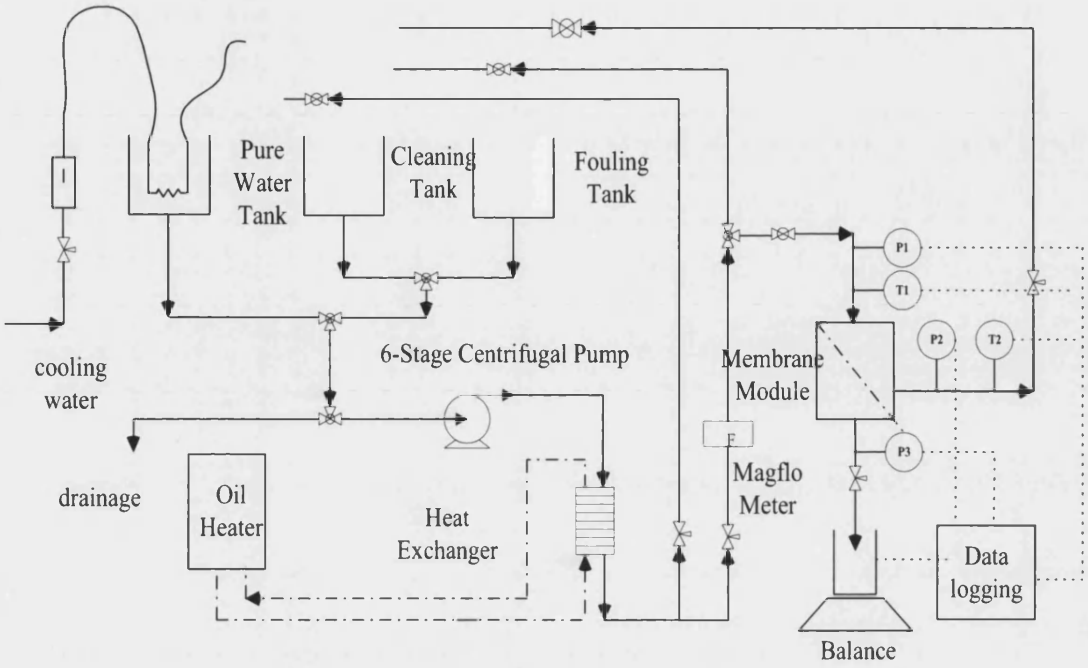

Figure 3.8 Schematic diagram of the fouling and cleaning rig

3.2.4 Experimental Methods

3.2.4.1 Pretreatment of membrane

Most commercial membranes are coated with a hydrophilic agent, such as glycerin in order to prevent it from drying out completely. According to the study of Weis (2004), it is necessary to remove the glycerin before investigating the performance of membrane fouling and cleaning. In his study, membranes were treated for 90 mins at 60 °C (polyethersulphone / polysulphone membranes) and 50 °C (regenerated cellulous membrane) with pure water. Surface analysis, namely FTIR and contact angle measurements were carried out to establish that this was an efficient protocol. This protocol was therefore used in the current system. The polysulphone membranes and the fluoropolymer membranes were rinsed with reverse osmosis water at 60 °C and 50 °C separately for 90 minutes by considering different temperature resistances of these two membranes.

3.2.4.2 Fouling and cleaning protocol

The short-term performance of three different kinds of membrane was investigated in this part of study. There are three major operations in each fouling and cleaning cycle, namely pure water flux measurement (mentioned as PWF in the following paragraphs), fouling and cleaning. The detail procedure is shown in Table 3.2.

Table 3.2 The procedures of a fouling and cleaning cycle

PWF1:	This measurement is to determine the permeate flux before fouling.
Fouling:	The prepared tea solution of a certain concentration is separated into retentate and permeate.
PWF2:	This measurement will determine the effect of fouling.
Rinsing:	The membrane is rinsed with RO water to remove loose deposits.
PWF3:	This measurement will determine the effect of rinsing.
Cleaning:	The membrane is cleaned with cleaning reagent.
Rinsing:	The membrane is rinsed again to ensure remaining cleaning reagent is flushed from the membrane and system.
PWF4:	This measurement will determine the effect of cleaning.

The pure water flux measurement is carried out by using reverse osmosis water at 1 bar, 22 °C, with a cross flow velocity (CFV) 0.58 m s^{-1} in the small rig, and 1 bar, 22 °C, and 4.86 m s^{-1} in the large rig for 5 minutes. All the pure water flux measurements were undertaken under these standard conditions unless stated otherwise.

The fouling conditions applied were decided by referring to the industrial conditions used during the manufacture of black iced tea. Fouling is operated at 3 bar, 50 °C, with a CFV of 0.58 m s^{-1} in the small rig and 4.86 m s^{-1} in the big rig using black tea solution of different concentrations.

Two cleaning reagents, namely sodium hydroxide and *P3 Ultrasil 11* were used in the cleaning procedure. The cleaning conditions were varied with different experiments.

The rinsing step was performed using RO water at 22 °C, with a CFV of 0.58 m s^{-1} in the small rig and 22 °C, 4.86 m s^{-1} in the large rig. The transmembrane pressure was less than 1.0 bar in both cases.

3.2.5 Method of analysis of fouling and cleaning performance

For the experiments mentioned above, the permeate flux is considered to be an important parameter to evaluate the performance of membrane fouling and cleaning. The changes in permeation during fouling and cleaning can be easily obtained by plotting the permeate fluxes of product solution and cleaning solution against time. In addition, the flux recovery is also very helpful to compare the extent of fouling and cleaning under different conditions.

The definition of flux recovery is described in e.q. 3.1 and e.q.3.2.

$$\text{Flux recovery (\%)} = \frac{\text{Pure water flux after fouling or after cleaning}}{\text{Pure water flux before fouling}} \times 100\% \qquad (3.1)$$

Resistance of membrane (R_m) is another effective parameter to analyse the experiment results. According to the equation:

$$J = \frac{\Delta P}{\mu R_{tot}} \qquad (3.2)$$

Permeate flux is proportional to the driving force (ΔP). The resistance towards convective flow through an original membrane should be the resistance of the membrane only. However, if fouling occurs, additional resistance will be added. By knowing the value of the permeate flux (J) and that of the driving force (ΔP), namely transmembrane pressure (TMP), the total resistance (R_{tot}) can be calculated easily.

3.2.6 Visualization of membrane fouling and cleaning by Transmission Electronic Microscope (TEM)

To investigate the differences between the membranes after conditioning, fouling, and cleaning processes, transmission electron microscope was used to characterise the cross-section structures of these membrane samples.

The TEM used was 1200EX TEM, which is fitted with a scanning transmission to provide high contrast imaging. The preparation of membrane samples for TEM was quite complicated and time consuming. Generally, it started with the embedding of sample in resin, followed by sectioning with glass knife on Sorvall ultra microtome, and finally imaging at 80 kV at appropriate magnifications using optimized microscope settings. The detail steps of operation are given in Appendix 9.6 (Reilly, 2004).

3.3 Results and discussion

3.3.1 Fouling and cleaning performance on Polysulphone (PSF GR61PP) membrane with MWCO 20 kD using *P3 Ultrasil 11* as cleaning reagent

3.3.1.1 The error analysis of DSS separation system

To ensure the reliability of the experimental results, it is very important to be aware of the repeatability and accuracy of the experimental rig. The errors of the experiments carried out on the small rig have been determined by multiple measurements of the pure water fluxes through the membranes after conditioning. The results shown in Figure 3.9 indicated that the error bar of the average values of triple measurements was approximately ± 3 %. Consequently, the estimate of global error is considered to be around ± 3 %, which is acceptable for the study of membrane fouling and cleaning.

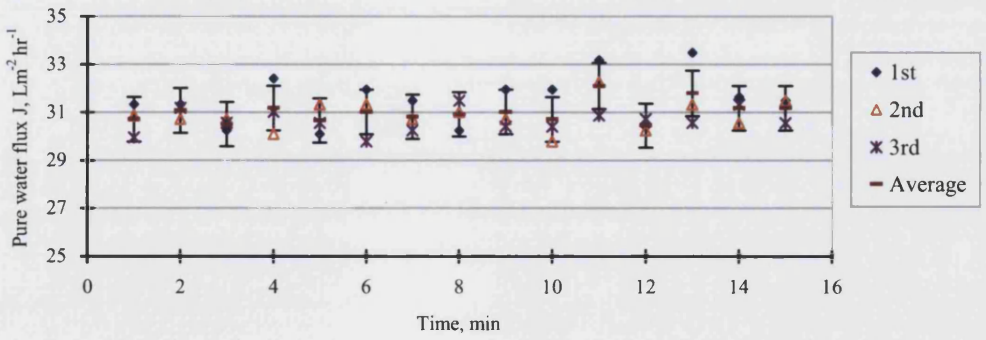

Figure 3.9 The error analysis of small rig. Pure water flux measurement conditions: RO water, Temperature 22 °C, CFV 0.214 m s^{-1}, TMP 1 bar.

3.3.1.2 The influence of conditioning upon the permeability of membrane

As mentioned above, most commercial membranes are normally coated with glycerine before drying. This hydrophilic agent covering on the membrane surface will probably have impact upon membrane ultrafiltration, and thus provide unreliable information about membrane fouling and cleaning behaviors. To avoid this problem, the pretreatment was carried out to remove glycerine by passing reverse osmosis water at 58 °C through the membrane with a transmembrane pressure 1.15 bar, and a cross flow velocity of 0.93 m s^{-1}. The pure water fluxes of membrane after different treatments were measured subsequently so as to indicate the effects of conditioning.

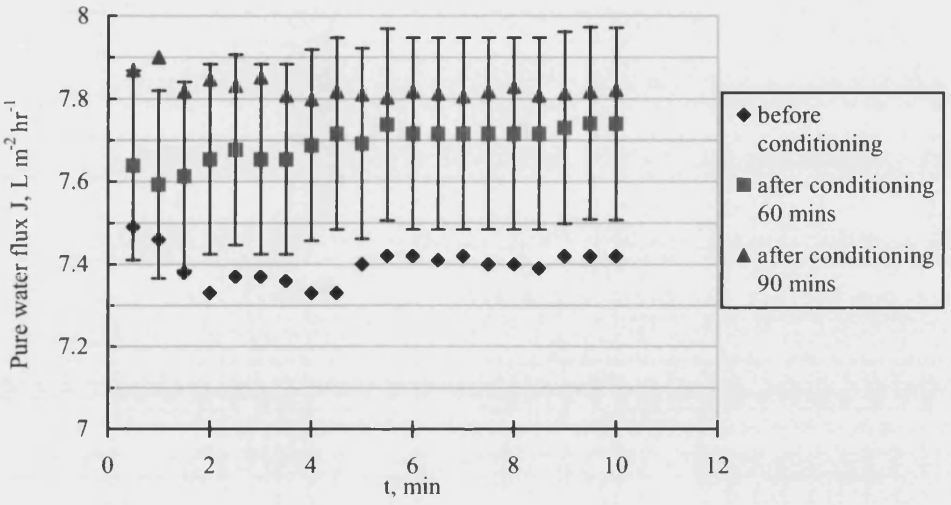

Figure 3.10 The influence of conditioning upon the pure water flux of membrane. Conditioning: RO water, 58 °C, 1.15 bar, CFV 0.926 m s^{-1}.

Table 3.3 Contact angles of unconditioned and conditioned PSF (GR61PP) membranes.

Membrane	Contact angle (°)
Unconditioned virgin PSF GR61PP	57.5 ± 3.2
Conditioned virgin PSF GR61PP	67.4 ± 4.0

As shown in Figure 3.10, there was an increase from approximately 7.4 LMH to 7.7 LMH in pure water flux after conditioning the membrane for 60 minutes. This indicates that the removal of glycerine will improve the pure water flux of membrane itself. The increase of pure water flux after conditioning for another 30 minutes was not significant, implying that the membrane surface should be clean of the preservatives

after conditioning for 60 minutes. To further confirm the effectiveness of conditioning, the contact angles of unconditioned and conditioned membrane were measured. From Table 3.3, the contact angle increased form 57.5 ± 3.2° to 67.4 ± 4.0° after conditioning. The higher hydrophilicity of an unconditioned membrane compared with the conditioned one is presumably due to the presence of glycerine which is highly hydrophilic with three hydroxyl groups. When this layer of glycerine is completely removed, the membrane becomes more hydrophobic, giving the confidence of the effectiveness of membrane conditioning.

3.3.1.3 The influence of the operating conditions upon the membrane ultrafiltration performance

Before any fouling and cleaning experiments can be carried out on the membranes, some preliminary tests by means of pure water flux measurement over a sixteen-minute period had been undertaken to attain a better understanding of the membranes, as well as the impact of operating conditions, such as pressure, temperature and cross flow velocity.

Transmembrane Pressure

As shown in Figure 3.11, the permeate flux of the reverse osmosis water increased with the increasing transmembrane pressure. This was expected since the permeate flux is proportional to the driving force across the membrane below the limiting flux value. Higher transmembrane pressure will force more water to permeate through the membrane in unit time. Moreover, an obvious jump observed between 2 and 3 bar implied that a fouling transmembrane pressure of 3 bar might be more appropriate with the aim to achieve a high productivity in the experiment.

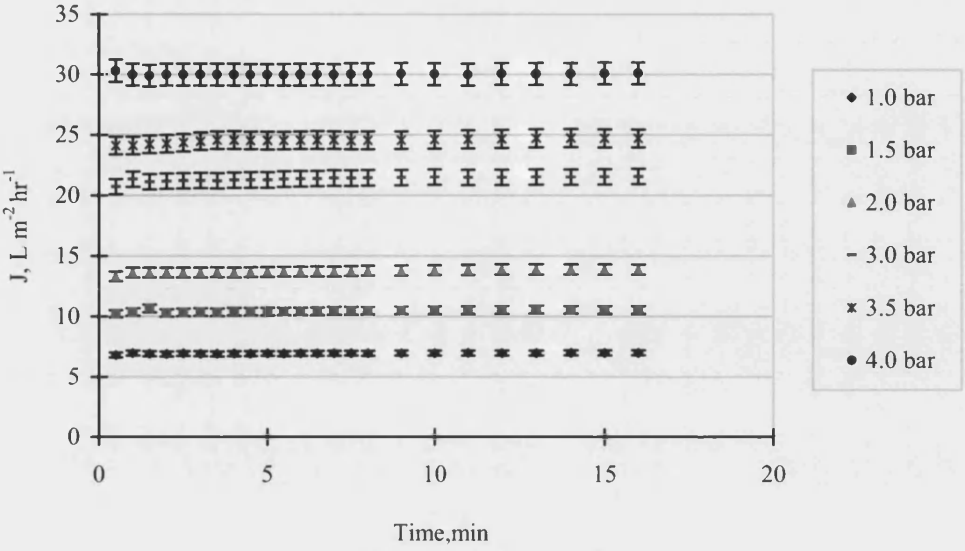

Figure 3.11 The influence of transmembrane pressure upon pure water permeate fluxes. Conditions: RO water, Temperature 20 °C, CFV 0.214 m s^{-1}, varied TMP

The linear relationship between transmembrane pressure and permeate flux was obtained by plotting the average of permeate fluxes against TMP in Figure 3.12. This is consistent with the equation (3.2) when the viscosity of RO water and membrane resistance are kept constant under certain conditions.

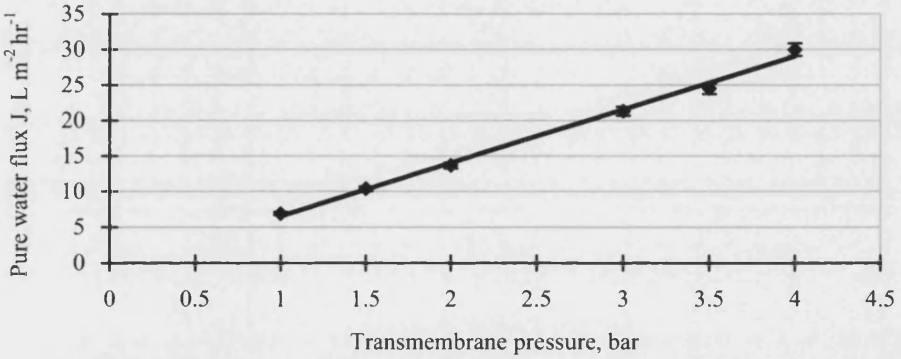

Figure 3.12 The relationship of permeate flux and transmembrane pressure

Temperature

As was expected, an increase in the flux of the reverse osmosis water was observed with a rise in the temperature in Figure 3.13. This is mainly due to the decrease of the RO

water's viscosity with the increase of temperature as the membrane resistances remained constant as shown in Figure 3.14.

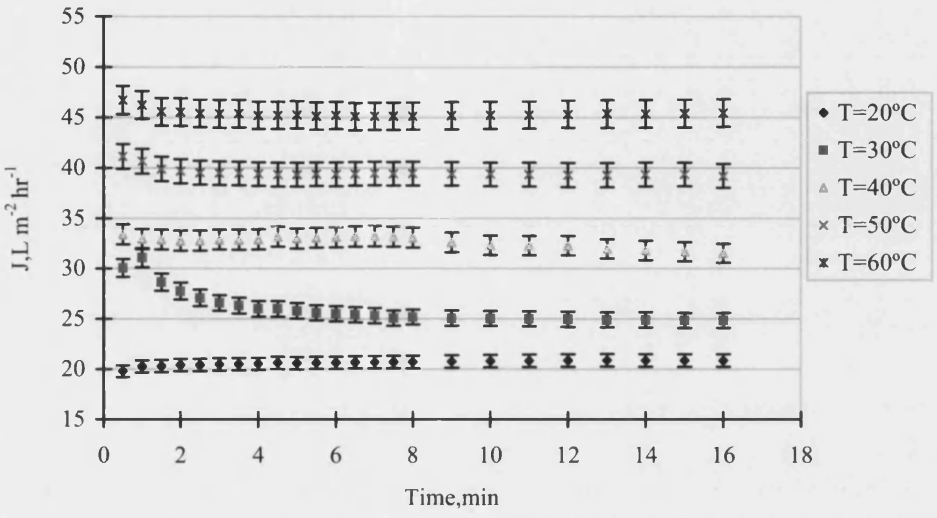

Figure 3.13 The impact of temperature upon permeate fluxes. Conditions: TMP 3 bar, CFV 0.214 m s^{-1}, varied temperature

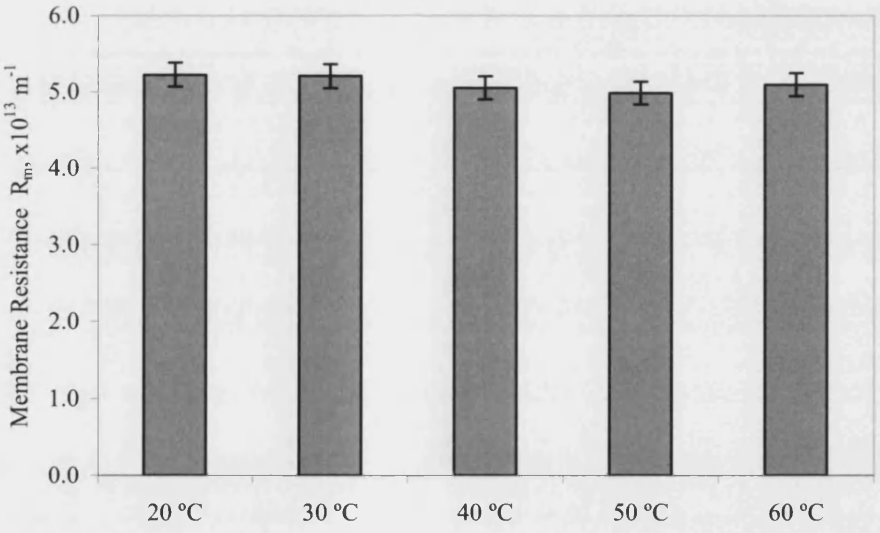

Figure 3.14 The averaged membrane resistances during rinsing by pure water at various temperatures.

Cross flow velocity

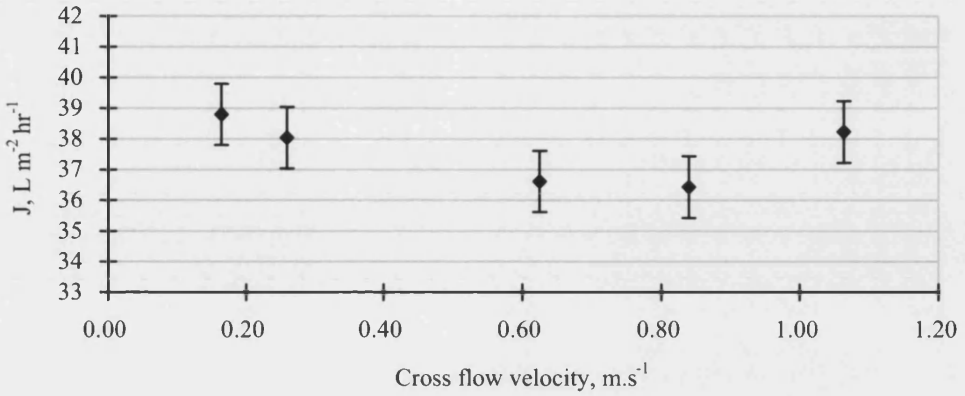

Figure 3.15 The effect of cross flow velocity upon permeate fluxes. Conditions: TMP 3 bar, Temperature 49 °C, varied CFV

Figure 3.15 indicates the influence of cross flow velocity upon the performance of pure water flux through the membrane. With the increase of cross flow velocity from 0.16 m s^{-1} to 0.84 m s^{-1}, the average value of permeate fluxes decreased from 38.8 LMH to 36.4 LMH. However, an increase of permeate flux was observed when higher cross flow velocity, namely 1.06 m s^{-1} was applied. As the estimate of global error is around $\pm 3\%$, the increase in the cross flow velocity has little effect upon the flux within experimental error. This is also in agreement with the studies of Kim *et al.,* (1993), Bird and Bartlett (1995).

3.3.1.4 Impact of tea concentration on fouling process

The concentration of the foulant is another important factor determining permeate flux.

During the manufacture of RTD tea products, the solid concentration in the initial extract ranges from 2 – 4 wt% (Pierre, 2004). A lower concentration 1 wt% and the highest value 4 wt% were investigated in these preliminary experiments on this small rig. The fouling operations had been carried out for 50 minutes to make sure a steady state was obtained.

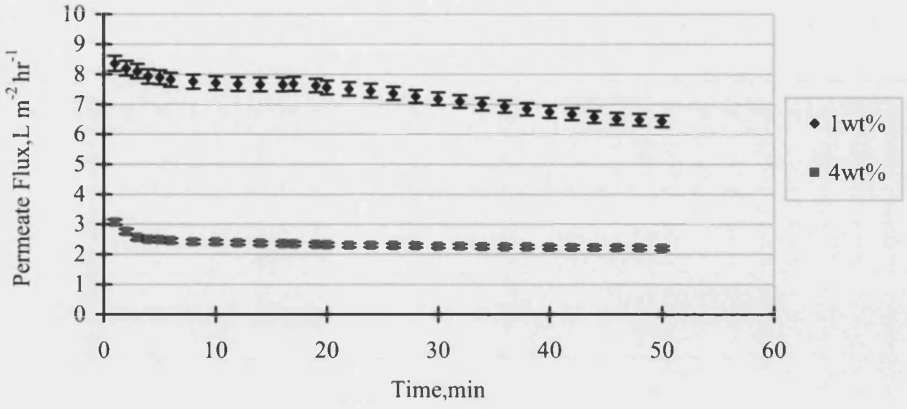

Figure 3.16 The influence of tea concentration on fouling flux decline. Fouling: TMP 3 bar, 50 °C, CFV 0.58 m s^{-1}, using 1 wt% and 4 wt% tea

According to Figure 3.16, the use of 1 and 4 wt % tea solutions lead to permeate flux values of 6 and 2 LMH respectively after 50 minutes for the conditions tested. There is a gradual flux decline from 8.36 to 6.44 LMH when 1 wt % tea solution was filtered, while 4 wt% tea solution resulted into a more severe membrane fouling in the first 5 minutes. This is because the tea solution of high concentration has much more undissolved particulates, and is therefore easier to induce instant fouling.

3.3.1.5 Effect of the concentration of *P3 Ultrasil 11* on membrane cleaning

During the process of chemical cleaning, the fouling particles might swell when certain level of porosity is achieved according to the model described in the section of literature survey (Gallott-Lavalle and Lalande, 1985). It is hypothesized that there might well be an optimal cleaning concentration to obtain a better cleaning quality. Four different concentrations of *Ultrasil 11* were compared, and the flux recovery was used to assess the efficiency of cleaning.

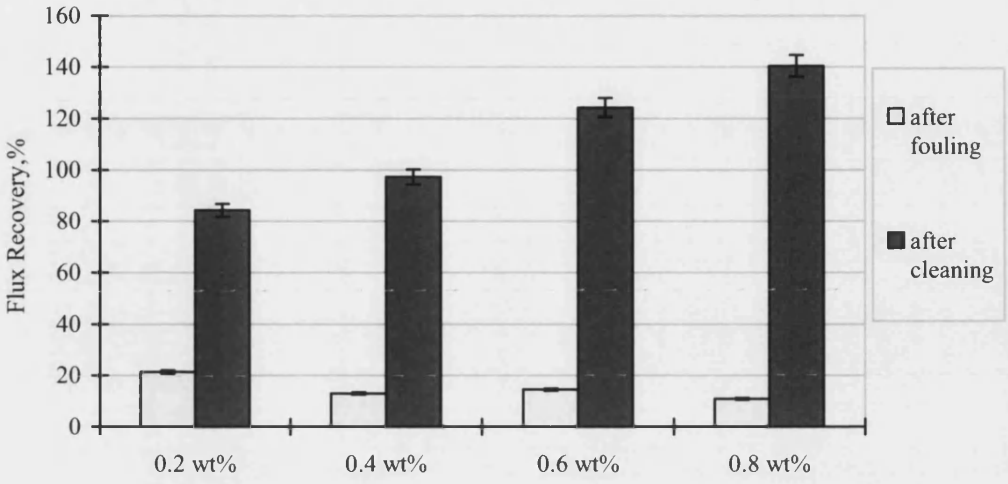

Figure 3.17 Flux recoveries after fouling and cleaning as a function of the *Ultrasil 11* concentration. Fouling: TMP 3 bar, 50 °C, using 1 wt% tea, CFV 0.58 m s^{-1}. Cleaning: TMP 2 bar, 50 °C, CFV 0.58 m s^{-1}

Figure 3.17 demonstrates that the use of *Ultrasil 11* resulted in an increase in flux recovery with increasing concentration from 0.2 to 0.8 wt%. This is presumably due to an increase in the surfactant adsorption with concentration. Flux values of over 100% resulted, and give little confidence that the surface is clean of either deposit or surfactant.

3.3.1.6 Impact of *P3 Ultrasil 11* upon virgin membrane

Because of the presence of surfactant in *Ultrasil 11*, it might have a function of activation on membrane. To validate this hypothesis, four new membranes which are the same as those used in the experiments above were treated with 0.04 wt% *Ultrasil 11* solution by passing the solution through membrane under low temperature (14 °C), at 1 bar for 10 minutes after removing glycerine. The pure water fluxes measured subsequently were used to compare the permeability of membranes.

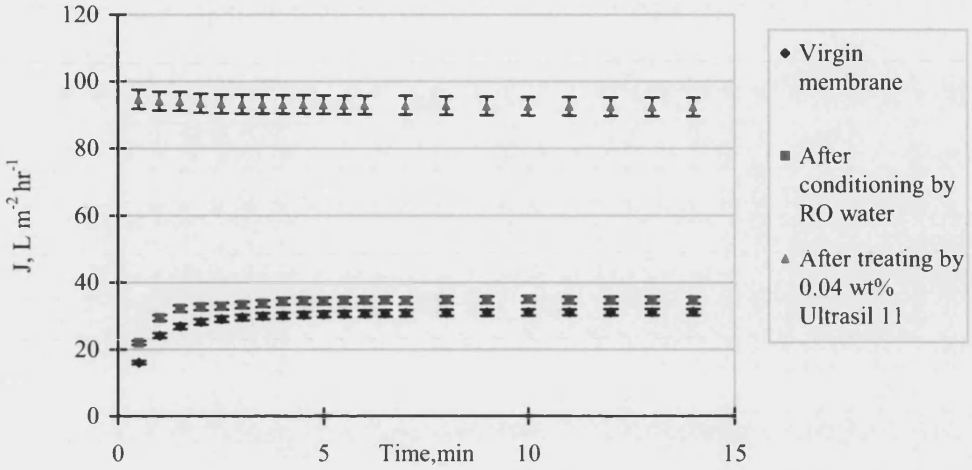

Figure 3.18 The influence of *Ultrasil 11* on virgin membranes by comparing the RO water fluxes before and after rinsing with 0.04 wt% *Ultrasil 11*. Conditioning: RO water, 58 °C, 1.15 bar, CFV 0.926 m s^{-1}. *Ultrasil 11* treatment: 0.04 wt% *Ultrasil 11*, Temperature 14 °C, TMP 1 bar, 10 minutes

Figure 3.18 shows a large jump in the permeate fluxes between the membranes after conditioning and that after rinsing with *Ultrasil 11*. This indicates that *Ultrasil 11* has a great effect on membrane permeability. As *Ultrasil 11* is a compound comprising sodium hydroxide and other surfactants, it is hard to tell the roles of these components in membrane cleaning without further investigation. To answer this question, the effect of sodium hydroxide upon the virgin membrane has been investigated.

3.3.1.7 Impact of sodium hydroxide upon virgin membrane

Four new polysulphone membranes (GR61PP) were rinsed with 0.02 wt% sodium hydroxide solution at 19 °C, 1 bar for 10 minutes after removal of glycerine from the membrane surface.

The pure water fluxes before, after conditioning, and after treating with 0.02 wt% NaOH solution are presented in Figure 3.19. After conditioning, the permeate flux of the pure water passing through the membrane was slightly higher than that before conditioning. However, after rinsing with sodium hydroxide, the permeate flux reduced to the level which was more or less the same as that before conditioning. This

phenomenon ascertained the influence of *Ultrasil 11* on the membrane was most likely because of the surfactant it contained rather than the alkali component.

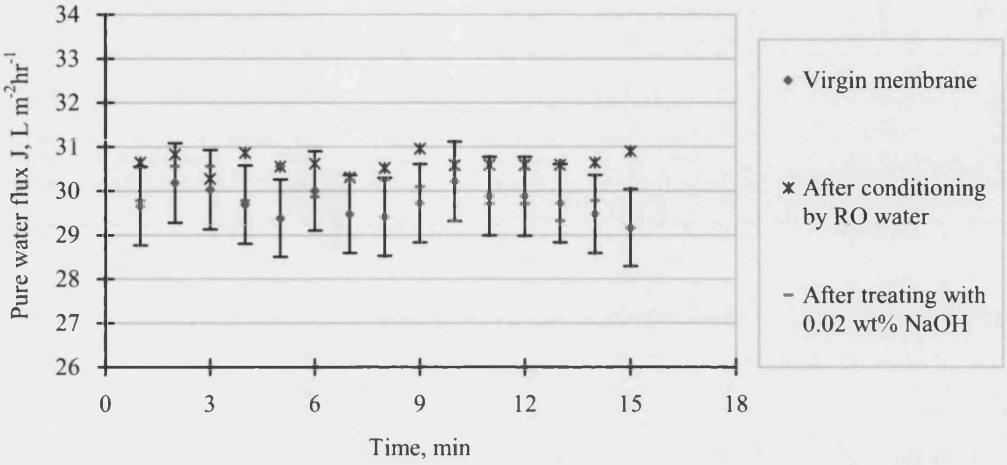

Figure 3.19 The influence of NaOH on virgin membranes by comparing the RO water fluxes before and after rinsing with 0.02 wt% NaOH. Conditioning: RO water, 58 °C, 1.15 bar, CFV 0.926 m s^{-1}. NaOH treatment: 0.02 wt%, Temperature 19 °C, TMP 1 bar, 10 minutes

3.3.2 Fouling and cleaning of Polysulphone (PSF) membrane (MWCO 30 kD) using sodium hydroxide as cleaning agent

3.3.2.1 The error analysis of the pilot scale rig

The errors of the experiments carried on the pilot scale rig had been worked out by multiple measurements of the pure water fluxes through the membranes after conditioning. As showed in Figure 3.20, the error bar of the average values in the figure was $\pm 3.5\%$.

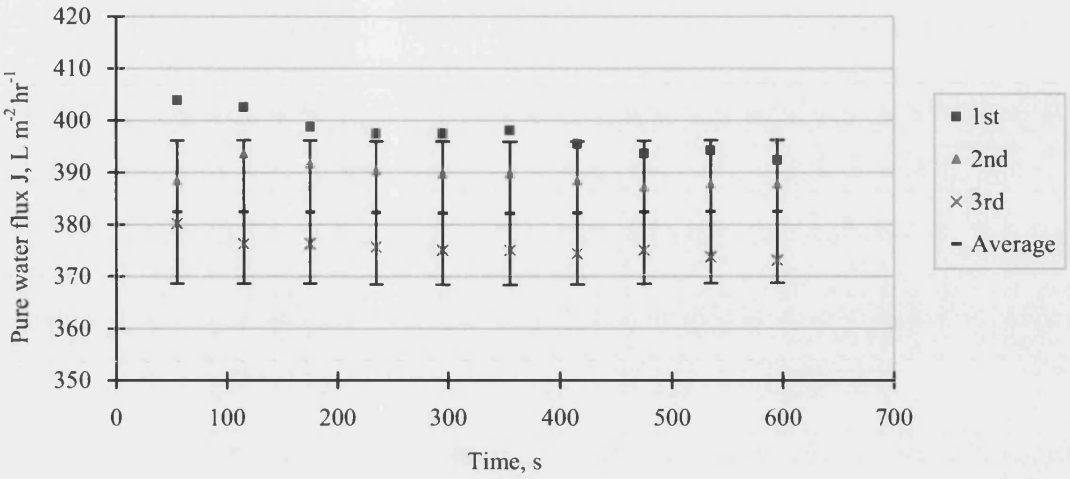

Figure 3.20 The error analysis for the large rig. Pure water flux measurement conditions: RO water, Temperature 22 °C, CFV 4.86 m s^{-1}, TMP 1 bar

3.3.2.2 The effect of cleaning fluid's concentration

The membranes were fouled by 2 wt% tea solution at 50 °C, at a TMP of 3 bar for 30 minutes. After rising with reverse osmosis water for 10 minutes, the membranes were cleaned with sodium hydroxide solutions of different concentrations: 0.1, 0.2, 0.3, and 0.4 wt%. Each cleaning was carried out at 50 °C, at a TMP of 2 bar for 15 minutes. The range of concentration of NaOH selected was chosen by referring to maximum pH value (13) of the membrane as well as the previous studies of membrane cleaning using *Ultrasil 11*, which contains around 40 wt% of sodium hydroxide.

From Figure 3.21, the permeate flux for 0.2 and 0.3 wt % of sodium hydroxide were higher than those for other concentrations in the range 0.1 to 0.4 wt %. This indicates that either 0.2 or 0.3 wt % might be the better concentration for membrane cleaning within the range tested. The comparison of flux recoveries in Figure 3.22 confirmed the better performance of 0.1wt % to 0.3 wt % sodium hydroxide than any others. However, as the estimate of global error is ± 3.5%, it is difficult to determine which concentration is more suitable for cleaning between 0.2 and 0.3 wt%. From this point of view, the subsequent product fluxes of membranes after cleaning by NaOH of different concentrations were compared in Figure 3.23. The initial product fluxes of membranes cleaned by 0.1 and 0.2 wt% NaOH were approximately 30 LMH, which are higher than

those cleaned by either 0.3 or 0.4 wt% NaOH. The highest final and averaged permeate fluxes were observed on the membrane cleaned by 0.2 wt% NaOH, indicating the optimal cleaning agent concentration. As a result, 0.2 wt% of sodium hydroxide was used in the following cleaning experiments. This concentration optimum was also found by Bird and Bartlett (1995, 2002) in their studies on the cleaning of whey protein fouled membranes. Bird and Fryer (1991) suggested the gel swelling during alkali cleaning of whey protein fouled hard surface. It is possible that the optimum cleaning agent concentration is associated with the highest voidage in the fouling cake during cleaning.

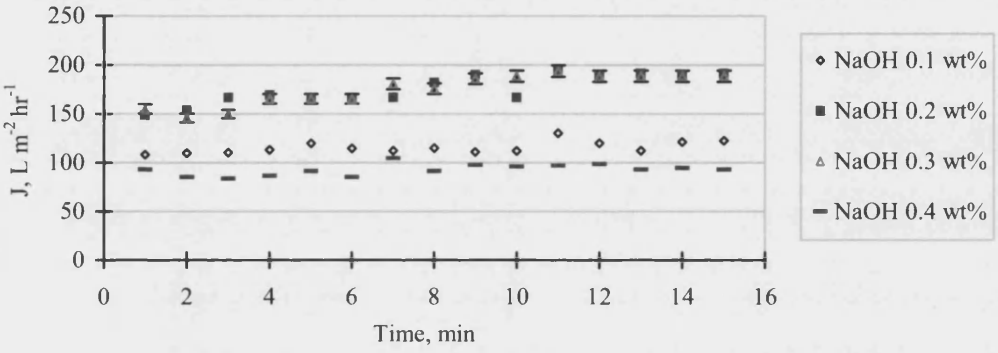

Figure 3.21 The influence of concentration of NaOH on cleaning fluxes. Fouling: TMP 3 bar, 50 °C, CFV 4.86 m s^{-1}, using 2 wt% tea. Cleaning: TMP 2 bar, 50 °C, CFV 4.86 m s^{-1}, NaOH of varied concentration

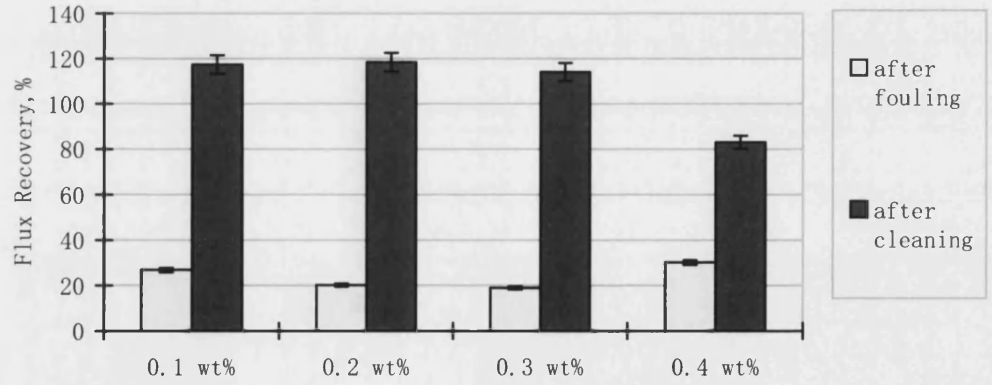

Figure 3.22 Flux recoveries after fouling and cleaning as a function of NaOH concentration. Fouling: TMP 3 bar, 50 °C, CFV 4.86 m s^{-1}, using 2 wt% tea. Cleaning: TMP 2 bar, 50 °C, CFV 4.86 m s^{-1}, NaOH of varied concentration

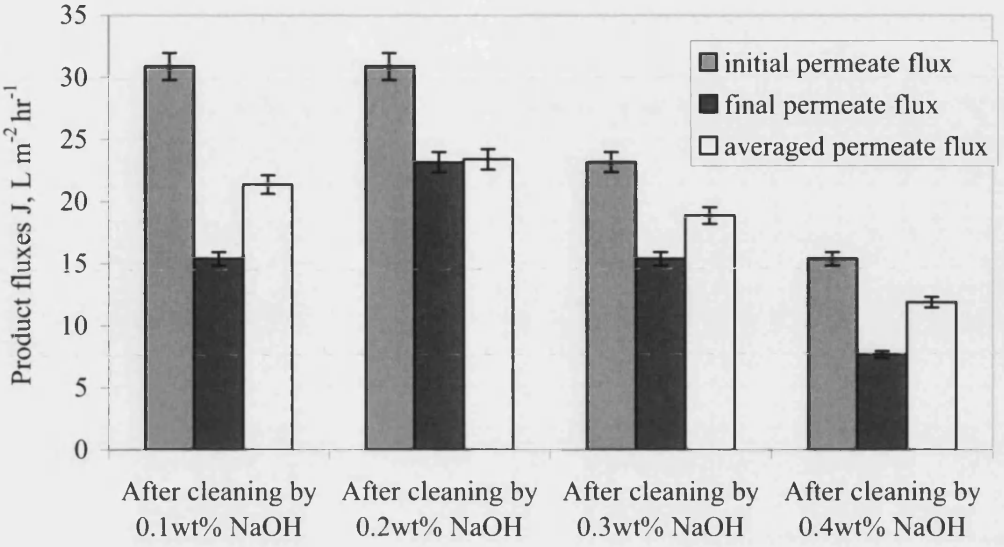

Figure 3.23 The influence of concentration of NaOH on product fluxes. Fouling: TMP 3 bar, 50 °C, CFV 4.86 m s^{-1}, using 2 wt% tea. Cleaning: TMP 2 bar, 50 °C, CFV 4.86 m s^{-1}, NaOH of varied concentration

3.3.2.3 The influence of cleaning agent temperature

The membranes were fouled by 2 wt% tea solution at 50 °C, at a TMP of 3 bar for 30 minutes. After rinsing with reverse osmosis water for 10 minutes, the membranes were cleaned by 0.2 wt% sodium hydroxide solutions at different temperatures: 30, 40, 50, 60 and 70 °C. Each cleaning experiment was carried out at a TMP of 2 bar for 15 minutes.

Referring to the Figure 3.24, an increase of permeate flux can be observed with increasing temperatures from 30 to 70 °C. This is expected since the increase of cleaning solution's temperature will reduce its viscosity; hence increase the flow through the membrane. In addition, higher temperature will provide more energy; accelerate the reaction rate and diffusion coefficients, which will make membrane cleaning more effective.

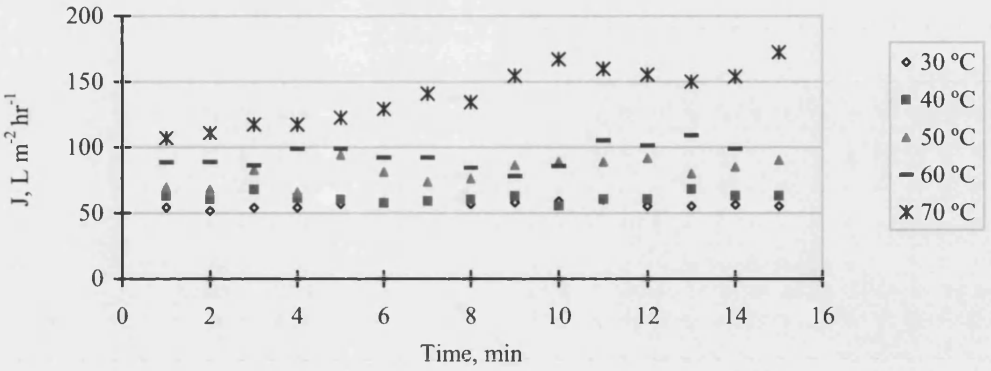

Figure 3.24 The influence of NaOH temperature on the cleaning flux. Fouling: TMP 3 bar, 50 °C, CFV 4.86 m s^{-1}, using 2 wt% tea. Cleaning: TMP 2 bar, CFV 4.86 m s^{-1}, 0.2 wt% NaOH, varied cleaning temperatures

To further ascertain whether the increase of permeate flux is as a result of the cleaner being more active at higher temperature or simply as a result of viscosity decrease, in Figure 3.25, the flux data are converted to the membrane resistances during cleaning at the temperatures tested. The plots of the membrane resistances for cleaning at 30, 50 and 60 °C appeared to be clustered, indicating that variations in flux were predominantly accounted for by viscosity variations with temperature. The membrane resistances were slightly higher when cleaning was carried out at 40 °C. This could be explained by the fact that the membrane was not 100% recovered after cleaning by NaOH at 30 °C (see Figure 3.26). Cleaning at 70 °C significantly decreased the membrane resistances as cleaning reagent became highly reactive at this highest temperature.

From Figure 3.26, the pure water flux recoveries of membranes cleaned at 40 °C and 50 °C were 107%, and 114% respectively, giving the confidence that membranes were highly cleaned of deposits after cleaning at these temperatures. These values being slightly over 100% indicated that the membrane structure might be more opening after cleaning. However, unexpected findings were found on the membranes after cleaning at 60 °C and 70 °C. The flux recoveries of the membranes became 186% and 218%, indicating that the active layer of the membranes might swell up after cleaning at these high temperatures. In this case, the membrane permeability could be significantly

changed. To further investigate this problem, the subsequent product fluxes for membranes being cleaned at different temperatures were compared in Figure 3.27.

According to the graph, with the temperature ranging form 30 to 60 °C, the highest values were observed on the membrane after cleaning at 50 °C. This indicated that the optimal cleaning agent temperature could be 50 °C. The remarkable similarities in initial and final product fluxes for the membranes cleaned at 30, 40, and 60 °C implied that there were no critical modifications of membrane permeability after NaOH cleaning at these temperatures. The insignificant increase in averaged product flux at these three temperatures showed cleaning being slightly more effective at higher temperature. However, after membrane being cleaned at 70 °C, the averaged product flux became even higher than that for 50 °C. This is indicative of the tremendous change of membrane surface as well as the membrane permeability after reacting with NaOH at 70 °C.

Considering the possibility that this membrane has been damaged after cleaning at 70 °C, a new conditioned membrane was used in the following experiments.

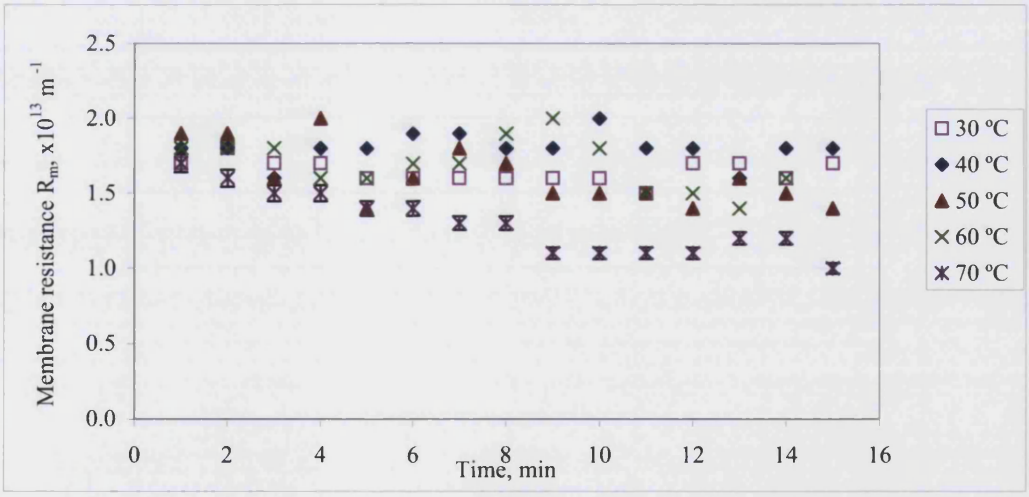

Figure 3.25 The influence of NaOH temperature on the membrane resistance. Fouling: TMP 3 bar, 50 °C, CFV 4.86 m s^{-1}, using 2 wt% tea. Cleaning: TMP 2 bar, CFV 4.86 m s^{-1}, 0.2 wt% NaOH, varied cleaning temperatures

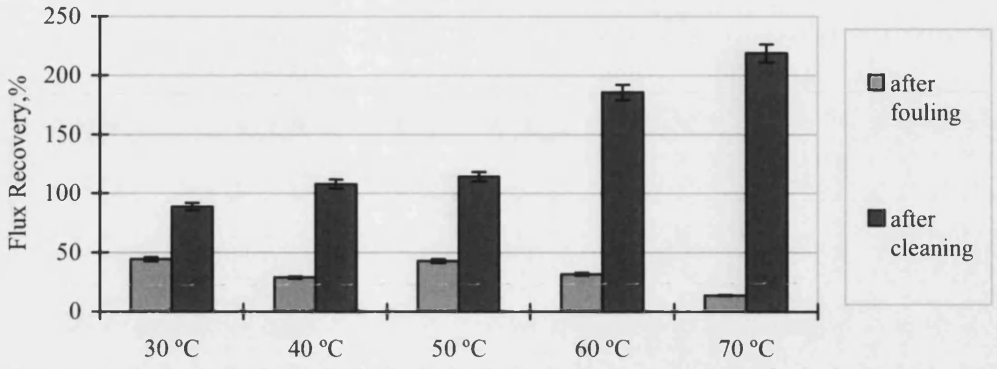

Figure 3.26 Flux recoveries after fouling and cleaning as a function of NaOH temperature. Fouling: TMP 3 bar, 50 °C, CFV 4.86 m s^{-1}, using 2 wt% tea. Cleaning: TMP 2 bar, CFV 4.86 m s^{-1}, 0.2 wt% NaOH, varied cleaning temperatures

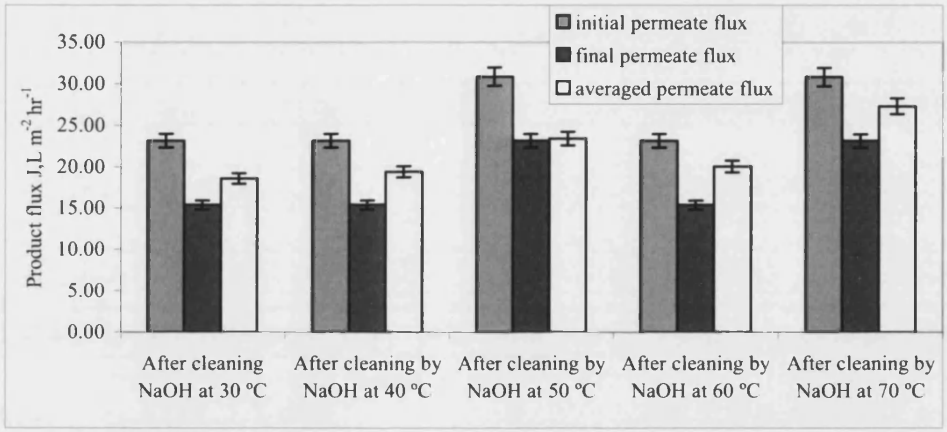

Figure 3.27 Subsequent product fluxes as a function of NaOH temperature. Fouling: TMP 3 bar, 50 °C, CFV 4.86 m s^{-1}, using 2 wt% tea. Cleaning: TMP 2 bar, CFV 4.86 m s^{-1}, 0.2 wt% NaOH, varied cleaning temperatures

3.3.2.4 The influence of transmembrane pressure upon membrane cleaning

The membranes were fouled by 2 wt% tea solution at 50 °C, at a TMP of 3 bar for 30 minutes. After rising with reverse osmosis water for 10 minutes, the membranes were cleaned by 0.2 wt% sodium hydroxide solutions at 50 °C at TMP: 1 bar and 2 bar. The cleaning fluxes were compared in Figure 3.28.

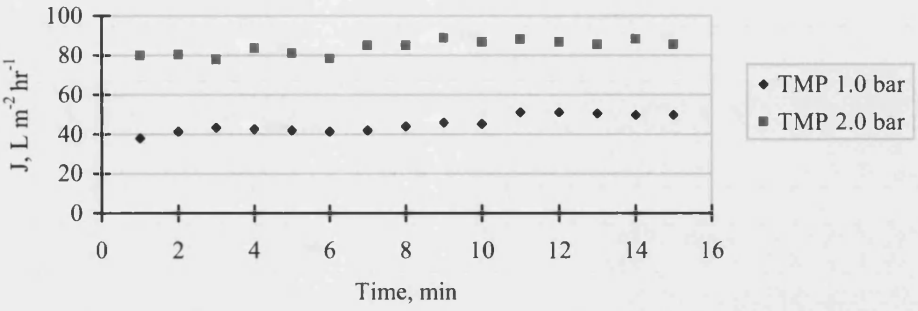

Figure 3.28 Influence of cleaning TMP upon the cleaning agent fluxes. Fouling: TMP 3 bar, 50 °C, CFV 4.86 m s^{-1}, using 2 wt% tea. Cleaning: Temperature 50 °C, CFV 4.86 m s^{-1}, 0.2 wt% NaOH, varied TMPs

As it is shown in Figure 3.28, the fluxes through the membrane for the cleaning taking place at a TMP of 2 bar were higher than those for cleaning at TMP 1 bar. This was expected as the usage of higher transmembrane pressure was able to push more permeate passing through the membrane. However, did the cleaning fluxes reflect the effectiveness of membrane cleaning? To answer this question, the pure water flux recoveries after cleaning at different TMPs were plotted in Figure 3.29.

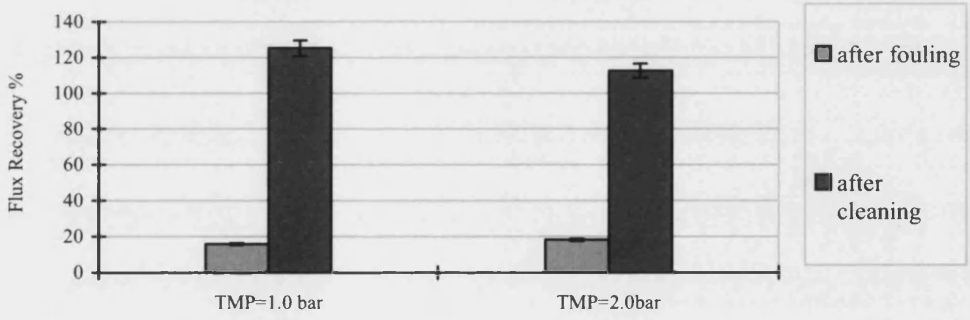

Figure 3.29 Pure water flux recoveries after fouling and cleaning as a function of TMP. Fouling: TMP 3 bar, 50 °C, CFV 4.86 m s^{-1}, using 2 wt% tea. Cleaning: Temperature 50 °C, CFV 4.86 m s^{-1}, 0.2 wt% NaOH, varied TMPs

Referring to Figure 3.29, the flux recovery after cleaning for TMP 1 bar was even higher than that for TMP 2 bar. A possible explanation is that the higher TMP during cleaning leads to a compact deposit that partially blocks the membrane pores, and therefore results in cleaning difficulties. Other researchers (Bird and Bartlett, 1995)

have demonstrated that it is important to clean at TMP values considerably less than those applied during fouling.

3.3.3 Fouling and cleaning of Fluoropolymer (FS50PP) membrane with MWCO 30 kD using sodium hydroxide as a cleaning agent

3.3.3.1 The influence of cleaning agent concentration

The membranes were fouled by 2 wt% tea solution at 50 °C, at a TMP of 3 bar for 30 minutes. After rinsing with reverse osmosis water for 10 minutes, the membranes were cleaned by sodium hydroxide solutions of different concentrations: 0.1, 0.2, 0.3, and 0.4 wt%. The temperature for cleaning was 50 °C, while the TMP was 2 bar. The cleaning fluxes were compared in Figure 3.30.

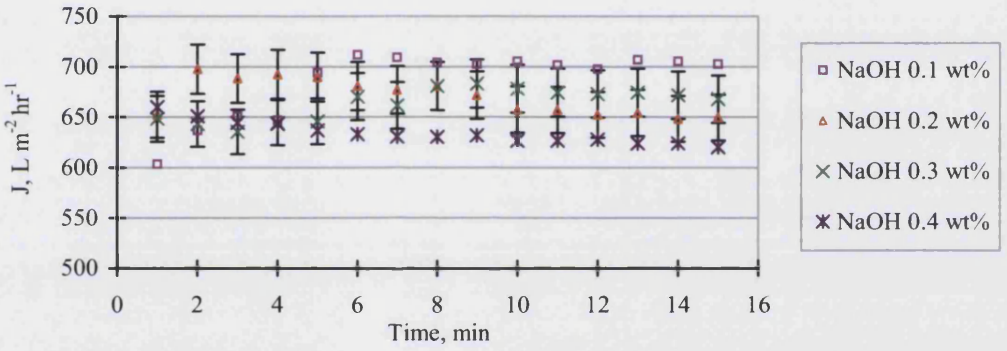

Figure 3.30 The impact of NaOH concentration upon the cleaning fluxes. Fouling: TMP 3 bar, 50 °C, CFV 4.86 m s^{-1}, using 2 wt% tea. Cleaning: Temperature 50 °C, TMP 2 bar, CFV 4.86 m s^{-1}, varied NaOH concentrations

Considering the estimate of global errors (3.5%), there were no apparent differences between the values of permeate fluxes for cleaning with sodium hydroxide concentrations ranging from 0.1 to 0.4 wt%. However, 0.1 wt% seemed to behave slightly better than those from 0.2 to 0.4 wt% especially in the last three minutes. It is reported that the viscosities of sodium hydroxide solutions of concentrations 0 wt% and 2.0 wt% are 0.8900 cp and 0.9017 cp respectively (Vazquez, *et al.*, 1996). Consequently, the increase of viscosity of aqueous sodium hydroxide solutions as concentration increases from 0.1 to 0.4 wt% should be too small to contribute to this flux decline. As a result, other possible explanations could be the cleaning being slightly

more effective at lower concentration or there were some additional random errors during the measurement. To further investigate this problem, Figure 3.31 compared the flux recoveries after fouling and after cleaning with sodium hydroxide of each concentration. The results demonstrated the use of lower concentration 0.1wt% of NaOH was not sufficient as a poorer flux recovery of less than 90% was obtained after membrane cleaning. Either 0.2 wt% or 0.3 wt% NaOH appeared to be more effective as the flux recoveries of both membranes were approximately 100%. However, the value of membrane cleaned by 0.4 wt% NaOH appeared to be over 100%, indicating that membrane surfaces could be modified to a certain extent by sodium hydroxide solution of this concentration. To further study this point, the product fluxes after cleaning with each concentrations of sodium hydroxide were displayed in Figure 3.32.

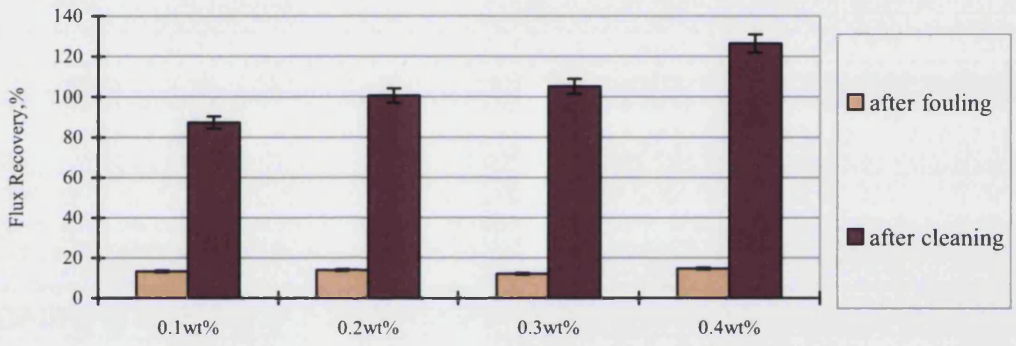

Figure 3.31 Pure water flux recoveries after fouling and cleaning as a function of NaOH temperature. Fouling: TMP 3 bar, 50 °C, CFV 4.86 m s^{-1}, using 2 wt% tea. Cleaning: Temperature 50 °C, TMP 2 bar, CFV 4.86 m s^{-1}, varied NaOH concentration

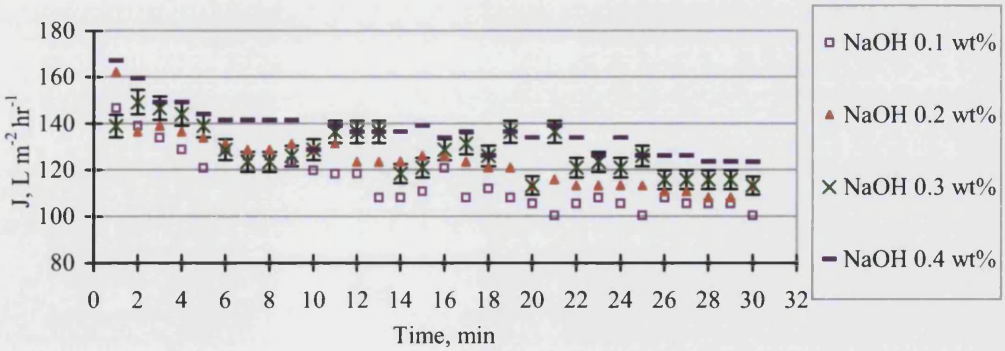

Figure 3.32 Subsequent product fluxes as a function of cleaning agent concentration. Fouling: TMP 3 bar, 50 °C, CFV 4.86 m s^{-1}, using 2 wt% tea. Cleaning: Temperature 50 °C, TMP 2 bar, CFV 4.86 m s^{-1}, varied NaOH concentrations

As shown in Figure 3.32, the product fluxes after cleaning with sodium hydroxide of different concentrations from 0.1 to 0.4 wt% increased with increasing concentrations. The increase in product flux when the concentration of NaOH changed from 0.1 to 0.2 wt% presumably arose from the improvement in membrane cleanliness after cleaning. After the membrane was cleaned by 0.3 wt% NaOH, the product fluxes fluctuated with time although the averaged value (approximately 128 LMH) appeared to be slightly higher than that (124 LMH) for membrane being cleaned by 0.2 wt% NaOH. Further increase of product flux when NaOH of higher concentration 0.4 wt% was used during cleaning was also observed. These might indicate the small modification of membrane surface after cleaning at concentrations above 0.2 wt%.

3.3.3.2 The effect of cleaning temperature

The membranes were fouled by 2 wt% tea solution at 50 °C, at a TMP of 3 bar for 30 minutes. After rising with reverse osmosis water for 10 minutes, the membranes were cleaned by 0.2 wt% sodium hydroxide solutions at a TMP of 2 bar at different temperatures: 40, 50, and 60 °C.

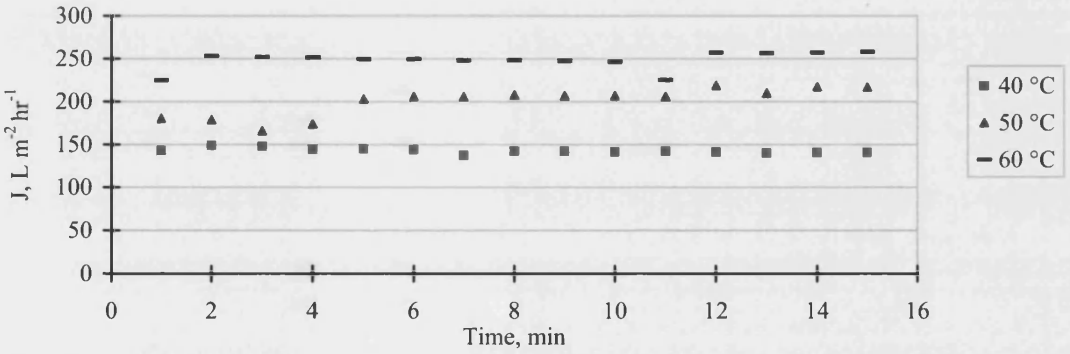

Figure 3.33 The influence of cleaning temperature upon permeate flux during cleaning. Fouling: TMP 3 bar, 50 °C, CFV 4.86 m s^{-1}, using 2 wt% tea. Cleaning: 0.2 wt% NaOH, TMP 2 bar, CFV 4.86 m s^{-1}, varied cleaning temperatures

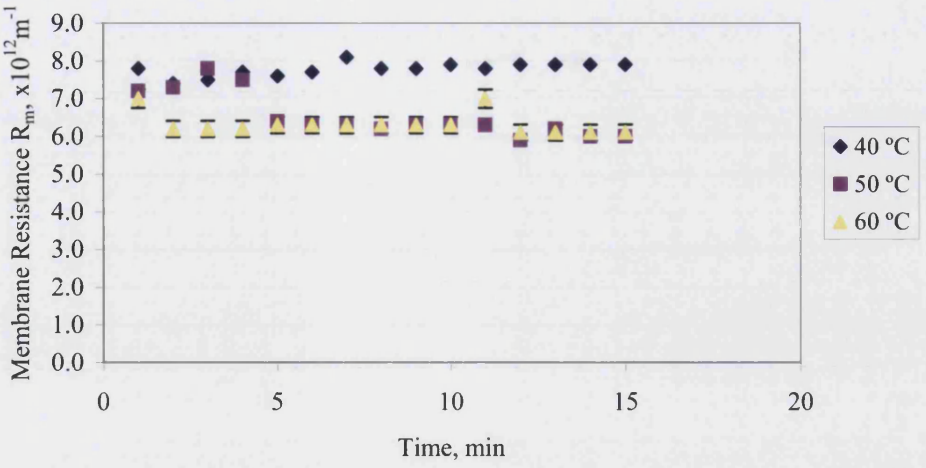

Figure 3.34 The membrane resistances as a function of cleaning temperature. Fouling: TMP 3 bar, 50 °C, CFV 4.86 m s^{-1}, using 2 wt% tea. Cleaning: 0.2 wt% NaOH, TMP 2 bar, CFV 4.86 m s^{-1}, varied cleaning temperatures

According to Figure 3.33, the permeate flux increased as the temperature of cleaning solution rose. The most likely explanation for this is that the increased temperature resulted into the decrease of viscosity of cleaning solution, which therefore assisted the flow through the membrane. However, the possibility of the cleaning reagent being more effective at higher temperatures should also be considered. Figure 3.34 illustrated the changes of membrane resistances as a function of cleaning reagent temperature. As shown in the graph, there was a decline in the membrane resistance from the sixth minute when cleaning was carried out at 50 °C. This indicated that the higher temperature speed up diffusion and / or the chemical reaction between cleaning reagent and deposit, leading to a break up and dissolution the foulants. There were therefore the significant decrease of membrane resistance after cleaning for 6 minutes. However, when the cleaning temperature increased form 50 °C to 60 °C, few changes of membrane resistances implied that the flux improvement was merely a result of viscosity reduction as temperature increase in this situation.

As to the efficiency of membrane cleaning, the plots of flux recoveries shown in Figure 3.35 can give an indication.

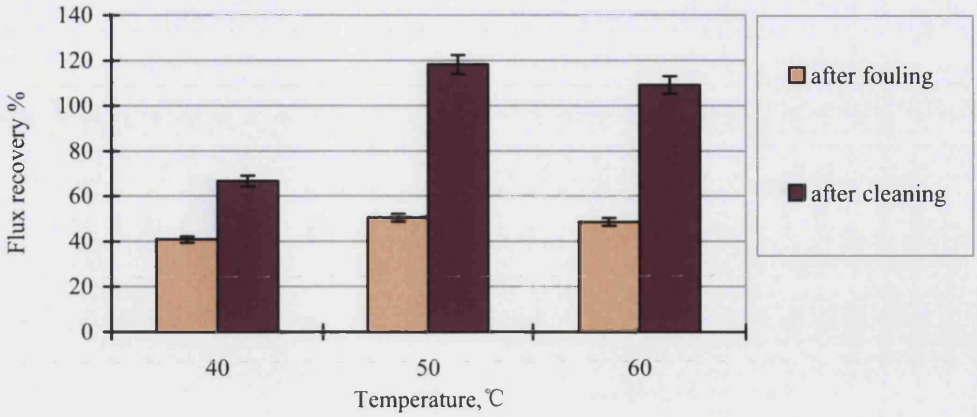

Figure 3.35 The influence of temperature upon fluxes during cleaning. Fouling: TMP 3 bar, 50 °C, CFV 4.86 m s^{-1}, using 2 wt% tea. Cleaning: 0.2 wt% NaOH, TMP 2 bar, CFV 4.86 m s^{-1}, varied cleaning temperatures

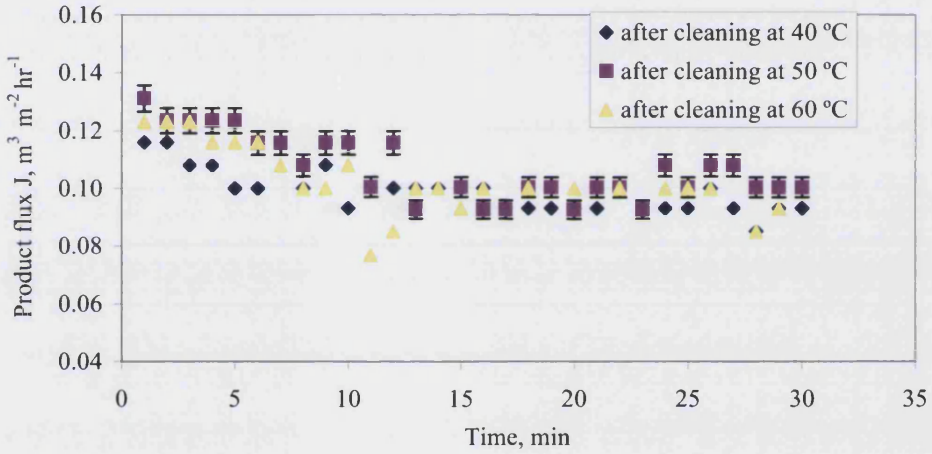

Figure 3.36 The influence of cleaning temperature upon product fluxes. Fouling: TMP 3 bar, 50 °C, CFV 4.86 m s^{-1}, using 2 wt% tea. Cleaning: 0.2 wt% NaOH, TMP 2 bar, CFV 4.86 m s^{-1}, varied cleaning temperatures

Figure 3.35 illustrates the maximum pure water flux recovery was obtained on the membrane which was cleaned at 50 °C rather than 60 °C. It is possible that the kinetics of reaction between the polyphenol based deposits and FS50PP membrane containing the pore forming additives polyvinylpyrrolidone (PVP) (Lipnizki, 2006) is speeded up at 60 °C, thereby resisting cleaning at higher temperature. PVP has been reported to have good capability of absorbing polyphenols by Borneman, *et al.*, 2001. To further investigate this problem, the corresponding product fluxes after cleaning at different

temperatures were displayed in Figure 3.36. According to the graph, the cleaning at 50 ºC was slightly more effective than those at the other two temperatures, indicating 50 ºC is the optimal temperature for cleaning.

3.3.3.3 The impact of TMP upon membrane cleaning

The membranes were fouled by 2 wt% tea solution at 50 °C, at a TMP of 3 bar for 30 minutes. After rising with reverse osmosis water for 10 minutes, the membranes were cleaned by 0.2 wt% sodium hydroxide solutions at 50 °C at TMP: 1 bar and 2 bar. The cleaning fluxes were compared in Figure 3.37.

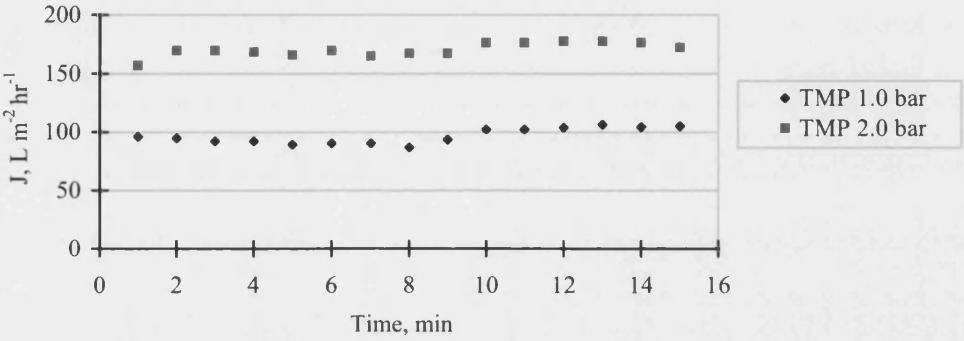

Figure 3.37 The influence of cleaning transmembrane pressure upon cleaning fluxes. Fouling: TMP 3 bar, 50 °C, CFV 4.86 m s^{-1}, using 2 wt% tea. Cleaning: 0.2 wt% NaOH, Temperature 50 °C, CFV 4.86 m s^{-1}, varied transmembrane pressures

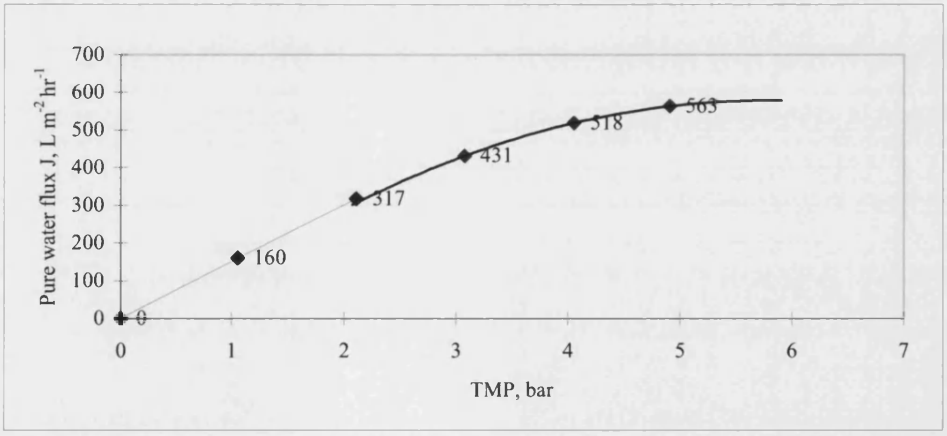

Figure 3.38 Curve showing the relationship between pure water flux of virgin conditioned FS membrane and transmembrane pressure

There was a large jump of cleaning fluxes as cleaning TMP increased from 1.0 bar to 2.0 bar. It should be noticed that this increase of cleaning flux was not proportional to the increase of transmembrane pressure, indicating that this is not within the linear pressure dependent region. Figure 3.38 plotted the averaged pure water flux of the virgin conditioned FS membrane against TMP. It is clear that pure water flux is linear proportional to TMP up to 2 bar. Further increase of transmembrane pressure from 2 to 5 bar led to the approach of limiting flux of this virgin conditioned membrane. Once the membrane has been fouled by tea solution, it is reasonable that lower TMP is required to obtain the limiting flux during membrane cleaning. As a result, the cleaning flux at 2 bar was observed to be less than double of that at 1 bar. To further understand the function of TMP during cleaning, the flux recoveries of membranes after different cleaning were shown in Figure 3.39. Both membranes were not fully recovered after cleaning. The similarity of the values indicated that transmembrane pressure had little effect upon the cleaning of fluoropolymer membrane.

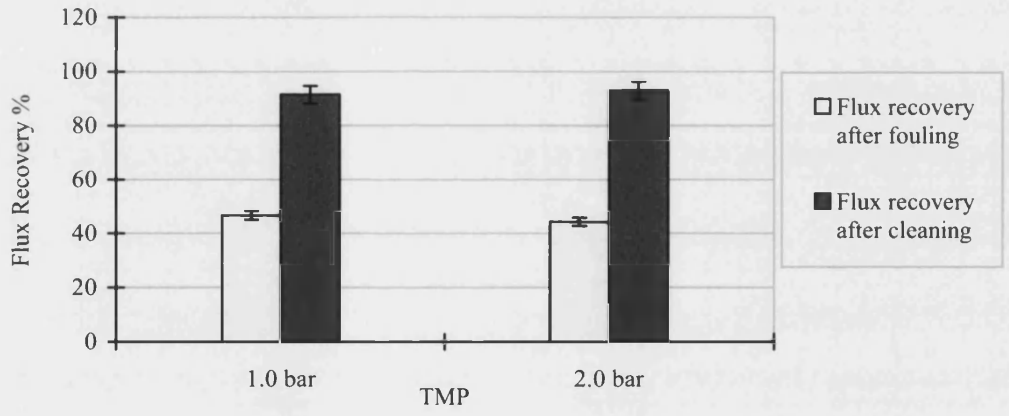

Figure 3.39 The influence of cleaning transmembrane pressure upon pure water flux recovery after cleaning. Fouling: TMP 3 bar, 50 °C, CFV 4.86 m s^{-1}, using 2 wt% tea. Cleaning: 0.2 wt% NaOH, Temperature 50 °C, CFV 4.86 m s^{-1}, varied transmembrane pressures

3.3.4 Visualization of membrane fouling and cleaning by TEM

3.3.4.1 Polysulphone membrane (MWCO 30 kD)

The TEM images of polysulphone membranes after conditioning, fouling and cleaning were compared and explained in this section. The conditions for these three operations, namely conditioning, fouling and cleaning, were presented as follows:

Conditioning: RO water, 60 °C, TMP 1.0 bar, 90 mins

Fouling conditions: 2 wt% tea solution, 50 °C, TMP 3.0 bar, 30 mins

Cleaning :0.2 wt% NaOH, 60 °C, TMP 2.0 bar, 15 mins

Figure 3.40 showed the TEM image of the cross-section structures of conditioned PSF membrane. The dark area represents the presence of polymer, while the white area is absent of polymer. The active layer which is a very thin and dense layer is indicated by the arrow. The white and finger like areas observed in the membrane sublayer are the irregular columnar macrovoids (Mulder, 1996; Lin, *et al.*, 2002; Lin, *et al.*, 2003; Wu. *et al.*, 2006). They are roughly parallel to each other, resembling the so-called finger structure. Figure 3.41 displayed overall cross - section structures of the fouled and the cleaned PSF membranes under low magnification. There was clear line of active layer in the fouled membrane. However, the active layer appeared to be thinner because of the removal of deposits on the membrane surface after cleaning by sodium hydroxide.

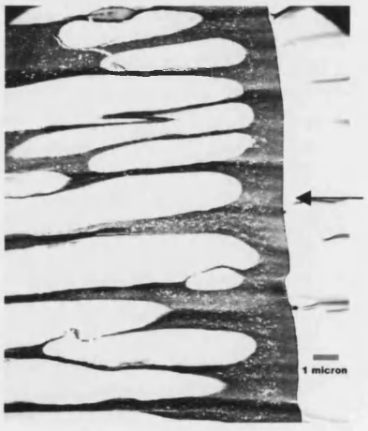

Figure 3.40 TEM image of the cross-section structure of conditioned PSF membrane 30 kD (x 5000)

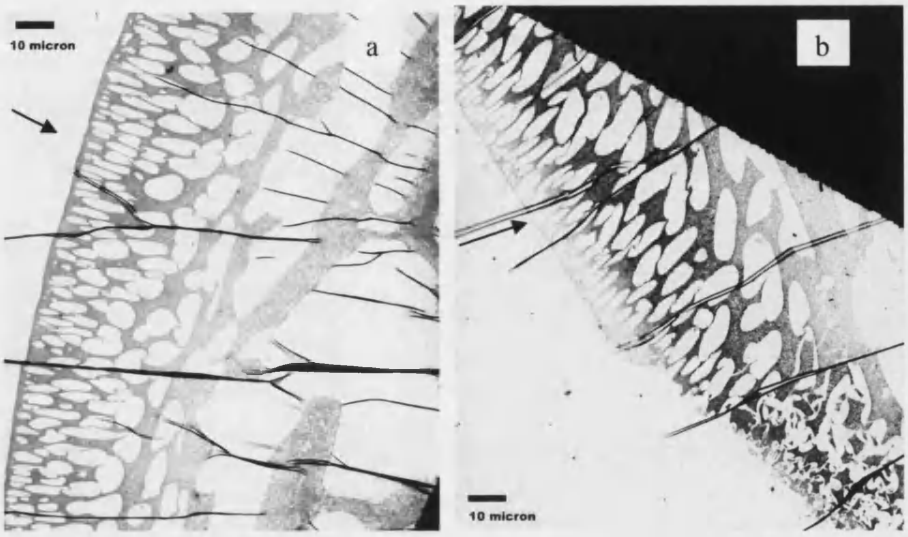

Figure 3.41 TEM images of the cross-section structure of PSF membranes: (a) fouled membrane(x 600); (b) cleaned membrane (x 600)

Figure 3.42 (a) and (b) illustrated different top layer surface structures of PSF membrane after fouling and cleaning. The membrane surface after fouling appeared to be covered by a layer of contaminants, which certified the presence of fouling. However, after cleaning, the membrane surface became smoother and denser, giving certain confidence that the surface is clean of deposits.

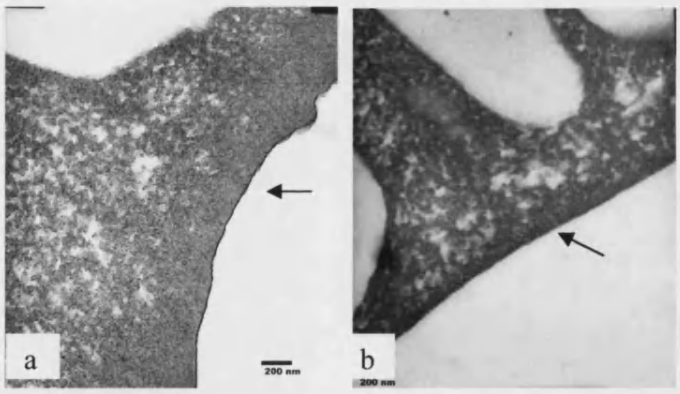

Figure 3.42 TEM images of top-layer surface structure of PSF membranes: (a) fouled membrane (x 30000); (b) cleaned membrane (x 30000)

The sublayers of the fouled membrane and the cleaned membrane have been inspected in Figure 3.43 and 3.44. The differences between (a) and (b) in both figures indicated that majority of the foulants have been removed from membrane sublayer after cleaning

although few residues were observed in the surrounding of membrane macrovoids. This might give some support to the protein-swelling model estabilished by Bartlett *et al.*, (1995).

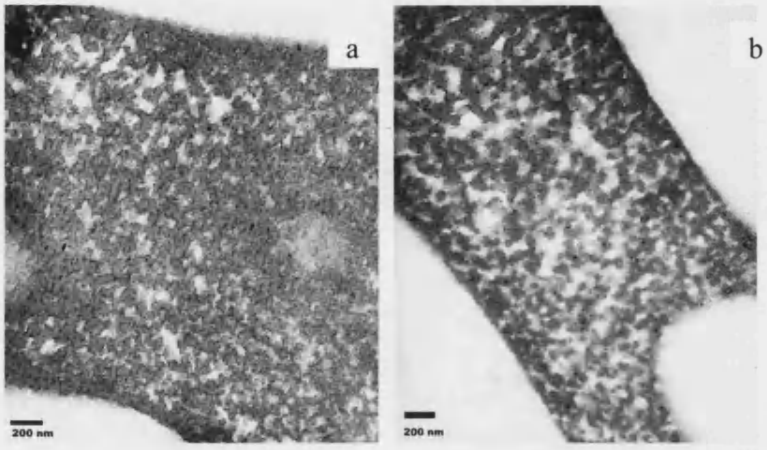

Figure 3.43 TEM images showing changes of PSF membrane structure before and after cleaning: (a) fouled membrane (x 30000); (b) cleaned membrane (x 30000)

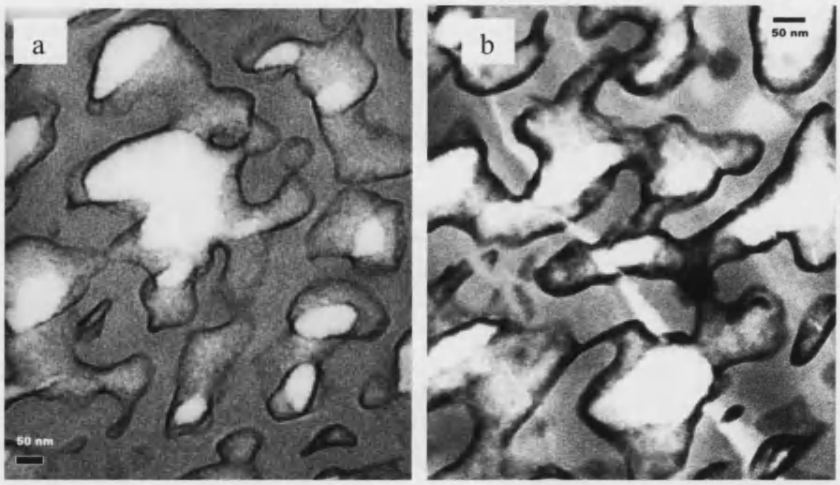

Figure 3.44 TEM images showing sub-layer structures of PSF membranes: (a) fouled membrane (x 100000); (b) cleaned membrane (x 100000)

3.3.4.2 Fluoropolymer membrane (MWCO 30 kD)

Fluoropolymer membranes after conditioning, fouling and cleaning under the conditions showed as follows were also examined by using TEM.

Conditioning: RO water, 50 °C, TMP 1.0 bar, 90 mins.

Fouling conditions: 2 wt% tea solution, 50 °C, TMP 3.0 bar, 30 mins

Cleaning : 0.2 wt% NaOH, 50 °C, TMP 2.0 bar, 15 mins

The cross-section structures of FS membranes after conditioning, fouling and cleaning were displayed in Figure 3.45 (a), (b) and (c). Compared to the PSF membrane, the active layer in FS membrane is not as clear as that in PSF membrane. The surface of FS membrane also seemed to be less compacted. The image of the fouled FS membrane appeared to be slightly darker than that of conditioned membrane, indicating the presence of foulants. After cleaning process, any differences between the images of the fouled and the cleaned membranes are not obvious with this low magnification.

Figure 3.46 (a), (b), (c), and (d) showed the top-layer surface structures of FS membranes after conditioning, fouling and cleaning. According to the grey colour in the image, severe fouling was observed in image (b). After cleaning with sodium hydroxide solution, there was still a certain amount of residue remaining on the membrane surface. Compared with PSF membrane, FS50PP has relatively weak cleanability as polysulphone membrane surface was observed to be clean of residues despite of the few deposits remaining in the sublayer. This is in accordance with the fact that PVP contained in this FS50PP membrane has relatively good capability to absorb polyphenols (Borneman, *et al.*, 2001).

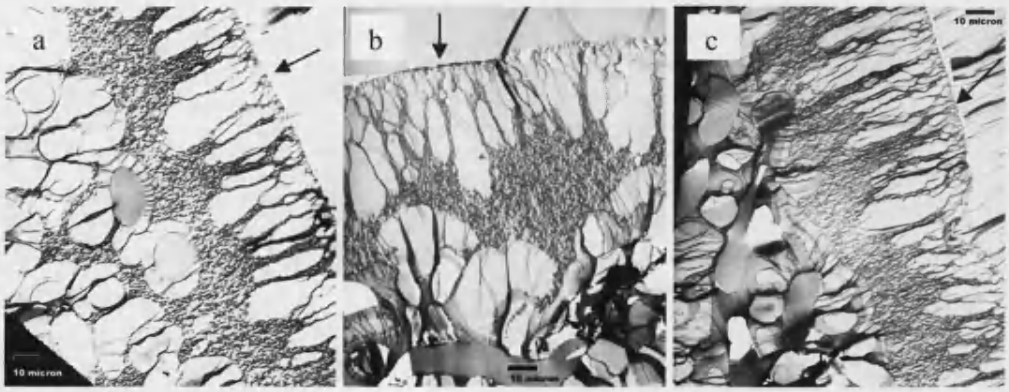

Figure 3.45 TEM images of cross-section structure of FS membranes: (a) conditioned membrane (x 600); (b) fouled membrane (x600); c) cleaned membrane (x 600)

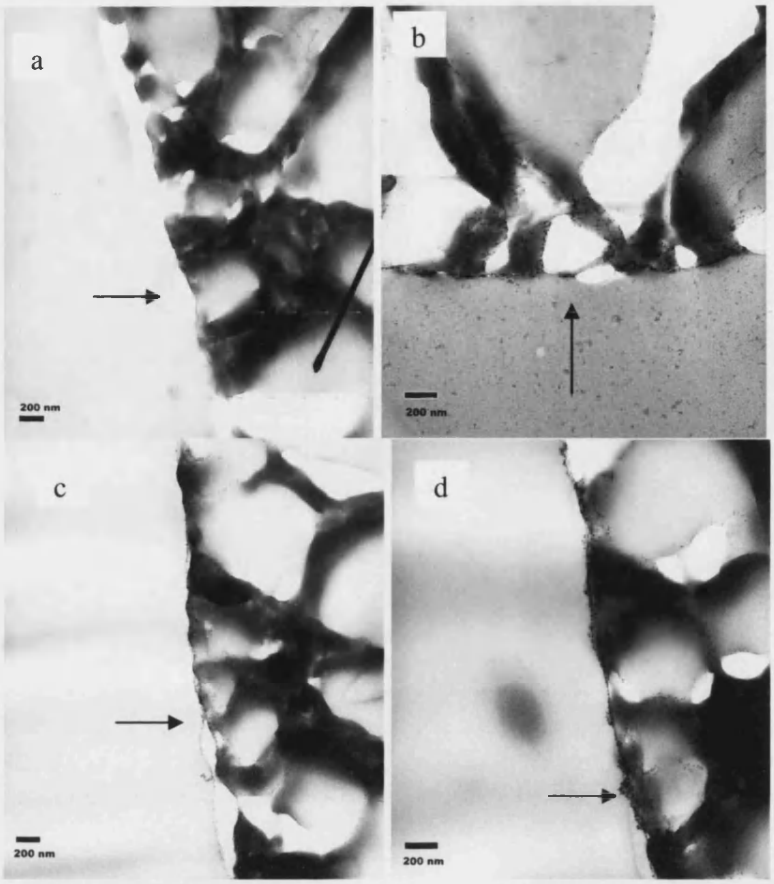

Figure 3.46 TEM images of top-layer surface structure of FS membranes: (a) conditioned membrane (x 25000); (b) fouled membrane (x 30000); (c) cleaned membrane (x 20000); (d) cleaned membrane (x 30000)

3.4 Conclusion

The fouling and cleaning performance of three different UF membranes for the processing of cold black tea is reported in this chapter. The polysulphone membranes with MWCO 20 kD were evaluated using a small DSS rig with the aim to get a better understanding of membrane filtration. The other two membranes, namely polysulphone membranes with MWCO 30 kD and fluoropolymer membranes with MWCO 30 kD, were applied on a large-scale rig that was designed to simulate industrial operating conditions.

The measurements of the pure water fluxes and the contact angles of membranes before and after conditioning showed the effectiveness of removing glycerine coated outside the membrane surface. Sixty minutes conditioning was able to take away the majority of glycerine, and consequently increased membrane hydrophobicity.

During the characterization of PSF (MWCO 20 kD) membranes, the permeate flux of membrane was found to be linear proportional to the temperatures of RO water from 20 to 60 °C and the TMP from 1 to 4 bar. Cross flow velocity appeared to have an irregular impact on the permeate flux through membrane, which is consistent with the studies from Kim *et al* (1993), Bird and Bartlett (1995).

The formulated cleaning agent *P3 Ultrasil 11* was proved to be effective because the values of flux recoveries were over 100% after cleaning. The most favorable concentration of *Ultrasil 11* was 0.8 wt% within the range tested. In addition, according to the study of the influence of *Ultrasil 11* as well as NaOH upon virgin membranes, the fact that *Ultrasil 11* enhanced the permeate fluxes is most likely due to the function of surfactant materials contained rather than the alkali.

From the experiments using the small DSS rig, the pure water flux of the virgin polysulphone membrane with MWCO 20 kD was approximately 30 LMH. During the fouling of membranes by 1 wt% tea solution at TMP 2 bar, 50 °C , CFV 0.58 m s^{-1}, the permeate flux was about 6 LMH. When using 0.4 wt% *Ultrasil 11* to clean the membrane under the conditions of TMP 2 bar, 50 °C , CFV 0.58 m s^{-1}, the permeate flux was about 45 LMH.

Cleaning agent temperature, the concentration of cleaning fluids, and the TMP, were tested to determine the best cleaning operating conditions using the large apparatus. The main findings are concluded in the following paragraphs. The optimum cleaning conditions for both membranes are summarized in Table 3.4.

Table 3.4 The summary of the optimal cleaning conditions for PSF and FS 50PP membranes

Membrane / Cleaning conditions	PSF (30 kD)	FS 50PP (30 kD)
Cleaning agent	NaOH solution	NaOH solution
Cleaning agent concentration (wt%)	0.2	0.2
Cleaning agent temperature (°C)	50	50
Transmembrane pressure (bar)	Lower TMP 1.0 bar	No trend

As far as PSF membranes (MWCO 30 kD) are concerned, sodium hydroxide of the concentration 0.2 wt% seemed to be the optimal cleaning concentration by referring to the comparison of the cleaning flux, pure water flux recovery and subsequent product flux. Higher cleaning temperature in the range from 30 °C to 60 °C resulted in higher permeate fluxes due to the viscosity variation with temperature. However, maximum of product flux was observed on the membrane after cleaning at 50 °C within this range. Membrane cleaning at 70 °C significantly changed the membrane resistance and the corresponding permeability. It is possible that the active layer swelled up after cleaning at this highest temperature used. The increased transmembrane pressure resulted in more cleaning solution passing through the membrane. Moreover, higher TMP probably caused the compaction of the deposit on the membrane, which made the cleaning less efficient. A higher pure water flux recovery was observed when 1.0 bar cleaning agent TMP was used, rather than a TMP of 2.0 bar.

For the FS50PP membrane, a higher concentration of sodium hydroxide cleaner lead to a higher flux recovery within the range tested. 0.3 wt% and 0.4 wt% NaOH, which are relatively higher concentrations tested, showed flux recoveries of over 100% after cleaning. This is presumably due to changes in membrane surfaces after cleaning. In terms of the product fluxes after cleaning, the increasing tendency also implied this possibility. Consequently, 0.2 wt% appeared to be the most appropriate concentration used for FS50PP membrane cleaning. A cleaning agent temperature of 50 °C resulted in a higher flux recovery than that recorded for 60 °C. The most likely explanation is that high temperature enhanced the absorption of polyphenols to the polyvinylpyrrolidone

(PVP) contained in FS50PP membrane. The membrane is therefore more difficult to clean at 60 °C. In this case, it is risky to use relatively high temperature, such as 60 °C during cleaning of fluoropolymer membrane. Furthermore, flux recovery was less sensitive to TMP changes after cleaning though the cleaning fluxes were higher at higher TMP values.

The inspection of PSF (MWCO 30 kD) membranes and FS50PP (MWCO 30 kD) membranes under TEM showed better cleanability of the former membrane than the latter. The surface of PSF membranes appeared to be smoother and more porous after cleaning. Although small amount of residues were visualized in the sub layer of membranes, the surface area was cleaned of deposits for PSF membranes. For FS50PP membranes, there was still certain amount of residues remaining on the membrane surface, which indicated poor cleaning of this membrane under the conditions tested.

Chapter 4 Product stabilities and qualitative analysis by gel filtration and High Performance Gel filtration Chromatography

4.1 Introduction

The optimisation of the conditions for membrane cleaning has been discussed in Chapter 3. However, the influence of membrane ultrafiltration on the product quality is not clear yet. From this point of view, the product stabilities, including the content of polyphenol and colour stabilities have been investigated in this chapter. The permeates from membrane ultrafiltration were also analysed by using gel filtration and High Performance Gel Filtration Chromatography with the aim to identify the composition in the products.

4.2 Experimental

4.2.1 Materials

Folin-Ciocalteu's phenol reagent, 2N, F9252-500ML from *Sigma*, UK

Sodium Carbonate Anhydrous (ACs reagent) from *Sigma-Alorich*, UK

3,4,5-Trihydroxybenzoic acid (Acide gallique), MW 188.14, $C_6H_2(OH)_3COOH{\cdot}H_2O$, general purpose grade from *Fisher*, UK

Ultra pure ProtoGel® 30% (w/v) (g/ml) Acrylamide : 0.8% (w/v) Bis-Acrylamide Stock solution (37.5 :1) Protein & Sequencing electrophoresis Grade (Gas stabilized) from *Bio – Rad*, UK

Mili Q H_2O

1.5M Tris pH8.8 buffer

0.5M Tris HCl pH6.8 buffer

10% SDS

10% Ammonium persulfate (m/v)

TEMED: N,N,N',N'-Tetramethylethylene-diamine 100mL, $C_6H_{16}N_2$ FW 116.2, 99% *Sigma*, UK

Silver Stain Kit for Polyacrylamide Gels, from *Sigma*, UK

Protein Quantification Kit-Rapid 51254 (*Sigma*, UK)

4.2.2 *Folin – Ciocalteu* assay (Referring to beverages standard analytical methods, SAM 945/005 V.4, 2003, provided by *Unilever*, UK)

The polyphenols in the tea extracts and permeate were determined colorimetrically using *Folin-Ciocalteu* reagent. The reagent consists of phosphor-tungstic acids as oxidants, which on reduction by readily oxidized phenolic hydroxyl groups yield a blue colour with a broad maximum absorption at λ 765 nm due to the formation of tungsten and molybdenum blues. As *Folin-Ciocalteu* reagent acts with a wide range of polyphenolic compounds, selection of a suitable standard enables useful total polyphenol data to be obtained. Gallic acid was chosen as standard in this assay. The methods are described in Appendix 9.7 (Peilow and Samuel, 2004).

4.2.3 The measurement of solid concentrations

The solid concentrations of tea solution and permeate were measured by weighing the mass of a certain amount of samples before and after drying in the 77 °C oven for 48 hours.

4.2.4 Colour analysis of tea product

Colour parameters, namely lightness (L^*), redness (a^*), and yellowness (b^*) values of the permeates collected from different ultrafiltions were determined by using UVPC Color Analysis Personal Spectroscopy Software (Version 3.0). For comparison, the

colour parameters of the tea solutions of equivalent solid concentrations were also measured under the same conditions. The specific operations are as follows:

The sample was scanned from 200 nm to 900 nm under the transmission mode in a UV – visible spectrophotometer (Shimazu 1601). The data was saved and then analysed by UVPC Color Analysis software to determine the L^*, a^* and b^* values. The content of haze was also indicated by the absorbance of sample at 900 nm.

4.2.5 Protein quantification based on Coomassie Brillant Blue G (CBB) assay

This assay was performed by referring to the protocol of Protein Quantification Kit-Rapid 51254 (*Sigma*, UK) and Bradford, 1976.

As a popular, simple and reproducible assay for quantification of proteins, CBB protein assay is based on the binding of Coomassie brilliant blue G dye (CBBG) and specific amino acid residues which are exposed on the surface of the protein under acidic conditions. Because of the six phenyl groups and two sulfonic acid groups contained in the dye molecule, the interactions are generally noncovalent, and normally occur via hydrophobic (Tryptophan, Tyrosine, Histidine and phenylalanine) and electrostatic (arginine, Lysine) residues. Coomassie blue, in its protonated form, has a maximum absorption of light at 465 nm. However, after interacting with protein, the maximum change in the absorbance of the complex becomes 595 nm. The staining reaction is completed within 1 min and colour is stable for 30 minutes. Therefore, the amount of protein can be easily detected by a spectrophotometer under this wavelength. (http://sbio.uct.ac.za/Sbio/documentation/Bradford%20assay.html).

The protein detection range is from 10 $\mu g\ mL^{-1}$ to 5000 $\mu g\ mL^{-1}$ by standard method, and is from 0.1 $\mu g\ mL^{-1}$ to 50 $\mu g\ mL^{-1}$ by micro method. Bovine serum albumin (BSA) is used as standard protein for calibration. This method is relatively reliable and unaffected by many chemicals, such as sucrose, urea, and glycerol. However, due to the fact that the sensitivity of this assay also depends on the type of proteins, there might be protein – to – protein variation during quantification (Protein quantification kit-rapid protocol, *Sigma*, UK). The detailed procedures of both standard and micro assay are explained in Appendix 9.8.

4.2.6 Sodium dodecyl sulphate - PolyAcrylamide Gel Electrophoresis (SDS-PAGE)

Sodium dodecyl sulphate - PolyAcrylamide Gel Electrophoresis is a typical method in separating and identifying protein under denaturing conditions. As an anionic detergent, sodium dodecyl sulphate (SDS) denatures proteins and confers a negative charge to the polypeptide in proportion to its length. The binding mass ratio of SDS to proteins is 1.4:1. As a result, the denatured polypeptides become equally negative charged and have similar shapes. When electrophoresis is undertaken, migration of denatured protein is determined not by intrinsic electrical charge but only by molecular weight. The rate of migration also depends on the size of molecules rather than the nett charge or the shape of polypeptide during electrophoresis. Therefore, proteins of different sizes can be easily separated by this method (http://en.wikipedia.org/wiki/SDS-PAGE).

The molecular mass of unknown protein can also be determined in SDS – PAGE. There is a linear relationship between the logarithm of the molecular weight of an SDS-denatured polypeptide and its Rf. The Rf is calculated as the ratio of the distance migrated by the molecule to that migrated by a marker dye-front. Consequently, by plotting a standard curve of distance migrated against lg(MW) for known samples, the relative molecular mass of unknown sample can be calculated according to the distance migrated on the sample gel (Coyne, *et al.*, 1996). The protocols for SDS – PAGE and subsequent silver staining are given in Appendix 9.9 (Thompsett, 2005 and ProteoSilverTM Stain Kit protocol, *Sigma*, UK).

4.2.7 Qualitative analysis of tea, permeate and retentate after ultrafiltration by gel filtration

With the initial intention of analyzing tea haze contained in the tea powder before and after ultrafiltration, gel filtration was selected as a separating tool in the first step as tea haze is considered to be the complex of polyphenols and tea protein.

Gel filtration is a method that separates molecules according to their size and shape. It is also referred to as molecular sieve chromatography, and is commonly used as an analytical method to determine the molecular mass of an uncharacterised molecule. The gel filtration matrix, namely the stationary phase of the chromatograph, consists of

microscopic beads containing pores and internal channels. Larger molecules tend to flow around and in between the beads, while smaller molecules tend to spend more time in the maze of channels and pores in the bed. Consequently, the smaller, lower molecular weight molecules are eluted from the column after larger molecules.

Before fractionation of samples by gel filtration, it is important to pack the chromatography column with gel beads symmetrically. To do so, the beads presented in the chosen buffer are poured into the chromatography column of suitable dimensions slowly, and allowed to settle by gravity. Once the packing is finished, it is necessary to wash and equilibrate the column by buffer overnight. After that, the sample dissolved in buffer can be applied to the top of column and the eluate is collected in a series of fractions (Gel filtration principles and methods. Amersham Biosciences. www.acabs.dk/submenus/Files/Gel%20filtration%20Amersham.pdf).

The matrices available for gel filtration are of great variety. To obtain the optimal separation of sample investigated, it is critical to choose proper type of gel. Use of an inappropriate gel type will result into the poor resolution of fractionation. From this point of view, five different kinds of beads were used in our experiments so as to find out a suitable matrix for the samples examined. They were Bio-gel P60, Sephadex G-100, Sephadex G-75, Sepharcyl HR 100 and Sepharcyl HR 200. The separation ranges of the beads above are showed as follows (www.life.sci.qut.edu.ac/epping/LSB 6070LT/607GFCmedia.html):

Table 4.1 The fraction range of different gel filtration beads

Name medium	Type of matrix	Particle size of hydrated beads (μm)	Fraction range for globular proteins (Da)
Bio-gel P60	Polyacrylamide	90-180	1000-6000
Sephadex G-75	Dextran	40-120	1000-50000
Sephadex G-100	Dextran	40-120	1000-100000
Sepharcyl HR 100	Corss-linked allyldextran/ bisacrylamide	25-75	1000-100000
Sepharcyl HR 200	Corss-linked allyldextran/ bisacrylamide	25-75	5000-250000

For each of the gel filtration experiment, the sample injected into the column was prepared by dissolving the freeze-dried powder from feed solution or permeate or retentate, which were from the ultrafiltration of black tea liquor on PSF (MWCO 30 kD) membrane, in 0.01 M acetate buffer at a pH of 5.0. The eluate was connected to a flow cell which was emplaced in a UV – visible spectrophotometer (*Shimadzu* 1601), in order to record the absorbance of eluate at the wavelength of 280 nm. The fractions were then collected for further analysis. The calibration curve was obtained by injecting a series of standards including Immunoglobulin (IgG, MW: 150000 Da), Bovine serum albumin (BSA, MW: 66000 Da), Chicken egg albumin (Ovalbumin, MW: 43000 Da), Blue dextran (MW: 17000 Da), Lysozyme (MW: 14000 Da), Cytochrome C (MW: 12000 Da) and PEG-blue (MW: 4000).

4.2.8 High Performance Gel Filtration Chromatography

High performance gel filtration chromatography is a more precise technique for separating and analysing protein, peptides or other biological macro-molecules. To achieve higher exactitude for this analysis, the samples injected are required to be relatively pure. Therefore, this high performance gel fltration chromatography was applied to analyse the fractions of tea, permeate and reatentate from gel filtration column mentioned above.

TSK – gel SEC columns are well known and have demonstrated good results for gel filtration of various biological macro-molecules. There is a great variety of TSK – gel SEC columns available as shown in Table 4.2.

Table 4.2 TSK gel filtration column

Column type	MW separation range		Common Applications
	Proteins	Dextrans	
TSK gel G1000 PW	< 2K	-	Water-soluble polymers Polysaccharides, Nucleic Acids, Basic Protein
TSK gel G 2000 PW	< 5K	-	
TSK gel G 3000 PW	500-800K	<60K	
TSK gel G 4000 PW	10K-1500K	1K-700K	
TSK gel G 5000 PW	< 10,000K	50K-7000K	

TSK gel G5000 PWXL 7.8mm (ID × 30 cm) was selected finally in this part of study. The TSK-PW series are particularly suitable for smaller peptides (< 1000 Da), protein aggregrates, DNA fragments and viruses. The running conditions were as follows:

Buffer: 0.2M phosphate buffer, pH 6.7;

Flowrate: 0.5mL min^{-1};

Temperature: 22 °C.

4.3 Results and discussion

4.3.1 Stabilities of phenolic components and colour paramenters of products from ultrafiltrations on PSF membrane and FS membrane

To compare the efficiency of PSF and FS membranes of the same molecular weight cut off, the stabilities of products, (including the stabilities of total polyphenols and the colour parameters) have been investigated.

Prior to the measurements on ultrafiltration products, the sensitivity of UV-spectrophotometer was determined by measuring the absorbance of gallic acid standard solution of a concentration of 30 μg ml^{-1} for five times at λ 765 nm. The averaged value was 0.121, and the corresponding standard deviation was 0.004. This indicated the relatively high accuracy of UV-spectrophotometer. Figure 4.1 - 4.4 show the relatively good stabilities of total polyphenols and colour, namely lightness, redness, and yellowness in two different products. The averaged concentrations of total polyphenol in the permeates from PSF membrane and FS membrane were 1257 and 1673 μg ml^{-1} respectively. According to the comparison of colour parameters, the product obtained from PSF membrane ultrafiltration appeared to be lighter, less reddish and less yellowish, indicating that more components were retained by the PSF membrane than by fluoropolymer membrane. This is in accordance with the results of the measurement of solid concentrations remained in both permeates, which are 0.78 wt% and 0.92 wt% for PSF and the FS permeate respectively. The minus values of redness (a^*) shown in Figure 4.3 implied that the permeate from PSF membrane ultrafiltration was not red enough to be detected.

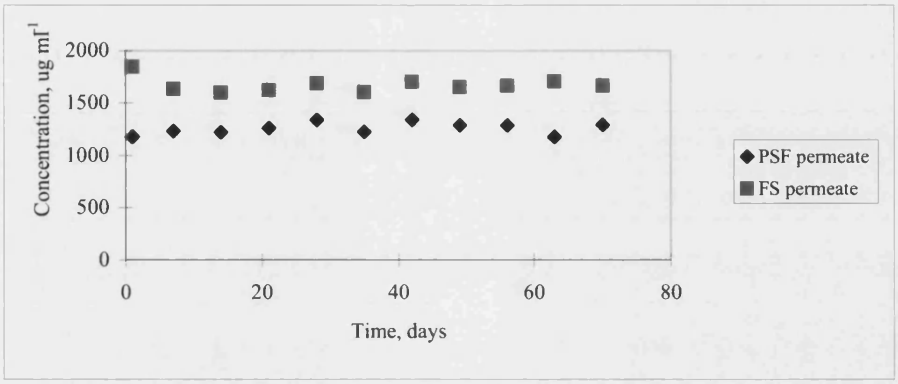

Figure 4.1 The stabilities of total polyphenols in the permeates from PSF and FS membranes

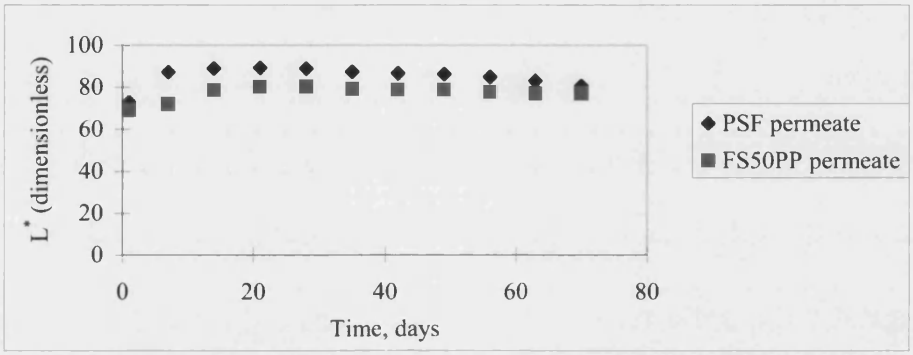

Figure 4.2 The stabilities of lightness (L^*) colour in the permeates from PSF and FS membranes

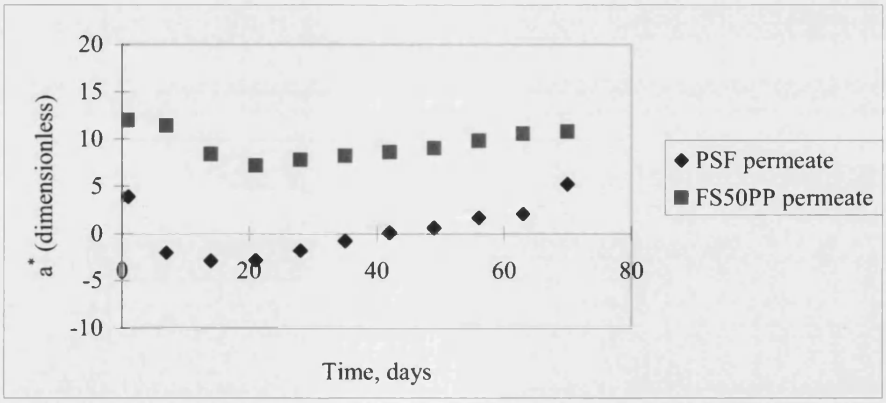

Figure 4.3 The stabilities of Redness (a^*) colour in the permeates from PSF and FS membranes

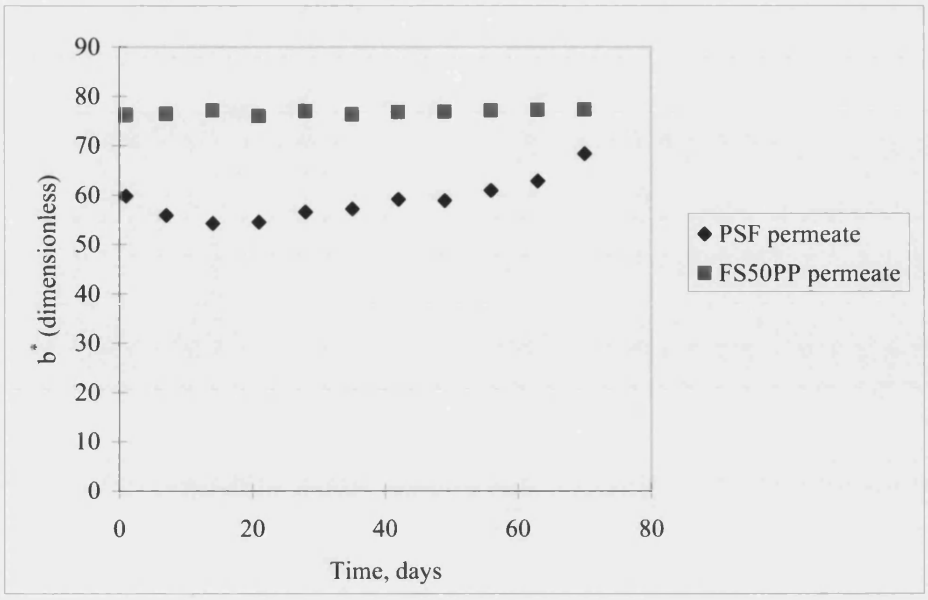

Figure 4.4 The stabilities of yellowness (b^*) colour in the permeates from PSF and FS membranes

To further investigate the effect of membrane ultrafiltration, the colour parameters as well as the haze of the permeates from both membranes and the tea solutions of equivalent solid concentrations were compared in Table 4.3. From this table, the permeates were much lighter, less reddish and more yellowish than their corresponding tea solutions. As mentioned in Chapter 2, TFs are mainly responsible for the yellowish colour, while TRs contribute more to the reddish colour. The changes of a^* and b^* values indicated the retention of large molecules (TRs) but the transmission of relatively small molecules namely TFs during membrane ultrafiltration. Haze was measured via the absorbance at 900 nm. As shown in the table, the absorbance values for both permeate samples were 0.005 and 0.006 respectively, which are much lower than those for the tea solutions of equivalent solid concentrations. Considering the accuracy of the readings from UV-spectrophotometer, there was almost no haze measurable in these permeate samples. Figure 4.5 demonstrated the stabilities of tea haze in the permeates from PSF and FS membrane ultrafiltration. The values fluctuated slightly around zero as both samples were too clear to give sufficient absorbance. This indicated that no haze was observed in both permeates for more than two months.

Table 4.3 Comparison of colour parameters and haze of the permeates and the corresponding tea solutions of equivalent solid concentrations

Colour parameter / Tea samples	Lightness (L^*) (dimensionless)	Redness (a^*) (dimensionless-)	Yellowness (b^*) (dimensionless)	Haze (dimensionless absorbance unit)
PSF permeate (solid concentration 0.78 wt%)	72.8	3.90	59.8	0.005
0.78 wt% tea	16.3	26.2	27.8	0.329
FS permeate (solid concentration 0.92 wt%)	69.2	12.0	76.2	0.006
0.92 wt% tea	7.79	22.4	13.3	0.447

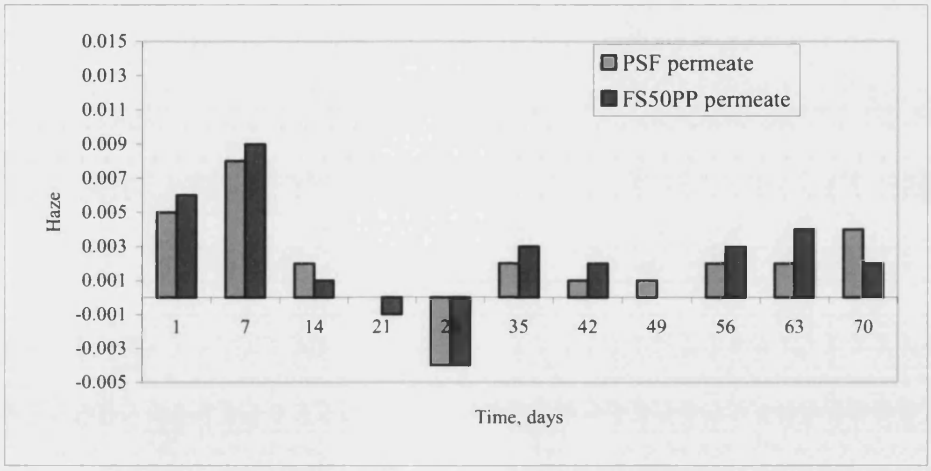

Figure 4.5 The observation of tea haze in the permeates from PSF and FS membranes

4.3.2 The qualitative analysis of tea product before and after ultrafiltration by gel filtration

According to the studies of stabilities of permeates from ultrafiltration of black tea on PSF membrane and FS50PP membrane, both membranes appeared to be effective on ultrafiltration in terms of removal of haze and maintenance of polyphenol and colour in the products after ultrafiltration. However, the FS50PP membrane appeared to be more difficult to be cleaned by standard NaOH cleaning procedure as shown in previous chapter. Therefore, subsequent studies have focused on the polysulphone membranes, together with the filtration products obtained from this membrane.

With the expectation of separating tea haze so as to further understand the influence of ultrafiltration on product compositions, the permeate, retentate as well as the feed solution were collected from the ultrafiltration of 2 wt% tea solution by using a polysulphone membrane at 50 ºC, TMP 3 bar for 30 minutes. These samples were all freezed dried and then made up into solutions of certain concentrations by using buffer solution as required for gel filtration.

4.3.2.1 Selection of proper type of beads for gel filtration

As mentioned previously, the separating capabilities of five different gel filtration columns have been investigated here. The first gel filtration column chosen was Bio-gel P6, which are porous polyacrylamide beads derived from copolymerzation of acrylamide and N, N'-methylene-bis-acrylamide. These gels are extremely hydrophilic, essentially free of charge and are able to separate the molecules within the range from 1000 to 6000 Da (www.life.sci.qut.edu.ac/epping/LSB 6070LT/607GFCmedia.html).

0.5 mL 4.35 mg mL^{-1} permeate dissolved in elution buffer, namely 0.01 M acetate buffer with pH 5.0 and ionic strength 100 mM, was injected into this column with a flowrate of 1 ml min^{-1} at 25 °C. The typical profile was displayed in Figure 4.6.

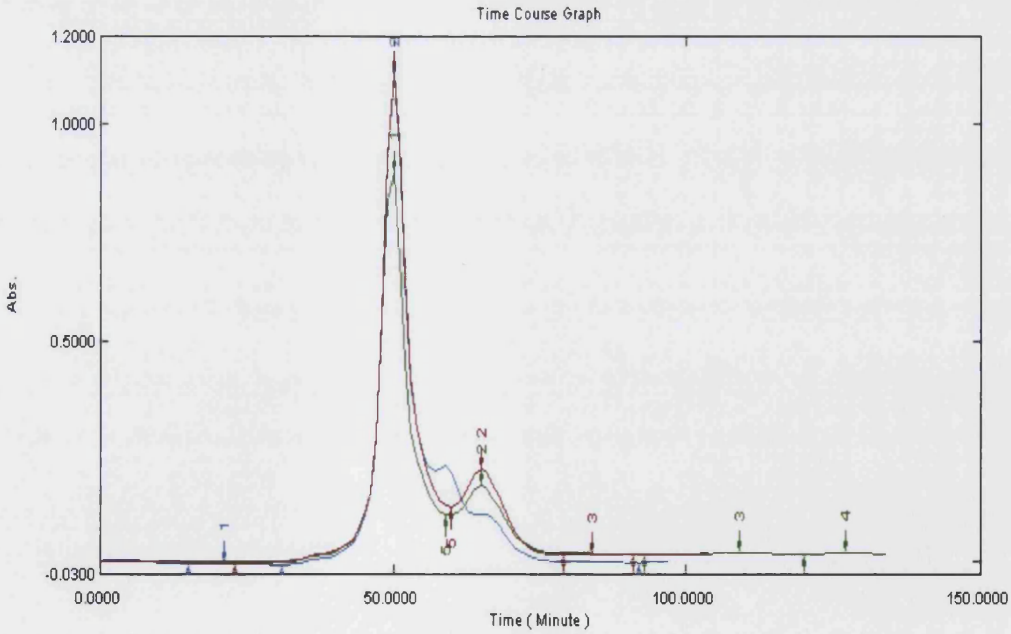

Figure 4.6 SEC profile on Bio-gel P6 column of the tea permeate (triple injections) at flowrate 1.0 ml min^{-1}, 25 °C, with 0.01 M acetate buffer pH 5.0 as mobile phase

From the graph, there were only two fractions at 68.9 minutes and 88.4 minutes respectively. These fractions were collected and scanned from 200 nm to 600 nm in a UV-visible spectrophotometer (*Shimadzu* 1601). The scanning spectrum of the first fraction showed the only one absorbance at around 273 nm. While the absorbance of the second fraction was at 265 nm. From these results, protein or amino acid may exist in the fractions as proteins in solution normally absorb ultraviolet light with absorbance maxima at around 280 nm. However, this needs further investigation. Compared with the scanning spectrum of polyphenol standard, these results also indicate the removal of pigment from the sample injected after gel filtration as there was absorbance near 400 nm when the polyphenol standard was scanned under the same conditions. This was also certified by the change of colour as the sample became colourless after passing through the Bio-gel P6 gel filtration column.

Because of the relatively small fraction range available for Bio-gel P6, other kinds of gel filtration beads had been taken into consideration in our study. Sephadex Gel-Filtration Resins are another series of highly specialized chromatographic media commonly used in the field of gel filtration. From a wide range of Sephadex G products available for gel filtration, Sephadex G 75 and Sephadex G 100 of fraction capabilities of 1000 – 50000 Da and 1000 – 100000 Da respectively, were selected here to separate the same sample applied on Bio-gel P6 column. Figure 4.7 and Figure 4.8 showed the SEC profiles obtained from these columns.

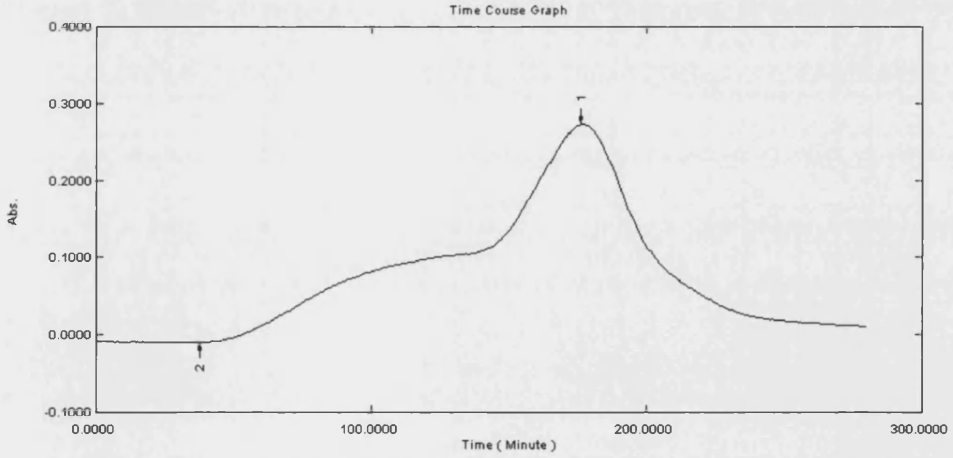

Figure 4.7 SEC profile on Sephadex G-75 column of the tea permeate at flowrate 1.0 ml min^{-1}

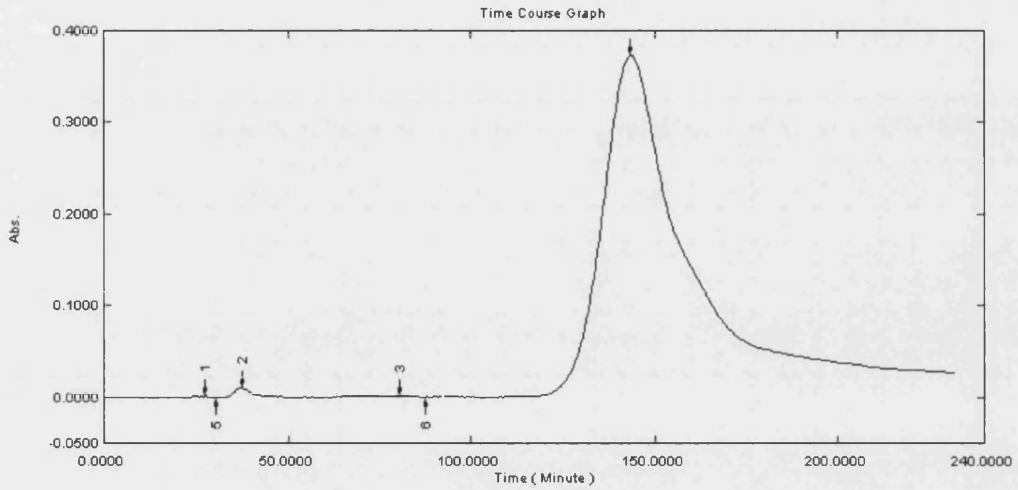

Figure 4.8 SEC profile on Sephadex G-100 column of the tea permeate at flowrate 1.2 ml min^{-1}

Unfortunately, Sephadex G 75 did not result in a clear fractionation of the sample. Meanwhile, the resolution of fractionation on Sephadex G100 was not sufficiently good compared to that of Bio-gel P6 gel filtration. This implied that Sephadex G gels, prepared by the crosslink of polysaccharide and dextran, are probably not suitable for the separation of tea product.

Despite of the disappointing results from Sephadex G columns above, some success in sample fractionation was achieved when an attempt was made on Sepharcyl HR 100, which is a versatile gel filtration media possessing a rigid hydrophilic matrix.

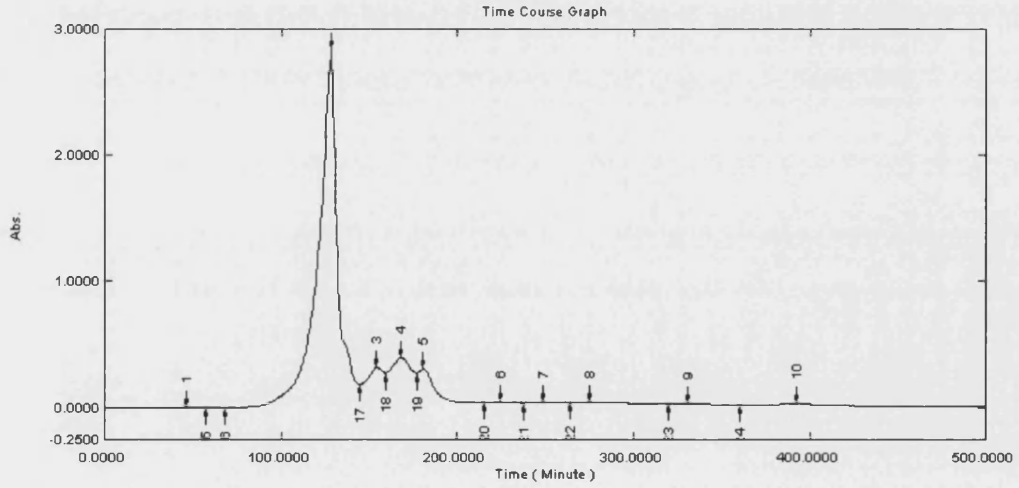

Figure 4.9 SEC profile on Sepharcyl HR 100 column of the tea 10mg.ml^{-1} at flowrate 1.2 ml min^{-1}

As shown in Figure 4.9, there were four fractions eluted from the column when 2 mL tea solution of concentration 10 mg mL^{-1} were injected and eluted by 0.01 M pH 5.0 acetate buffer with Ionic strength 100 mM at flowrate 1.2 mL min^{-1} at 25 °C. Similar resulted were displayed in Figure 4.10 when 4.35 mg mL^{-1} permeate as well as 10 mg mL^{-1} retentate were applied on the column with the operating conditions remained the same.

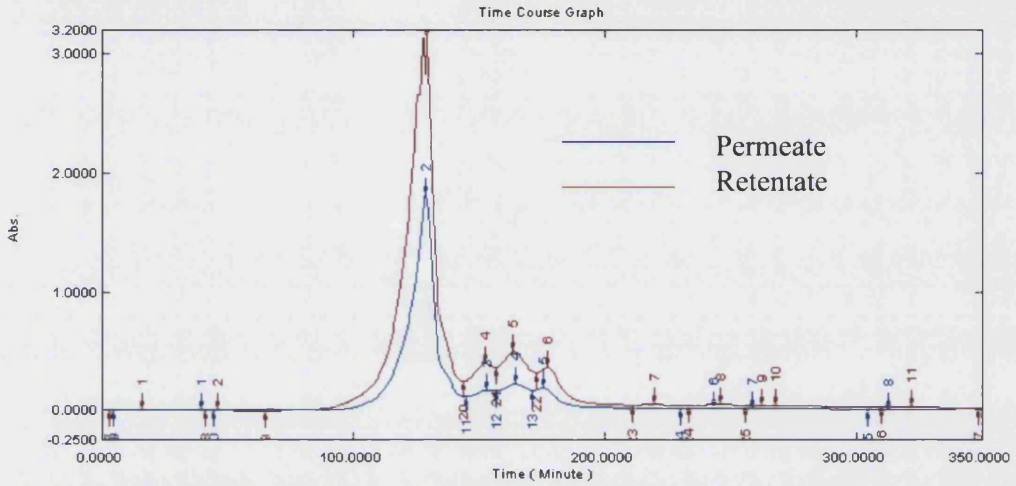

Figure 4.10 SEC profile on Sepharcyl HR 100 column of the tea permeate and retentate samples at flowrate 1.2 ml min^{-1}

To ensure the entire sample fractionation, all the samples above were injected into another column packed with Sepharcyl HR 200 gels, which offer even wider range of fractionation capability from 5000 Da to 250000 Da. However, the results resembled to those from Sepharcyl HR 100, giving the evidence that the samples had been fractionated at relatively higher resolutions on both columns. An example is shown in Figure 4.11.

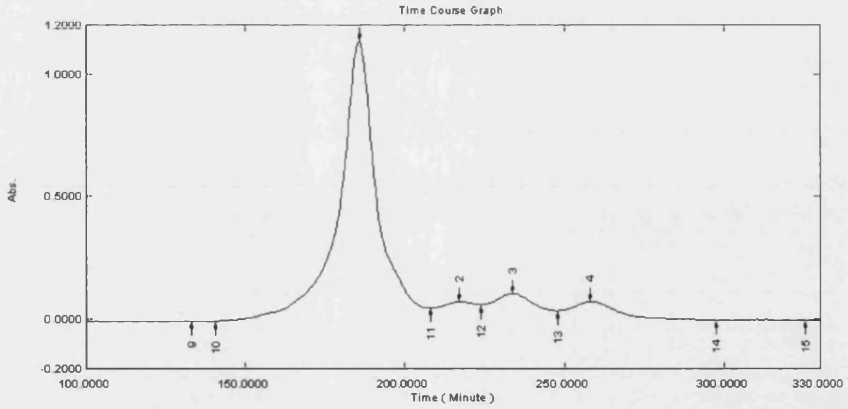

Figure 4.11 SEC profile on Sepharcyl HR 200 column of the tea permeate at flowrate 1.0 ml min^{-1}

To obtain basic understandings of possible compositions of fractions eluted from gel filtration, the fractions of the permeate, retentate and feed solutions from Sepharcyl HR 200 were all collected and scanned from 200 nm to 600 nm in a UV-visible spectrophotometer (*Shimadzu* 1601). The results presented the UV absorbances at around 220 nm and 280 nm for each fraction investigated. These are more or less the same as those from the fractions of permeate sample from Bio-gel P6 column, confirming the absence of coloured phenol components and possible existence of protein or amino acids.

As gel filtration can be used to estimate the molecular mass of unknown samples eluted from the column due to the linear relationship between lg(MW) and retention time, the molecular mass of the major fraction from the tea sample was calculated by referring to a series of protein standards. Figure 4.12 illustrates the calibration curve for the Sepharcyl HR 200 column. As the retention time for the major fraction from tea sample was 157 min, the molecular mass of this fraction was determined to be 5080 Da. Nevertheless, it should be noted that this value was only an estimation, as the elution of molecules from gel filtration will be affected not only by the size but also the shape of molecules.

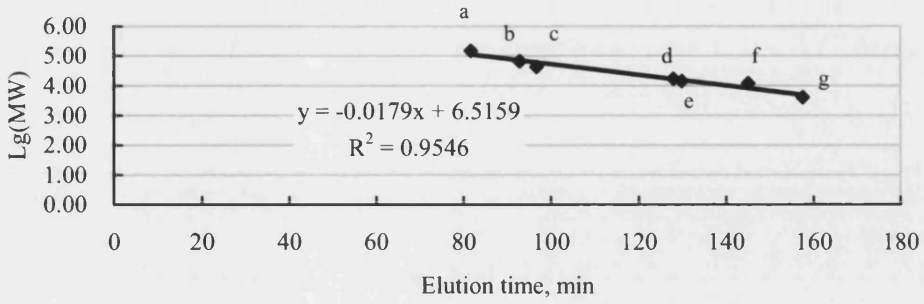

Figure 4.12 Calibration curve indicating the relationship between the logarithms of the molecular weights and retention times of the standards on S200 column: a. IgG; b. BSA; c. Ovalbumin; d. Blue dextran; e. Lysozyme; f. Cytochrome C; g. PEG-blue

4.3.2.2 Characterization of fractions from gel filtration on Sepharcyl HR 200 column

The composition of gel filtration fractions were assumed to consist of protein based components. However, this needs further investigation. As a result, SDS-PAGE, HPLC, CBB assay, and Polyphenol assay were subsequently conducted to analyse the fractions from gel filtration.

On the assumption that the gel filtration eluates were protein based species, the fractions were applied to SDS-PAGE according to the methods described in Appendix 9.9. However, no protein bands were observed on the SDS gels even after the samples had been concentrated using methanol and chloroform precipitation. This could be accounted for by the fact that the fractions obtained from gel filtration might be amino acid residues rather that protein. Consequently, the molecules were too small to be detected by SDS-PAGE.

Now that the gel filtration fractions might not be protein according to SDS-PAGE results, high performance liquor chromatography (HPLC) was used for further investigation. The column used for HPLC was a TSK gel G5000 column. By referring to the operation instruction along with the HPLC column applied, 0.2M phosphate buffer with pH 6.7, ionic strength 100 mM was selected as elution buffer. The flowrate was 0.5 mL min^{-1}. The HPLC profiles of different tea sample fractions from Sepharcyl HR 200 column were illustrated from Figure 4.13 to Figure 4.24. The differences between tea permeate fractions, retentate fractions and tea fractions were comparatively small. Therefore, instead of repeating all of the HPLC profile explanations, the HPLC

profiles of the four fractions from tea permeate were taken as an example, and full explanations were as follows.

In fraction 1 as showed in Figure 4.13, two peaks were obtained at 35 min and 44 min. However, in fraction 2, there were peaks at 22.2 min, 25 min, 28 min, 32 min, 34.5 min, and 43.5 min. While two peaks at approximately 21 min and 25 min were presented in both fraction 3 and fraction 4. Providing that fractions eluted from Sepharcyl HR 200 column were monomers, the retention time of the peaks observed in the HPLC profile of the latter fraction should be longer than those in the HPLC profiles of earlier fractions according to separating principle of gel filtration. In other words, if taking fraction 1 and 2 as examples, the molecular mass of the first fraction from Sepharcyl HR 200 column would be larger than that of second fraction if they were monomers. Then when fraction 1 and fraction 2 were injected into HPLC column, theoretically the peaks of fraction 1 would have been eluted earlier than those of fraction 2. Nevertheless, the results showed in HPLC profiles were totally opposite to the supposition above, implying that the fractions obtained from Sepharcyl HR 200 gel filtration were possibly compounds rather than monomers.

So what are the compositions of these compounds? To answer this question, both polyphenol and protein quantifications had been carried out on all the fractions from Sepharcyl HR 200 gel filtration. The results are displayed in detail in Table 4.4 and Table 4.5. According to the results of CBB assay, there were protein residues, namely amino acids contained in the fractions although the concentrations were very low, generally less than 1mg mL^{-1}. As to the results of *Folin-Ciocalteu* assay, there were also polyphenols detectable in the samples examined. Despite of rather low concentrations, these results indicated the existence of colourless phenol components as well as residues of protein or amino acids in the fractions from gel filtration.

Table 4.4 Concentration of protein contained in fractions of different tea samples

No of sample	Name of Sample	Concentration of protein detected (mg ml^{-1})
1	Tea permeate fraction 1	0.73
2	Tea permeate fraction 2	0.13
3	Tea permeate fraction 3	0.17
4	Tea permeate fraction 4	0.19
5	Tea retentate fraction 1	0.86
6	Tea retentate fraction 2	0.12
7	Tea retentate fraction 3	0.17
8	Tea retentate fraction 4	0.10
9	Tea fraction 1	0.58
10	Tea fraction 2	0.14
11	Tea fraction 3	0.18
12	Tea fraction 4	0.11

Table 4.5 Concentration of total polyphenols contained in fractions of different tea samples

No of sample	Name of sample	Concentration of phenols detected (µg ml^{-1})
1	Tea permeate fraction 1	2.24
2	Tea permeate fraction 2	3.25
3	Tea permeate fraction 3	2.45
4	Tea permeate fraction 4	4.26
5	Tea retentate fraction 1	3.86
6	Tea retentate fraction 2	1.79
7	Tea retentate fraction 3	3.66
8	Tea retentate fraction 4	1.84
9	Tea fraction 1	3.66
10	Tea fraction 2	2.24
11	Tea fraction 3	3.05
12	Tea fraction 4	2.04

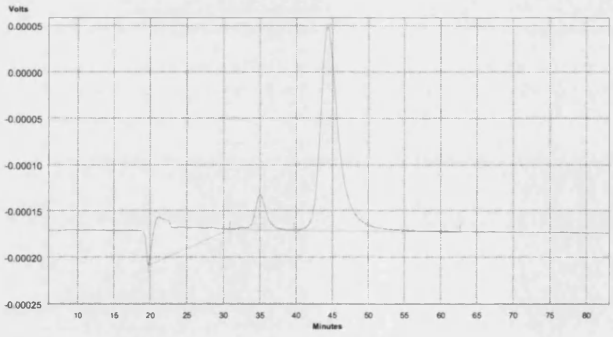

Figure 4.13 HPLC profile of the 1st fraction of permeate from S200 gel filtration column

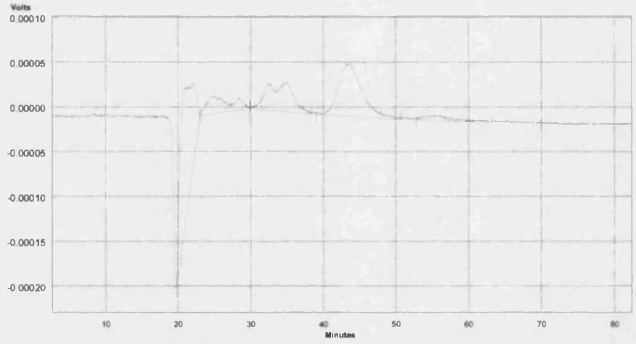

Figure 4.14 HPLC profile of the 2nd fraction of permeate from S200 gel filtration column

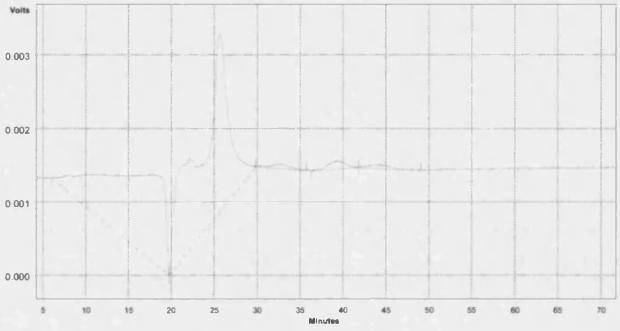

Figure 4.15 HPLC profile of the 3rd fraction of permeate from S200 gel filtration column

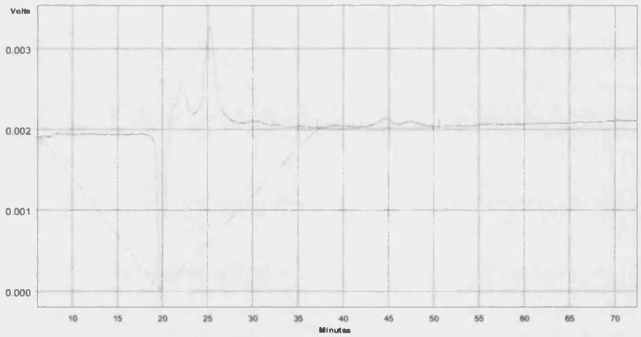

Figure 4.16 HPLC profile of the 4th fraction of permeate from S200 gel filtration column

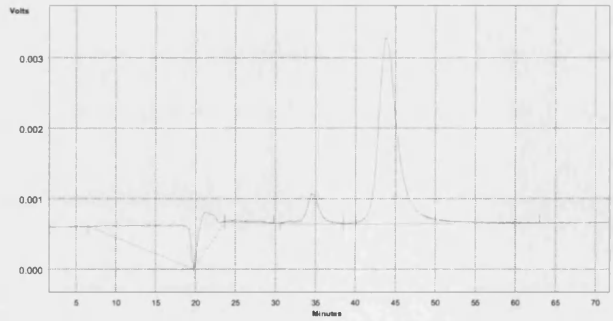

Figure 4.17 HPLC profile of the 1st fraction of retentate from S200 gel filtration column

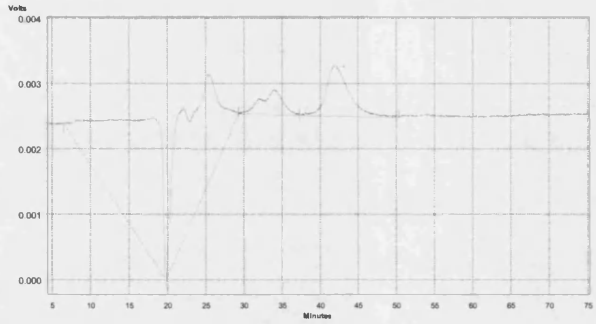

Figure 4.18 HPLC profile of the 2nd fraction of retentate from S200 gel filtration column

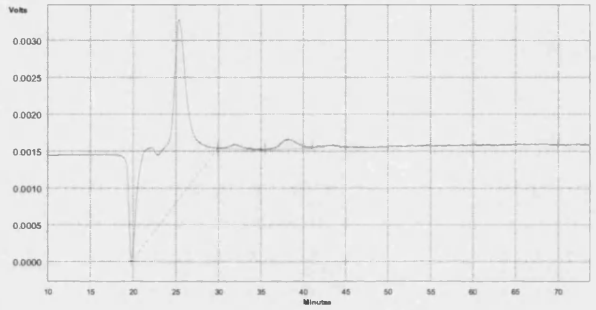

Figure 4.19 HPLC profile of the 3rd fraction of retentate from S200 gel filtration column

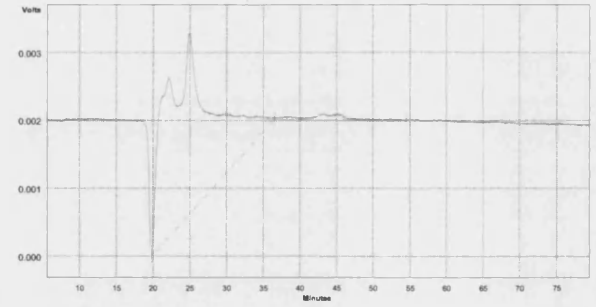

Figure 4.20 HPLC profile of the 4th fraction of retentate from S200 gel filtration column

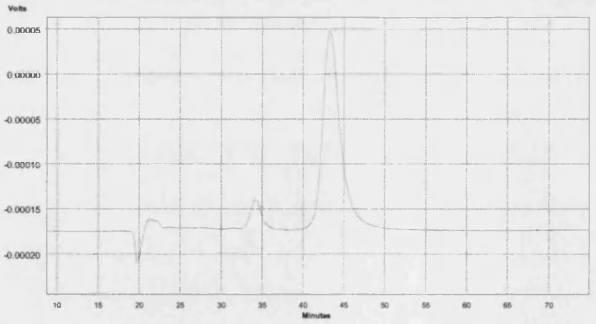

Figure 4.21 HPLC profile of the 1st fraction of tea from S200 gel filtration column

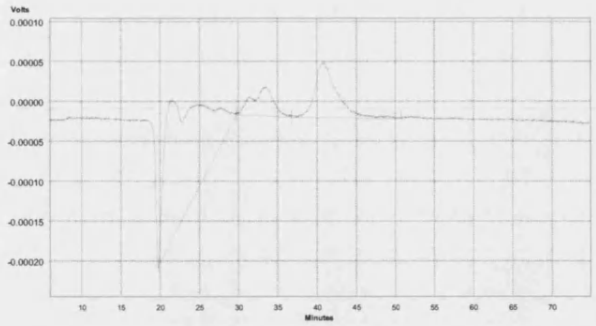

Figure 4.22 HPLC profile of the 2nd fraction of tea from S200 gel filtration column

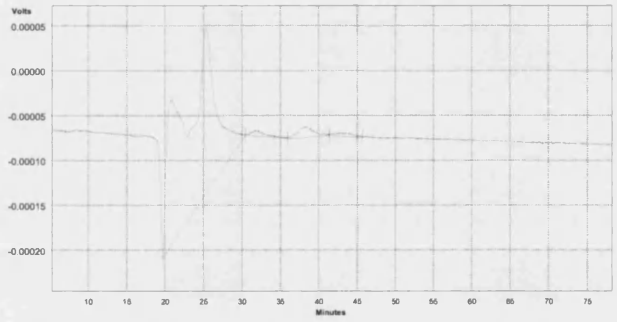

Figure 4.23 HPLC profile of the 3rd fraction of tea from S200 gel filtration column

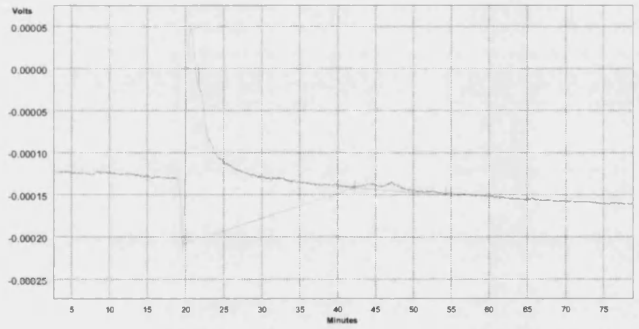

Figure 4.24 HPLC profile of the 4th fraction of tea from S200 gel filtration column

4.4 Conclusions

The colour and the content of total polyphenol of the permeates obtained from both PSF (MWCO 30 kD) and FS50PP (MWCO 30 kD) membranes were relatively stable during the period inspected. No haze was measured in these products for over two months investigated, indicating the efficiency of membrane ultrafiltration applied. The

concentration of total polyphenol contained in the permeate from FS50PP membrane was slightly higher than that in permeate from PSF membrane. The permeate from FS50PP membrane also appeared to be darker, more reddish and more yellowish compared with the product from PSF ultrafiltration. However, due to the better cleanability of the PSF membrane, it was chosen for the subsequent experiments.

The initial objective of the gel filtration experiments described in this chapter was to separate the tea haze from the feed, permeate and retentate solutions after ultrafiltration on polysulphone membranes (MWCO 30 kD). However, according to the analytical results from SDS-PAGE, high performance gel filtration chromatography, CBB protein quantification and *Folin Ciocalteu* assay, the use of gel filtration was unable to separate the haze from tea samples. The fractions eluted form Sepharcyl HR 200 column were probably the compounds of colourless phenol components and amino acids. The molecular mass of the major fraction was approximately 5000 Da.

Chapter 5 Separation and purification of tea protein and polyphenol species and the study of their binding capabilities by ITC

5.1 Introduction

Although numerous studies have been reported in the literature concerning haze formation in beverages, few have involved tea products. The direct separation of tea haze from the tea product by using gel filtration did not succeed as described in Chapter 4. Therefore, the objectives of the experiments described in this chapter were to use a range of techniques to isolate both protein and polyphenols independently from spray dried black tea powder; then to understand the mechanism of interaction between tea proteins and polyphenols by resorting to Isothermal Titration Microcalorimetry (ITC).

5.2 Experimental

5.2.1 Materials and chemicals

Lipton's spray dried instant tea powder, produced in Sri Lanka, manufactured and shipped by *Unilever Bestfoods*, UK

A mixed theaflavin standard was provided by *Unilever Bestfoods*, UK

5.2.2 Separation of tea protein

20 g of *Lipton*'s spray dried instant tea powder was extracted using 200 ml of a 1 wt% NaOH solution. The extracted solution was centrifuged at 20000 rpm at 4 °C using a *Koolspin* centrifuge (*Biotech Instruments Ltd*, UK) for 10 minutes. The supernatant was collected, and precipitated by adding saturated $(NH_4)_2SO_4$ solution (42.9 wt%) until the protein began to be salted out. It was subsequently stored in a refrigerator at 4 °C for 24 hours. Thereafter the precipitate was dialyzed against distilled water using dialysis

tubing (DTV01350, *Medicell International Ltd*, UK) of molecular weight cut off (MWCO) 1350 Da for 8 days. Tea protein powder was finally generated by freeze drying the dialysed solution.

5.2.3 Estimation of molecular mass of tea protein by Gel filtration chromatography

The freeze-dried tea protein powder was dissolved in 0.2 M phosphate buffer at a pH of 6.8. The dissolved protein sample with a final concentration 1.0 mg ml^{-1} was injected into G4000 PWXL gel filtration column with a Shimadzu HPLC system, and UV-VIS Detector (SPD-10AV VP *Shimadzu*, UK) at 280 nm. The calibration curve was obtained by injecting a series of proteins, including thyroglobulin bovine (669 kD), apoferritin from horse spleen (443 kD), β- amylase from sweet potato (200 kD), alcohol dehydrogenase from yeast (150 kD), bovine serum albumin (BSA, 66 kD), carbonic anhydrase from bovine erythrocytes (29 kD), and lysozyme from chicken egg white (14.3 kD).The details are given in Table 5.1.

Table 5.1 Running conditions of gel filtration HPLC analysis of tea protein sample

HPLC column	TSK Gel G4000 PW_{XL}, 7.8 mm ID x 30 cm, *Tosoh Bioscience Ltd*
Injection volume	20 μL
Column temperature	25 °C
Mobile Phase	0.2 M phosphate buffer, pH 6.8
Flow rate	0.6 mL min^{-1}

5.2.4 Determination of molecular mass of tea protein by Sodium Dodecyl Sulfate Polyacrylamide Gel Electrophoresis (SDS-PAGE)

The freeze-dried tea protein powder was dissolved in 10 mM Acetate buffer with pH 5.0 and ionic strength 0.1 M to obtain a concentration of 10 mg ml^{-1}. The protein sample and broad range molecular mass standard (*Bio-Rad*) were applied to SDS-PAGE by using 17% separating gel with 4% stacking gel. The gel after electrophoresis was visualized by Coomassie Blue staining and silver staining (ProteoSilverTM Silver Stain Kit, *Sigma*, UK) afterwards.

5.2.5 Protein quantification by Coomassie Brilliant Blue (CBB) Assay

This assay was depicted in detail in Appendix 9.8.

1.7 mg freeze-dried tea protein powder was dissolved in 10 mM pH 5.0 Acetate buffer. The colourimetric detection was carried out in a UV-visible spectrophotometer (*Shimadzu* 1601) at 600 nm. The standard curve was obtained by plotting the absorbance values of CBB with BSA (*Sigma*, UK) against known protein concentrations.

5.2.6 Determination of possible secondary structure using FTIR

Fourier Transform Infrared Spectroscopy (FTIR) was used to compare the functional groups and structure of tea protein separated above with pure proteins. It was performed on a *Bruker*-equinox 55 FT-IR spectrometer. The freeze-dried samples were finely ground with 100 times its bulk of pure potassium bromide and the mixture pressed into tablets under vacuum. For each sample, 100 scans were recorded from 4000 to 600 cm^{-1} with a resolution of 2 cm^{-1}.

5.2.7 Separation of tea polyphenol by Zn^{2+} precipitation

This separating method is based on the initial formation of aggregates of Zn^{2+} and phenolic hydroxyl groups under alkali conditions, and subsequent degradation of these precipitations when pH is adjusted to acidic conditions. The principle can be illustrated by following equations:

$$n\ R\text{-}OH + M^{n+} \rightleftharpoons M(R\text{-}O)_n \downarrow + n\ H^+ \rightleftharpoons n\ H_2O$$

$$M(R\text{-}O)_n + n\ H^+ \rightleftharpoons n\ R\text{-}OH + M^{n+}$$

5 gram of *Lipton*'s spray dried tea powder was dissolved in 500 ml boiling distilled water, and stirred on a hot plate for 30 minutes. 2.5 g of $ZnCl_2$ was added into the dissolved tea solution. Then the pH of solution was titrated to 7.5 by using 5% $NaHCO_3$ gradually in order to fully settle polyphenols contained in the solution. The precipitation was collected after 10 minutes centrifugation at 20000 rpm at 4 °C, and then acidified using 6 M hydrochloric acid until the pH paper appeared to be red (pH ≈ 1-2). After

that, the sample was extracted by ethyl acetate of the same volume twice, followed by rotary evaporation under vacuum and freeze drying.

5.2.8 Assessment of total polyphenol

The concentration of polyphenols in the samples separated by cation precipitation was determined colorimetrically using a *Folin-Ciocalteu* Assay (detailed method described in Appendix 9.7). Polyphenol samples of 0.01g were dissolved in 25 ml of hot distilled water (60 °C) with 1ml acetonitrile added to stabilize the solution. Following cooling down to room temperature, the sample was made up to 50 ml in a volumetric flask with distilled water, then diluted 1 in 10. A 1 ml tea polyphenol solution with final concentration 0.02 mg ml^{-1} was mixed with 5 ml of 10 – fold diluted *Folin-Ciocalteu* reagent for 6 minutes, and 4 ml of 7.5 % Na_2CO_3 solution was then added to stop the reaction. The assay mixtures were allowed to stand for one hour before the absorbance at 765 nm was measured in a UV – visible spectrophotometer (*Shimadzu* 1601). The standard solutions for calibration were prepared with gallic acid solutions of concentrations ranging from 0 to 60 μg ml^{-1}. To improve the measurement of purity of the sample separated by cation precipitation, 0.1 mg ml^{-1} of black tea solution was also analysed as a reference.

5.2.9 Determination of components in separated tea polyphenol samples by Reverse Phase High Performance Liquid Chromatography

The tea polyphenol powder mentioned above was dissolved in acetonitrile stabilizer solution, made of 2 % glacial acetic acid, 20 % acetonitrile, and 0.25 g L^{-1} of ascorbic acid and 0.25 g L^{-1} EDTA. This was subsequently filtered using a 0.2 μm prefilter (FP 30/0.2 CA-S, *Schleicher & Schuell*, UK). The filtrate was injected into a Gilson 715 HPLC system to determine the contents of polyphenols. Further details are given in Table 5.2.

Table 5.2 Running conditions of Reverse Phase HPLC analysis of separated tea polyphenol samples

HPLC column	KR100-5C18-4498, *Hichrom*, UK
Injection volume	20 µL
Column temperature	25 °C
Mobile Phase	20% solvent A – 2% acetic acid in acetonitrile 80% solvent B – 2% acetic acid in distilled water
Flow rate	1 ml min^{-1}
Detector	UV detector *(Gilson* Model 116, UK) at 274 nm
Sensitivity	2.0%

5.2.10 Characterization of binding interaction by Isothermal Titration Calorimeters

The binding properties of tea protein towards the theaflavin standard and the polyphenol mixture separated from tea powder were studied using Isothermal Titration Calorimetry (ITC) in an OMEGA ITC instrument (*Microcal Ltd*).

5.2.10.1 The interaction of theaflavin standards and tea protein under different concentrations and pH environments

The influence of tea protein concentrations on binding reactions with the theaflavin standard was studied at pH 5.0, a value corresponding to that present during tea extraction. Tea protein was dissolved in 5 mM pH 5.0 acetate buffer of ionic strength 100 mM at room temperature, filtered with a 0.2 µm syringe filter (FP 30/0.2 CA-S, *Schleicher & Schuell*, UK) and the monomer concentrations (MW:11 kD) were adjusted to 0.251 mM, 0.502 mM and 0.593 mM before use. The titrant sample of mix theaflavin standard (average molecular mass 768.1 g mol^{-1}), was diluted to a final concentration of 3.520 mM. Titrations were run at 25 °C, and all the samples degassed at 15 °C prior to use. In each case, 50 injection of 4 ml of mixed theaflavin solution were automatically added at 2 minutes intervals into the tea protein solution stirred at 300 rpm to ensure thorough mixing. The heat evolved after each injection was measured by the cells feedback network as differential heat effects between sample and reference cell.

The effect of different pH environments upon binding abilities was also studied by preparing a 0.502 mM tea protein solution and a 3.52 mM theaflavin solution in 5 mM acetate buffers of pH 4.0, 5.0 and 5.5.

In all cases, control experiments were carried out using identical theaflavin injections into a cell-containing a buffer without protein and the relative heats of dilution and mixing were subtracted from the heats of binding relative to the actual titration experiment.

5.2.10.2 Binding model of tea protein and tea polyphenols

Assuming that the molecular mass of the tea polyphenol powder was the same as the theaflavin standard (768.1 g mol^{-1}), 3.52 mM of tea polyphenol solution prepared in 5mM acetate buffer at pH 5.0 was titrated into the sample cell where 0.0133 mM tea protein was placed as a sequence of 50 injections of 4 µl aliquots at 300 rpm. The duration of each injection was 4 seconds, and the interval between each successive injection remained 2 minutes.

The titration of tea polyphenol into the buffer was also conducted as a control experiment. The corrected experimental data have had the corresponding control subtracted.

The final experiment result, represented by heat developed versus the cell ligand ratio, was fitted to a theoretical curve by using three in-built curve fitting models. These were (i) one set of sites per monomer, (ii) two sets of sites per monomer and (iii) sequential binding sites per monomer models, provided by Origin ITC Data Analysis Software (*Microcal Ltd*).

5.3 Results and discussion

5.3.1 Analytical results for tea protein

5.3.1.1 Gel filtration chromatography

As introduced in Chapter 4, gel filtration is a simple and easy method to separate a wide range of biological molecules, especially proteins, based on the differences in their size and shape. Due to the linear relationship between lg(protein molecular weight) versus elution time, gel filtration is also used as a general method to determine the molecular weight of unknown protein by reference to the standard curve obtained from standard proteins of known molecular masses. However, it should be borne in mind that the shape of protein molecules has an important impact upon gel filtration. Generally, polypeptides and proteins of long or extended structures tend to behave as if they were larger than globular protein molecules. Therefore a calibration curve is only as accurate as the nature of the protein standards used to construct it will allow.

The TSK Gel PW_{XL} column applied in this study is polymer-based, and is designed for size exclusion chromatography of water soluble polymers, for example proteins, peptides polysaccharides, DNA, RNA and so on. The molecular weight separation range for G4000 PW_{XL} column of globular proteins is from 10 to 1500 kD. The logarithm values of the molecular weights of the protein standards and tea protein sample against retention times were plotted in Figure 5.1. From the graph, the molecular weight of the tea protein dissolved in 0.2 M pH 6.8 phosphate buffer was calculated to be approximately 22.2 kD.

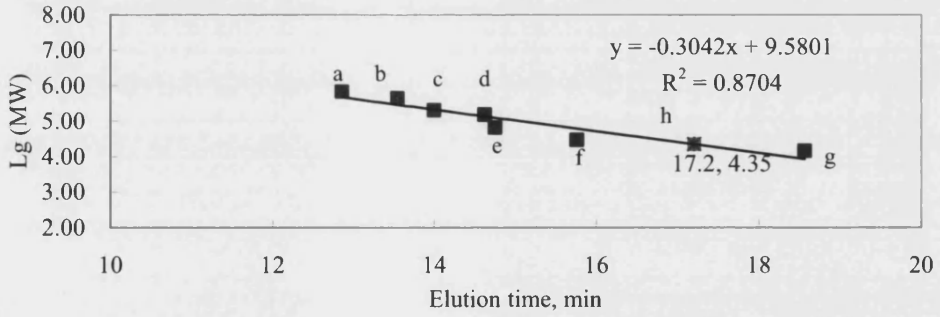

Figure 5.1 The relationship between the logarithms of the molecular masses and retention times of the protein standards and tea protein sample on TSK G 4000 PW_{XL} column: (a) Thyroglobulin Bovine (669 kD), (b) Apoferritin from horse spleen (443 kD), (c) β- Amylase from sweet potato (200 kD), (d) Alcohol Dehydroegenase from yeast (150 kD), (e) BSA (66 kD), (f) Carbonic Anhydrase from Bovine Erythrocytes (29 kD), (g) Lysozyme (14.3 kD), (h) tea protein

5.3.1.2 SDS-PAGE results

Seventeen vol% SDS-PAGE preparative gel was used to purify the tea protein isolate. Coomassie Blue staining, followed by silver staining was applied to visualize the protein bands as haze-active proteins were reported to be too weak to stain well with Coomassie Blue dye (Wu and Siebert, 2002).

Figure 5.2 shows that the strongest protein bands were displayed in the middle of 6.5 kD and 16.5 kD. Therefore, the molecular mass of this tea protein isolate was *ca* 11 kD. This result was nearly half of the value obtained from HPLC analysis using a TSK G4000 PW_{XL} gel filtration column. This can be accounted for by the aggregation of two protein molecules below pH 6.8. However, this protein isolate appeared to contain impurities as there was a dark area above the protein band. This indicated that there might be some other proteins of larger molecular mass between 16.5 kD and 32.5 kD. This phenomenon is in agreement with existing studies on proteins contained in wine, grape juice and apple juice (Hsu and Heatherbell, 1987; Waters *et al.*, 1992; Wu and Siebert, 2002).

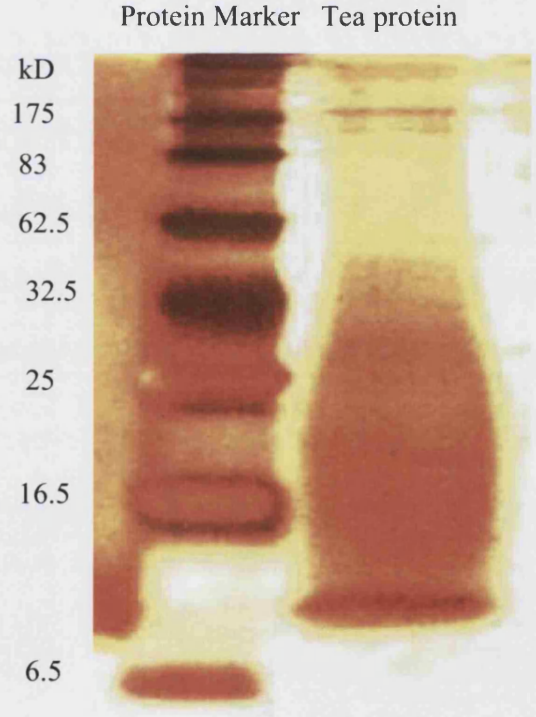

Figure 5.2 Image of a silver-stained SDS-PAGE gel of tea protein purified from *Lipton* spray dried tea powder. Molecular mass markers are shown in kD and tea protein loadings

5.3.1.3 Assay of protein contents

As proteins typically have a maximum absorbance at around 280 nm, the measurement of the tea protein's intrinsic UV absorbance can be used to determine the concentration of protein. However, the presence of brown color in the tea protein sample exerted extra absorbance at around 280 nm, which would have influenced the accuracy of the result. For this reason, the CBB assay was chosen in this study. This assay is based on the maximum absorbance at 600 nm of a protein sample after interaction with Coomassie Brilliant Blue G and being stained blue under acidic conditions. Bovine serum albumin (BSA) solutions of concentrations ranging from 32 to 500 μg ml^{-1} were used as standards for calibration. The concentration of protein in 1.7 mg ml^{-1} of tea protein sample was found to be 87.3 μg ml^{-1}. Consequently, the purity of this tea protein isolate was 51.4 wt%. Although not high, this value has to be seen in the context of an original tea protein concentration in the product of < 1 wt% (http://www.fmltea.com/Teainfo/tea-chemistry%20.htm). However, CBB has been reported to provide little response to proteins that lack basic and aromatic amino acids, such as wine and grain haze-active proteins. Therefore tea haze-active proteins might be possibly underestimated by this assay (Siebert, 1999). To investigate this possibility, a bicinchoninic acid (BCA) assay was used as a cross check on the accuracy of the CBB assay. However, interference by phenolic compounds resulted in a gross overestimation of the tea protein content. Therefore, the use of BCA assay seems inappropriate for this system.

5.3.1.4 Characterization of tea protein by FTIR

To further investigate the purity of the tea protein, Fourier Transform Infrared Spectroscopy (FTIR) was used to compare the isolate with protein standard BSA. FTIR is also reported to be a novel and useful technique in determining the secondary structure of protein (Jabs, 2005).

The FT-IR absorption spectrum of the BSA standard is shown in Figure 5.3. A broad band at 3296 cm^{-1} and a relative smaller band at 2960 cm^{-1} observed were mainly due to N-H stretching vibration. The other two characteristic bands in the protein, namely Amide I (1600-1700 cm^{-1}) and Amide II (1510-1580 cm^{-1}) were confirmed at 1654 cm^{-1}

and 1539 cm^{-1} in BSA, which also indicated the typical α-helix structure of BSA (Smith and Franzen, 2002).

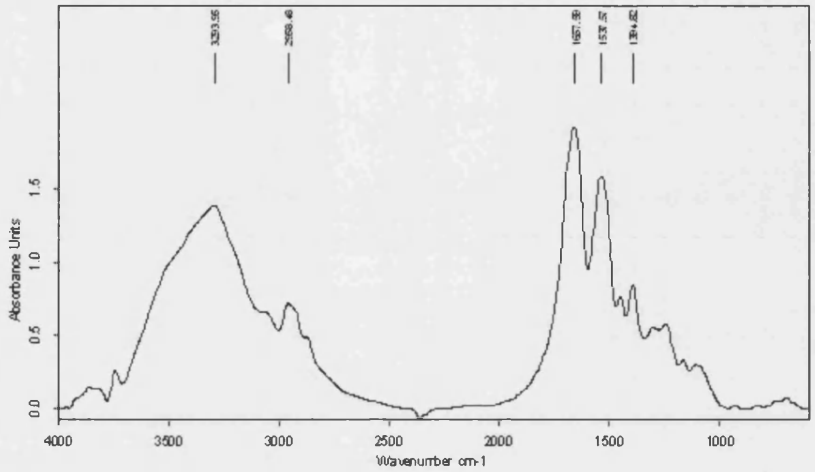

Figure 5.3 FT-IR spectrum of Bovine Serum Albumin (BSA)

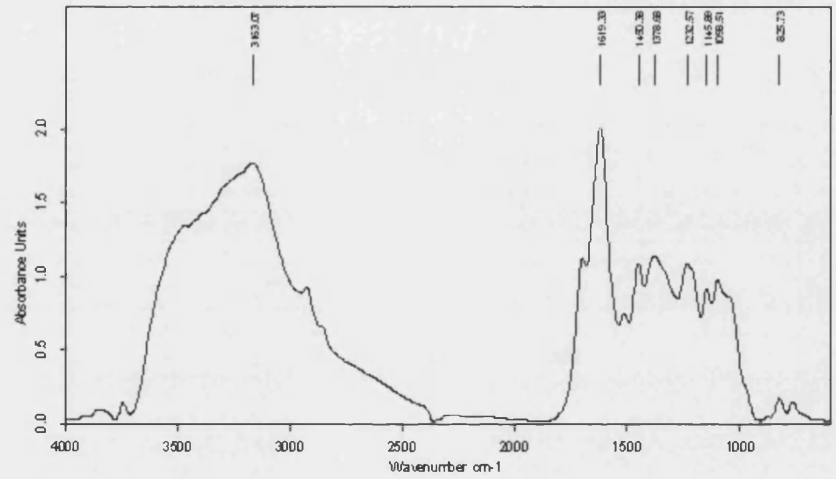

Figure 5.4 FT-IR spectrum of tea protein

Figure 5.4 shows the FT-IR absorption spectrum of the tea protein sample. Compared to that of BSA, the Amide A band ranging form 3500 to 3100 cm^{-1} was also observed in the tea protein sample, resulting from N-H stretching vibration. However, Amide I and Amide II bands in tea protein sample spectrum appeared to have moved to 1698 cm^{-1} and 1619 cm^{-1}, either because of the presence of some impurity or a different secondary structure of the protein. www.imb-jene.de mentioned that for proteins with β-sheet structure, two bands can be observed at approximately (i) 1629 cm^{-1} (with a minimum of 1615 cm^{-1} and a maximum of 1637 cm^{-1}), and (ii) 1696 cm^{-1} (with a minimum of

1685 cm^{-1}). This corresponds to the absorption spectrum of the tea protein sample, indicating that the secondary structure of the tea protein might indeed be mainly β-sheet rather than α-helix.

5.3.2 Quantitative analysis of tea polyphenols

5.3.2.1 Determination of total polyphenols in samples purified from tea by Zn^{2+} precipitation

The *Folin-Ciocalteu* assay has been widely used in the measurement of total phenols in wine, tea and fruit juice (Wu and Siebert, 2002; Degenhardt *et al.*, 2000). It is a simple, sensitive and accurate method based on the formation of blue complexes with the oxidation of phenolic hydroxyl groups by phospho tungstic acids. Gallic acid standard solutions of concentrations from 10 to 60 μg ml^{-1} were used for the calibration. The concentrations of polyphenol in 0.02 mg ml^{-1} tea polyphenol sample and 0.1 mg ml^{-1} tea sample were found to be 13.13 μg ml^{-1}, and 21.52 μg ml^{-1} respectively. The purities of the tea polyphenol sample and black tea sample were 65.7 wt% and 21.6 wt%. As a result, the amount of total polyphenol was three times more than that in original black tea powder after precipitation by Zn^{2+}.

5.3.2.2 Components of tea polyphenols separated by cationic precipitation

Analysis of tea polyphenols separated using the method described above was carried out using Reverse Phase HPLC. Figure 5.5 shows the profiles of tea polyphenols samples separated using cationic precipitation and those of the standards, for example, theaflavin, theobromine and caffeine. Accordingly, theaflavin, theobromine, and caffeine had the maximum absorbances at 3.98, 4.60 and 6.78 minutes respectively. For the polyphenol sample separated, three obvious peaks exist at 3.99, 4.65 and 6.63 minutes, which indicate that theaflavin, theobromine, and caffeine are the major contents of the tea polyphenol sample. The concentrations of these three components were 48.09 mg ml^{-1}, 4.54 mg ml^{-1}, and 1.95 mg ml^{-1} separately, calculated by calibration curves. From the data shown in Table 5.3, theaflavin is the major components in the tea polyphenol isolate.

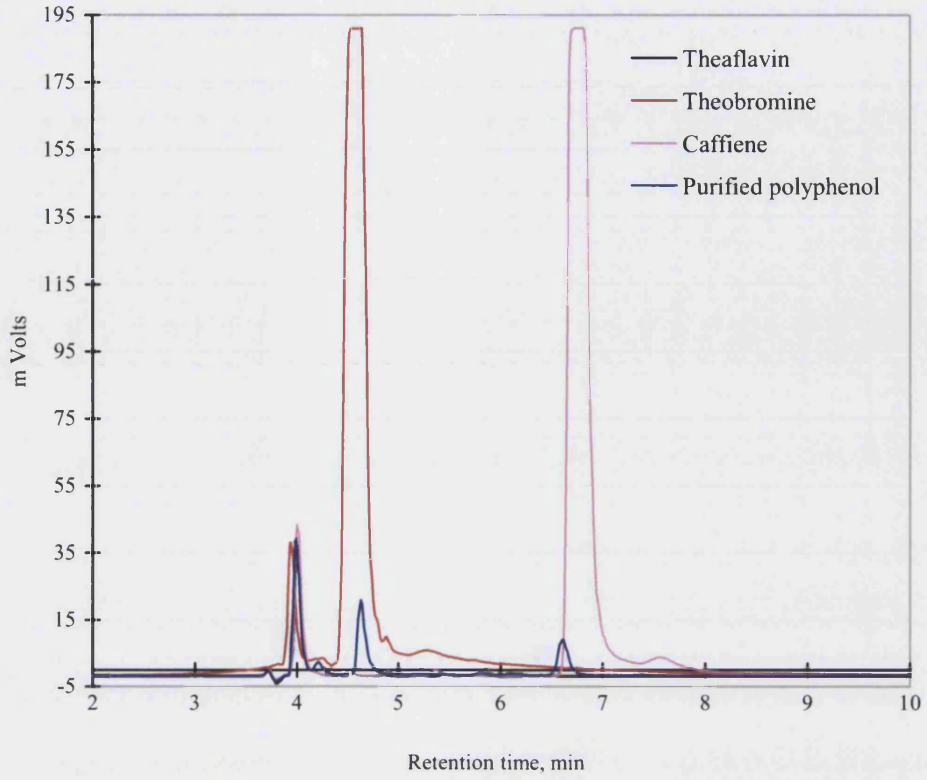

Figure 5.5 Reverse phase HPLC profiles of purified tea polyphenols, theaflavin, theobromine and caffeine standards on a KR100-5C18-4498 (*Hichrom*, UK) column, with 20% solvent A (2% acetic acid in acetonitrile) and 80% solvent B (2% acetic acid in distilled water) as mobile phase, flow rate: 1 ml min^{-1}

Table 5.3 Information on theaflavin, theobromine, and caffeine peaks in the Reverse-phase HPLC profile of tea polyphenol isolate

Peak Name	Retention time, min	Area, mV min	Area %	Concentration, mg ml^{-1}
Theaflavin	3.99	$3.38x10^5$	44.4	48.09
Theobromine	4.65	$2.09x10^5$	27.5	4.55
Caffeine	6.63	$1.05x10^5$	13.8	1.95

5.3.3 Binding capacity of tea protein with theaflavin standard determined by ITC

Isothermal Titration Microcalorimetry (ITC) is used extensively in ligand binding studies. The ligand is titrated into a solution containing the binding protein (here tea protein), and the heat evolved or absorbed during binding is measured. Deconvolution of data obtained from a sequence of additions yields the binding constant, enthalpy and

entropy of binding, and the stoichiometry of the interaction. Raw data was obtained by plotting heat flow in μcal $second^{-1}$ against time in minutes, after the integration baseline had been subtracted. For further analysis, the enthalpy change per mole of injectant (kcal mol^{-1}) was plotted as a function of the molar ratio of the ligand to the tea protein after normalizing and integrating the raw data.

5.3.3.1 Tea protein – theaflavin interaction

The interaction of tea protein and theaflavin (3.52 mM) was studied at different concentrations of protein, namely 0.251, 0.502 and 0.593 mM. The results are presented in Figures 5.6 – 5.8. Negative heat flows in raw data correspond to exothermic changes, while positive heat flows represent endothermic changes. Therefore, the interaction between tea protein and theaflavin at pH 5.0 appears to be accompanied by the release of heat according to the negative peaks.

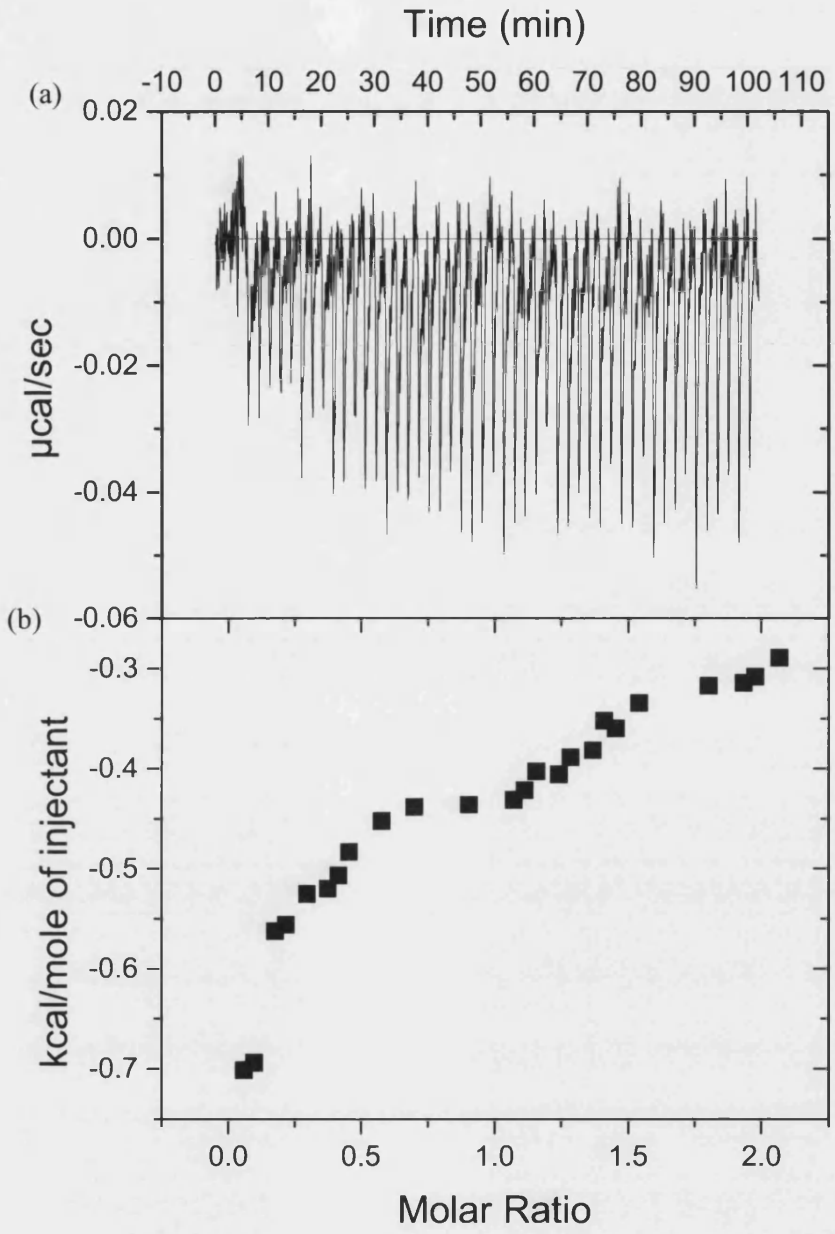

Figure 5.6 ITC figure for the titration of 0.251 mM tea protein against 3.52 mM theaflavin at pH 5.0. (a) Typical raw data – a plot of heat flow against time. (b) corresponding plot of molar enthalpy change against theaflavin / protein molar ratio after normalization and peak-by-peak integration

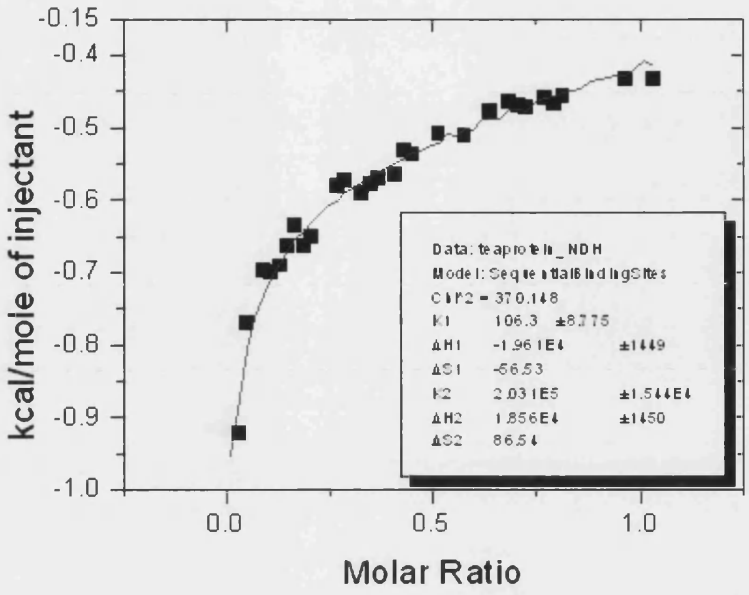

Figure 5.7 ITC figure for the titration of 0.502 mM tea protein against 3.52 mM theaflavin at pH 5.0. A plot of molar enthalpy change against theaflavin / protein molar ratio after normalization and peak-by-peak integration. The smooth solid line represents the best fit of the experimental data using the sequential binding site model

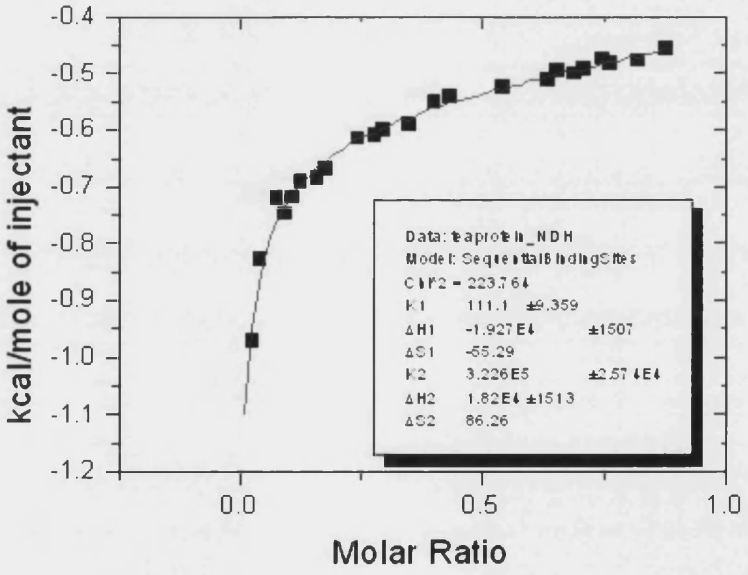

Figure 5.8 ITC figure for the titration of 0.593 mM tea protein against 3.52 mM theaflavin at pH 5.0. A plot of molar enthalpy change against theaflavin / protein molar ratio after normalization and peak-by-peak integration. The smooth solid line represents the best fit of the experimental data using the sequential binding site model

Figures 5.6 – 5.8 indicate that the concentration of tea protein strongly affected the amount of heat evolved as well as the saturation of the binding sites. In a typical exothermic reaction, when the macromolecule in the cell becomes saturated with added ligand, the heat signal diminishes until only the background heat of dilution and mixing is observed. The irregular change of heat flows in the raw data plot shown in Figure 5.6 indicate that the lowest concentration of 0.251 mM tested was too low to approach the saturated binding conditions. Consequently, the binding constants could not be determined in this case due to the lack of sufficient information.

For both of the higher concentrations examined (0.502 and 0.593 mM), the data was fitted to the sequential binding sites model. This means that the macromolecule has dependent sites, where the binding of a ligand to one of the sites will be affected by whether the ligands are bound to any other sites. A fixed sequence of binding is assumed in this model. For example, the first ligand which associates with an individual molecule always binds to site 1, the second ligand which binds to an individual molecule always binds to site 2, *etc*. Therefore, only two parameters, K and H are used to determine the best fit as the number of sequential sites must be integral and chosen by the operator. Two sequential site bindings were suitable for these tea protein-theaflavin interactions. Thermodynamic parameters, including the binding constants K and enthalpy change ΔH are showed in Table 5.4.

Table 5.4 Thermodynamic parameters concerning the interaction of tea protein and 3.52 mM theaflavin interactions at pH 5.0

Protein Concentration (mM)	K_1 mol^{-1}	ΔH_1 Cal mol^{-1}	K_2 mol^{-1}	ΔH_2 Cal mol^{-1}
0.502	$1.06x10^2 \pm 8.78$	$-1.96x10^4 \pm 1.45x10^3$	$2.03x10^5 \pm 1.54x10^4$	$1.86x10^4 \pm 1.45x10^3$
0.593	$1.11x10^2 \pm 9.36$	$-1.93x10^4 \pm 1.51x10^3$	$3.22x10^5 \pm 2.57x10^4$	$1.82x10^4 \pm 1.51x10^3$

The values of K_1 and K_2 for both experiments were $1.06x10^2$ mol^{-1}, $2.03x10^5$ mol^{-1}, $1.11x10^2$ mol^{-1}, and $3.22x10^5$ mol^{-1} respectively. The similarity of these binding constants of titration for different protein concentrations implies that there is little influence of protein concentration upon the binding mechanism as long as the saturating

binding conditions were approached. Furthermore, the fact that K2 was nearly 10^3 times larger than K1 indicates macroscopic positive cooperativity, meaning that the theaflavin already titrated into the tea protein possibly activated new binding reactions. This is in accordance with the findings from Charlton *et al.* (2002) concerning cooperative effects in PRP-tanning binding.

The impact of pH value upon the binding phenomena was also investigated at three different pH values, namely 4.0, 5.0 and 5.5. The results were compared in Figures 5.9, 5.7 and 5.10.

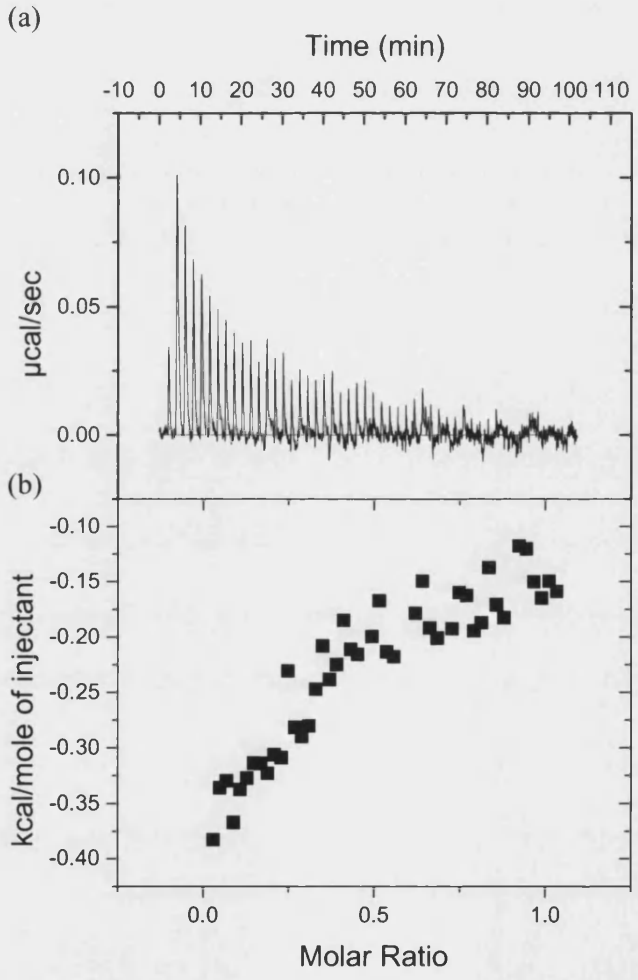

Figure 5.9 ITC figure for the titration of 0.502 mM tea protein with 3.52 mM theaflavin at pH 4.0. (a) Typical raw data – plot of heat flow against time. (b) corresponding plot of molar enthalpy change against theaflavin / protein molar ratio after normalization and peak-by-peak integration

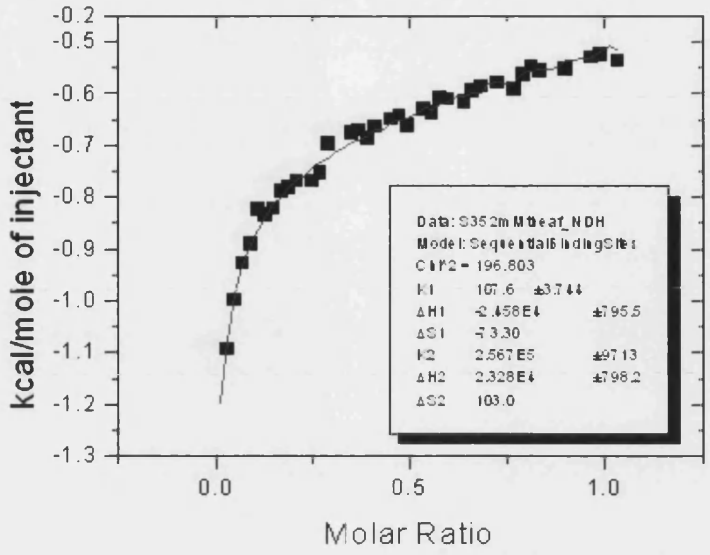

Figure 5.10 ITC figure for the titration of 0.502 mM tea protein with 3.52 mM theaflavin at pH 5.5. Plot of molar enthalpy change against theaflavin / protein molar ratio after normalization and peak-by-peak integration. The smooth solid line represents the best fit of the experimental data using the sequential binding site model

From these graphs, prominent differences lie in the raw data panel in Figure 5.9, where heat flow values appeared to be positive. This is because the dilution or deaggregation of theaflavin, which caused to endothermic effects, became dominate under pH values of 4.0. Therefore the binding of 3.52 mM theaflavin to 0.502 mM tea protein was possibly not strong enough to counteract other enthalpy changes from processes such as ligand dilution and deaggregation. An identical binding mechanism was observed for the reaction occurring in pH 5.5 acetate buffer (see Table 5.5). Nevertheless, the binding constants K1 and K2, were slightly higher than those titrated at pH 5.0. This may imply an increased affinity of theaflavin and tea protein with the increase of pH within the range from pH 4 to 5.5.

Table 5.5 Thermodynamic parameters of 0.502 mM tea protein and 3.52 mM theaflavin interactions at pH 5.0 and pH 5.5

pH	K_1 mol^{-1}	ΔH_1 Cal mol^{-1}	K_2 mol^{-1}	ΔH_2 Cal mol^{-1}
5.0	$1.06x10^2 \pm 8.78$	$-1.96x10^4 \pm 1.45x10^3$	$2.03x10^5 \pm 1.54x10^4$	$1.86x10^4 \pm 1.45x10^3$
5.5	$1.08x10^2 \pm 3.74$	$-2.45x10^4 \pm 7.96x10^2$	$2.57x10^5 \pm 9.71x10^3$	$2.33x10^4 \pm 7.98x10^2$

5.3.3.2 Tea protein-tea polyphenol interaction

The possible mechanism of the interaction between tea protein and tea polyphenols separated by cationic precipitation was also determined by ITC. The data is presented in Figure 5.11.

A sequential sites fitting model was also applied to this binding isotherm. However, only one binding site was used in the best fit. The value of the strength of the associate (K) was also much lower than that of K2 when considering the binding occurring between tea protein and theaflavin. Although the reason for the difference in the number of binding sites is not particularly clear, the impurity as well as the low concentration of polyphenol sample compared with theaflavin standard must be taken into consideration. Nevertheless, a lower protein concentration 0.0133 mM was found to be sufficient to obtain the saturating binding conditions. This is probably due to the fact that the real concentration of the tea polyphenol solution is much lower than desired 3.52 mM, as the total polyphenol in this tea polyphenol isolate is only 65.7 wt%. As a result, the ITC model conclusions regarding tea protein-polyphenol reactions can only be considered as an approximation, despite of the indication of sequential binding possibilities.

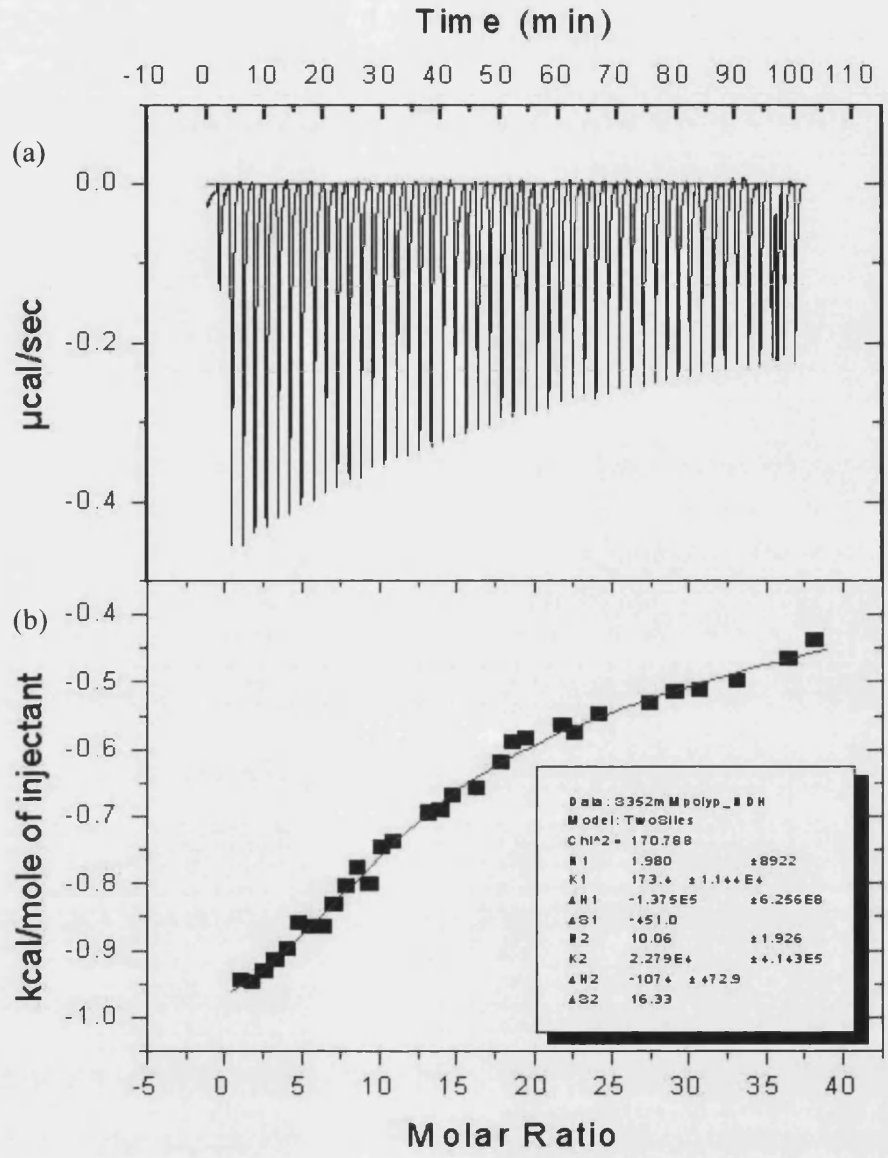

Figure 5.11 ITC figure for the titration of 0.0133 mM tea protein with 3.52 mM theaflavin at pH 5.0. (a) typical raw data – plot of heat flow against time. (b). corresponding plot of molar enthalpy change against theaflavin / protein molar ratio after normalization and peak-by-peak integration. The smooth solid line represents the best fit of the experimental data using the sequential binding site model

5.4 Conclusions

Tea protein was successfully separated by alkali extraction, followed by centrifugation, sedimentation and dialyzation from *Lipton* spray dried black tea powder. The purity of this tea protein isolate was approximately 50 wt%. The results from TSK gel G4000 PW_{XL} gel filtration chromatography indicated that the molecular mass of tea protein was approximately 22.2 kD at pH 6.8. This value was nearly double of that obtained from SDS-PAGE, where the tea protein was dissolved in pH 5.0 acetate buffer. This implied the aggregation of protein molecules under pH 6.8. The existence of a broad band ranging from 3500 cm^{-1} to 3100 cm^{-1} in the FTIR spectrum of tea protein verified the presence of amidocyanogen, which is a specific functional group in the protein. The secondary structure of tea protein was considered to be β-sheet rather that α-helix according to the excursion of infrared absorbance within Amide I and Amide II areas.

Tea polyphenols were also purified from black tea powder by precipitating interactions between Zn^{2+} and phenolic hydroxyl groups of polyphenols under alkali conditions. The Reversed-phase HPLC analysis of this tea polyphenol isolate demonstrated the presence of theaflavin, theobromine, and caffeine. The amount of total phenols in this isolate was also determined to be approximately 65wt% using a *Folin-Ciocalteu* assay, a value which is 3 times larger than that in the original tea powder.

The interactions of (i) tea protein and theaflavin, (ii) tea protein and mixed tea polyphenols were investigated by ITC. Both interactions were fitted to sequential sites binding models with different numbers of binding sites. Mixture (i) was fitted by two sequential sites binding, and exhibited great positive cooperativity. The concentration of tea protein had a marked effect upon the magnitude of the enthalpy change, but little impact upon the mechanism of tea protein-theaflavin binding once saturation had been obtained. The pH value applied during titration had a great influence on the total enthalpy change for the processes occurring in the sample cell. A slightly higher pH within the range studied (4 – 5.5) tended to be preferable, as the strength of binding associate became larger than when higher pH values were used.

The interaction in mixture (ii) was found to fit a one site sequential binding model. The affinity was found to be weaker than that of the tea protein / theaflavin interaction.

Chapter 6 Membrane fouling by model tea component solutions

6.1 Introduction

Proteins and polyphenols are the principle fouling constituents in the ultrafiltration (UF) of black tea liquor. The aim of this study was to determine the relative importance of individual components in the fouling process, and to investigate any synergetic interactions that were occurring. A 30 kD Molecular Weight Cut Off (MWCO) polysulphone UF membrane in dead end mode was challenged with model solutions of tea components. Model solutions consisted of tea proteins, theaflavins (TFs), and thearubigins (TRs).

6.2 Experimental methods

6.2.1 Apparatus

As model components were only available in small quantities, a dead-end rather than a cross-flow system was developed in this part of experiments. Figure 6.1 shows the schematic diagram of dead-end filtration rig used in these fouling experiments. The fouling apparatus consisted of a 50-mL *Amicon* stirred cell (model 8050) that provided an effective membrane filtration area of 17.3 cm^2. Nitrogen gas was chosen as a pressuring medium to prevent the oxidization of polyphenols during the filtration process.

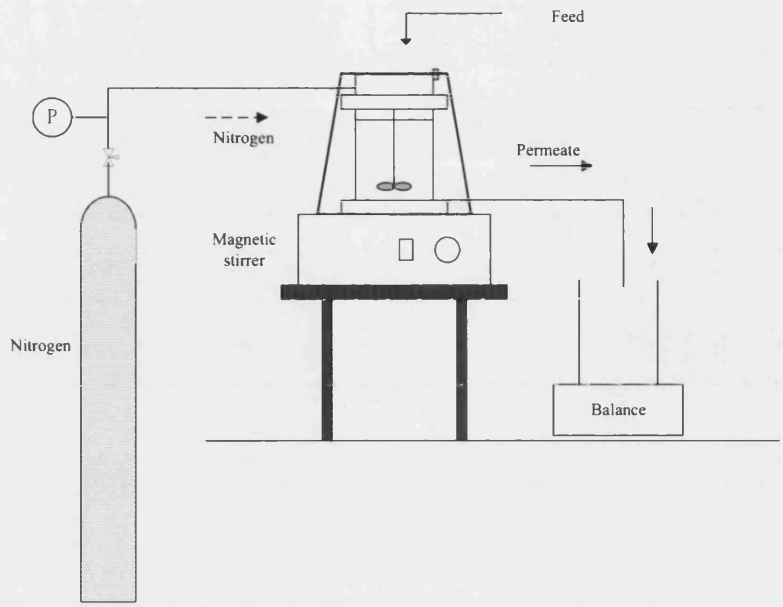

Figure 6.1 Schematic diagram of dead-end filtration rig

6.2.2 Membranes and materials

The polysulphone membrane disks (*Osmonics*, 30 kD MWCO) of 47 mm diameter were used in this study. Membranes for each fouling experiments were cut from the same sheet of UF membrane to reduce membrane variability.

Polyphenol standards, namely theaflavin (TF, 91 wt% purity, 564 g mol^{-1}), theaflavin–3-gallate (TF-3-G, 82 wt% purity, 716 g mol^{-1}), theaflavin-3'-gallate (TF-3'-G, 95 wt% purity, 716 g mol^{-1}), theaflavin -3,3'-gallate (TF-3,3'-G, 90 wt% purity, 868 g mol^{-1}), and Thearubigins (TR, average molecular mass 3000 Da), were all provided by *Unilever R&D Colworth*, UK. Tea protein with a molecular mass 11 kD and a purity of 51.4wt% was isolated from *Lipton*'s spray dried tea powder as described in chapter 5. Caffeine (purity ≥ 99%, *Fluka*) was bought from *Sigma Ltd*, UK.

6.2.3 Model solution set up and fouling protocol

To understand the relative importance of individual tea components on membrane fouling, as well as to investigate whether there are any synergetic interactions between different fouling species, three groups of model solutions were applied in this part of study. They are described in Table 6.1.

Table 6.1 Composition of various tea model solutions

Group 1 Individual tea components :	
A	25 mg L^{-1} Theaflavin
	25 mg L^{-1} Theaflavin - 3 - gallate
	25 mg L^{-1} Theaflavin - 3' - gallate
	25 mg L^{-1} Theaflavin - 3,3' - gallate
	25 mg L^{-1} Thearubigins
	25 mg L^{-1} Tea protein
B	50 mg L^{-1} Theaflavin
	50 mg L^{-1} Theaflavin - 3 - gallate
	50 mg L^{-1} Theaflavin - 3' - gallate
	50 mg L^{-1} Theaflavin - 3,3' - gallate
	50 mg L^{-1} Thearubigins
	50 mg L^{-1} Caffeine
	50 mg L^{-1} Tea protein
Group 2 Binary mixtures of polyphenols and tea protein :	
	25 mg L^{-1} Theaflavin and 25 mg L^{-1} Tea protein
	25 mg L^{-1} Theaflavin - 3 – gallate and 25 mg L^{-1} Tea protein
	25 mg L^{-1} Theaflavin - 3' – gallate and 25 mg L^{-1} Tea protein
	25 mg L^{-1} Theaflavin - 3,3' – gallate and 25 mg L^{-1} Tea protein
	25 mg L^{-1} Thearubigins and 25 mg L^{-1} Tea protein
	25 mg L^{-1} caffeine and 25 mg L^{-1} Tea protein
Group 3 Multiple mixtures of tea components	
	12.5 mg L^{-1} TF, 12.5 mg L^{-1} TF-3-G, 12.5 mg L^{-1} TF-3'-G, and 12.5 mg L^{-1} TF-3,3'-G
	10 mg L^{-1} TF, 10 mg L^{-1} TF-3-G, 10 mg L^{-1} TF-3'-G, 10 mg L^{-1} TF-3,3'-G, and 10 mg L^{-1} Tea protein
	10 mg L^{-1} TF, 10 mg L^{-1} TF-3-G, 10 mg L^{-1} TF-3'-G, 10 mg L^{-1} TF-3,3'-G, and 10 mg L^{-1} Thearubigins
	7.7 mg L^{-1} TF, 7.7 mg L^{-1} TF-3-G, 7.7 mg L^{-1} TF-3'-G, 7.7 mg L^{-1} TF-3,3'-G, 7.7 mg L^{-1} Thearubigins, 7.7 mg L^{-1} Tea protein and 4 mg L^{-1} caffeine

All the model solutions were made up using 5 mM acetate buffer with a pH of 5 and ionic strength 100 mM. The acetate buffer was used to maintain the pH value of different fouling solutions to a consistent value of pH 5, which is also the value of black tea extract during the Ice tea making process. In addition, this also corresponded to the conditions used when investigating the binding capabilities of theaflavins and tea protein by ITC. To ensure the comparability of membrane fouling by different model solutions, a standard protocol was used in all the experiments (See Table 6.2).

Table 6.2 Standard protocol of membrane fouling by model solutions

Step	Operation	Operating Conditions		
1	Membrane Conditioning	Prefiltered distilled water	TMP 3.0 bar	55 °C
2	Pure water flux measurement	Prefiltered distilled water	TMP 1.5 bar	22 °C
3	Pure water flux measurement	Prefiltered distilled water	TMP 2.0 bar	22 °C
4	Membrane fouling	Model solutions	TMP 2.0 bar	22 °C
5	Rinsing	Prefiltered distilled water	TMP 1.0 bar	22 °C
6	Pure water flux measurement	Prefiltered distilled water	TMP 1.5 bar	22 °C

Prior to membrane fouling, new membranes were conditioned by passing 180 ml of prefiltered distilled water through the membrane at 55 °C and a transmembrane pressure (TMP) of 3.0 bar to remove the glycerin. Following conditioning, the pure water flux (J_w) of each membrane at 1.5 bar was measured so as to compare the extent of fouling by different model solutions. The pure water fluxes at 2.0 bar of each membrane were also measured as the reference of membrane permeability before fouling. All fouling experiments were undertaken at 22 °C, with a TMP of 2.0 bar. Permeate flux during fouling (J_f) was recorded. The operating conditions used for conditioning, pure water flux measurement and fouling were determined by previous experiments in our laboratory concerning the ultrafiltration of black tea liquor using PSF membranes on a pilot scale cross flow rig (See Chapter 3). A magnetic stirrer suspended just above the membrane surface was rotated at a constant speed of 610 rpm during the filtration process to reduce the effects of concentration polarization and gelation.

6.2.4 Evaluation of the fouling process and membrane performance

As mentioned in Chapter 2, membrane fouling normally induces the flux decline during ultrafiltration when the transmembrane pressure is kept constant. By recording the changing of permeate flux value, an indication of membrane fouling is given. Therefore, permeate flux has been chosen as one of the most important parameters to evaluate fouling process in this study. However, as each single fouling experiment was carried out on a new membrane although the standard protocol was applied, there will still be some errors caused by the heterogeneity of different parts of membrane. To reduce these errors, the normalized permeate flux (J_n) was used. This is defined as the ratio of the flux measured during fouling (J_f) to the pure water flux measured under the same conditions (TMP 2.0 bar) prior to fouling (J_w).

Apparent rejection coefficient (R) is another parameter generally used to determine membrane fouling during ultrafiltration process. The rejection coefficients of either polyphenol or protein were calculated using equation (6.1):

$$R\%=(1-\frac{C_p}{C_b})\times 100\% \quad (6.1)$$

Where C_b and C_p are the concentrations of a component in the bulk and the permeate respectively. C_b was calculated using a simple mass balance.

To further understand fouling behaviours, the separate mass fluxes of total polyphenols, protein, caffeine, TF and its derivatives, namely TF-3-G, TF-3'-G and TF-3,3'-G components were also determined.

In addition, membrane resistances after different operations were calculated from pure water flux measurements according to Darcy's law:

$$J_w = \frac{TMP}{\mu \cdot R_m} \quad (6.2)$$

Where μ is the filtrate viscosity.

6.2.5 Visualization of membranes after fouling by Scanning Electron Microscope (SEM)

Scanning electron microscopy (SEM) was applied to observe the state of membrane surface after different fouling processes. Air and vacuum dried membranes were stuck to SEM stubs with conductive paste, followed by coating with a thin layer of gold. Afterwards, the specimens were viewed with a JSM 6310 scanning electron microscope in combination with a microanalysis system, LINK AN10000 (Oxford Instruments).

6.2.6 Determination of concentration

The concentration of total polyphenols was determined using the *Folin-Ciocalteu* assay. The concentration of individual theaflavins was measured by high-performance liquid chromatography (HPLC) as described in Table 6.3 (Samuel, 2005):

Table 6.3 Operating conditions for determining individual TFs concentrations by HPLC

HPLC column	Hypersil C18, 3μ, 100 x 4.60mm
Injection volume	20 μL
Column temperature	30 °C
Mobile Phase	20% solvent A – 2% acetic acid in acetonitrile 80% solvent B – 2% acetic acid in distilled water
Flow rate	1.8 ml min^{-1}
Detector	UV detector at 274 nm
Sensitivity	2.0%

The Coomassie Brilliant Blue G (CBB) assay was used to quantify protein concentration. C_b was calculated using a simple mass balance. The concentration of caffeine was measured according to the method described by Yao *et al.*, 2006. The detailed method is given in Appendix 9.10.

6.3 Results

6.3.1 Effects of filtration of individual polyphenol components and tea protein

To understand different filtration behaviours of the individual components, TF, TF-3-G, TF-3'-G, TF-3,3'-G, TRs, and tea protein were each dissolved into 5 mM acetate buffer of pH 5 to obtain sets of feed solutions with concentrations of 25 mg L^{-1} and 50 mg L^{-1}. The low concentrations selected reflect the small amount of these pure components available for experimentation, and the concentrations used by other workers in model solution filtration (Eagles and Wakeman, 2002). TFs account for approximately 1 – 2% of the dry weight of black tea (Balentine,1992; Degenhardt, *et al.*, 2000). The solubility of each component at the temperature of the experiments also provides an upper concentration limit.

Typical flux decline profiles for 50 mg L^{-1} solutions are shown in Figure 6.2. Initial fluxes varied considerably. After 1 minute the 50 mg L^{-1} TF feed displayed a normalized flux of 0.96, whilst TR and protein solutions of an equivalent concentration

had declined to normalized fluxes of 0.46 and 0.4 respectively after 1 minute had elapsed. Fluxes of all components continued to decline gradually, and were still declining when filtration was stopped after 60 minutes. From the values recorded at the 1st to those seen at the 60th minute, the flux declines of each tea component, namely theaflavin, theaflavin-3-gallate, theaflavin-3'-gallate, theaflavin-3,3'-gallate, thearubigins and tea protein, were 52%, 80%, 70%, 85%, 76% and 72% respectively.

Owing to the rapid loss of filtration volume in the dead end mode, it was necessary to add additional feed solutions of the same volume to all the feeds at particular time intervals. These time intervals varied with different filtrations experiments due to the variation in fluxes between the samples. The corresponding jumps in the flux seen for TF and TF-3'-G filtrations at those intervals are typical of the reductions in the concentration polarization resistances. The increases in the normalized flux for TF and TF-3'-G were approximately 0.37 and 0.055 on average. These values indicated that concentration polarization was less significant for membrane fouling by TF-3'-G (Molecular mass 716 g mol^{-1}) than the smaller molecule TF (564 g mol^{-1}). No jumps in the flux of the other individual components were seen when fresh feed was added, implying that concentration polarization was not significant for these systems under the conditions investigated.

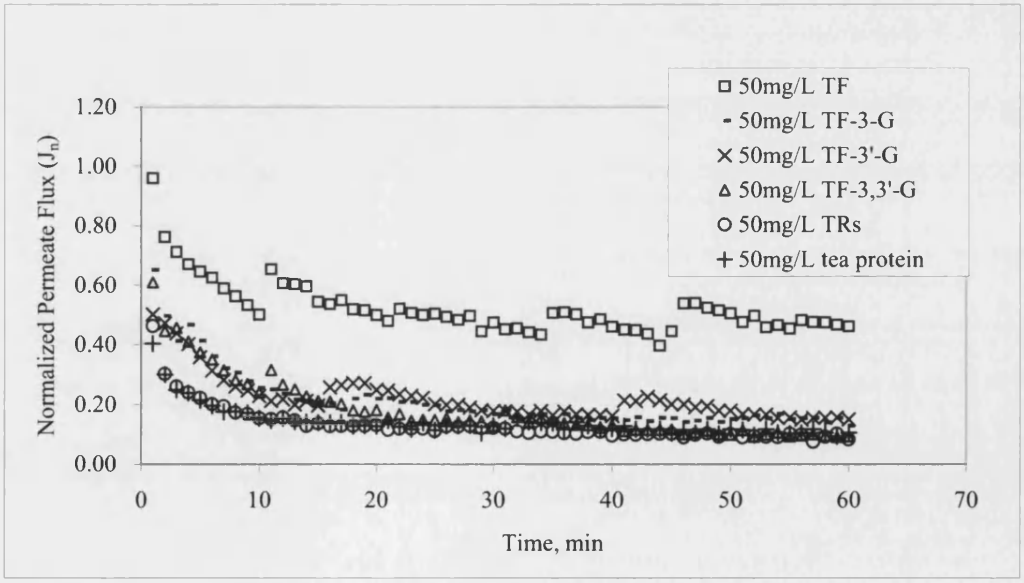

Figure 6.2 Normalised permeate flux (J_n) vs time for various tea components

Table 6.4 Initial apparent percentage rejections of individual components during filtration

Foulant	tea protein	Caffeine	TF	TF-3-G	TF-3'-G	TF-33'-G	TRs
Concentration, mg L^{-1}	50	50	50	50	50	50	50
R %	100	52.7	65.2	73.3	79	70.5	90.1

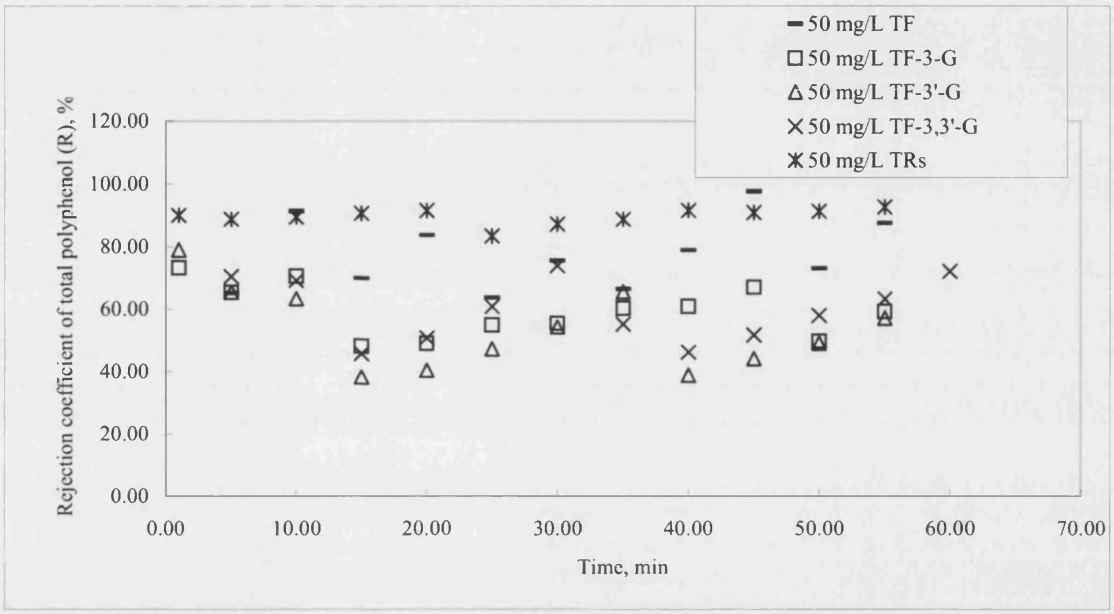

Figure 6.3 The rejection coefficients of total polyphenols during fouling by individual tea components

The apparent rejection coefficients of the individual components over the first 5 minutes are shown in Table 6.4. There is good agreement between the rank order of the normalized flux curves (highest to lowest) and the reverse order of the apparent rejection coefficients (ie a high permeate solution flux is associated with a low rejection of a component). Rejections range from 65 % for TF (molecular mass 564 g mol^{-1}) through 90 % for TR's (average molecular mass 3 kD), to 100% for protein (average molecular mass 11 kD). Figure 6.3 shows the changing trends of rejection coefficients of total polyphenols during membrane filtration of these different single component solutions. There were decreases in apparent rejection coefficients when extra feed solutions were added, especially for those membrane fouled by TFs. As the concentration in the bulk solution (C_b) is calculated according to the mass balance, its

value significantly decreased as a result of dilution. Consequently the apparent rejection coefficients declined at these intervals. However, the real rejection coefficient is likely to be more stable, it depends upon the concentration adjacent to the membrane surface which is less likely to be susceptible to substantial fluctuation on addition of fresh feed.

The high rejection of relatively small molecule such as TF indicates that molecular mass of fouling species does not control the filtration process. The fact that a protein with a mean molecular mass of 11 kD is completely rejected by a 30 kD membrane is perhaps not surprising, given that concentration polarization and irreversible fouling were found to play an important role in the flux decline of the protein solution.

The mass fluxes of total polyphenols ($J_{phenols}$) with filtration time are shown in Figure 6.4. The transfer flux of all the TF's declined as time progressed. This is to be expected, as the liquid permeate fluxes are also declining (Figure 6.2). Indeed, the decline in the transfer flux of the TF's matches the decline of the liquid permeate flux, indicating that no additional selectivity took place as a result of cake deposition or concentration polarization increasing with time. As for TF-3'-G, increases in mass flux were observed at the intervals when additional feed solutions were added. Such jumps in permeate flux occur due to reductions in the effect of concentration polarization.

The transfer flux of TRs increases slightly over the first 30 minutes of the filtration (from 1.77 to 1.92 mg m^{-2} min^{-1}), even though the liquid permeate flux declines during fouling. It appears likely that the mass transfer of TRs across the membrane is controlled by the concentration driving force across the active layer of the membrane, and is largely independent of the liquid permeate flux. The feed concentration is increasing during the dead-end filtration process, and this increase in driving force could lead to an increase in TRs component flux. After 30 minutes, the addition of fresh feed took place, with a little decrease in the mass flux following addition due to dilution effects. This indicates that membrane fouling is key to controlling the process. Inspection of a membrane following TRs solution filtration supports this, revealing a substantial cake layer on the surface (Figure 6.33 (a)). Membranes fouled by TF show a much less substantial deposit layer (Figure 6.29 (a)).

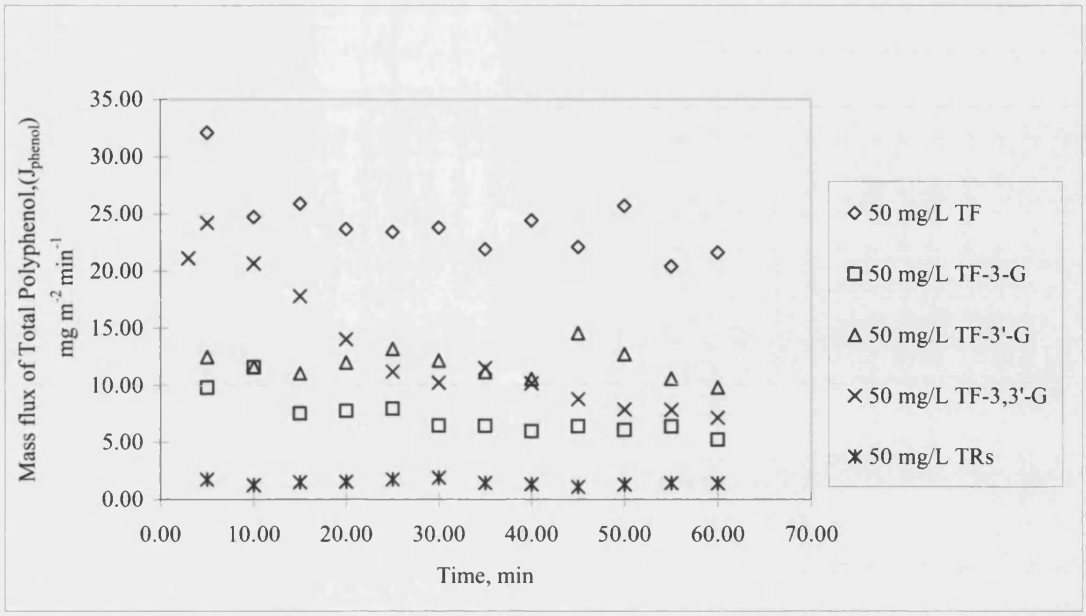

Figure 6.4 Mass fluxes of total polyphenols vs time during fouling by individual polyphenol components

A decrease in concentration from 50 mg L^{-1} to 25 mg L^{-1} led to an increase in both initial flux and steady permeate solution fluxes when membranes were fouled with TF, TF-3-G, TF-3'-G, TF-3,3'-G, TRs and tea protein (Figure 6.5-6.10). The raised percentages of initial flux for these components were 54%, 31%, 48%, 38%, 47% and 47% respectively. Corresponding permeate solution steady state fluxes values, which are the average of last 10 minutes' permeate fluxes, increased by 51%, 56%, 81%, 110%, 167% and 82% respectively. Generally, the concentrations of these tea components exerted a stronger effect on steady fouling fluxes than on the initial fouling value.

Colour parameters (lightness (L*), redness (a*), and yellowness (b*)) of permeate and feed solution were also determined by using a UV spectrophotometer (Shimazu 1601). Unfortunately, the tea component concentrations used in this part of experiments displayed colour values that were too close to those of water to be statistically significant.

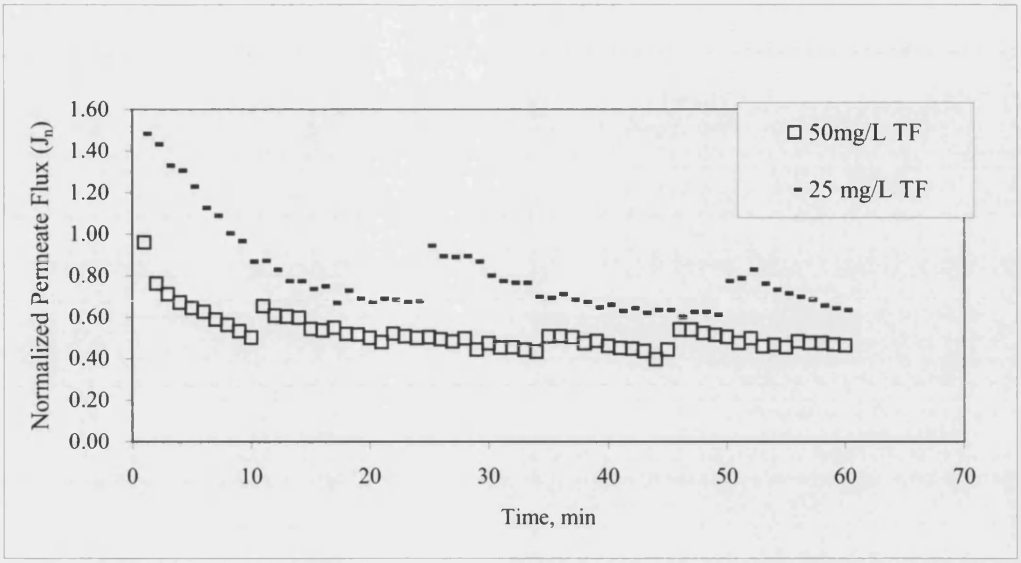

Figure 6.5 Normalized permeate flux (J_n) vs time for fouling by TF of different concentrations

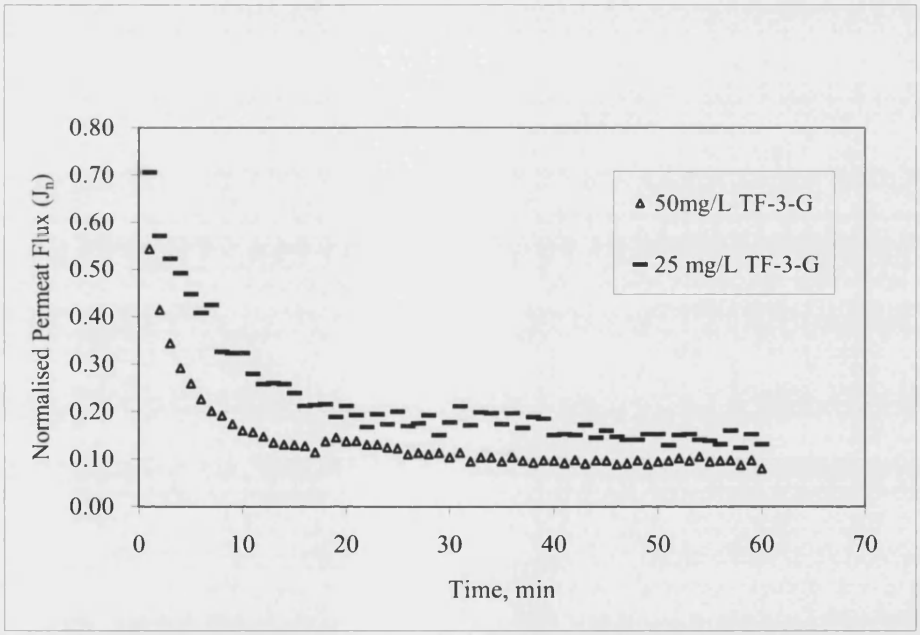

Figure 6.6 Normalized permeate flux (J_n) vs time for fouling by TF-3-G of different concentrations

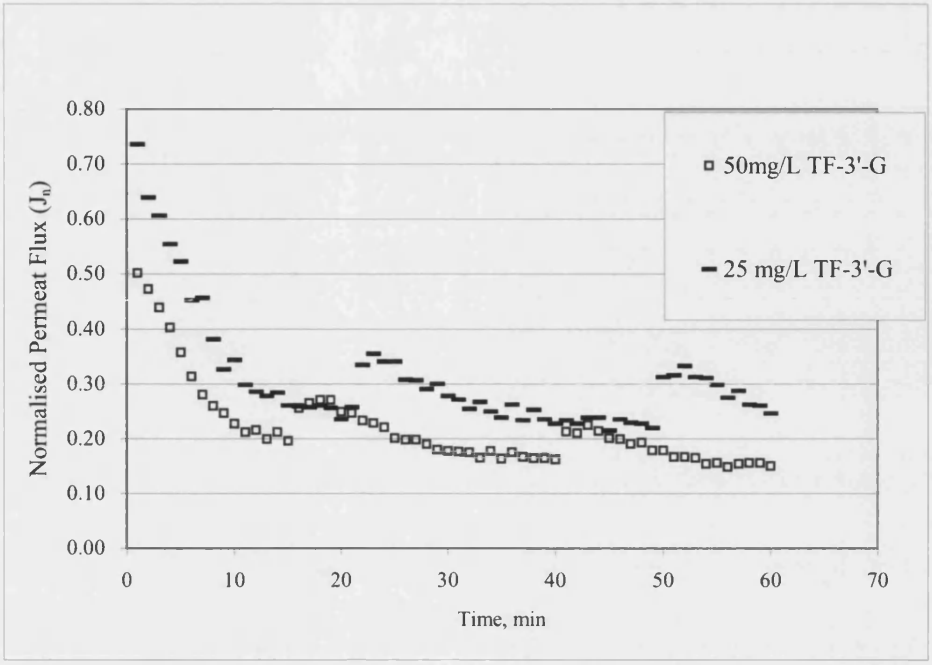

Figure 6.7 Normalized permeate flux (J_n) vs time for fouling by TF-3'-G of different concentrations

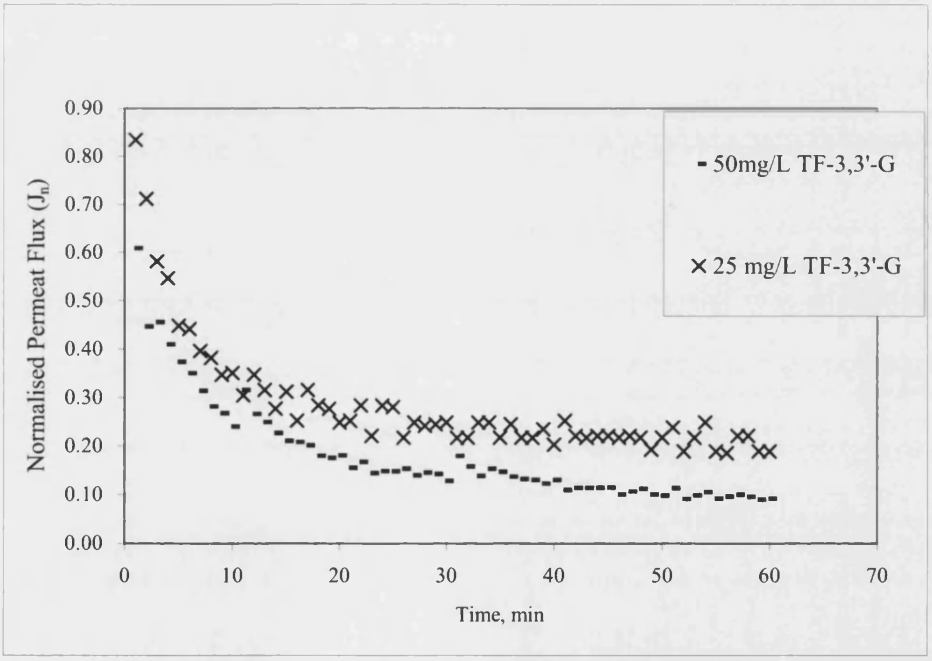

Figure 6.8 Normalized permeate flux (J_n) vs time for fouling by TF-3,3'-G of different concentrations

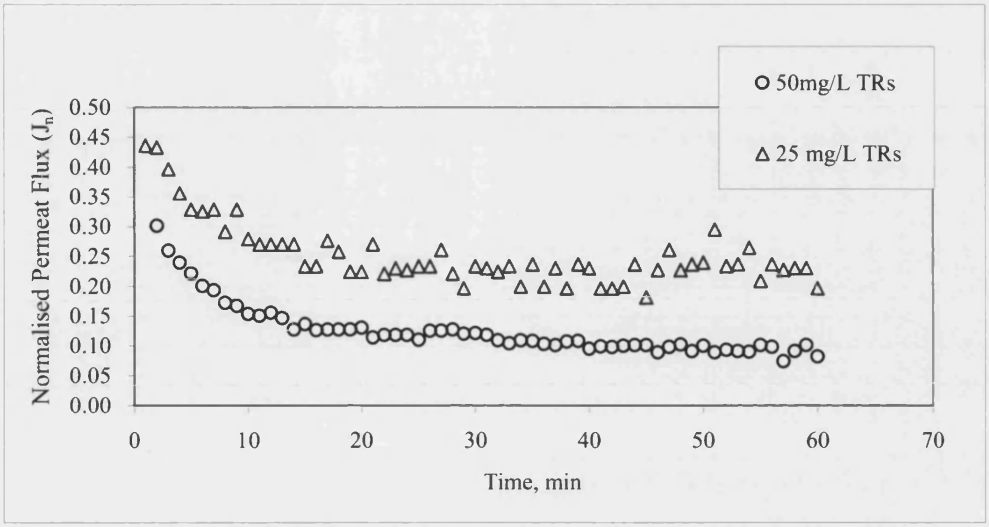

Figure 6.9 Normalized permeate flux (J_n) vs time for fouling by TRs of different concentrations

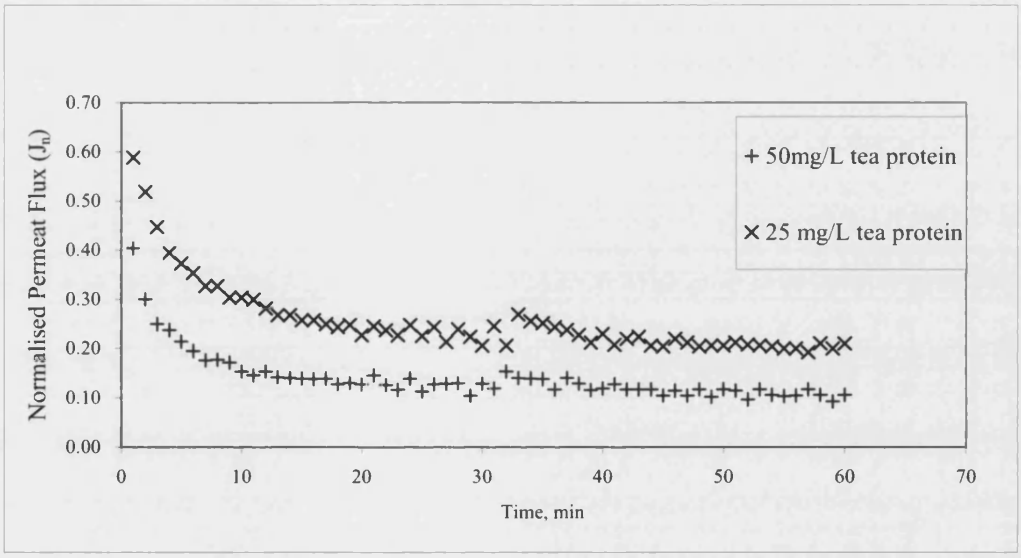

Figure 6.10 Normalized permeate flux (J_n) vs time for fouling by tea protein of different concentrations

6.3.2 Influence of binary mixtures of polyphenols and tea protein on membrane fouling

Previous work as described in Chapter 5 concerned Isothermal Titration Microcalorimetry (ITC). The interactions of (i) tea protein and theaflavin, (ii) tea protein and mixed tea polyphenols were investigated by ITC. Both interactions were fitted to sequential sites binding models with different numbers of binding sites.

Mixture (i) was fitted by two sequential sites binding. The concentration of tea protein had a marked effect upon the magnitude of the enthalpy change, but little impact upon the mechanism of tea protein-theaflavin binding once saturation had been obtained. The molar concentration of polyphenols were approximately 7 times more than those of tea protein when saturation conditions had been obtained. The pH value applied during titration had a great influence on the total enthalpy change for the processes occurring in the sample cell. A slightly higher pH within the range studied (4 – 5.5) tended to be preferable, as the strength of binding associate became larger than when lower pH values were used. The interaction in mixture (ii) was found to fit a one site sequential binding model. The affinity was found to be weaker than that of the tea protein / theaflavin interaction.

The interaction between tea protein and specific TFs or TRs will have a direct impact upon the mechanism and the extent of membrane fouling. Investigations into component interaction during filtration concerned binary mixtures. A series of model solutions containing (i) 25 mg L^{-1} tea protein and (ii) 25 mg L^{-1} of either TFs or TRs were filtered under the same conditions.

Figures 6.11 – 6.15 show the flux decline of each TF / protein mixtures where the concentration of each component is 25 mg L^{-1}. The filtration curves for binary TF / protein mixtures (25 mg L^{-1} each) tend to resemble those for 50 mg L^{-1} protein. Much higher rejection coefficients for TF's were also noticed after adding tea protein (See Figure 6.16). The two possible mechanisms for the increase in TF retention are due to (i) an increase in solute size due to protein / TF binding and (ii) an increased filtration resistance due to fouling of the membrane by protein or protein / TF species. However, after *ca* 15 minutes filtration, the rejection coefficients of total polyphenol in the binary mixtures of different theaflavins and tea protein began to reduce slightly, indicating some TF is still transmitted through membranes that reject 100% of the protein present. It is therefore clear that some unbound TF is still present in solution.

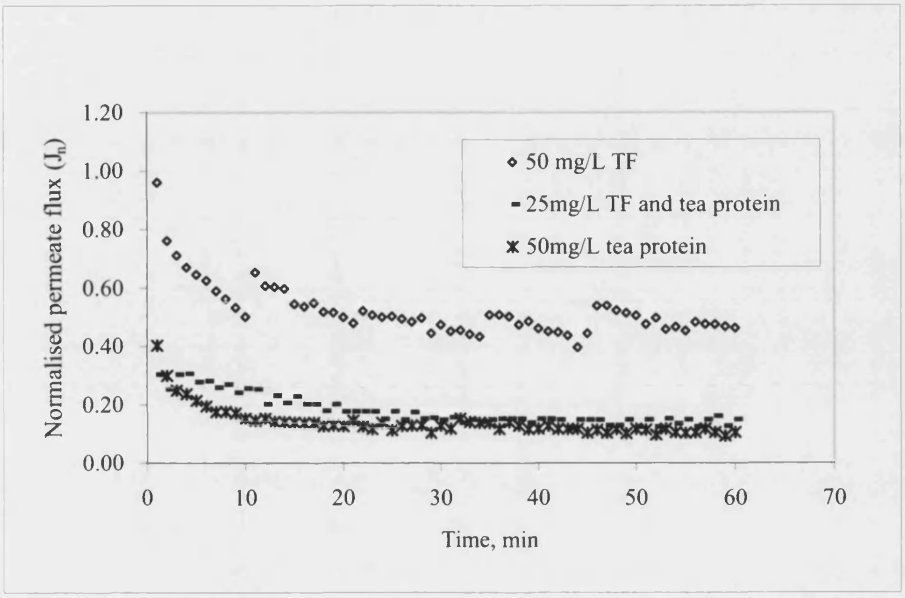

Figure 6.11 Normalized permeate flux (J_n) vs time for fouling by TF, tea protein, and a binary mixture of the two

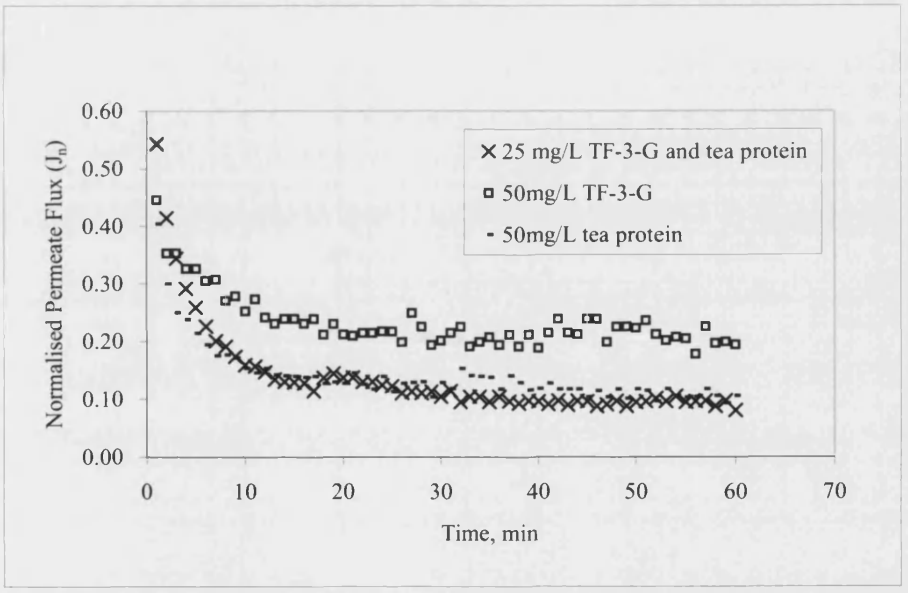

Figure 6.12 Normalized permeate flux (J_n) vs time for fouling by TF-3-G, tea protein, and a binary mixture of the two

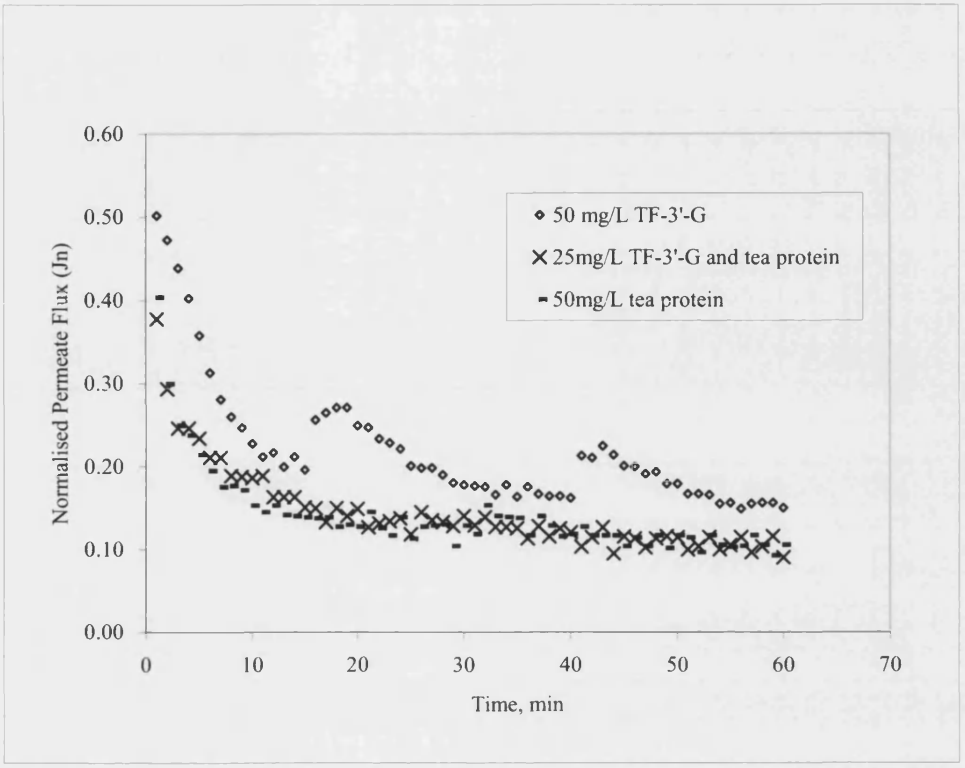

Figure 6.13 Normalized permeate flux (J_n) vs time for fouling by TF-3'-G, tea protein, and a binary mixture of the two

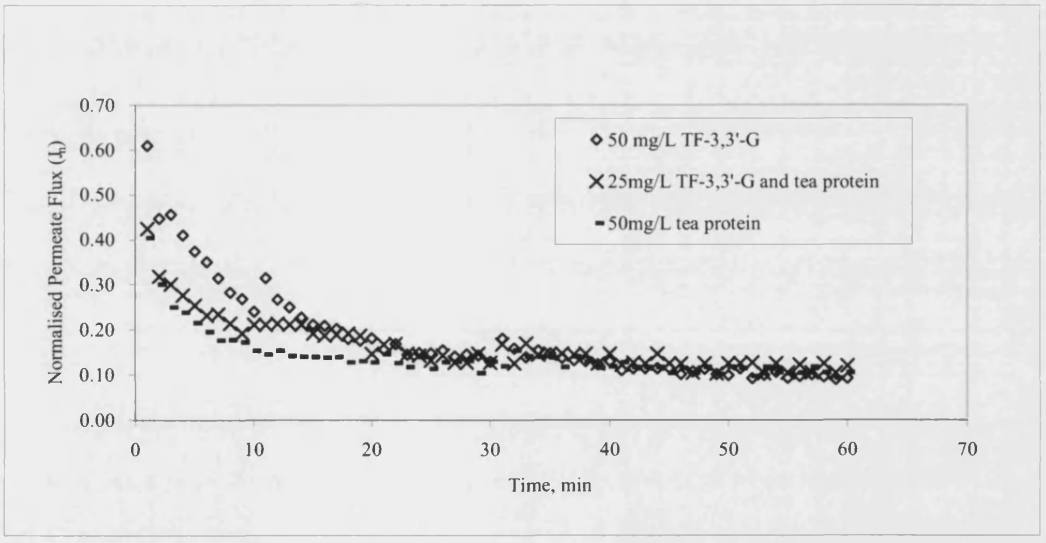

Figure 6.14 Normalized permeate flux (J_n) vs time for fouling by TF-3,3'-G, tea protein, and a binary mixture of the two

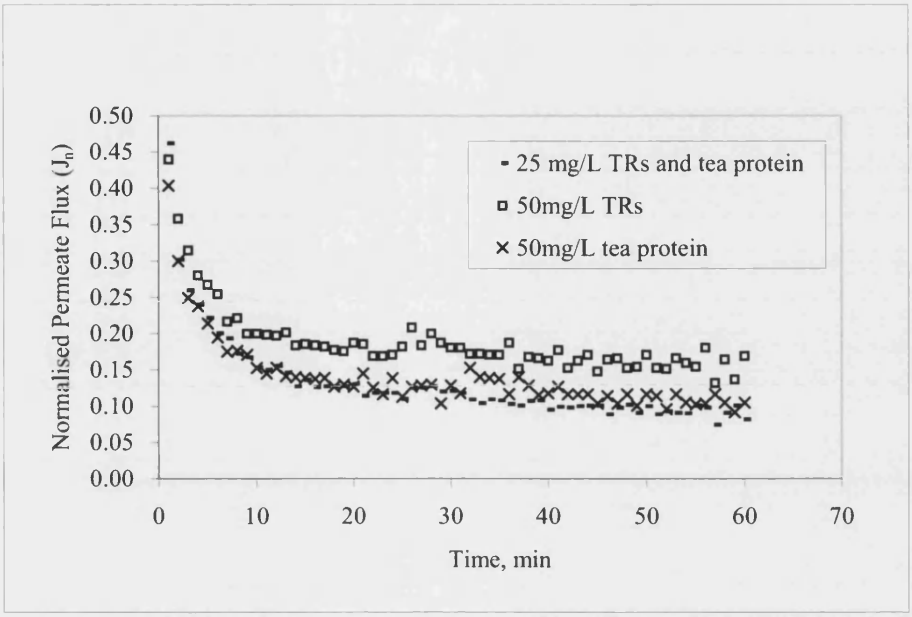

Figure 6.15 Normalized permeate flux (J_n) vs time for fouling by TRs, tea protein, and a binary mixture of the two

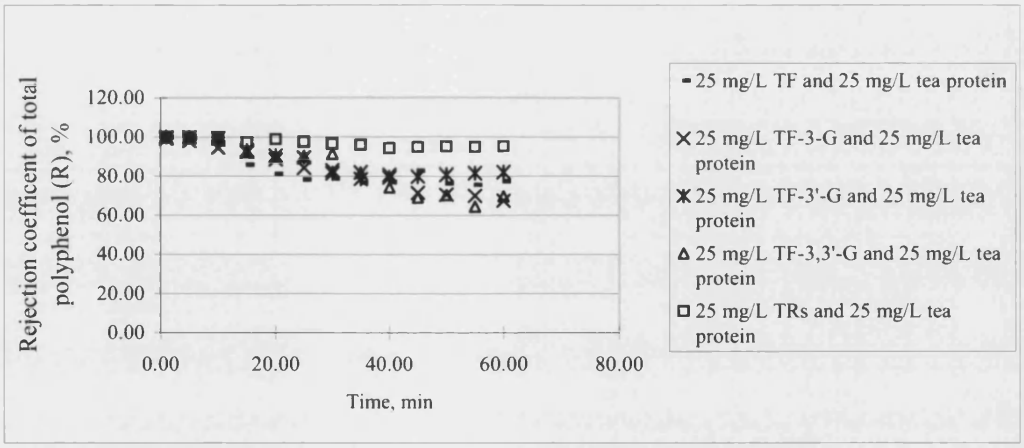

Figure 6.16 The rejection coefficients of total polyphenols during fouling by binary mixtures

Figure 6.17 shows the rejection coefficients of protein in binary protein / polyphenol mixtures during ultrafiltration. The majority of the rejection coefficients are between 70 – 90%. This compares to 100% protein rejection when 50 mg L^{-1} tea protein was filtered under the same conditions. These values indicate that more protein was transmitted through the membranes after mixing with polyphenol components. This result is confirmed by the recorded permeate mass fluxes during filtration.

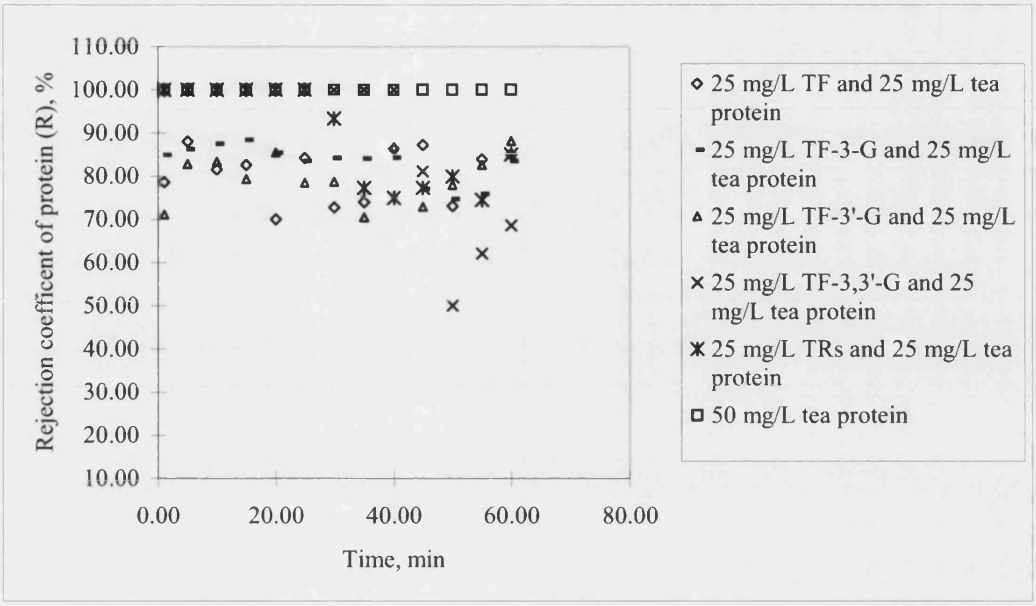

Figure 6.17 The rejection coefficient of protein during filtration of binary protein / polyphenol mixtures

The average values of total polyphenol and protein mass fluxes for both single component and binary mixtures are shown in Table 6.5.

Table 6.5 Average permeate mass fluxes of polyphenols and protein during filtration of individual tea components and protein / polyphenol mixtures

Average of mass fluxes / Model solution	J_{phenol}, mg m^{-2} min^{-1}	$J_{protein}$, mg m^{-2} min^{-1}
50 mg L^{-1} TF	24.2	-
50 mg L^{-1} TF-3-G	7.31	-
50 mg L^{-1} TF-3'-G	11.8	-
50 mg L^{-1} TF-3,3'-G	13.3	-
50 mg L^{-1} TRs	1.48	-
50 mg L^{-1} tea protein	-	0.0
Mixture of TF and tea protein	0.50	0.63
Mixture of TF-3-G and tea protein	0.87	2.55
Mixture of TF-3'-G and tea protein	1.04	3.67
Mixture of TF-33'-G and tea protein	0.72	0.40
Mixture of TRs and tea protein	0.27	2.10

It is clear that in addition to the disproportional drop in the all of the binary mixture TF fluxes compared to single components, there is also an increase in the protein transmission when binary TF / protein mixtures are filtered. A 50 mg L^{-1} solution of protein was completed rejected by the membrane. However, all five of the 25 mg L^{-1} TF / protein binary solutions displayed a non-zero protein component flux (Table 6.5 and

Figure 6.18). Moreover, compared with Figure 6.4, there were increases in permeate mass fluxes with filtration time of polyphenols for all of the binary TF / protein mixtures examined (See Figure 6.19). This finding is significant, as it implies that a membrane that completely rejects a protein solution can be made to transmit some protein when it is a component of a mixture containing polyphenols.

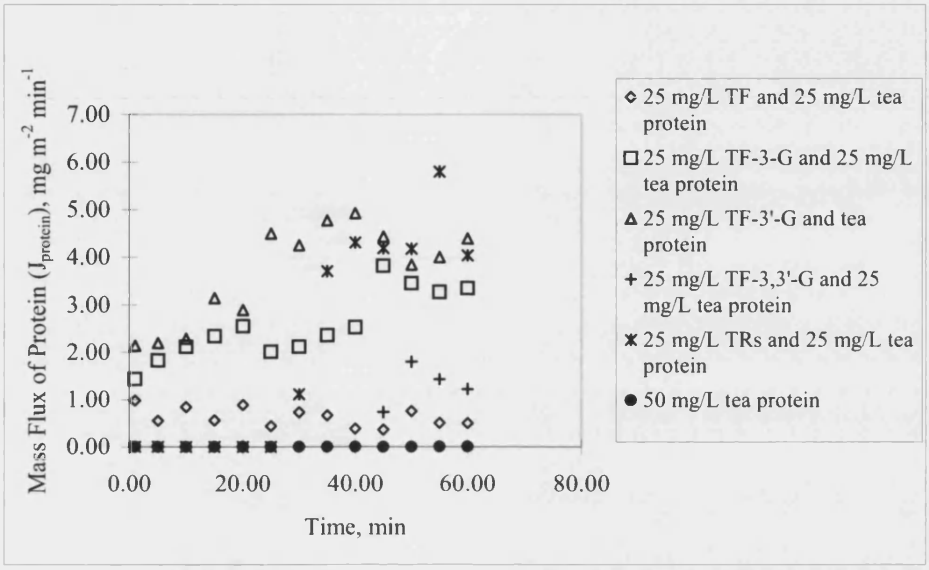

Figure 6.18 Mass transfer of tea protein vs time during fouling by binary mixtures

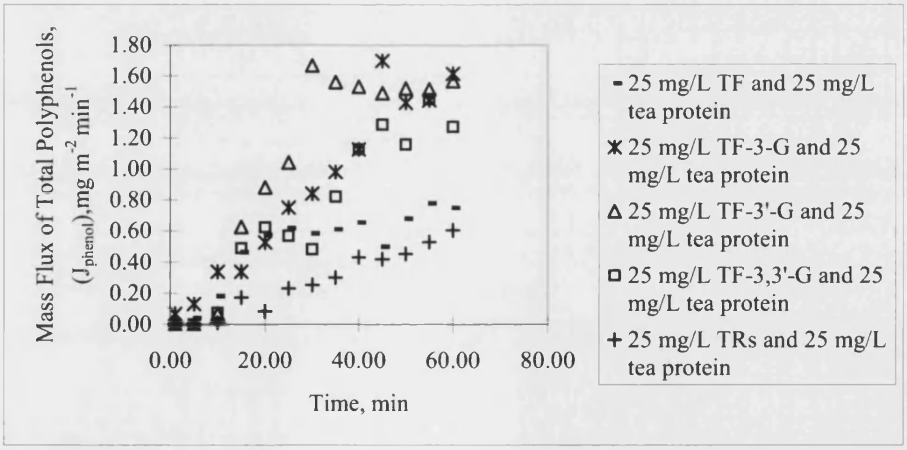

Figure 6.19 Mass transfer of total polyphenols vs time during fouling by binary mixtures

6.3.3 Influence of caffeine on membrane fouling

In addition to protein and polyphenol interactions, caffeine has been implicated in the formation of insoluble tea cream aggregates. To determine the effect of caffeine upon membrane filtration and fouling performance, another group of experiments were carried out, including membrane filtration by (i) 50 mg L^{-1} caffeine, (ii) a binary mixture of 25 mg L^{-1} caffeine and 25 mg L^{-1} protein, and (iii) a mixture of 4 mg L^{-1} caffeine, 7.7 mg L^{-1} tea polyphenols and 7.7 mg L^{-1} tea protein.

Figure 6.20 shows flux declines during fouling by different model solutions. Caffeine of concentration 50 mg L^{-1} presented the highest permeate fluxes. At the beginning of the filtration, the normalized permeate flux was 1.06. While after 45 minutes, the permeate flux dropped to 0.44, indicating a flux decline of 58%. This value is generally lower than those values seen during filtration of individual phenol components mentioned in the section 6.3.1. This could be explained by the fact that caffeine is a relatively small molecule (Molecular mass 194 g mol^{-1}), and so caused less fouling than the other components examined. Fluxes increased by an average value of 0.26 at those intervals when extra feed solution was added into the tank. This is a clear sign of concentration polarization occurring during caffeine ultrafiltration.

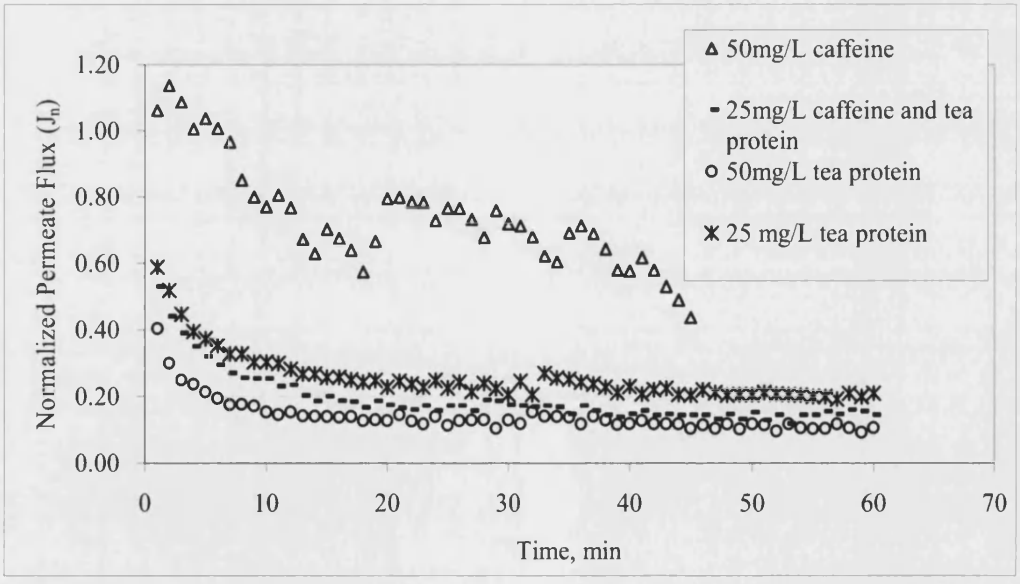

Figure 6.20 Normalised permeate flux (J_n) vs time for fouling by various model solutions

The ultrafiltration of a binary mixture of 25 mg L^{-1}caffeine and 25 mg L^{-1} protein, lead to initial and final normalized fluxes of 0.53 and 0.16 respectively (see Figure 6.20). The fouling flux curve recorded is between that for membranes fouled by 25 mg L^{-1} and 50 mg L^{-1} tea protein. The increase of total solid concentration from 25 to 50 mg L^{-1} in feed solution resulted in a slight decline in permeate fluxes when caffeine was mixed with protein.

Multiple species interaction was investigated by the filtration of a mixture of 4 mg L^{-1} caffeine, 7.7 mg L^{-1} tea protein and 7.7 mg L^{-1} of each of five tea polyphenols. Fouling fluxes resembled those seen in TFs / TRs / tea protein fouling (Figure 6.23). This indicated that caffeine exerted little impact on membrane fouling as long as the total concentration of feed solution remained the same. This hypothesis is confirmed by the comparison of membrane resistances before and after different fouling treatments. According to Figure 6.21, the membrane resistances of three conditioned membranes used for the ultrafiltration of caffeine, binary mixture and multi-mixture, were 7.3 x 10^6 m^{-1}, 1.2 x 10^7 m^{-1}, and 2.1 x 10^7 m^{-1} respectively. After fouling, these values increased to 1.0 x 10^7 m^{-1}, 5.3 x 10^7 m^{-1} and 1.0 x 10^8 m^{-1}, which were 1.4, 4.5, and 4.9 times more than those before fouling for the three mixtures respectively. The relatively small increase in membrane resistance recorded after fouling indicates that the severe decline of permeate seen during filtration of 50mg L^{-1} caffeine was mainly due to concentration polarization rather than membrane fouling.

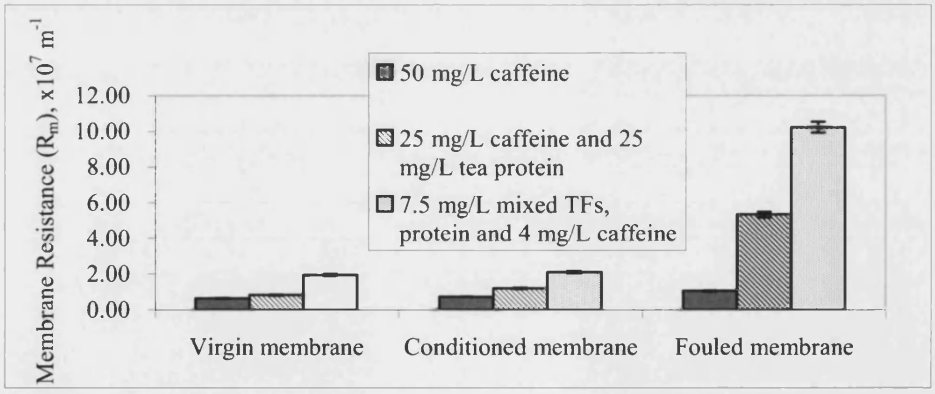

Figure 6.21 Changes of membrane resistances after fouling by different solutions

As can be seen from Figure 6.22, there was a tremendous drop in caffeine mass transfer fluxes from an average of 65.1 mg m^{-2} min^{-1} to only 3.17 mg m^{-2} min^{-1} when caffeine

was mixed with tea protein. This is because of the severe fouling caused by tea protein. The decreasing tendency of caffeine mass transfer was observed on fouling by both individual caffeine and binary mixtures. However, the mass fluxes of protein when membrane was fouled by binary mixture remained zero, which was the same as that seen during fouling by 50 mg L^{-1} tea protein. This result varied from those fouled by binary mixtures of polyphenols and tea protein, implying that the addition of caffeine probably did not change the conditions of either membrane surface or protein. As a result, no additional transmission of protein occurred in this system.

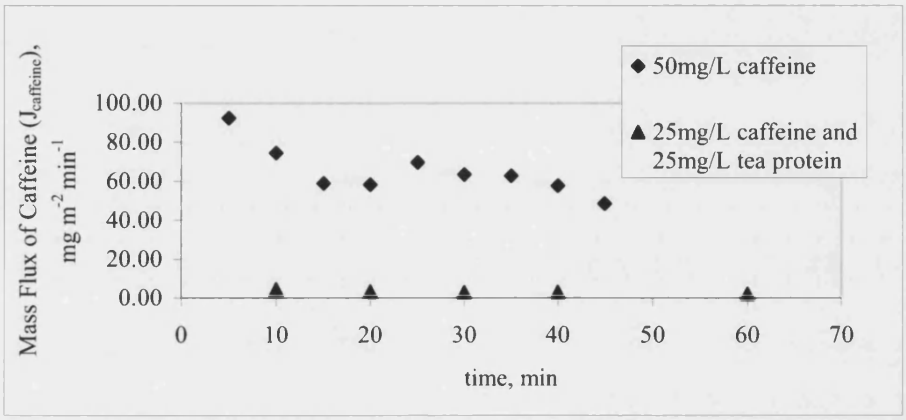

Figure 6.22 Mass flux of caffeine vs. time during filtration of caffeine and a caffeine / protein mixture

6.3.4 Membrane fouling by multiple mixtures

In order to investigate the interactions between multiple components, the following mixtures were filtered (See Table 6.1):

(i) TF, TF-3-G, TF-3'-G, and TF-3,3'-G; 12.5 mg L^{-1} of each component.

(ii) TF, TF-3-G, TF-3'-G, TF-3,3'-G and [1] TRs; 10 mg L^{-1} of each component.

(iii) TF, TF-3-G, TF-3'-G, TF-3,3'-G and tea protein; 10 mg L^{-1} of each component

(iv) 4 mgL^{-1} Caffeine, TF, TF-3-G, TF-3'-G, TF-3,3'-G, TRs and tea protein; (7.7 mg L^{-1}.of each component).

Figure 6.23 shows the flux declines during filtration of the four mixtures detailed above. Mixture (i) (four different theaflavins) had a relatively higher permeate flux than the

other mixtures. The jumps in permeate fluxes during the addition of feed solution were also observed when filtering theaflavins. This can be explained mainly by concentration polarization. The normalized permeate flux during filtration was initially 0.82, and declined to approximately 0.2 after 60 minutes. However, when larger molecules were involved (mixtures (ii) – (iv)), both initial and steady state fluxes decreased considerably. For the mixture of theaflavins with thearubigins, the initial normalized permeate flux was 0.71, and the value declined to 0.12 after 60 minutes. The corresponding values for the fouling by the mixture of theaflavins with tea protein were 0.55 and 0.16 respectively.

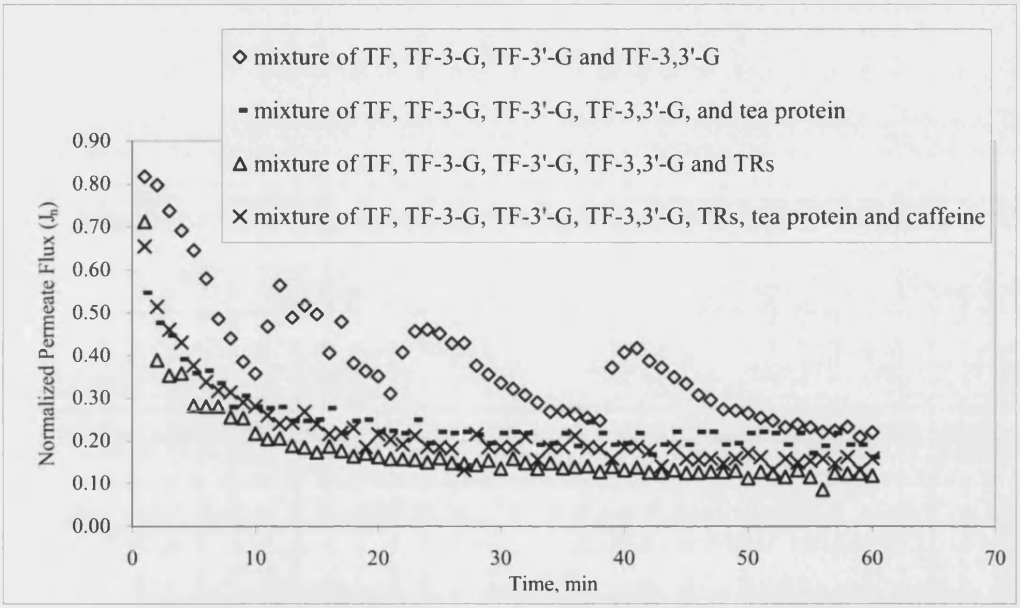

Figure 6.23 Normalised permeate flux (J_n) vs time for fouling by multiple mixtures

The mass fluxes of the theaflavins for mixtures (i) - (iv) are shown in Figure 6.24, 6.25, 6.26 and 6.27 respectively. From Figure 6.24, the masses fluxes of TF were slightly higher than its derivatives. However, few differences could be observed in terms of the shape of mass flux curves of these four theaflavins. When theaflavins were mixed with thearubigins, there were considerable drops in the mass fluxes, especially the initial mass flux values as shown in Figure 6.25. The mass fluxes during first five minutes were 0.3, 0.24, 0, and 0.25 mg ml^{-1} min^{-1} for TF, TF-3-G, TF-3'-G and TF-3,3'-G, while the equivalent values were 12.85, 8.66, 64, and 8.92 mg mL^{-1} min^{-1} respectively before mixing with thearubigins. The percentages of the decrease of the averaged mass

fluxes for TF, TF-3-G, TF-3'-G and TF-3,3'-G were 80%, 63%, 65%, and 73% respectively .

Adding tea protein to the theaflavins (mixture (iii)) resulted in even lower mass fluxes of TF and its derivatives (Figure 6.26). For these solutions, steady state fluxes after 60 minutes were less than a quarter of the value seen when filtering the TFs alone.

Similar trends were obtained for filtration of mixture (iv) (theaflavins, thearubigins, tea protein and caffeine), see Figure 6.27. Even lower values of mass fluxes were seen, and the delay of the start of mass transfer due to the presence of both tea protein and thearubigins is apparent.

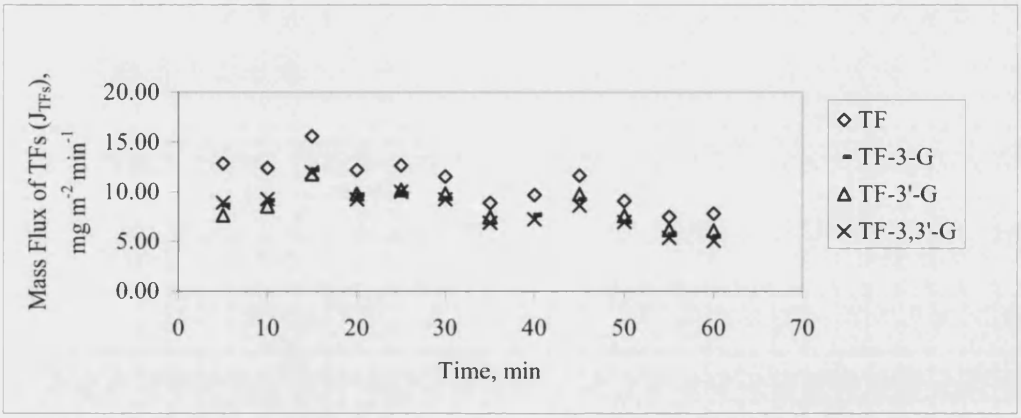

Figure 6.24 Mass flux of TF components vs time during filtration of theaflavin mixture

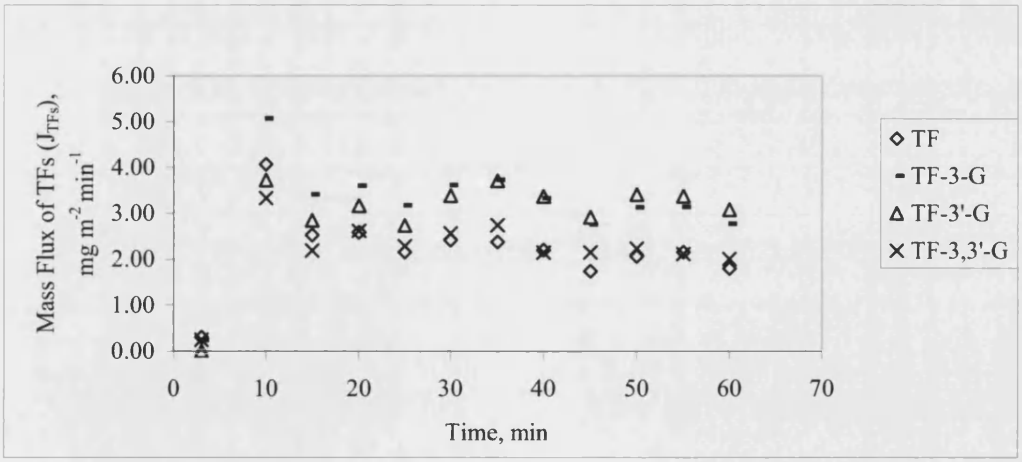

Figure 6.25 Mass flux of TF components vs time during filtration of theaflavin / thearubigin mixture

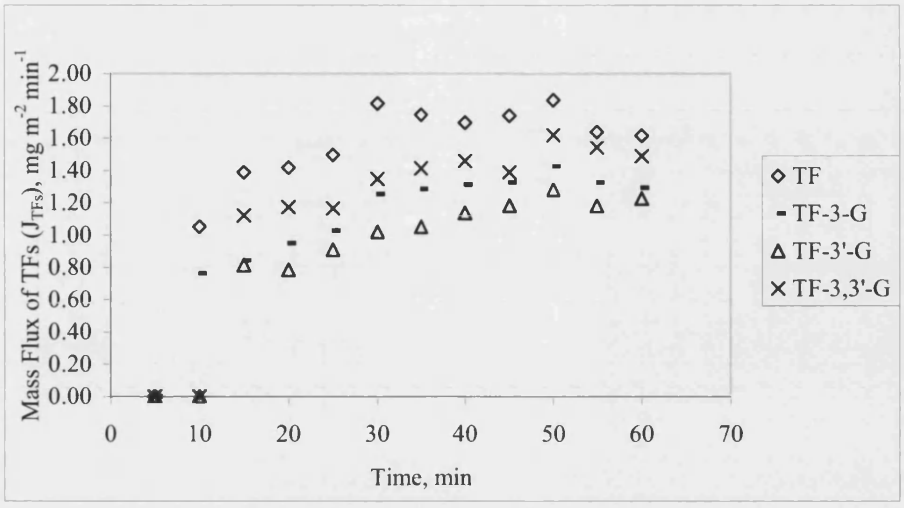

Figure 6.26 Mass flux of TF components vs time during filtration of theaflavin / tea protein mixture

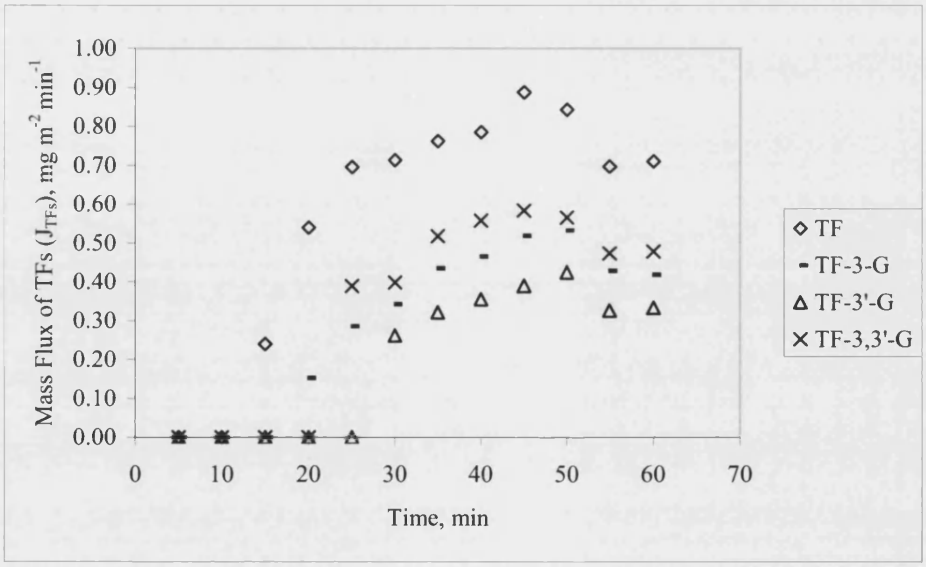

Figure 6.27 Mass fluxes of TF components vs time during filtration of theaflavin, thearubigin, tea protein and caffeine mixture

6.3.5 SEM

The morphology of fouled deposits on membrane surfaces for a range of different conditions has been inspected using SEM. The morphology of the deposits showed considerable variation.

For comparison, Figure 6.28 shows the SEM image of conditioned PSF membrane (MWCO 30 kD) before fouling. The membrane surface appeared to be flat, smooth, and clear of any deposits. Although high magnification of 20,000 was applied, no clear membrane micro-structure was observed. This is presumably due to the even smaller membrane pore size of an average of approximately 8 nanometers according to the molecular weight cut off. After fouling by different model solutions, distinctly different surface images were displayed in Figure 6.29 to 6.34.

As showed in Figure 6.29 (a), a rough surface with a few residues was observed for the membrane fouled by TF. Figure 6.29 (b) showed a layer of foulant formed on the membrane surface after ultrafiltration of tea protein. The porous cake layer is typical of proteinacous deposit seen previously in our laboratory (Shorrock and Bird, 1998, Bartlett *et al*, 1995). X-ray diffraction revealed no difference in elemental composition over the surface of the deposit. The deposit formed from the filtration of a binary mixture of TF and tea protein is seen in Figure 6.29 (c). A considerable aggregate deposition is seen, with nodules of *ca* 0.3 μm being present. It is uncertain whether the formation of these aggregates is a bulk or surface controlled phenomenon.

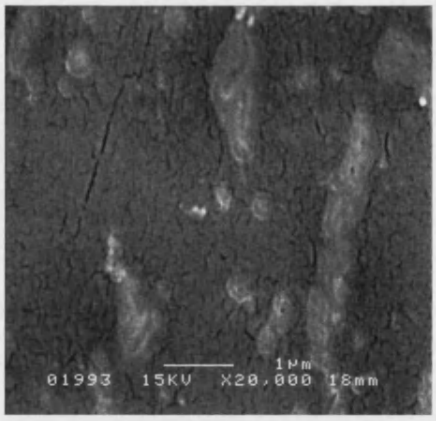

Figure 6.28 Scanning electron micrographs of conditioned PSF (MWCO 30 kD) membrane

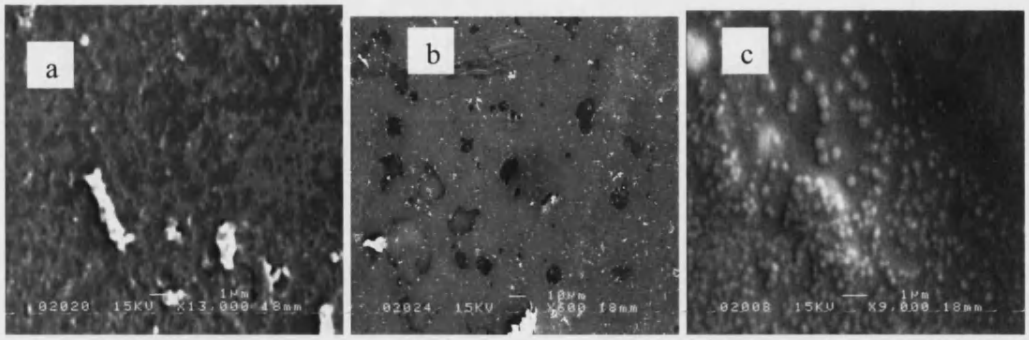

Figure 6.29 Scanning electron micrographs of PSF membranes fouled by a) TF, b) tea protein, and c) binary mixture of TF and tea protein

The SEM images of foulants produced when membranes were fouled by TF-3-G and the binary mixture of TF-3-G and tea protein were compared in Figure 6.30. There was a certain amount of deposition distributed unevenly on the membrane surface, which was fouled by single TF-3-G. While a layer of compact foulant was observed on the membrane fouled by the binary mixture.

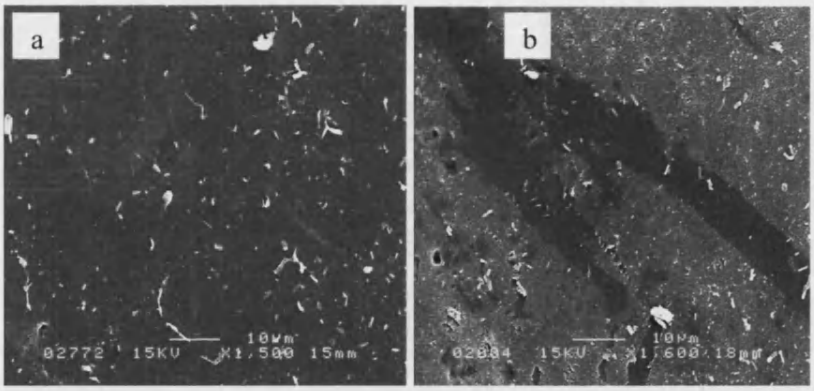

Figure 6.30 Scanning electron micrographs of PSF membranes fouled by a) TF-3-G, and b) binary mixture of TF-3-G and tea protein

In terms of surface morphologies of membranes fouled by the isomer of TF-3-G, namely TF-3'-G, and the corresponding binary mixture with tea protein, total different and unexpected results were found in Figure 6.31. As a result of relative strong self-polymerization of TF-3'-G itself, large quantity of globular aggregations were discovered on the membrane surface. The diameter of each aggregate was nearly 1 μm. However, when TF-3'-G were mixed with tea protein, the shapes of aggregates appeared to become irregular, and they are not as closely distributed as those showed in Figure 6.31 (a).

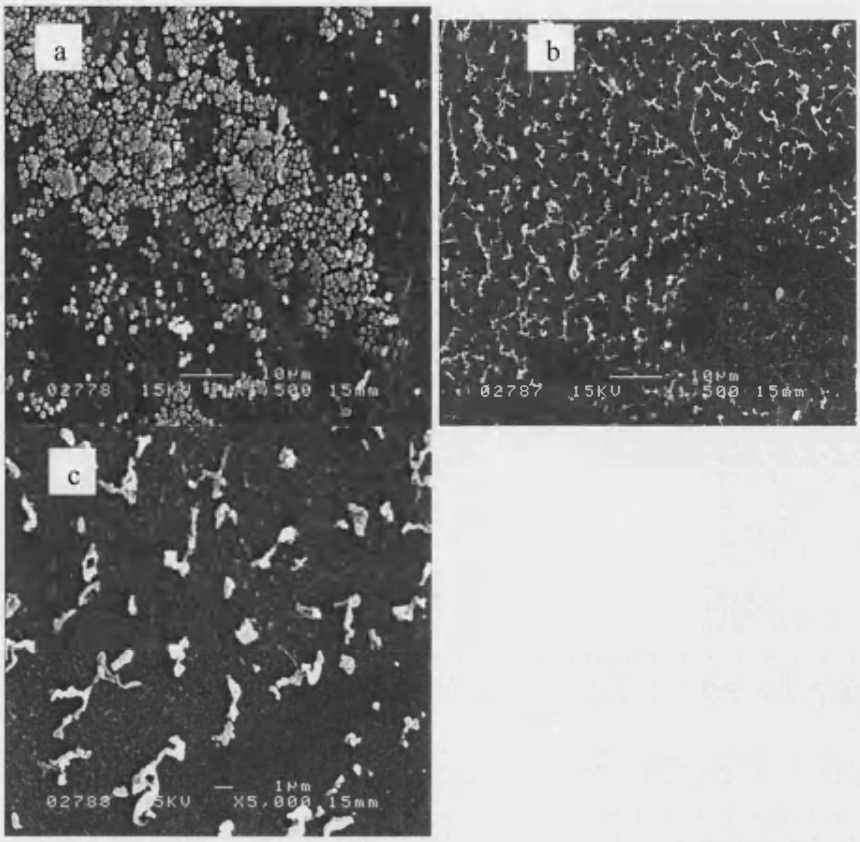

Figure 6.31 Scanning electron micrographs of PSF membranes fouled by a) TF-3'-G at magnification x 1500, b) binary mixture of TF-3'-G and tea protein at magnification x 1500, and c) binary mixture of TF-3'-G and tea protein at magnification x 5000

As to the membranes fouled by TF-3,3'-G, the SEM image resembled to that of membrane fouled by binary mixture of TF-3'-G and tea protein. A large amount of residue remained on the membrane after filtration of TF-3,3'-G (See Figure 6.32 (a)). Similar results were found on the membrane which was fouled by the binary mixture of TF-3,3'-G and tea protein. Nevertheless, a new deposit was also visible with a crystalline structure as showed in Figure 6.32 (b). Unfortunately, X-ray diffraction of the crystalline deposit did not provide much useful information as the foulant and membrane are all organic based materials.

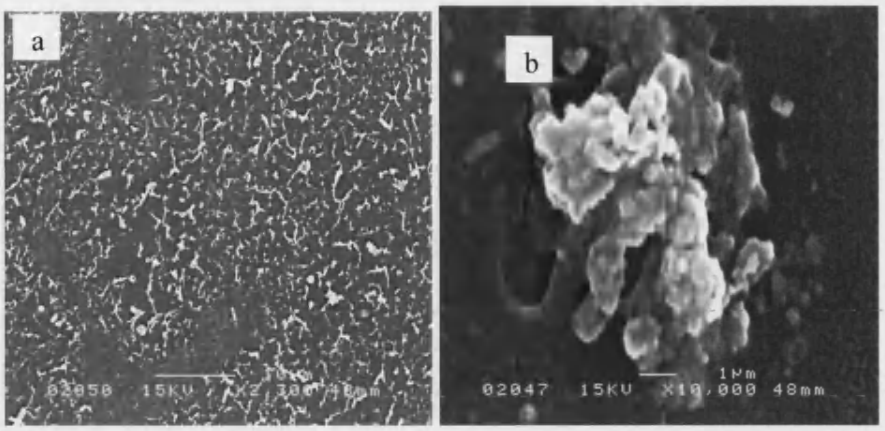

Figure 6.32 Scanning electron micrographs of PSF membranes fouled by a) TF-3,3'-G, b) binary mixture of TF-3,3'-G and tea protein

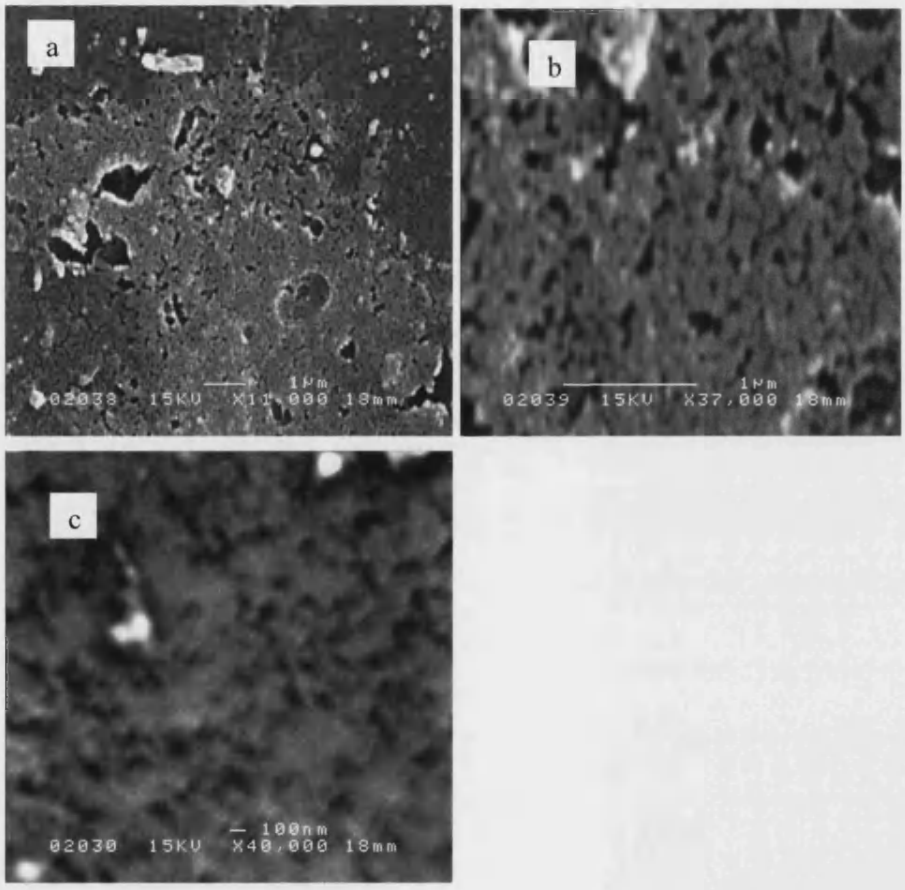

Figure 6.33 Scanning electron micrographs of PSF membranes fouled by a) TRs at magnification x 11,000, b) TRs at magnification x 37,000, and c) binary mixture of TRs and tea protein

Figure 6.33 illustrated the SEM pictures of membrane surfaces fouled by TRs and the mixture of TRs and tea protein. Cake-like layer of foulant visualized on both membranes confirmed the much more severe fouling caused by these relatively larger molecules compared with other smaller molecules such as TFs.

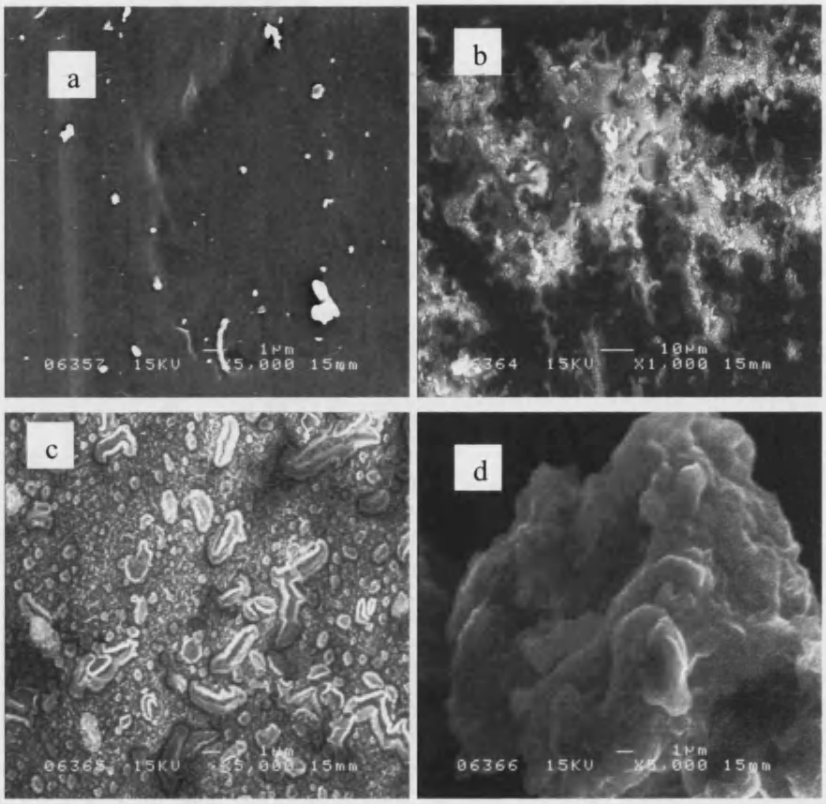

Figure 6.34 Scanning electron micrographs of PSF membranes fouled by a) caffeine at magnification x 5000, b) binary mixture of caffeine and tea protein at magnification x 1000, c) binary mixture of caffeine and tea protein at magnification x 5000, d) binary mixture of caffeine and tea protein at magnification x 5000

Figure 6.34 showed the images of the membranes fouled by caffeine and the mixture of caffeine and tea protein. There were huge differences between these two membranes. For the membrane fouled by only caffeine, few deposits remained on the membrane surface after filtration. While relatively large amount of foulants were observed on the membrane fouled by binary mixture. Moreover, the foulants appeared to have two different structures as shown in Figure 6.34 (c) and (d). The crystal-like foulant could be derived from the aggregation of protein itself as similar structure was visualized on

the membrane fouled by binary mixture of TF-3,3'-G and tea protein. While the other structure might be due to the interaction between caffeine and tea protein.

It is clear that protein / TF mixtures still readily foul surfaces, so another explanation for the improved transfer of protein in the binary mixture must be sought. Changes in membrane hydrophobicity have been found to affect membrane permeability during membrane filtration of tea liquor (Evans and Bird, 2006). Surface charge has also been proved to be a key parameter, and may facilitate the transmission of protein based complexes that would otherwise be repelled by the surface and left in the retentate. This hypothesis was investigated by measuring the zeta potential of membranes in determining the filtration characteristics of lignosulphonates (Weis *et al*, 2003, 2005). It is possible that both modification of membrane hydrophobicity and the masking of repulsive charges present in the surface bound proteinaceous deposition are taking place during filtration of the protein / TF system, inducing the additional transmission of protein and increasing transfer of TF components. This hypothesis is examined by measuring the contact angles and the zeta potential of some selected fouled membranes. The results are shown in Chapter 7.

6.4 Conclusions

Filtration characteristics of a range of individual tea polyphenol and protein feeds were determined at a concentration of 50 mg L^{-1}. Liquid permeate flux declines recorded were typically severe, with more than 60% of the initial flux being lost within 15 minutes. An exception was TF filtration, where liquid permeate flux decline by 44 % after 15 minutes. Fluxes of all components continued to decline gradually, and were still declining when filtration was stopped after 60 minutes had elapsed.

Among the tea polyphenol component investigated, pure component TF filtration showed the most obvious signs of concentration polarization during filtration, though TF-3'-G also displayed this phenomenon.

There was good agreement between the rank order of the normalized flux curves (highest to lowest) and the reverse order of the initial apparent rejection coefficients (ie a high permeate solution flux is associated with a low rejection of a component). The high rejection of a relatively small molecule such as TF indicates that molecular mass do not control the filtration process.

The mass fluxes of total polyphenol (J_{phenol}) during filtration of all TF solutions declined as time progressed. The decline in the transfer flux of the TF's matched the decline of the liquid permeate flux, indicating that no additional selectivity took place as a result of cake deposition or concentration polarization increasing with time. The transfer flux of TR increased over the first 30 minutes of the experiment, even though the liquid permeate flux declined during filtration.

The filtration curves for binary TF / protein mixtures (25 mg L^{-1} each) tended to resemble those for 50 mg L^{-1} protein. Much higher rejection coefficients for all five polyphenol solutions were also noticed after adding tea protein. There was also an increase in the protein transmission when binary TFs / protein mixtures were filtered. This implies that a membrane that completely rejects a protein solution can be made to transmit some protein when small molecular weight polyphenols are added.

It is possible that the masking of repulsive charges present in the surface bound proteinaceous system is taking place in the protein / polyphenol binary systems, reducing the overall charge of the system, and allowing the transmission of protein based complexes.

Caffeine is associated with the formation of tea cream. However, as the smallest molecule in the tea components investigated here, it had little effect upon other components in the mixture. Concentration polarization was the main reason for the flux decline during filtration of caffeine alone. When caffeine was mixed with either protein or protein plus polyphenol mixtures of equivalent concentrations, the normalized filtration fluxes reduced significantly to a level which was nearly equal to that seen for 50 mg L^{-1} of tea protein. Caffeine was highly rejected during the filtration of binary mixtures. The average mass flux of caffeine after mixing with protein was less than 5 % of that when the membrane was fouled by caffeine alone. However, the addition of

caffeine did not modify the transmission behaviour of tea protein. Tea protein was 100% rejected by the membrane during the fouling despite of the presence of caffeine. This indicated that caffeine did not have significant influence upon membrane fouling under the conditioned investigated.

When the membranes were fouled by different groups of multiple mixtures, the results were similar to those by fouling of individual components and binary mixtures. The mixtures containing tea protein, thearubigins or both, led to lower permeate fluxes during fouling. The mass transfer of TF and its derivatives showed identical behaviours during each of the filtration experiments. The presence of thearubigins lowered the mass fluxes of each theaflavin due to severe fouling. The addition of tea protein also reduced the transmission of theaflavins.

SEM indicated that there was a considerable difference between the morphologies of different foulants generated by the filtration of the mixtures examined. Tea protein and TRs (alone or in combination) generated a more severe fouling than any of the TF components, as supported by the filtration data. A large quantity of spherical aggregates were present on the membrane fouled by TF-3'-G, indicating that a different aggregation phenomenon had occurred for this component.

Chapter 7 NaOH cleaning of membranes fouled by model tea component solutions

7.1 Introduction

The fouling behavior of different model solution has been described in Chapter 6. Once the membranes were fouled, they need to be cleaned. Therefore, the cleaning effectiveness of membranes fouled by different model tea components has been investigated in this chapter.

7.2 Experimental methods

7.2.1 Experimental equipment and cleaning protocol

The experimental equipment used in membrane cleaning studies is the same dead-end filtration system illustrated in Chapter 6 (see Figure 6.1). A standard cleaning protocol was applied throughout all the cleaning experiments to maintain comparability. Following the fouling protocols described in Chapter 6 (see Table 6.2), the cleaning step was carried out by passing 0.2 wt% NaOH solution through the membrane at 22 °C, TMP 1.5 bar for 15 minutes. This cleaning protocol was developed in cross flow filtration experiments performed in our laboratory. The cleaning flux (J_c) was recorded. Subsequently, a final pure water flux measurement (J_{wc}) at TMP 1.5 bar was used to determine the resistance of cleaned membrane (R_c). The initial membrane resistance (R_m) and resistance of fouled membrane (R_f) were calculated from the pure water flux measurements after conditioning (J_{wm}) and that after fouling (J_{wf}). The total irreversible fouling resistance (R_{if}) and the residual fouling resistance left after cleaning (R_{rf}) were defined in equation (7.1) and (7.2) respectively:

$$R_{if} = R_f - R_m \quad (7.1)$$

$$R_{rf} = R_c - R_m \quad (7.2)$$

7.2.2 Evaluation of cleaning efficiency

Reversible fouling is defined as that which is removed by water rinsing alone; i.e. loosely bound deposits and concentration polarisation layers. Irreversible fouling is that which is not removed by water rinsing. The membrane after fouling was rinsed with pure water at 22 °C, TMP 1.0 bar for 6 minutes with the aim to remove the loosely bound deposits remaining on the membrane surface.

Cleaning efficiency has been evaluated in terms of membrane permeability recovery. Two parameters are defined to facilitate a comparison of the membrane permeability before and after fouling and cleaning.

(i) the standard percent flux recovery. Defined as the ratio of the pure water flux after cleaning (J_{wc}) to the pure water flux of the virgin membrane (J_{wm}).

$$\text{Flux Recovery } \% = \frac{J_{wc}}{J_{wm}} \times 100\% \qquad (7.3)$$

(ii) the percentage fouling resistance recovery following cleaning. Defined as the ratio of the difference in the fouled and cleaned membrane resistances to the difference between the fouled and virgin membrane resistance. This quantity gives a measure of the fraction of the resistance recovered due to cleaning.

$$\text{Fouling resistance recovery } \% = \frac{R_{if}\text{-}R_{rf}}{R_{if}} \times 100\% \text{ (equal to } (R_f - R_c) / (R_f - R_m)) \qquad (7.4)$$

7.2.3 FTIR

As introduced in Chapter 2, Attenuated Total Reflection – Fourier Transform Infrared Spectroscopy (ATR-FTIR) is a very sensitive technique in examining the chemical components in and remained on the membrane. It is therefore useful to evaluate the cleaning effectiveness after membrane cleaning operation.

7.2.4 Visualization of membranes after cleaning by Scanning Electron Microscope (SEM)

Scanning electron microscopy (SEM) was also applied to inspect the membrane surface after cleaning processes. Air and vacuum dried membranes were stuck to SEM stubs with conductive paste, followed by coating with a thin layer of gold. Subsequently, the specimens were viewed with a JSM 6310 scanning electron microscope in combination with a microanalysis system, LINK AN10000 (Oxford Instruments).

7.2.5 Membrane hydrophobicity determination by contact angle measurement

The contact angles of selected membranes were measured using a sessile drop method. A drop of pure water was placed on the membrane surface and the contact angles from both side of drop were measured. This procedure was repeated 6 times at different points on the membrane surface, producing a total of 12 measurements, which were then averaged.

7.2.6 Zeta-potential measurement

As described in Chapter 2, Zeta-potential parameter has been used to indicate the surface charge conditions, which are highly associated with the separation properties and fouling tendencies of membranes. For ultrafiltration membranes, zeta-potential can be determined via streaming potential method, which has been proven to be the best method to characterize the surface charge densities of different membranes (Pihlajamäki and Nyström, 1995).

Zeta potential measurements reported in this paper were recorded using apparatus at the Lappeenranta University of Technology, Finland. Figure 7.1 illustrates the apparatus used for measuring the streaming potential simultaneously. The cross flow membrane module used in this system is designed for flat sheet membrane with area 10.4 cm^2. The main body of the module and the porous supports were made from polycarbonate and polyethylene respectively. The materials for other parts, such as electrode plugs and some supports were polyvinlchloride. A pair of Ag/AgCl electrodes that could measure the streaming potential developed across the membrane were fitted separately to both sides of the module and sealed with O-rings. All the important data were collected in a

computer via data acquisition software programmed with MS® quickBASIC version 4.5 and using an ADDA14 interface card.

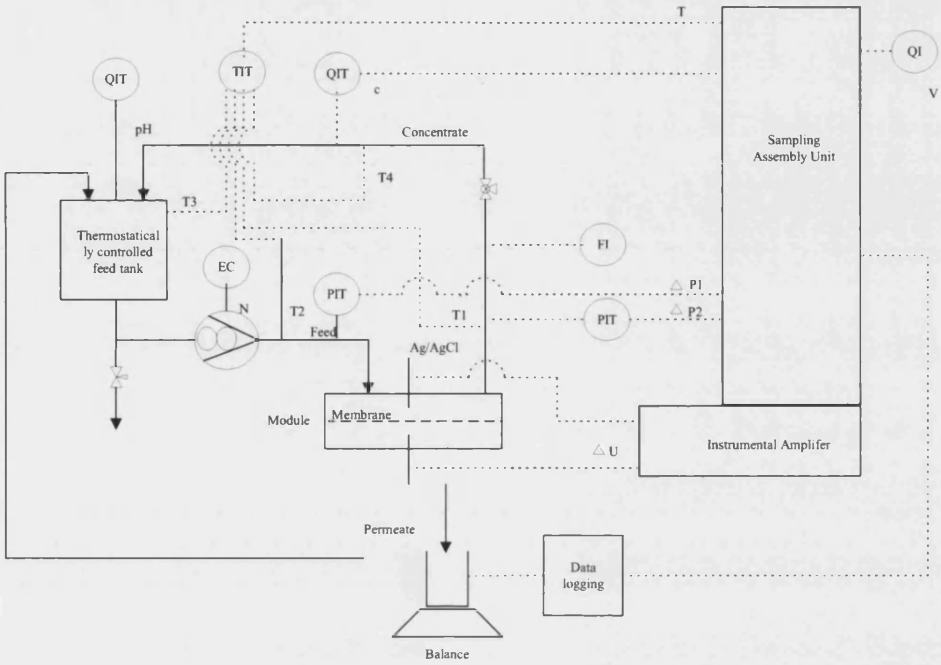

Figure 7.1 The schematic diagram of the apparatus for simultaneous streaming potential measurement

A potassium chloride (KCl) solution of concentration 0.001 mol L^{-1} was used as the electrolyte in these experiments. An approximate pH range 4 to 7 was covered during measurement of each membrane sample. At each pH, the streaming potentials across the membrane were measured under a series of pressures, while the flow rate was kept constant throughout the experiment. Apparent zeta potential (ζ) of the membrane at each pH was then calculated according to the Helmholtz-Smoluchowski equation (See eq.(7.5)) without corrections.

$$\zeta = \frac{\Delta E \times \eta \times \kappa}{\Delta P \times \varepsilon_0 \times \varepsilon_r} \qquad (7.5)$$

where ΔE is the streaming potential; P is the pressure; η is the viscosity of the solvent; κ is the conductivity of the electrolyte in the pores; ε_0 is the permittivity of a vacuum; ε_r is the relative dielectric constant of the electrolyte.

However, it should be noticed that the zeta-potential values measured here are just the apparent zeta potential rather than the real zeta as some problems should be taken into account when calculating zeta potential from the streaming potential. One is the variation in surface conductivity due to the difference in surface roughness. The other is the error caused by the overlapping of electrical double layer in small pores. To obtain the real zeta potential, the corrections of Helmholtz-Smoluchowski equation should be made in terms of these errors mentioned above. Nevertheless, this is rather difficult because of the lack of confident mathematical models as well as the accurate physical parameters, such as the pore size distributions of different membranes. As a result, the apparent zeta potential values were used to indicate how the surface has changed when it was treated by different operations.

7.3 Results

7.3.1 Cleaning effectiveness of membranes fouled by individual tea components

Membranes fouled by 50 mg L^{-1} individual tea components, namely TF, TF-3-G, TF-3'-G, TF-3,3'-G, TRs and tea protein were cleaned by 0.2 wt% NaOH solution under the same conditions. Figure 7.2 illustrated the standard percentage of flux recovery of membranes fouled by different tea components after cleaning. The results indicate that after cleaning the permeabilities of membranes fouled by the relatively small molecules of TF, TF-3-G, TF-3'-G and TF-3,3'-G have recovered to 83%, 75%, 82% and 74% of those for the conditioned membranes for the four components respectively.

Nevertheless, membranes fouled by larger molecules such as thearubigins and tea protein, had relatively poor flux recoveries of 62% and 69% respectively. This could be explained by the comparatively more severe fouling caused by thearubigins and tea protein. In addition, more than 80% of the irreversible fouling resistance was removed

by sodium hydroxide cleaning for membranes fouled by all the individual tea components mentioned above (see Figure 7.3). This indicated that membrane cleaning using 0.2 wt% NaOH is reasonably effective for the membranes fouled by tea components.

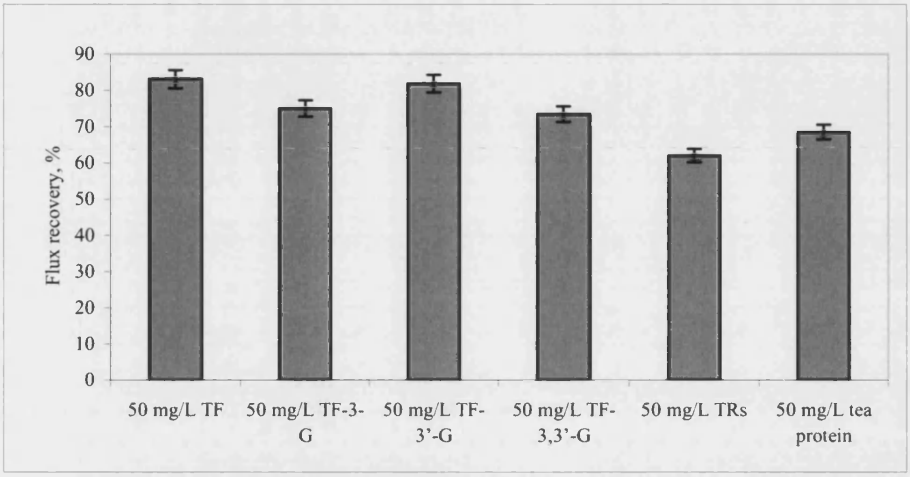

Figure 7.2 Percent flux recovery of different fouled membranes after cleaning

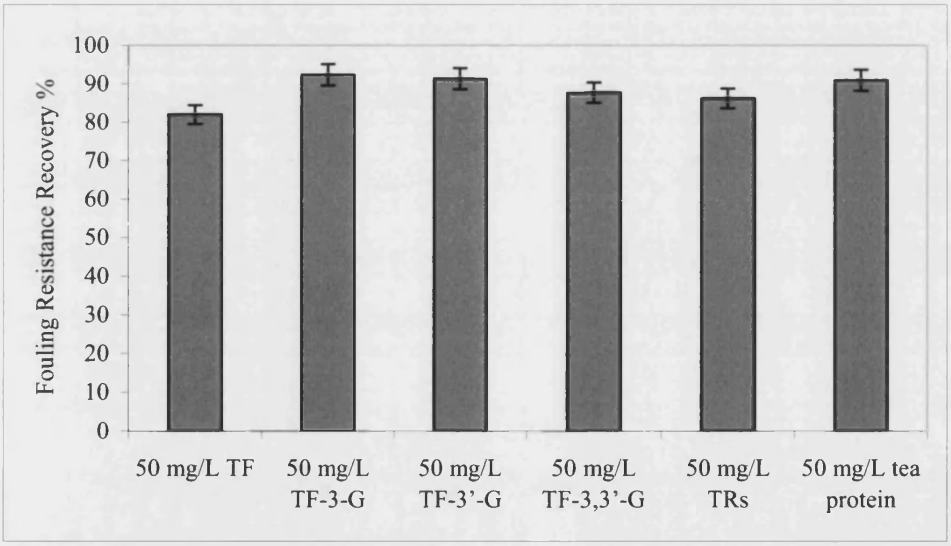

Figure 7.3 Fouling resistance recovery of different fouled membranes after cleaning

7.3.2 Cleaning efficiency of membranes fouled by binary mixtures of tea polyphenols and tea protein

According to the results in Chapter 6, tea protein dominated membrane fouling when membranes were fouled by binary mixtures of tea polyphenol components and tea protein. Fouling fluxes became to resemble to that of fouling by only tea protein. Higher rejections of total polyphenols were also observed. Table 7.1 shows that filtration of binary mixtures of TF's and protein tends to lead to higher irreversible fouling resistances than the filtration of equivalent concentrations of single polyphenols. After standard NaOH cleaning, more than 80% irreversible fouling resistance has been removed for membranes fouled by these binary mixtures. The flux recoveries after cleaning of membranes fouled by binary mixtures are shown in Figure 7.4.

Table 7.1 The irreversible fouling resistance of membranes fouled by individual components and the binary mixtures

Membrane fouled by model solution	R_{if}, x 10^7 m^{-1}
50 mgL^{-1} TF	1.23±0.04
50 mgL^{-1} TF-3-G	5.02±0.15
50 mgL^{-1} TF-3'-G	2.79±0.08
50 mgL^{-1} TF-3,3'-G	3.75±0.11
50 mgL^{-1} TRs	3.92±0.12
Mixture of 25 mgL^{-1}TF and 25 mgL^{-1}tea protein	9.14±0.27
Mixture of 25 mgL^{-1}TF-3-G and 25 mgL^{-1}tea protein	4.99±0.15
Mixture of 25 mgL^{-1}TF-3'-G and 25 mgL^{-1}tea protein	3.35±0.10
Mixture of 25 mgL^{-1}TF-33'-G and 25 mgL^{-1}tea protein	7.20±0.22
Mixture of 25 mgL^{-1}TRs and 25 mgL^{-1}tea protein	4.87±0.15

The flux recoveries of membranes fouled by mixtures of TF and tea protein, and TF-3,3'-G and tea protein, were 79%, and 72% separately. These values are slightly lower than those of membranes fouled by corresponding phenol components. However, unexpected results were found on the cleaning of membranes fouled by the mixtures of TF-3-G and tea protein, and TF-3'-G and tea protein. The flux recoveries of cleaned membranes for ultrafiltration of these two groups of mixtures were more than 90%. Tea protein and TRs in the mixture generated the deposit that was the most difficult to clean, with a flux recovery of only 57%.

Although some of the membranes were less cleaned than those fouled by the corresponding individual tea polyphenols, the sodium hydroxide cleaning of membranes were still effective to a certain extent as the fouling resistance recoveries after cleaning were more or less over 80% (see Figure 7.5).

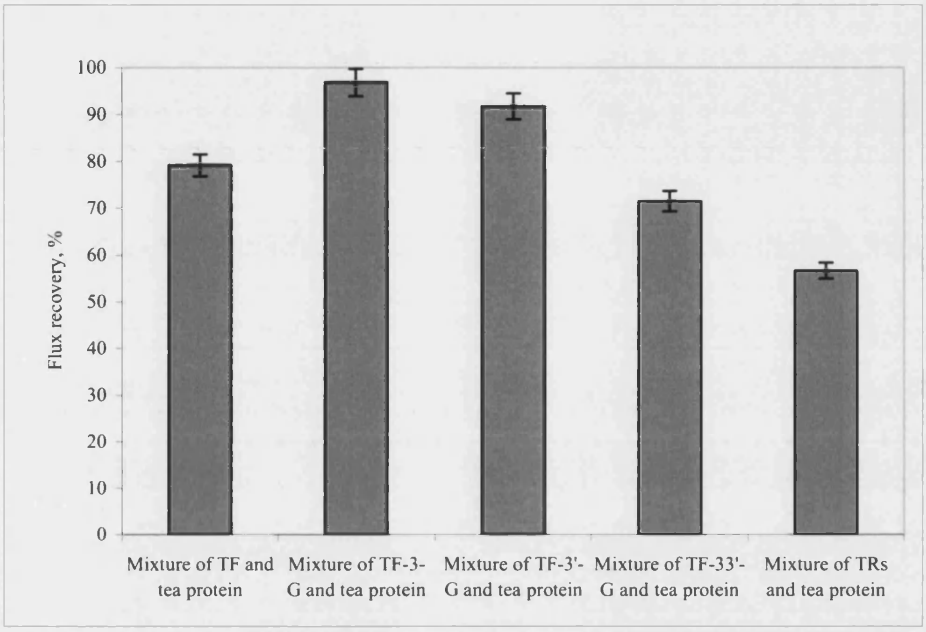

Figure 7.4 Percentage flux recovery of fouled membranes after cleaning

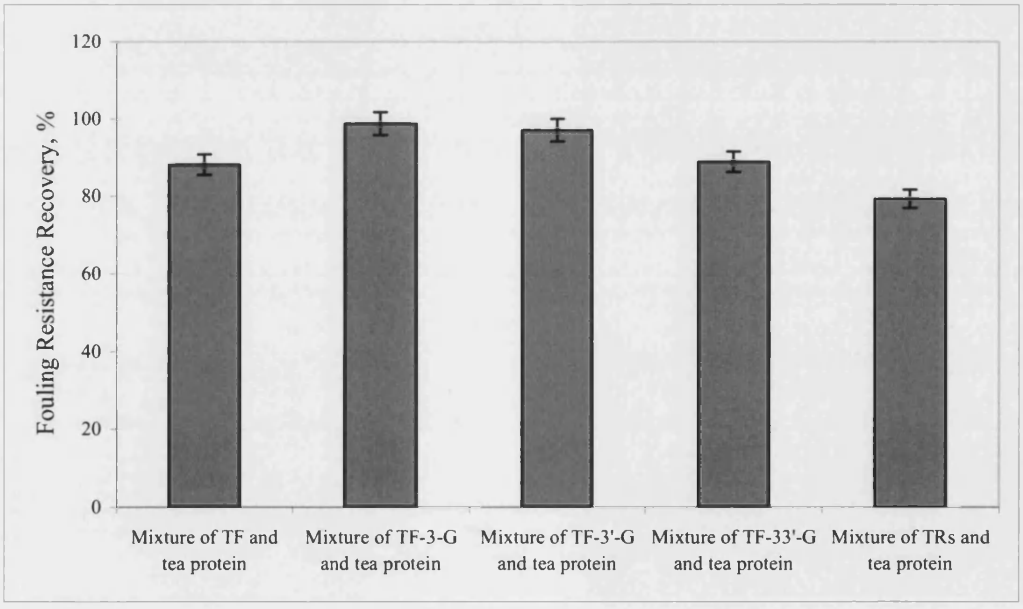

Figure 7.5 Fouling resistance recovery of different fouled membranes after cleaning

7.3.3 Membrane fouling and cleaning examined by using ATR-FTIR

The IR spectrum can be examined to identify small changes in the composition of material on the surface occurring as a result of fouling and cleaning processes

In theory, the use of IR spectrum can also help determine the structural information of either membrane or the materials remaining on the membrane surface. However, it is not easy to do so in this part of study. The interpretation of infrared spectra involves the correlation of absorption bands in the spectrum of an unknown compound with the known absorption frequencies for types of bonds, which are normally from the reference spectrum of pure materials. In reality, materials such as polysulphone membrane or tea components all consist of different substances, which augment the difficulties in data interpretation. Moreover, except for the frequency (cm^{-1}), the intensity and shape of the absorption band also need to be taken into account to make sure of the proper identification of the absorption band. All these enquire plenty of knowledge and experience. Consequently, it can be quite risky to achieve the correct interpretation.

The intensity of infrared absorption bands can be used to quantify the amount of material present on the membrane. However, in this study, the layers of foulant remaining on the membranes were too thin to generate data suitable for quantitative analysis. Therefore, the FTIR spectrum could only be used qualitatively to compare the surface conditions after fouling and cleaning.

Figures 7.6 (a) – (f) illustrate the FTIR spectra of membranes fouled by (a) tea protein, (b) TF, (c) binary mixture of TF and tea protein, (d) TF-3-G, (e) binary mixture of TF-3-G and tea protein, and (f) TF-3'-G respectively. In each of the figures, the black line represents the spectrum of the fouled membrane after the spectrum of the conditioned membrane has been subtracted. This signifies the infrared absorption bands attributable to the foulants. The grey lines represent the spectra of the corresponding cleaned membranes after subtraction of conditioned membrane spectrum. This indicates whether there were any foulant residues left on the membrane surface after cleaning. The spectra are presented at their natural intensities.

In Figure 7.6 (a), the bands highlighted at 1650 cm^{-1} and 1565 cm^{-1} are attributed to C=O stretch in amides. These are characteristic of protein bands (Smith and Franzen, 2002; Pudney, 2006, www.imb-jene.de). The differences in natural intensities of the two spectra show that 'tea protein' was largely removed by chemical cleaning. Figure 7.6 (b) indicates that partial removal of TF took place due to cleaning. The spectrum for the binary protein / TF mixture (Figure 7.6 (c)) is more similar to the spectrum of the membrane fouled by tea protein alone than to that of the membrane fouled by TF, indicating that protein dominated membrane fouling. This is in agreement with the permeate flux results shown in Figure 6.11. However, the spectrum indicates that the membrane shown in Figure 7.6 (c) is much cleaner than the one fouled by TF alone.

This trend is continued with TF-3-G (Figure 7.6 (d)). The spectra indicate that the cleaning procedure left residues of TF-3-G on the membrane surface. However, a binary mixture of TF-3-G and protein (Figure 7.6 (e)) was more effectively cleaned, leaving minimal residues detected by the FTIR trace. For both TF-3-G and the binary TF-3-G / protein mixture, a point in the spectra of the cleaned membranes around 1660 cm^{-1} showed an increase over that of the fouled membrane. It is possible that these peaks correspond to hydrolysed TF-3-G.

In contrast with TF, TF-3-G and TF-3'-G appeared to have been very effectively removed from the membrane surface by the cleaning protocol (Figure 7.6 (d) (f)). This result is supported by the high flux recovery seen for this compound recovery (Figure 7.4).

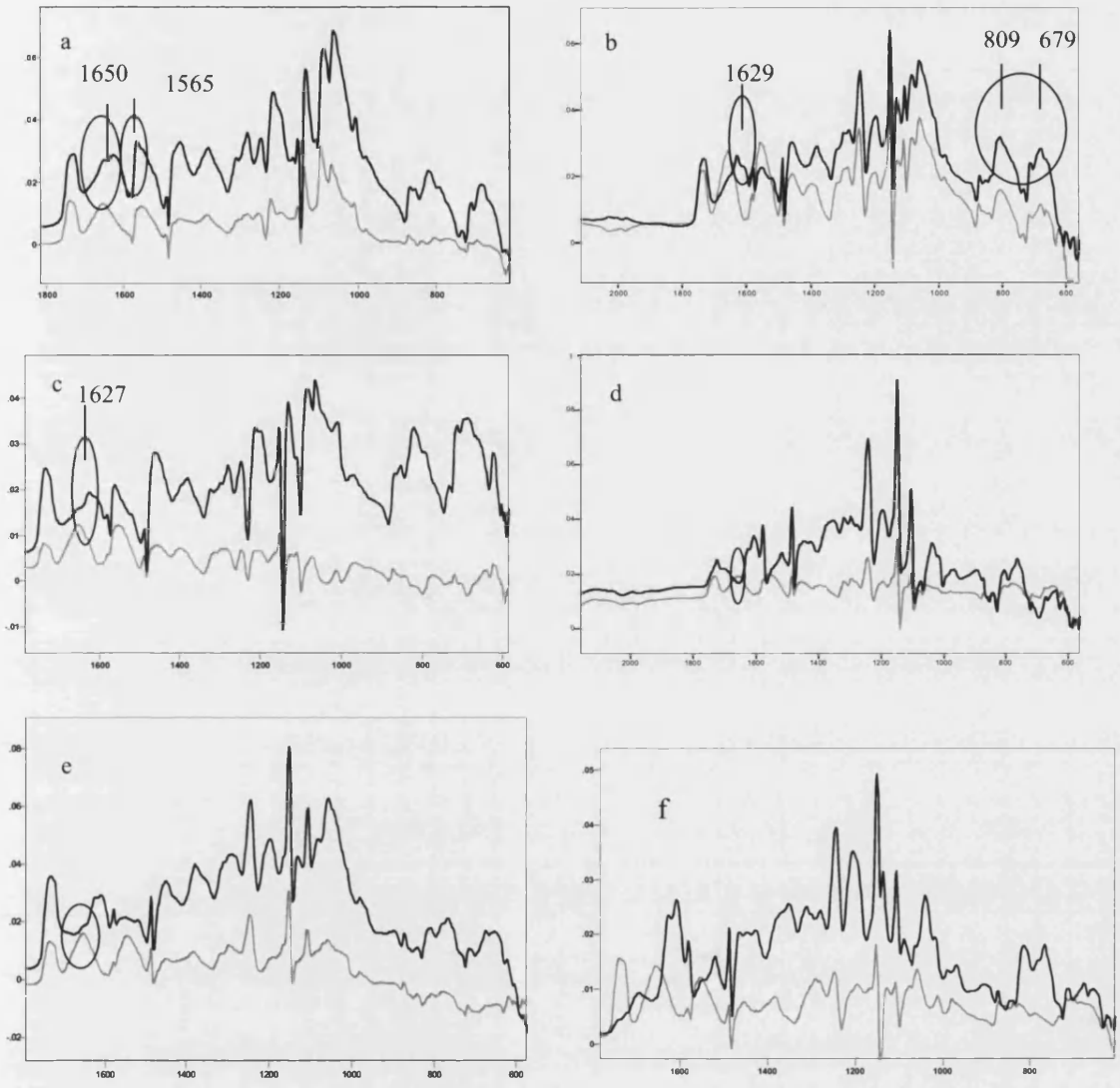

Figure 7.6 (a)-(f). FTIR spectrum of fouled membranes and fouled & cleaned membranes. (a). Tea protein fouled membrane and corresponding cleaned membrane; (b). TF fouled membrane and corresponding cleaned membrane; (c). TF / tea protein binary mixture fouled membrane and corresponding cleaned membrane; (d). TF-3-G fouled membrane and corresponding cleaned membrane; (e). TF-3-G / protein fouled membrane and corresponding cleaned membrane; (f). TF-3'-G fouled membrane and corresponding cleaned membrane

7.3.4 SEM

To confirm the cleaning effects on the membranes fouled by different model solutions, scanning electron microscopy (SEM) was used to examine membrane surfaces after cleaning. As shown in Figure 7.7, the membranes fouled by either individual phenol components or the binary mixtures appeared to be generally cleaned after the standard NaOH cleaning step, though residues of *ca* 0.3 μm remained on some surfaces. The fact that flux recoveries of 55 – 90% were seen on surfaces that appeared relatively clean is not surprising, given that in pore deposition is likely, and that permeate flux recovery in itself is a poor indication of surface condition.

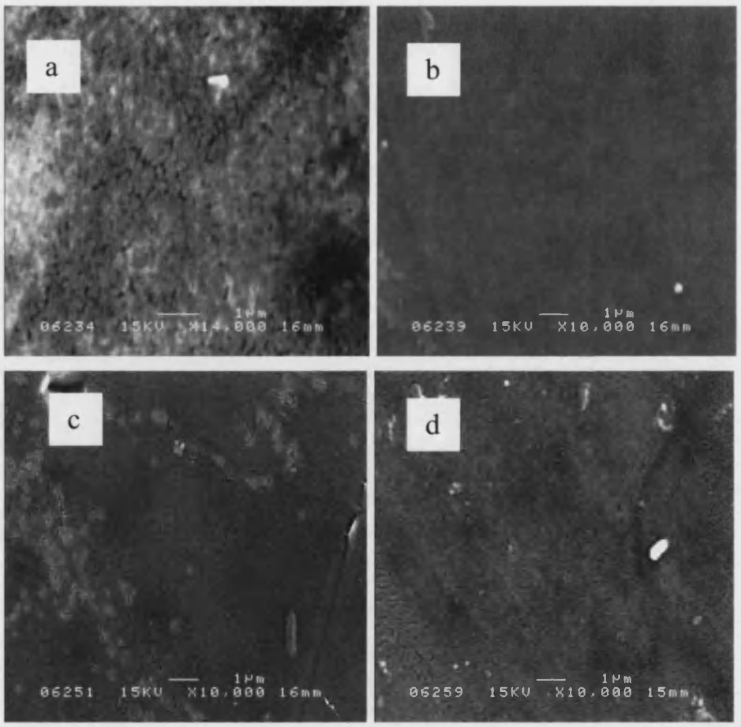

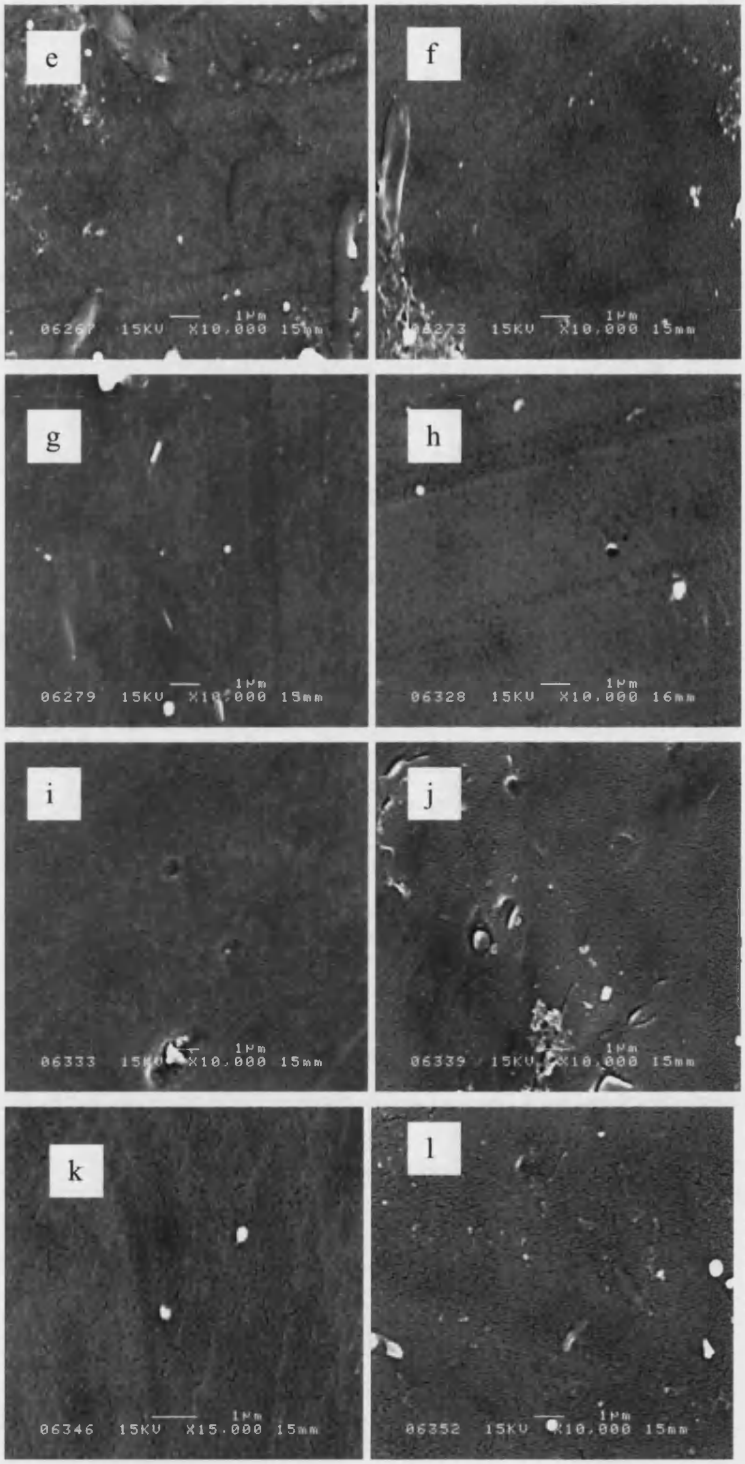

Figure 7.7 SEC images of virgin membrane (a) and cleaned membranes fouling by (b) tea protein; (c) TF and tea protein; (d) TF; (e) TF-3-G and tea protein; (f) TF-3-G; (g) TF-3'-G and tea protein; (h) TF-3'-G; (i) TF-3,3'-G and tea protein; (j) TF-3,3'-G; (k) TRs and tea protein; (l) TRs

7.3.5 Contact angle and Zeta potential results

The samples examined were the following PSF membranes (i) virgin conditioned, (ii) fouled by 50 mg L^{-1} tea protein, (iii) fouled by 50 mg L^{-1} TF-3,3'-G, (iv) fouled by a binary mixture of tea protein and TF-3,3'-G (25 mg $L^{-1}$of each component), and (v) fouled by 50 mg L^{-1} tea protein, and cleaned using 0.2 wt% NaOH solution. Table 7.2 shows the contact angles of the samples mentioned above. The contact angles of membranes fouled by tea protein and its binary mixture with TF-3,3'-G are 43.7 ± 3.5° and 37.2 ± 4.4° respectively. These values are much lower than those for the conditioned membrane (61.6 ± 3.6°), indicating that these membranes became more hydrophilic after fouling by protein based solutions. For membrane fouled by TF-3,3'-G alone, the value is 55.8 ± 4.1°. Although this is also slightly lower than that of conditioned membrane, the change in membrane hydrophobicity is not significant when the standard deviation is considered. After cleaning, the contact angle of the membrane initially fouled by tea protein returns to 57.9 ± 3.0°. This shows the membrane is generally cleaned after standard NaOH cleaning protocol is applied.

Table 7.2 Contact angles measured using the sessile drop method for selected membranes

Membranes	Contact angle (°)
Virgin conditioned PSF	61.6 ± 3.6
PSF fouled by 25 mg L^{-1} TF-3,3-G and 25 mg L^{-1} protein mixture	37.2 ± 4.4
PSF fouled by 50 mg L^{-1} TF-3,3'-G	55.8 ± 4.1
PSF fouled by 50 mg L^{-1} tea protein	43.7 ± 3.5
PSF fouled by 50 mg L-1 tea protein, cleaned by 0.2wt% NaOH	57.9 ± 3.0

Figure 7.8 compares the zeta potential values of these different membranes between pH 4 and 7. Measurements below 3 were not carried out because the greater conductivity developed in this range prevents accurate measurement. Above pH 7, the silver coating of the electrodes is damaged by the alkaline conditions.

The zeta-potentials for the virgin conditioned PSF membrane were below zero, and decreased from –1.8 mV to –5.0 mV as pH increased from 4 to 7. This indicated that the PSF membrane surface was negatively charged initially, and tended to absorb negatively charged ions as pH increased. This result is in agreement with the ZP measurements on PSF membranes reported by Weis *et al*, 2003. When the membrane

was fouled by 50 mg L^{-1} tea protein, the membrane appeared to be even more negatively charged especially within the pH range 5 to 7. However, a different picture was observed for the membrane fouled with 50 mg L^{-1} TF-3,3'-G. The zeta potential values became less negative than those for other membrane treatments, changing from – 0.86 mV to – 4.61 mV within the pH range tested. This implied that the absorption of TF-3,3'-G decreased the negative charge on the membrane surface. This finding supports the hypothesis that TF addition to protein aids the transmission of protein by reducing the negative charge on membrane surface, hence allowing more protein molecules to pass.

Despite the reduction in surface charge during the filtration of single component TF-3,3'-G , a binary mixture of TF-3,3'-G and protein displayed the lowest zeta potential values recorded. As indicated from the ITC results, the ratio of the molar concentration of TF-3,3'-G to that of protein when binding sites are saturated should be approximately 7 to 1. However, the molar ratio of TF-3,3'G and tea protein in this binary mixture is 15.4 : 1. Excessive unbound TF-3,3'-G therefore remained in the mixture. According to the mass transfer and rejection coefficients of total polyphenols during filtration of its binary mixture with tea protein, there was no transmission of TF-3,3'-G during the first 10 minutes. Nevertheless, very small amounts of TF-3,3'-G were detected in the permeate after 15 minutes (see Figure 6.19). As the membrane became more hydrophilic during filtration, this surface modification enabled the flux of TF-3,3-G to increase and gradually reduced the magnitude of the negative charge on the membrane surface (i.e. making it more positive). It is postulated that this charge reduction facilitates the subsequent transmission of some protein / TF-3,3'-G aggregates as filtration continues. However, the majority of the tea protein / TF-3,3'-G aggregates (as seen in Figure 6.32) are retained by the membrane, and this leads to cake deposition. Therefore, the surface charge of the membrane is likely to be dominated by these aggregates. In this case, the structure of protein / TF3,3'-G aggregates will be directly related to the charge of the system. In their study on polyphenols and proline-rich proteins, Luck, *et al* (1994) suggested the formation of casein micelles by the sequestration of polyphenols by proteins. If this is the dominant mechanism in the current system, the charge of aggregates could be similar to that of tea protein, as the protein surrounds the polyphenol molecules. As the severe additional fouling was

proved to take place when this binary mixture was ultrafiltered, it is not surprising that membrane fouled by the binary mixture appeared to be even more negative charged than that fouled by tea protein alone, as the deposition leads to higher surface charge densities. The increase of this negative charge on membrane surface as fouling continued also restricts the transmission of protein / TF-3,3'-G aggregates, as the mass flux of protein appeared to decrease in the last 10 minutes of the 60 minute filtration period examined (Figure 6.18).

The effect of cleaning using NaOH on a membrane fouled by tea protein was examined. The zeta potential values recorded were between those of a virgin membrane and those of the membrane fouled by tea protein. This is also reflected in the rank order of the fluxes of these membrane samples.

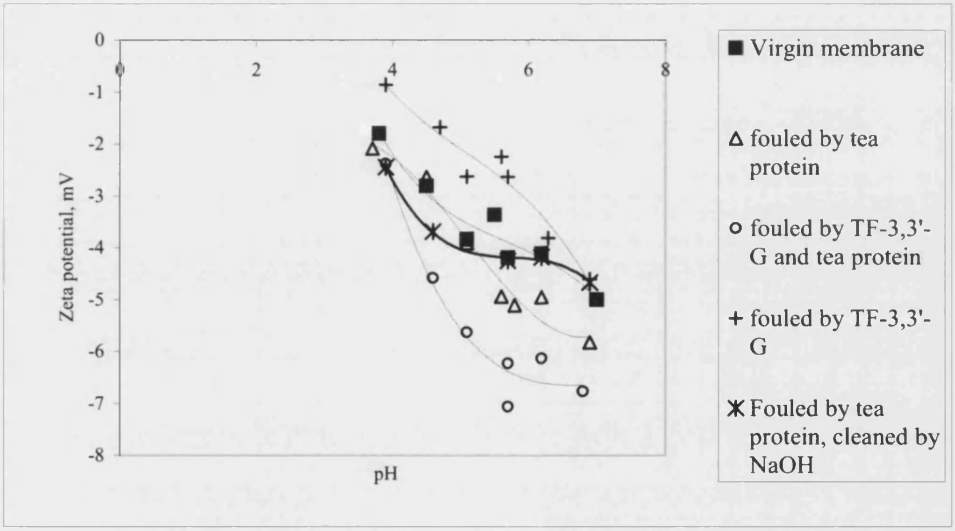

Figure 7.8 Zeta-potential values of different membranes examined. (r^2 >0.99 for streaming potential versus pressure the stand deviation < 0.7 (n = 7)

7.4 Conclusions

The cleanability of membranes fouled by different model tea components has been investigated by considering two parameters indicating recovery of membrane permeabilities after cleaning. For the membranes fouled by individual tea components,

the majority of the irreversible fouling resistance of each fouled membrane was removed after the standard cleaning protocol was applied. The pure water fluxes of cleaned membranes were recovered to more than 62% of that of conditioned membranes. Membranes fouled by binary mixtures generally showed poor cleanabilities due to the comparatively severe fouling present.

Exceptions to this were the membranes fouled by the mixture of TF-3-G with protein, and that of TF-3'-G with protein. Ninety eight and 97% respectively of irreversible fouling resistances of both membranes were removed after cleaning. The permeabilities of both membranes were highly recovered. There may be morphological or chemical variations resulting from the in the way these materials interact with sodium hydroxide that lead to a deposit that has a greatly reduced resistance.

The FTIR spectra of membranes after different fouling and standard cleaning treatments provided another indication of membrane cleanliness. Despite of the relatively small FTIR response given by the foulant remaining on the membranes, there were still apparent differences between the fouled and cleaned membranes. With the exception of the TF fouled membrane, there were clear signs of the effect of cleaning upon the membranes examined. The inspection of various cleaned membrane surfaces by scanning electron microscope (SEM) also confirmed the effects of cleaning, indicating that standard NaOH cleaning established was relatively effective at removing the top cake layer of deposition from the membrane surfaces.

The contact angle measurements of fouled membranes showed the modification of hydrophobicities of membranes following different fouling treatments. The membranes fouled by protein based deposit became highly hydrophilic. This appears to have altered membrane selectivities towards increased polyphenols tranmission. TF-3,3'-G was therefore able to pass through membrane gradually during fouling by the binary mixture.

Zeta potential measurements on selected membrane samples not only supported the assumption that the masking of repulsive charge was occurring on the surface bound proteinaceous system during the filtration of binary mixture, but also confirmed the effects of membrane cleaning.

The virgin conditioned PSF membrane was found to be negative charged within the tested pH range 4 to 7. When fouled by tea protein, the membrane surface became more negative charged. In contrast, fouling by TF-3,3'-G reduced the membrane surface charge. The reduction of surface charge could possibly aid the transmission of negatively charged protein based aggregates in a binary mixture of the two components. The zeta potential values of a membrane fouled with protein and then cleaned with NaOH recovered to values between those seen for the virgin membrane and the fouled membrane.

Chapter 8 Conclusions and Future Work

8.1 Conclusions

The research work in this study concerned membrane fouling and cleaning of ultrafilters for processing black tea solution, separation of tea protein and polyphenols, and studies on the interactions between these tea species and their effects upon membrane ultrafiltration. According to this study, membrane ultrafiltration appeared to be an effective solution to remove tea haze. The resulting tea products have appealing colours and relatively good stabilities. It is possible to use membrane ultrafiltration as a natural substitute for enzyme treatment during black tea processing in industry. The detailed results presented from Chapter 3 to 7 can be summarized in the following paragraphs.

8.1.1 Results of membrane ultrafiltration of black tea solutions

The ultrafiltration of black tea solutions started on three different hydrophobic UF membranes. The polysulphone membranes (PSF) with MWCO 20 kD were applied on a small DSS rig in the very beginning of this PhD study. The removal of preservatives coated outside the membrane surface, namely glycerine, was proved to be necessary. Sixty minutes conditioning was found to be sufficient to remove the majority of the glycerine, and consequently increase the pure water flux and the hydrophobicity of the virgin membrane. The temperature and TMP used during membrane filtration appeared to have positive effects on the permeate fluxes within the ranges tested (for temperature of 20 - 60 °C, and for a TMP of 1 - 4 bar). Varying cross flow velocity showed an irregular impact upon the permeate flux through membrane, which is in agreement with the studies by Kim *et al* (1993), and Bird and Bartlett (1995).

The studies on membrane cleaning by formulated cleaning agent *P3 Ultrasil 11* in this small cross flow rig showed that 0.8 wt% was the most effective concentration for membrane cleaning within the range investigated. The flux recoveries were found to be more than 100% after cleaning. The reason for this has been demonstrated to be the

presence of surfactant materials rather than the alkali components contained in this cleaning reagent.

After the trials on this small rig, a modified pilot - scale rig was used in black tea processing with the aim to simulate operating conditions applied in industry. Another two membranes, namely polysulphone membranes (MWCO 30 kD) and fluoropolymer membranes (MWCO 30 kD) were investigated here. With the concern of the effects of surface-active substance in *P3 Ultrasil* 11, a simple alkali cleaning reagent NaOH was decided to be used in the subsequent cleaning experiments.

The pilot scale cross flow rig had been modified by adding a removable cooling system in the feeding tanks so as to obtain a stable temperature control during membrane ultrafiltration. The cleaning conditions, including temperature, concentration of cleaning fluids, and TMP, had been optimized in this part of study. The effects of NaOH cleaning on both membranes had also been investigated by TEM. The comparison of the qualities of products obtained from both membranes showed the effectiveness of membrane ultrafiltration.

As to the experiments on PSF membranes (MWCO 30 kD), sodium hydroxide solution of the concentration of 0.2 wt% was observed to be superior to others. The maximum temperature of 50 °C appeared to be the most effective, according to relatively high product fluxes induced. Though more cleaning solution could pass through the membrane under higher TMP, a comparative lower TMP of 1.0 bar rather than 2.0 bar was found to be more efficient by referring to the membrane flux recoveries after cleaning.

As far as the FS50PP membrane was concerned, a NaOH solution of 0.2 wt% led to a flux recovery of nearly 100% after cleaning. However, higher concentrations resulted in flux recoveries of more than 100%. This phenomenon was considered to be related to membrane surface modification under higher alkali conditions. Consequently, 0.2 wt% was regarded as the optimal concentration for membrane cleaning. The cleaning temperature 50 °C was the optimum temperature investigated. Higher temperature 60 °C enhances the absorption of polyphenols by PVP which is a pore forming additive in FS

50PP membrane. Moreover, transmembrane pressure had little influence on flux recovery although the cleaning fluxes increased with the increased TMP.

The products obtained from ultrafiltrations on both membrane appeared to have relatively good stabilities on total polyphenol content and the colour. No haze was observed in these permeates for more than two months. The results from TEM showed the effects of NaOH cleaning on PSF (MWCO 30 kD) membrane and FS50PP (MWCO 30 kD) membrane. It is found that PSF membranes are easier to clean than FS membrane. From this point of view, PSF membranes were used in the subsequent experiments.

8.1.2 Results of separation and characterization of tea haze, tea protein and polyphenols

The separation of tea haze was not successful via the application of gel filtration. The characterization of gel filtration fractions by using SDS-PAGE, high performance gel filtration chromatography, CBB protein quantification and *Folin-Ciocalteu* assay indicated that the fractions eluted from the Sepharcyl HR 200 column were probably the compounds of colourless phenol components and amino acids. The molecular mass the major fraction was approximately 5000 Da.

Despite of the failure of separating out tea haze, tea protein was successfully separated by using NaOH extraction from *Lipton* spray dried black tea powder. Compared with the relative low concentration of protein in black tea, the protein isolate with the purity of approximately 50 wt% was highly concentrated. The molecular mass of tea protein was approximately 22.2 kD at pH 6.8 according to the results from TSK gel G4000 PW_{XL} gel filtration chromatography. However, the molecular mass was found to be half of this value by SDS-PAGE when pH is 5.0. This indicated the self aggregation of protein molecules under a pH of 6.8. The existence of a broad band ranging from 3500 cm^{-1} to 3100 cm^{-1} in the FTIR spectrum of tea protein verified the presence of amidocyanogen, which is a specific functional group in the protein. The secondary structure of tea protein was considered to be β-sheet rather that α-helix according to the excursion of infrared absorbance within Amide I and Amide II areas.

The experiments based on the precipitating interactions between Zn^{2+} and phenolic hydroxyl groups of polyphenols under alkali conditions effectively purified tea polyphenols from black tea powder. There were theaflavin, theobromine, and caffeine presented in this polyphenol isolate by resorting to the measurements by Reversed-phase HPLC. *Folin-Ciocalteu* assay also showed that the amount of total phenols in this isolate was approximately 65 wt% which is 3 times more than that in the original tea powder.

The interactions of (i) tea protein and theaflavin, (ii) tea protein and mixed tea polyphenols were investigated by Isothermal Titration Microcalorimetry (ITC). Both interactions were fitted to sequential sites binding models with different numbers of binding sites. Mixture (i) was fitted by two sequential sites binding. The concentration of tea protein had a marked effect upon the magnitude of the enthalpy change, but little impact upon the mechanism of tea protein-theaflavin binding once saturation had been obtained. The pH value applied during titration had a great influence on the total enthalpy change for the processes occurring in the sample cell. A slightly higher pH within the range studied (4 – 5.5) tended to be preferable, as the strength of binding associate became larger than when lower pH values were used. The interaction in mixture (ii) was found to fit a one site sequential binding model. The affinity was found to be weaker than that of the tea protein / theaflavin interaction.

8.1.3 Results of membrane fouling by tea model solutions

With the aim to understand the interactions between tea species and between them and membranes during membrane fouling, a series of model tea component solutions, involving individual tea component solutions, binary mixture solutions and complex mixture solutions, have been ultrafiltered by PSF (30 kD) membranes in dead-end filtration rig.

An initial concentration of 50 mg L^{-1} was used for a range of individual tea polyphenol and protein filtration. Typical permeate flux declines were observed during membrane fouling. More than 60% of the initial fluxes were lost within the first 15 minutes except for TF filtration, where liquid permeate flux decline by 43.8% after 15 minutes. TF filtration also displayed the most obvious signs of concentration polarization though it

was also inspected in TF-3'-G filtration. The higher the normalized fluxes were observed, the lower the initial apparent rejection coefficients were obtained. Molecular mass was proved to be less significant in controlling the filtration process due to the high rejection of a relatively small molecule such as TF. The mass transfer of total polyphenols among filtration of individual phenol components decreased with the filtration time, which accorded with the decline of permeate flux. This indicated that there was no additional selectivity occurred as a result of cake deposition or concentration polarization increasing with time.

The studies on membrane filtration by binary TF / protein mixtures (25 mg L^{-1} each) showed that tea protein dominated membrane fouling. The fouling curves for these binary mixture filtrations showed great similarities to that for filtration of 50 mg L^{-1} protein. More polyphenols were retained with the addition of tea protein. Nevertheless, more protein was found to be able to transmit after mixing with phenol components. This has been further investigated by contact angle and zeta potential measurements. The possible explanation was that the increase in membrane hydrophilicity after fouling by protein-based model solutions altered the membrane selectivity towards polyphenols. Resulting transmission of unbound polyphenols led to the charge reduction in the system. This allows the transmission of protein based complexes.

Caffeine has been examined to be less influential on membrane fouling. The flux decline showed in caffeine filtration was mainly due to concentration polarization rather than membrane fouling. During the filtrations of mixture of caffeine and protein, and the mixture of caffeine, tea protein and polyphenols, the normalized fouling fluxes resembled to those for 50 mg L^{-1} tea protein filtration. There was a significant reduction of caffeine transmission when tea protein was added. However, tea protein was still 100% rejected by the membrane, indicating that caffeine did not change the transfer behavior of tea protein during filtration.

As to membrane fouling by different groups of multiple mixtures, there were no unexpected results in terms of permeate fluxes and the tendency of mass transfer of each components. The presence of tea protein or thearubigins or both resulted into lower permeate fluxes during fouling. The addition of tea protein also restrained the transmission of theaflavins.

The membrane surfaces fouled by different model solutions appeared to have diverse foulant morphologies under scanning electron microscopy (SEM). Tea protein and TRs fouled membranes showed cake-like layer of foulants due to their much more severe fouling. The aggregations inspected on membranes fouled by binary mixtures of polyphenol components and tea protein as well as the mixture of caffeine and tea protein illustrated the possible reactions taking place in binary mixture systems. In addition, large quantity of orbicular aggregates presented on the membrane fouled by TF-3'-G, presumably indicated different aggregation phenomenon occurred during membrane ultrafiltration.

8.1.4 Results of membrane cleaning for model solution fouled membranes

The membranes fouled by different model tea component solutions showed relatively good cleanabilities by using standard NaOH cleaning protocol developed. Two parameters indicating membrane permeabilities after cleaning were used to evaluate the cleaning efficiency.

When considering the membranes fouled by individual tea components, the pure water fluxes of cleaned membranes were recovered to over 60% of that of conditioned membranes. More than 80% of the irreversible fouling resistance was removed after the standard cleaning. In terms of the membranes fouled by binary mixtures, membranes fouled by the mixture of TF-3-G with protein and that of TF-3'-G with protein were nearly 100% recovered after cleaning process. While the others appeared to be less cleaned with the flux recoveries of 79%, 72% and 57% for TF / protein, TF-3,3'-G / protein and TRs / protein respectively.

The examination of membranes after different fouling and standard cleaning by ATR-FTIR provided information of foulant and confirmed relatively good membrane cleanliness after cleaning. Characteristic protein amide bands were found in the spectrum of membrane fouled by tea protein alone. However, they were slightly overlapped by the phenol bands in the spectrum of binary mixtures. The apparent differences of nature intensities of the bands for fouled and cleaned membranes certified the efficiency of membrane cleaning by 0.2wt% NaOH. However, an exception was found in the membrane fouled by TF, which appeared to have certain deposits remained

after cleaning. The images of various cleaned membrane surfaces recorded using scanning electron microscope (SEM) also confirmed the effect of cleaning, indicating that the standard NaOH cleaning established was sufficient for cleaning membranes fouled by tea components.

The contact angles and zeta potentials of the protein fouled and subsequently cleaned membranes recovered to values between those seen for the virgin membrane and the fouled membrane. This again indicated the effect of NaOH cleaning, and explained the recovery of membrane permeability seen after cleaning.

8.2 Future work

During this three-year study, a significant amount of pioneering work has been carried out to investigate the influence of membrane fouling and cleaning upon black tea processing. Due to the success of this study, there is no doubt that membrane ultrafiltration can be applied to the manufacture of Ice tea products in industry. From a long term point of view, taste panel and the scale up of current UF system should be carried out in the future. Taste panel will help the company to investigate customer's attitudes towards the appearance, taste and overall quality of the products and to evaluate their market prospects. In terms of scaling up, a larger pilot scale UF system might be required. The structure will be similar to the large rig used in this study. Nevertheless, a larger pump, heater and single / multiple plate and frame membrane modules are needed. It is important to determine the possibility of increasing the output by increasing the surface area without increasing the module cleaning requirement. The effective process recovery and the energy consumed of the system should also be investigated.

From a short term point of view, as there are few researchers working on tea ultrafiltration, particular in the area of tea proteins, there are still a lot of interesting aspects awaiting further investigation.

Although tea protein has been separated successfully in this study, the basic properties of this protein, for example the isoelectric point and composition of amino acids have not been determined yet. The purity of this protein isolate could also be improved by ionic exchange chromatography or some other methods in future work.

Despite the finding that caffeine appeared to be less significant in membrane fouling, the interactions between caffeine and polyphenols, or caffeine with proteins can be further studied by ITC. This will possible be helpful to understand more about the tea cream formation and the transmission of functional components such as caffeine and polyphenols in tea ultrafiltration.

In their study on polyphenols and proline-rich proteins by Luck *et al.,* (1994), Ca^{2+} was considered to have an important role in the formation of casein micelles and the sequestration of polyphenols when milk was added into a tea infusion. Therefore, the impact of Ca^{2+} upon membrane fouling and cleaning could be interesting and should be investigated. The addition of Ca^{2+} in a model solution could be taken into account in future work. In addition, changes in pH, ionic strength and temperature could also be investigated in further model solution ultrafiltration studies.

Due to the limit of time and the availability of equipment, the measurement of apparent zeta-potentials has been carried out on only five membrane samples. Zeta-potential measurements on other samples should be completed so as to further prove the hypothesis advanced for explaining the increased transmission of protein in a binary mixture.

As mentioned in Chapter 2, it is possible to determine the fouling mechanism by using Hermia equation. However, the data fitting needs a lot of experience, and the modification of the equation is required for cross-flow filtration. The software "Scientist 3.0" can be used in this mathematical modeling work.

Polyphenols present in other beverages such as beer, wine and fruit juice also tend to interact with protein to from precipitates, which are detrimental to the taste and appearance of the product. Membrane filtration should be able to tackle these problems in producing these beverages rich in phenol components. It is believed that the findings

form this study on black tea ultrafiltration will be applicable to a range of beverage products. Therefore, it would be useful to apply membrane ultrafiltration on other polyphenol-based beverages to validate the findings from this study.

References

Allie, Z., Jacobs, E.P., Maartens, A. and Swart, P., 2003, 'Enzymatic cleaning of ultrafiltration membranes fouled by abattoir effluent', *Journal of Membrane Science*, **218**, 107-116.

Argüello, M.A., Álvarez, S., Riera, F.A. and Álvarez, R., 2003, 'Enzymatic cleaning of inorganic ultrafiltration membranes used for whey protein fractionation', *Journal of Membrane Science*, **216**, 121 – 134.

Arnot, T.C., Field, R.W. and Koltuniewicz, A.B., 2000, 'Cross-flow and dead-end microfiltration of oily-water emulsions Part II, mechanisms and modeling of flux decline', *Journal of Membrane Science,* **169**, 1-15.

Balentine, D.A. and Thomas, J., 1992, 'Manufacturing and Chemistry of Tea', *American Chemical Society.*

Bartlett, M., Bird, M.R. and Howell, J.A., 1995, 'An experimental study of the development of a qualitative membrane cleaning model', *Journal of Membrane Science*, **105**, 147-157.

Beveridge, T., Veto, L., and Harrison, J.E., 1998, 'Formation of chain-like structures in apple juice haze', *Lebensmittel-Wissenschaft & Technologie*, **31**, 74-77.

Bird, M.R. and Bartlett, M., 1995, 'CIP optimization for the food industry: relationships between detergent concentration, temperature and cleaning time', *Food and Bioproducts Processing*, **73** (C2), 63-70.

Bird, M.R. and Bartlett, M., 2002, 'Measuring and modeling flux recovery during the chemical cleaning of MF membranes for the processing of whey protein', *Journal of Food Engineering*, **52**, 4, 143 – 152.

Bird, M.R. and Fryer, P.J., 1991, 'An experimental study of the cleaning of surfaces fouled by whey proteins', *Transaction of the Institution of Chemical Engineers,* Part C **69**, 13-21.

Borneman, Z., Gökmen, V. and Nijhuis, H.H., 2001, 'Selective removal of polyphenols and brown colour in apple juices using PES/PVP membranes in a single ultrafiltration process', *Separation and Purification Technology,* **22-23**, 53 – 61.

Bowen, W.R., Calvo, J.I. and Hernandez, A., 1995, 'Steps of membrane blocking in flux decline during protein microfiltration', *Journal of Membrane Science,* **101**, 153-165.

Bowen, W.R. and Gan, Q., 1991, 'Properties of microfiltration membranes: flux loss during constant pressure permeation of Bovine Serum Albumin', *Biotechnology and Bioengineering*, **38**, 688 – 696.

Bradford, M.M., 1976, 'A rapid and sensitive method for the quantitation of microgram quantities of protein utilizing the principle of protein-dye binding', *Analytical Biochemistry,* **72**, 248 – 254.

Burns, D.B. and Zydney, A.L., 1999, 'Effect of solution pH on protein transport through ultrafiltration membranes', *Biotechnology and bioengineering,* **64**, No.1. July 5, 27-37.

Chai, X., Kobayashi, T. and Fujii, N., 1998, 'Ultrasound-associated cleaning of polymeric membranes for water treatment', *Separation and Purification Technology,* **15**, 139-146.

Chan, R. and Chen, V., 2004, 'Characterization of protein fouling on membranes: opportunities and challenges', *Journal of Membrane Science*, **242**, 169-188.

Charlton, A.J., Davis, A.L., Jones, D.P., Lewis, J.R., Davies, A.P., Haslam, E. and Williamson, M.P., 2000, 'The self-association of the black tea polyphenol theaflavin and its complexation with caffeine', *Journal of the Chemical Society Perkin Transactions* 2, 317 – 322.

Charlton, A.J., Baxter, N.J., Khan, M.L., Moir A.J.G., Haslam E., Davies A.P. and Williamson, M.P., 2002, 'Polyphenol/peptide binding and precipitation', *Journal Agricultural Food Chemistry,* **50**, 1593-1601.

Cheryan, M., 1986, *Ultrafiltration Handbook,* Technomic Publishing Company. Lancaster, USA.

Coyne, V.E., James, M.D., Reid, S.J. and Rybicki, S.P., 1996, *Molecular Biology Techniques Manual*, 3rd edition.

Czekaj, P., López, F. and Güell, C., 2000, 'Membrane fouling during microfiltration of fermented beverages', *Journal of Membrane Science*, **166**, 199 – 212.

De Barros, S.T.D., Andrade, C.M.G., Mendes, E.S. and Peres, L., 2003, 'Study of fouling in pineapple juice clarification by ultrafiltration', *Journal of Membrane Science,* **215**, 213-224.

De Freitas, V., Carvalho, E. and Mateus, N., 2003, 'Study of carbohydrate influence on protein – tannin aggregation by nephelometry', *Food Chemistry,* **81**, 4, 503-509(7).

Degenhardt, A., Engelhardt, U.H., Wendt, A.S. and Winterhalter, P., 2000, 'Isolation of black tea pigments using high-speed countercurrent chromatography and studies on properties of black tea polymers', *Journal Agricultural Food Chemistry*, **48** (11), 5200-5205.

Duriyabunleng, H., Petmunee, J. and Muangnapoh, C., 2001, 'Effects of the ultrasonic waves on microfiltration in plate and frame module', *Journal of Chemical Engineering of Japan,* **34** (8), 985-989.

Eagles, W.P. and Wakeman, R.J., 2002, 'Interactions between dissolved material and the fouling layer during microfiltration of a model beer solution', *Journal of Membrane Science,* **206**, 253 – 264.

Evans, P. and Bird, M.R., 2006, 'Solute – membrane interactions during the ultrafiltration of black tea liquor', *Food and Bioproducts Processing,* **84** (C4), 292-301.

Eykamp, W., 1995. Microfiltration and Ultrafiltration, in Noble, R. D., and Stern, S. A., (eds.), *Membrane Separation Technology Principles and Applications. Elservier*, Amsterdam, 1.

Frazier, R.A., Papadopoulou, A., Harvey, I.M., Kissoon, D. and Green, R.J., 2003, 'Probing protein-tanning interactions by isothermal titration microcalorimetry', *Journal Agricultural Food Chemistry,* **51**, 5189-5195.

Gallot-Lavalle, T. and Lalande, M.A., 1985, 'Mechanistic approach to pasteurized milk deposit cleaning', *Journal of Membrane Science,* **100**, 259-272.

Gan, Q., 2001, 'Beer clarification by cross-flow microfiltration – effect of surface hydrodynamics and reversed membrane morphology', *Chemical Engineering and Processing,* **40**, 413 – 419.

Gan, Q. and Allen, S.J., 1999, 'Crossflow microfiltration of a primary sewage effluent – solids retention efficiency and flux enhancement', *Journal of Chemical Technology and Biotechnology,* 74, 693 – 699.

Gan, Q., Howell, J.A., Field, R.W., England, R., Bird, M.R. and Mckechinie, M.T., 1999, 'Synergetic cleaning procedure for a ceramic membrane fouled by beer microfiltration', *Journal of membrane Science*, **155**, 277-289.

Gan, Q., Howell, J.A., Field, R.W., England, R., Bird, M.R., O'Shaughnessy, C.L. and Mekechinie, M.T., 2001, 'Beer clarification by microfiltration – product quality control and fractionation of particles and macromolecules', *Journal of Membrane Science*, **194**, 185 – 196.

Goldstein, J.I., Romig, A.D., Newbury, D.E., Lymen, C.E., Echlin, P., Fiori, C., Joy, D.C. and Lifshin, E., 1992, *Scanning electron microscopy and X-ray microanalysis.* 2nd Edition, Plenum Press, New York.

Goosen, M.F.A., Sablani, S.S., Al-Hinai, H., Al-Obeidani, S., Al-Belushi, R. and Jackson, D., 2004, 'Fouling of reverse osmosis and ultrafiltration membranes: a critical review', *Separation Science and Technology*, **39**, No 10, 2261-2297.

Grahan, H.N., 1992, 'The polyphenols of tea-biochemistry and significance – a review', *In Xue Journees Internationales Group Polyphenols; DTA: Lisbon, Portugal,* **2**, 32-43.

Haslam, E., 2003, 'Thoughts on thearubigins', *Phytochemistry,* **64**, 61 – 73.

Hermia, J., 1982, 'Constant pressure blocking filtration laws – application to power – law non-newtonian fluids', *Transaction of the Institution of Chemical Engineers,* **60**, 183-187.

Hertog, N.C.J.L., Hollman, P.C.H., Katan, M.B. and Kromhout, D., 1993, 'Intake of potentially anticarcinogenic flavonoids and their determinations in adults in The Netherlands', *Nutrition and Cancer,* **20**, 21-29.

Hunter, R.J., 1981, *Zeta potential in colloid science principles and applications.* Academic Press. London.

Hong, S. and Elimelech, M., 1997, 'Chemical and physical aspects of natural organic matter (NOM) fouling of nanofiltration membranes', *Journal of Membrane Science,* **132**, 159 – 181.

Hsu, J.C. and Heatherbell, D.A., 1987, 'Heat-Unstable Proteins in Wine. I. Characterization and Removal by Bentonite Fining and Heat Treatment', *American Journal of Enology and Viticulture,* **38,** 11-16.

Hu, Q., Pan, G.and Zhu, J., 2001, 'Effect of selenium on green tea preservation quality and amino acid composition of tea protein', *Journal of Horticultural Science & Biotechnology,* **76**(3), 344-346.

Jabs, A., 2005, 'Determination of Secondary Structure in Proteins by Fourier Transform Infrared Spectroscopy (FTIR)', Retrieved on August 1st, 2005 from the IMB Jena Image Library web page: http://www.imb-jena.de/ImgLibDoc/ftir/IMAGE_FTIR.html.

Johnson G., Donnelly, B.J. and Johnson, D.K. 1968, 'The chemical nature and recursors of clarified apple juice sediment', *Journal of Food Science.* **33**, 254-257.

Jonsson, A.S. and Tragardh, G., 1990, 'Fundamental principles of ultrafiltration', *Chemical Engineering and Processing*, **27** (2), 67-81.

Kang, S., Hoek, E., Choi, H. and Shin, H., 2006, 'Effect of membrane surface properties during the fast evalation of cell attachment', *Separation Science and Technology,* **41**, No. 7, 1475 – 1487 (13).

Kawakatsu, T., Kobayashi, T., Sano, Y. and Nakajima, M., 1995, 'Clarification of green tea extract by microfiltration and ultrafiltration', *Bioscience, Biotechnology and Biochemistry,* **59** (6), 1016 – 1020.

Kilduff, J.E., Mattaraj, S., Zhou, M. and Belfort, G., 2005, 'Kinetics of membrane flux decline: the role of natural colloids and mitigation via membrane surface modification', *Journal of Nanoparticle Research,* **7**, 525-544.

Kim, J.K., Sun, P., Chen, V., Wiley, D.E. and Fane, A.G., 1993, 'The cleaning of ultrafiltration membranes fouled by protein', *Journal of Membrane Science*, **80**, 241-249.

Krishnan, R. and Maru, G.B., 2006, 'Isolation and analyses of polymeric polyphenol fractions from black tea', *Food Chemistry*, **94**, 331 – 340.

Kulkarni, S.S., Funk, E.W. and Li, N.N., Applications and Economics, in ref 5, 446.

Lee, M.J., Prabbu, S., Meng, X.F., Li, C. and Yang C.S., 2000, 'An improved method for the determination of green and black tea polyphenols in biomatrices by High-Performance Liquid Chromatography with Coulometric Array Detection', *Analytical Biochemistry*, **279**, 164 – 169.

Li, J., Hallbauer, D.K. and Sanderson, R.D., 2003, 'Direct monitoring of membrane fouling and cleaning during ultrafiltration using a non-invasive ultrasonic technique', *Journal of Membrane Science*, **215**, 33 – 52.

Liang, Y., Lu, J. and Zhang, L., 2002, 'Comparative study of cream in infusions of black tea and green tea [Camellia Sinensis (L.) O.Kuntze]', *International Journal of Food Science and Technology,* **37**, 627 – 634.

Liang, Y.R., Lu, J., Zhang, L., Wu, S. and Wu, Y., 2003, 'Estimation of black tea quality by analysis of chemical composition and colour difference of tea infusions', *Food Chemistry,* **80**, 283 – 290.

Liang, Y.R. and Xu, Y.R., 2001, 'Effect of pH on cream particle formation and solids extraction yield of black tea', *Food Chemistry*, **74**, 155-160.

Liang, Y.R. and Xu, Y.R., 2003, 'Effect of extraction temperature on cream and extractability of black tea', *International Journal of Food Science and Technology,* **38**, 37-45.

Lin, D., Chang, C., Chen, T. and Cheng, L., 2002, 'On the structure of porous Poly(vinylidene fluoride) membrane prepared by phase inversion from water-NMP-PVDF system', *Tamkang Journal of Science and Engineering.* **5**, No. 2, 95 – 98.

Lin, D., Chang, C., Huang, F. and Cheng, L., 2003, 'Effect of salt additive on the formation of microporous poly(vinylidene fluoride) membranes by phase inversion from $LiClO_4$/water/DMF/PVDF system', *Polymer.* **44**, 413-422.

Lin, J. K., Lin, C.L., Liang, Y.C., Lin-Shiau, S.Y. and Juan, I.M., 1998, 'Survey of catechins, gallic acid and methylxanthines in green, oolong, pu-erh, and black tea', *Journal Agricultural Food Chemistry.* **46**, 3635-3642.

Lin, Y.L., Juan, I.M., Chen, Y.L., Liang, Y.C. and Lin, J.K., 1996, 'Composition of polyphenols in fresh tea leaves and association of their oxygen radical-absorbing capacity with antiproliferative actions in fibroblast cell', *Journal Agricultural Food Chemistry,* **44**, 1387-1394.

Lipnizki, F., 2006, *Alfa Laval*, personal communication.

Liu, C., Caothien, S., Hayes, J., Caothuy, T., Otoyo, T. and Ogawa, T., *Membrane chemical cleaing: from art to science.*

Luck, G., Liao, H., Murray, N.J., Grimmer, H.R., Warminski, E.E., Williamson, M.P., Lilley, T.H. and Haslam, E., 1994, 'Polyphenols, astringency and proline-rich proteins', *Phytochemistry*, **37** (2), 357-71.

Lunder, T.L., 1992, 'Catechins of green tea antioxidant activity', *American Chemical Society.*

Maartens, A., Swart, P. and Jacobs, E.P., 1996, 'An enzymatic approach to the cleaning of ultrafiltration membranes fouled in abattoir effluent', *Journal of Membrane Science,* **119**, 9-16.

Mangas, J.J., Suárez, B., Picinelli, A., Moreno, J. and Blanco, D., 1997, 'Differentiation by phenolic profile of apple juices prepared according to two membrane techniques', *Journal Agricultural Food Chemistry,* **45**, 4777-4784.

Marcos, A., Fisher, A., Rea, G. and Hill, S.J., 1998, 'Preliminary study using trace element concentrations and a chemometrics approach to determine the geographical origin of tea', *Journal of Analytical Atomic Spectrometry,* **13**, 521-525.

Marshall, A.D., Munro, P.A. and Trangardh, G., 1993, 'The effect of protein foiling in microfiltration and ultrafiltration on permeate flux, protein retention and selectivity-a literature review', *Desalination,* **91**, 65-108.

Masselin, I., Chasseray, X., Durand-Bourlier, L., Laine, J-M., Syzaret, P-Y. and Lemordant, D., 2001, 'Effect of sonication on polymeric membranes', *Journal of Membrane Science,* **181**, 213-220.

Miller, K.D., Weitzel, S. and Rodgers, V.G.J., 1993, 'Reduction of membrane fouling in the presence of high polarization resistance', *Journal of Membrane Science,* **76**, 77-83.

Mulder, M., 1991, *Basic Principles of Membrane Technology*, Kluwer Academic Publishers, Dordrecht.

Mulder, M., 1996, *Basic Principles of Membrane Technology*, Kluwer Academic Publishers, Second edition.

Nunes, S. P. and Peinemann, K.V., 2001, *Membrane Technology in the Chemical Industry.*

Nyström, M., Ruohomaki, K. and Kaipa, L., 1996, 'Humid acid as a fouling agent in filtration', *Desalination,* **106**, 78 – 86.

Nyström, M. and Zhu, H., 1997, 'Characterization of cleaning results using combined flux and streaming potential methods', *Journal of membrane Science*, **131**, 195-205.

Obanda, M., Owuor, P.O., Mang'Oka, R. and Kavoi, M.M., 2004, 'Changes in thearubigins fractions and theaflavin levels due to variations in processing conditions

and their influence on black tea liquor brightness and total colour', *Food Chemistry*, **85**, 163 – 173.

Palmisano, L., 2006, 'Coupling heterogeneous photocatalysis with other technologies: a tool for abatement of pollutants in water', Retrieved on August 30th 2006 from http://www.psa.es/webesp/projects/solarsafewater/documents/simposio/dia_17/7.%20Leonardo%20Palmisano.pdf

Papadopoulou, A., Green, R.J. and Frazier, R.A., 2005, 'Interaction of flavonoids with bovine serum albumin: a fluorescence quenching study', *Journal Agricultural Food Chemistry*, **53**, 158-163.

Peilow, A. and Samuel, D., 2004, *Unilever,* Personal correspondence.

Pierre F.X., 2004, *Unilever*, Personal communication.

Pihlajamäki, A. and Nyström, M., 1995, 'Streaming potential methods in characterization of membranes', *Proceedings of EuroMembrane 95*, Bath, UK I-521 - I-524.

Popescu, G., Nechifor, G.H. and Olteanu, M., 1994, 'The influence of surfactants on the wetting of hydrophobic microporous surfaces', *Colloids and surface A: physicochemical and Engineering Aspects,* **90**, 1-8.

Pudney, P.D.A., 2006, *Unilever,* Personal correspondence.

Reilly, A.O., 2004, University of Bath, Personal correspondence.

Reimer, L., 1984, *Transmission electron microscopy physics of image formation and microanalysis.* Pressed by Springer-Verlag Berlin Heidelberg.

Riedl, K., Girard, B. and Lencki, R.W., 1998, 'Interactions responsible for fouling layer formation during apple juice microfiltration', *Journal Agricultural Food Chemistry,* **46**, 2458 – 2464.

Romney, A.J.D., 1990, *Principles of cleaning. Cleaning in place* (A. J. D. Romney, ed), 1-6. Amersham: Halstan & Co. Ltd.

Samuel, D., 2005, *Unilever,* Personal correspondence.

Sanderson, G.W., 1972, *In structural and functional aspects of phytochemistry,* Academic Press Inc.: New York, 247-316.

Sanderson, Warner, G. (Englewood, NJ), Hoefler, Charles, A. (Cresskill, NJ), Graham, Nathaniel, H. (Englewood, NJ), Coggon and Philip (Orangeburg, NY), 1977, 'Cold water extractable tea leaf and process', *United States Patent: 4051264,* September 27, 1977.

Sandu, C., Lund, D. and Plett, E., 1985, 'Fouling and cleaning of heat exchangers-a definition of terms', *Fouling and cleaning in food processing*, University of Wisconsin-Madison (C. Sandu, D.Lund, Plett, E. eds), 3-21.

Scott, K., 1995, *Handbook of industrial membranes,* 1st edition. Oxford: Elsevier Science Publishers Ltd.

Shorrock, C.J. and Bird, M.R., 1998, 'Membrane cleaning: chemically enhanced removal of deposits formed during yeast cell harvesting', *Food and Bioproducts Processing,* **76** (C1), 30-38.

Siebert, K.J., 1999, 'Effects of protein-polyphenol interactions on beverage haze, stabilization, and analysis', *Journal Agricultural Food Chemistry*, **47** (2), 353-362.

Siebert, K. J., Troukhanova, N.V. and Lynn, P.Y., 1996, 'Nature of polyphenol-protein interaction', *Journal Agricultural Food Chemistry*, **44**, 80-85.

Smith, B.M. and Franzen, S., 2002, 'Single-pass attenuated total reflection Fourier transform infrared spectroscopy for the analysis of proteins in H_2O solution', *Analytical Chemistry,* **74** (16), 4076-80.

Su, Y.L., Leung, L.K., Huang, Y. and Chen, Z.Y., 2003, 'Stability of tea theaflavins and catechins', *Food Chemistry*, **83**, 189 – 195.

Suki, A., Frane, A.G. and Fell, C.J.D., 1984, 'Flux decline in protein ultrafiltration', *Journal of Membrane Science,* **21**, 269-283.

Thompsett, A.R., 2005, University of Bath, Personal correspondence.

Todisco, S., Tallarico, P. and Gupta, B.B., 2002, 'Mass transfer and polyphenols retention in the clarification of black tea with ceramic membranes', *Innovative Food Scicence and Emerging Technologies,* **3**, 255-262.

Tolstoguzov, V., 2002, 'Thermodynamic Aspects of Biopolymer Functionality in Biological Systems, Foods, and Beverages', *Critical Reviews in Biotechnology,* **22** (2), 89 – 174.

Trägårdh, G., 1989, 'Membrane cleaning', *Desalination*, **71**, 325-335.

Vaisanen, P., Bird, M.R. and Nyström, M., 2002, 'Treatment of UF membranes with simple and formulated cleaning agents', *Food and Bioproducts Processing*, **80** (C), 98-108.

Vazquez, G., Alvarez, E., Varela, R., Cancela, A. and Navaza, J.M., 1996, 'Density and viscosity of aqueous solutions of sodium dithionite, sodium hydroxide, sodium dithionite + sucrose, and sodium dithionite + sodium hydroxide + sucrose from 25 °C to 40 °C', *Journal of Chemical and Engineering Data,* **41**, 244 – 248.

Verge, S., Richard, T., Moreau, S., Richelme-David, S., Vercauteren, J., Prome, J.-C. and Monti, J.-P., 2002, 'First observation of non-covalent complexes for a tannin-protein interaction model investigated by electrospray ionisation mass spectroscopy', *Tetrahedron Letters,* **43**, 13, 2363-2366 (4).

Vernhet, A. and Moutounet, M., 2002, 'Fouling of organic microfiltration membranes by wine polyphenols and incidence of membrane properties', *Journal of Membrane Science,* **201**, 103 – 122.

Vuataz, L. and Branderberger, H., 1961, 'Plant phenols III separation of fermented and black tea polyphenols by cellulose column chromatography', *Journal of Chromatography,* **5**, 17 – 31.

Waters, E.J., Wallance, W. and Williams, P.J., 1992, 'The identification of heat-unstable wine proteins and their resistance to peptidases', *Journal Agricultural Food Chemistry*, **40**, 1514-1519.

Weis, A., 2004, 'Fouling and cleaning synergy in ultrafiltration membrane systems – chemical cleaning of spent sulphite liquor fouled UF membranes', PhD thesis, University of Bath.

Weis, A., Bird, M.R. and Nyström, M., 2003, 'The chemical cleaning of polymeric UF membranes fouled with spent sulphite liquor over multiple operational cycles', *Journal of Membrane Science*, **216**, 67 – 79.

Weis, A., Bird, M.R., Nyström, M. and Wright, C., 2005, 'The influence of morphology, hydrophobicity, and charge upon the long-term performance of ultrafiltration membranes fouled with spent sulphite liquor', *Desalination,* **175**, 73 – 85.

Wright, W.A., 1990, 'The chemistry of detergents', *CIP: Cleaning in Place,* Romney, A.J.D. (ed) 2nd edition, The Society of Dairy Technology.

Wu, L.C. and Siebert, K.J., 2002, 'Characterization of haze-active proteins in apple juice', *Journal Agricultural Food Chemistry,* **50**, 3828-3834.

Wu, L., Sun, J. and Wang, Q., 2006, 'Poly(vinylidene fluoride)/polyethersulfone blend membranes: effects of solvent sort, polyethersulfone and polyvinylpyrrolidone concentration on their properties and morphology', *Journal of Membrane Science*, **285**, 290-298.

Yao L., Liu, X., Jiang, X., Caffin, N., D'Arcy, B., Singanusong, R., Datta, N. and Xu, Y., 2006, 'Compositional analysis of teas from Australian supermarkets', *Food Chemistry,* **94**, 115-122.

Zeman, L.J. and Zydney, A.L., 1996, *Microfiltration and Ultrafiltration-Principles and Applications*, Marcel Dekker.

Web references

http://en.wikipedia.org/wiki/SDS-PAGE. Retrieved on May 3rd 2005.

http://en.wikipedia.org/wiki/Scanning_electron_microscope. Retrieved on Jun 23rd 2006.

http://en.wikipedia.org/wiki/Contact_angle. Retrieved on July 2nd 2006.

http://en.wikipedia.org/wiki/Tea. Retrieved on July 15th 2006.

http://sbio.uct.ac.za/Sbio/documentation/Bradford%20assay.html. Retrieved on March 6th 2005.

http://66.102.9.104/search?q=cache:c-bIorwCA2UJ:www.che.utoledo.edu/nams/2006/viewpaper.cfm%3FID%3D1346+streaming+potential+electroosmosis&hl=en&gl=uk&ct=clnk&cd=1. Retrieved on July 11th 2006.

www.acabs.dk/submenus/Files/Gel%20filtration%20Amersham.pdf. 'Gel filtration principles and methods', Amersham Biosciences. Retrived on Feb 17th 2005.

www.fao.org/waicent/ois/press_ne/PRESSENG/1999/pren9955.htm. Retrieved on July 15th 2006.

www.fmltea.com/Teainfo/tea-chemistry%20.htm. Retrieved on May 20th 2006.

www.freshpatents.com/Fluoropolymer-membrane-dt200602/ptan20060032813.php. Retrieved on Jun 16th 2006.

www.life.sci.qut.edu.ac/epping/LSB 6070LT/607GFCmedia.html. Retrieved on Feb 17th 2005.

www.micromemanalytical.com/ATR-Ken/ATR.htm. Retrieved on July 11th 2006.

www.micromemanalytical.com/CAngle/ConAngl.htm. Retrieved on July 2nd 2006.

www.teatalk.com/science/chemistry.htm. Retrieved on May 24th 2006.

www.unl.edu/CMRAcfem/semoptic.htm. Retrieved on Jun 23rd 2006.

www.unl.edu/CMRAcfem/temoptic.htm. Retrieved on Jun 24th 2006.

Appendix

9.1 Scanning electron microscope

The Scanning electron microscope is one of the most commonly used techniques for membrane characterization. It provides three-dimensional images of samples with high resolutions. Consequently, it is very useful for visualizing the sample surface structures, especially in the membrane research area.

A typical SEM consists of the electron gun, a series of condenser lens, pairs of scan coils, objective lens, sample holder and detecting instruments (See Figure 9.1) http://www.unl.edu/CMRAcfem/semoptic.htm). During a scanning process, a stream of monochromatic electrons whose energy normally ranges from a few hundred eV to 50 keV is emitted from the electron gun, and is focused by two condenser lens which work in conjunction with the condenser aperture to form a beam with a focal spot sized 1 nm to 5 nm. The beam is then scanned by a set of coils in the form of raster, followed by being focused onto the specimen via the objective lens. When the sample is stroke by the beam, interactions will take place in the area where the primary electrons scattered by atoms in sample spread and extend into the surface. The consequent emission of electrons is detected subsequently to produce the image of sample surface (http://en.wikipedia.org/wiki/Scanning_electron_microscope).

SEM is heavily used in various research areas including biology, pharmacy, material science and chemical engineering. Sample preparation for SEM is relatively simple. Take a membrane sample for example, the sample is coated with a conductive material (ie. gold) and can then be examined directly in a regular SEM. (Goldstein, *et al.*, 1992; Mulder, 1996)

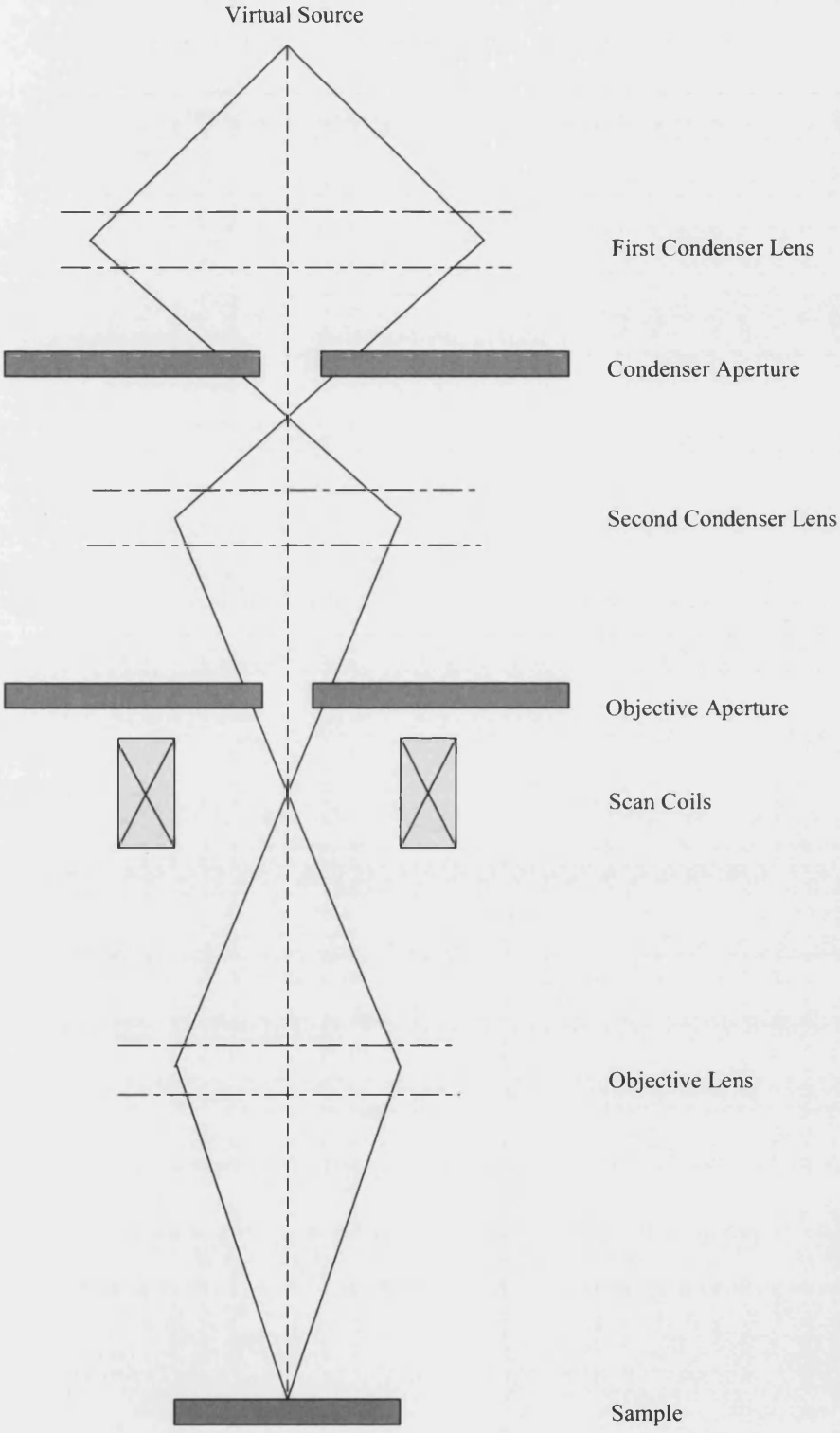

Figure 9.1 Schematic diagram of Scanning Electron Microscope

9.2 Transmission electron microscope

In spite of effective and relatively easy usage of SEM when visualizing membrane structures, the resolution of the SEM can not fall to the atomic scale due to the limits of both spot size and the interaction volume which lies on the extent of material interacting with electron beam. To compensate this disadvantage, another technique called transmission electron microscope (TEM) can be applied to inspect the sample.

Similar to the initial steps in the scanning process for SEM, electrons produced by the electron gun are accelerated by an electric field and then focused by two condenser lens into a thin, tight and coherent beam. Afterwards, instead of being deflected by pairs of coils in SEM, the beam directly strikes on the specimen and parts of it transmitted. The transmitted electrons hit a fluorescent screen, which generates the image of sample detected (See Figure 9.2), (Reimer, 1984; http://www.unl.edu/CMRAcfem/temoptic.htm).

The application of TEM is also involved in many research areas, such as material science and biological sciences. The sample for TEM must be thin enough to be electron transparent and resistant to vacuum. Therefore, the sample preparations are generally extensive and time consuming, compared with other imaging techniques for example SEM. In addition, the potential of sample damage by the electron beam, particularly for biological materials should be borne in mind when using TEM.

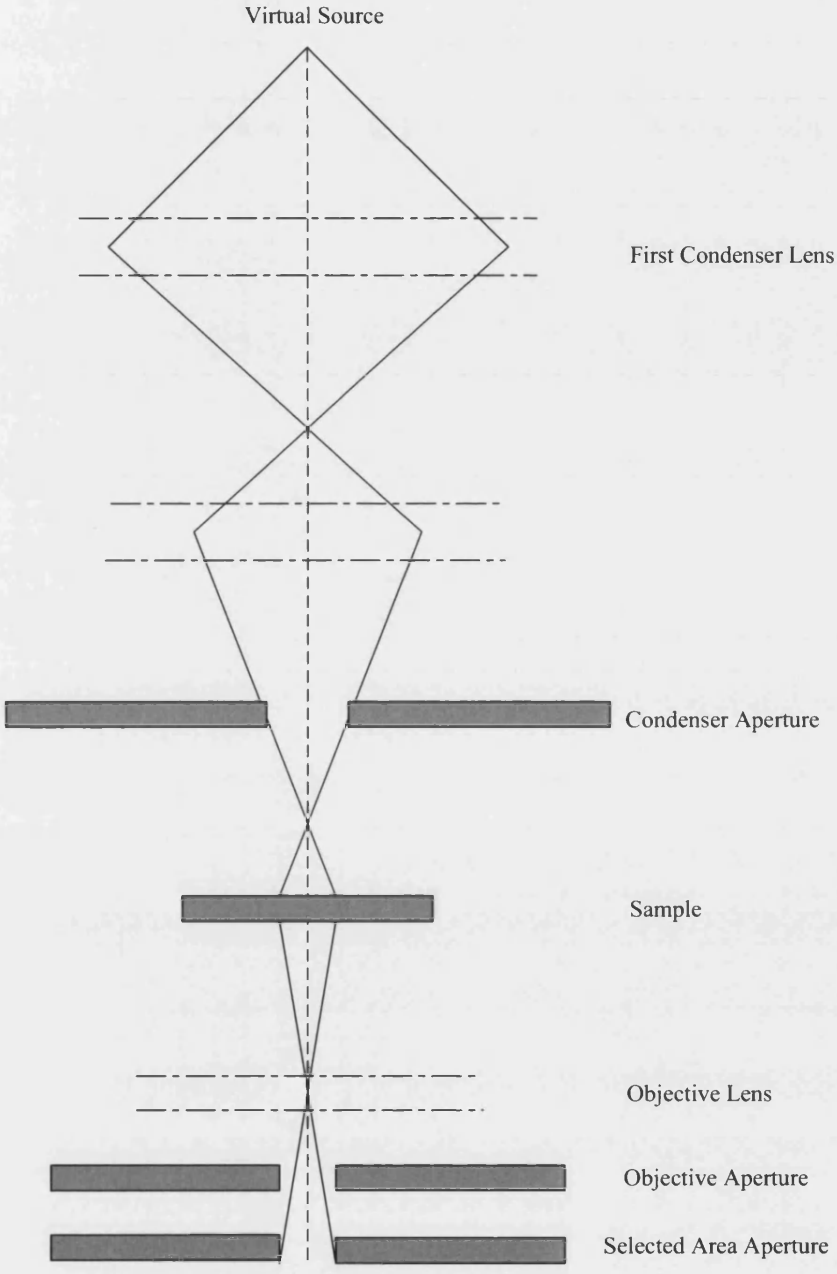

Figure 9.2 Schematic diagram of Transmission Electron Microscope

9.3 Attenuated Total Reflection – Fourier Transform Infrared Spectroscopy (ATR-FTIR)

The infrared spectra has been extensively used for the identification of functional groups in chemicals by resorting to the characteristic IR bands which correspond to specific types of molecular vibrations. In a simple Fourier Transform Infrared Spectroscopy, a continuum source of light generated over a broad range of infrared wavelengths pass through the sample, and the intensity is measured by an infrared detector. The IR spectrum is therefore obtained. As to the membranes, this becomes difficult, as membranes are generally too thick to allow the IR waves to penetrate. However, the use of attenuated total reflection FTIR offers a good resolution of this problem. The membranes can be examined simply and directly via this in situ infrared technique (Chan and Chen, 2004).

In this method, a small piece of membrane is pressed against an internal reflection element (IRE), namely crystal here, with the active layer facing the crystal. With the right angle of incidence and the right refractive index of crystal, the total internal reflection is taking place. In other words, the light enters the crystal and reflects down the length of the crystal, giving rise to a wave of IR radiation called an evanescent wave. During each of the internal reflection, this evanescent wave actually penetrates a short distance approximately 1 μm from the surface of crystal into the polymer membrane, which hence makes it possible to obtain the infrared spectrum of the sample. Schematic representation of path of a ray of light for total internal reflection is shown in Figure 9.3 (www.micromemanalytical.com/ATR-Ken/ATR.htm)

The sensitivity of ATR-FTIR is comparatively high. Nevertheless, it could be difficult to analyse a layer that is too thin compared with the penetration depth, typically ranging from 0.1 to 5 μm.

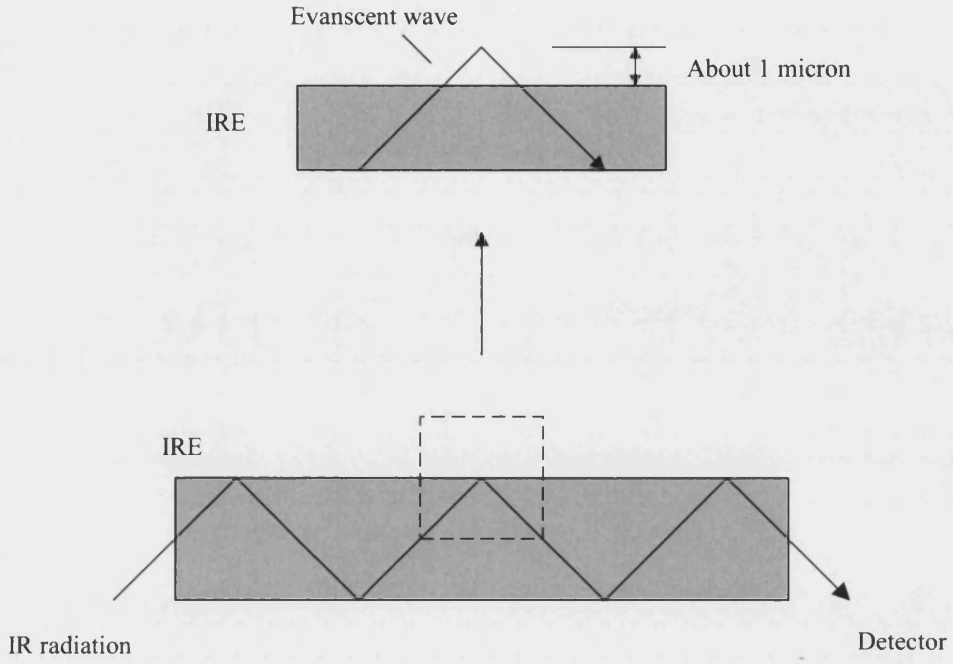

Figure 9.3 Schematic representation of light path in ATR-FTIR

9.4 Contact angle measurement

The contact angle is the angle at which a liquid / vapor interface meets the solid surface. It is normally used as a measure of wettability and adhesion properties of a certain solid surface by calculating its solid-vapour surface tension. Due to the fact that the wettability of a solid surface usually stands for its hydrophobicity / hydrophilicity, contact angle measurement can be used to predict these properties of the solid surface. This is particularly useful for the study of fouling on polymer membranes as the hydrophobicity of the membrane is highly related to its filtration performance and fouling potential. In general, the greater the contact angle, the greater the hydrophobicity of the polymer surface (Mulder, 1996).

Nowadays, there are five methods available for contact angle measurement. They are illustrated in the following paragraphs (http://en.wikipedia.org/wiki/Contact_angle).

Static or Sessile Drop method

Static or Sessile drop method is the most commonly used one for contact angle measurement. It is an optical method based on the measurement of the angle between the baseline of the drop line and the tangent at the drop boundary. The experimental hysteresis is relatively high as sample prehydration, surface roughness, chemical heterogeneity and evaporation have to be taken into account when using this method.

Wilhemly Plate method

The Wilhemly plate method is a dynamic method by measuring the wetting force on a double-sided sample when it is immersed in or withdrawn from a liquid of known surface tension. The average advancing and receding contact angles are calculated afterwards. The sample detected must have uniform geometry of both sides.

Captive air bubble method

Captive air bubble method is an alternative to the Wilhemly plate method. In this method, a sample is submerged into a liquid reservoir where an air bubble is introduced underneath. The contact angle is therefore generated between the air bubble and the hydrated sample surface. The value of the angle in degree is subsequently obtained by measuring the bubble's height and diameter at the interface.

Tilted – drop measurement

The tilted – drop measurement presents a technique by measuring contact angle when the surface is tilted up until the droplet reaches a point where it almost moves. In this method, both the advancing and receding contact angles can be observed at the same time.

For these methods mentioned above, static or sessile drop method and captive air bubble method are reported to be used in membrane surface analysis (http://www.micromemanalytical.com/CAngle/ConAngl.htm). In spite of the shortcoming of static contact angle measurement, it is still used in this study due to the availability of contact angle measurement equipment.

According to the Laplace equation (eq. 9.1), the contact angle is dependent on the membrane and the liquid used when Δ P keeps constant.

$$\cos\theta = \frac{\gamma}{2\beta} \times \Delta P \qquad (9.1)$$

where γ is the pore size of membrane; β is the surface tension of the liquid; θ is the surface energy of the membrane material.

9.5 Zeta potential measurement

Apart from the hydrophobicity of a membrane, surface charge is another property of great significance influencing membrane permeability and the fouling potential. Zeta potential measurements serving as a good technique for determining surface charge properties and are therefore suitable for membrane characterization.

Zeta potential is defined to be the electrical potential existing at " shear plane " or " slipping plane ", which is an imaginary boundary in particle – liquid interface. When a charged particle is suspended in a liquid, there will be an electrical double layer formed in the interfacial region which consists of a stern / fixed layer where the counterions will be relatively strongly bound and a diffuse layer in which the ions will be loosely bound. The concentration of counterions within this area decreases with the distance from the surface. This phenomenon leads to the presence of a potential which decays as the distance from the particle surface increase, and becomes zero finally at a sufficient distance. When an electric field is applied, particles accompanied by the double layer will move through the solution as a unit. The potential at the boundary between this unit, namely the " shear plane " mentioned above, and the surrounding medium is termed " zero potential ". From this point of view, zeta potential depends on the surface charge, the absorbed layer at the interface and the nature and composition of the surrounding liquid solution (Hunter, 1981).

Nowadays, several experimental methods containing streaming potential, sedimentation potential, electroosmosis and electrophoresis, are available for the measurement of zeta-potential. Streaming potential method is becoming more and more popular owing to its versatility and feasibility on the measurements of different surfaces like planar surfaces, cylindrical capillaries, and packed beds of granular or fibrous materials.

(http://66.102.9.104/search?q=cache:c-IorwCA2UJ:www.che.utoledo.edu/nams/2006/viewpaper.cfm%3FID%3D1346+streaming+potential+electroosmosis&hl=en&gl=uk&ct=clnk&cd=1).

In this study, the zeta potentials of the membrane samples are obtained via the measurement of streaming potential which is a difference of electric potentials derived from the forced flow of the liquid across the membrane when a voltage is applied.

According to the Helmholtz-Smoluchowski equation, (eq. 7.5), the zeta potential (ξ) can be calculated as follows.

$$\zeta = \frac{\Delta E \times \eta \times \kappa}{\Delta P \times \varepsilon_0 \times \varepsilon_r} \qquad (7.5)$$

where Δ E is the streaming potential; P is the pressure; η is the viscosity of the solvent; κ is the conductivity of the electrolyte in the pores; ε_0 is the permittivity of a vacuum; ε_r is the relative dielectric constant of the electrolyte.

9.6 Sample preparation protocol for TEM

After Reilly, 2004.

1. Embedding

Day one

Cut samples using sharp implement, without pressure;

Rinse sample three times in water buffer (leave 1/2 – 1 hour between rinses)

Leave samples at room temperature for 24 hours in 0.5% aqueous Ruthenium tetroxide

Wash samples three times in pure water (leave 1/2 – 1 hour between rinses)

Day two

Dehydrate samples in increasing amounts of acetone in water (leave 20-30 minutes between changes) from 20%, 30% and so on to 95%, and two changes of 100%

Dehydrate samples in 3 or 4 changes of dry acetone

Place samples in 3 to 1 dry acetone to Spurr's resin, then mix for at least an hour

Place sample in 1 to 1 dry acetone to resin, then mix for at least an hour

Place in 1 to 3 dry acetone to resin, then mix for at least an hour

Place in resin, and mix at room temperature over night

Day three

Change the resin and mix samples for 1 hour

Embed samples in appropriate trays with paper labels

Place trays of samples at 70°C for 7-8 hours

Leave samples at room temperature until ready to remove for trimming and sectioning

2. Sectioning

Place each sample block in a holder

Trim down blocks with razor, until sample in exposed

Reduce area to be cut to 1mm x 2mm

Section area with glass knife on Sorvall ultra microtome until full sections of required material can be cut

When 500nm sections can be floated onto water, change holder

Cut final sections with diamond knife on Ultracut microtome

Immobilise sections on prepared copper grids

Dry with gentle heat

Store until ready for imaging

3. TEM imaging

Examine sections at 80 KV on Jeol 1200 at appropriate magnifications using optimized microscope settings

Develop negatives of images collected

Scan in negatives (avoiding information area)

Convert to digital. Tif images using Adobe Image Ready 3.0

Add micron bar and appropriate measurement

Digital images are now ready for study

9.7 *Folin – Ciocalteu* assay protocol

After Peilow and Samuel, 2004.

Preparation of chemicals:

7.5% sodium carbonate:

Weigh 37.5 g of anhydrous sodium carbonate in a clean and dry beaker. Add enough distilled water and stir to dissolve. Allow solution to cool to room temperature. Transfer to a 500 ml volumetric flask, and make up to volume with distilled water. Store the solution at room temperature.

Dillute *Folin-Ciocalteu* phenol reagent:

Using a pipette to transfer 20 ml to a 200 ml volumetric flask. Dilute to mark with water. This reagent should be prepared fresh daily.

Standard Gallic Acid stock solution:

Weigh approximately 0.110 g of gallic acid monohydrate (record exact weight) in a clean and dry beaker. Transfer to 100 ml volumetric flask and make up to volume with distilled water.

Gallic acid dilute standard solutions (A to F):

Pipette 1, 2, 3, 4, 5, and 6 ml aliquots of standard gallic acid solution into separate 100 ml volumetric flasks. Make up to mark with distilled water and mix well.

Sample preparation:

Tea powder: weigh approximately 0.5 g of tea powder (record exact weight) into a dry and clean beaker. Add 25 ml of hot distilled water, swirl sample to dissolve contents, and then transfer the sample to 50 ml volumetric. Allow sample to cool and add 5 ml acetonitrile. Make flask up to volume and mix well. Dilute samples by 1 to 100.

Tea solution, permeate and retentate are diluted with distilled water.

Colorimetric Assay Procedure:

Using a pipette to transfer 1 ml of gallic acid standards solutions (A to F) into separate tubes.

Pipette 1 ml of water into disposable tube as reagent blank.

Using a pipette to transfer 1 ml of sample into separate tubes.

Using a pipette to add 5 ml of *Folin-Ciocalteu* working reagent into each tubes.

Within 3 to 8 minutes after the addition of *Folin-Ciocalteu* reagent, pipette 4 ml of 7.5% sodium carbonate solution into each tube.

Stand at room temperature for 1 hour, then measure absorbance at 765 nm in a UV – visible spectrophotometer (*Shimadzu* 1601).

9.8 Coomassie Brillant Blue G (CBB) assay protocol

After Protein Quantification Kit-Rapid 51254 protocol (*Sigma*, UK) and Bradford, 1976.

Preparing BSA standard solutions:

Dilute BSA standard stock solution (4000 μg mL^{-1}) with distilled water to obtain various concentrations of standard solutions by multiple dilutions: 2000 μg mL^{-1}, 1000 μg mL^{-1}, 500 μg mL^{-1}, 250 μg mL^{-1}, 125 μg mL^{-1}, 62.5 μg mL^{-1}, 31.25 μg mL^{-1}, and 0 μg mL^{-1}.

Add 50 μL of BSA standard solutions and sample solutions to separate test tubes.

Add 2.5 mL CBB solution to each of the test tubes above.

Transfer the mixed solution to a cell and measure the absorbance of the solution at 600 nm in a UV-visible spectrophotometer (*Shimadzu* 1601).

Determine the protein concentration of the sample solution using the calibration curve.

Micro assay:

Dillute 100 μg mL^{-1} BSA standard solution with distilled water to prepare various concentrations of standard solution by multiple dilutions: 50 μg mL^{-1}, 25 μg mL^{-1}, 12.5 μg mL^{-1}, 6.3 μg mL^{-1}, 3.2 μg mL^{-1}, 1.6 μg mL^{-1}, 0.8 μg mL-1 and 0 μg mL^{-1}.

Add 1.5 mL of BSA standard solutions and sample solutions to separate test tubes.

Add 1.5 mL CBB solution to each of the test tubes above.

Transfer the mixed solution to a cell and measure the absorbance of the solution at 600 nm in a UV-visible spectrophotometer (*Shimadzu* 1601).

Determine the protein concentration of the sample solution using the calibration curve.

9.9 SDS-PAGE and silver staining protocol

After Thompsett, 2005 and ProteoSilverTM Silver Stain Kit protocol, *Sigma*, UK.

Assembling gel apparatus

Assemble two glass plates (one notched) with two side spacers, clamps, and grease. Stand assembly upright using clamps as supports, on glass plate. Insert the comb into the chamber. Draw a line at about 1 cm under the line of the comb as a sign of the height of separating gel.

Preparing the separating gel and stacking gel

17% separating gel:

Components	Volume
Milli Q water	3.5 ml
30% acrylamide	11.2 ml
1.5 M Tris-HCl (pH 8.8)	5 ml
10 % SDS	200 µL
10% APS (mg ml^{-1})	100 µL
TEMED (add last)	20 µL

Mix ingredients in the order shown above, ensuring no air bubbles form. Pour into glass plate assembly carefully. Overlay gel with isopropanol to ensure a flat surface and to exclude air. Wash off isopropanol with water after gel has set after approximately 15 minutes.

Stacking gel:

Components	Volume
Milli Q water	5.8 ml
30% acrylamide	1.4 ml
1.5 M Tris-HCl (pH 8.8)	2.5 ml
10 % SDS	200 µL
10% APS (mg ml^{-1})	100 µL
TEMED (add last)	10 µL

After the separating gel is ready, mix the solutions of stacking gel as above. Pour the gel solution onto top of set separating gel. Then insert the comb carefully. After the gel is set, remove the comb and fill with electrophoresis buffer, which consists of 10 fold SDS

running buffer (30.3 g Trincine, 144 g glycine and 10 g SDS) and Milli Q water at the ratio 1 : 9.

Sample preparation

Add 15 μL protein sample and 5 μL dye (sample buffer) into centrifugal tube. Centrifuge for only 15 seconds to mix the sample and dye well. Put the samples in a "float" in a water bath (about 100°C) to denature for 3 mins, then centrifuging for 15 s again.

If the concentration of the sample is relatively low, the following method can be used to concentrate the sample.

Mix 400 μL diluted protein in buffer with 400 μL methanol and 100 μL chloroform. Centrifugate the mixture at 10000 rpm for 2 minutes. Then remove the top layer which is water/methanol carefully from the mixture. Add 600 μL methanol into the rest of liquid and centrifugate again at 14000 rpm for 2 minutes. Remove the supernate, and protein is concentrated at the bottom of centrifugal tube.

Sample loading and electrophoresis running

Load 17 μL of protein samples and 10 μL of protein markers into each slot of on the stacking gel.

Plug in electrodes, set to the mode of constant voltage. Set the voltage to 50 V, 70 mA and running the electrophoresis for 10 minutes initially to remove some extra acrylamide. Then change the setting to 250 V, 70 mA, running for another 45 minutes.

Staining of gel by Coomassie Brilliant Blue

After finishing electropheresis, stop running, using comb to separate two glass plates, remove stacking gel, then take out the gel carefully by using the comb.

Make up stain: 0.2 % CBB in 45:45:10 % methanol : water : acetic acid. Cover gel with staining solution, seal in plastic box and leave for one hour on shaker with agitation. Destain with 5% 88% 7% methanol water acetic acid mix, with agitation overnight.

Silver staining of gel after CBB staining

To increase the sensitivity to allow the detection of even small amounts of protein, silver staining can be applied on the gels after CBB staining. Generally, all silver staining techniques are 100 – fold more sensitive than those using Coomassie Brilliant Blue. The method described here is referred to the protocol provided with Silver Stain Kit for Polyacrylamide Gels from *Sigma*, UK.

Silver Stain Reagents:

Silver equilibration solution for gels of 0.5 mm thickness or greater – dilute 1.5 ml of Silver Concentrate to 300 ml with deionized water (dH_2O).

Development Solution – dilute 30 ml of Developer 1 Concentrate to 300 ml with dH_2O. Then add 0.17 ml of Developer 2 Concentrate to this solution.

Reducer Solution – mix 2.0 ml of Reducer A Concentrate, 4.0 ml of Reducer B Concentrate and 0.7 ml of Reducer C Concentrate together. Then dilute this mixture to 300 ml with dH_2O.

Procedure for silver staining of polyacrylamide gels following CBB staining:

a) Water rinse

Rinse the gel three times with 300 ml of deionized water for 10 minutes each rinse.

b) Silver equilibration

Place the gel in 300 ml of silver equilibration solution and allow it to equilibrate with gentle agitation for 30 minutes. Pour off the solution before proceeding to next step.

c) Rapid water rinse

Rinse the gel for only 10 – 20 seconds with 300 ml of dH_2O.

d) Development of gel

Place one - half of the 300 ml of developer solution over the gel. After 5 – 8 minutes discard the first half of the developer solution and add the remaining developer solution. Watch carefully to achieve the darkest bands while minimizing the yellowing of darkening of the gel.

e) Stopping the development

Pour off the developer solution and rapidly replace with stop solution for 5 minutes.

f) Water rinse

Rinse the gel three times with 300 ml of dH_2O for 10 minutes each rinse.

g) Reducer wash

Place gel in 300 ml of the reducer solution for 10 – 30 seconds. Remove reducer solution from gel and immediately rinse under running tap water for 1 minutes.

h) Final water rinse

Rinse the gel three times with 300 ml of dH_2O for 10 minutes each rinse.

9.10 Protocol for measuring caffeine concentration

After Yao *et al.*, 2006.

Preparing lead acetate solution, hydrochloric acid solution, sulfuric acid solution and diluted caffeine stock solution.

Lead acetate solution: $(CH_3COO)_2Pb.3H_2O$ 29.150 g was dissolved and made up to 50 ml with distilled water.

Hydrochloric acid solution: Hydrochloric acid (32%, specific gravity 1.16) 0.5 ml was diluted to 500 ml with distilled water.

Sulfuric acid solution: sulfuric acid (98%, specific gravity 1.84) 83.5 ml was diluted to 500 ml with distilled water.

Diluted caffeine stock solution: caffeine solution of concentration 1 mg ml^{-1} (W/V) was diluted to 200 ml with distilled water.

Calibration curve

0, 10, 20, 30, 40, 50 ml of the diluted caffeine stock solution were separately mixed with 5 ml HCl solution and 1 ml lead acetate solution. The mixture was left overnight and then made up to 100 ml with distilled water. The solution was allowed to stand for 1 hour, and then was filtrated through Whatman No.1 qualitative filter paper. The filtrate (25 ml) and 0.3 ml sulfuric acid solution were mixed and diluted to 50 ml by distilled water. This mixture was left for 30 mins and filtered using the same type of filter paper afterwards. The absorbance of the filtrate was measured using a UV-visable spectrometer (Shimazu 1601) at 274 nm.

Sample measurement

10 ml tea permeate sample, 5 ml HCl solution and 1 ml lead acetate solution were mixed and allowed to standard for at least 12 hours before being diluted to 100 ml with

distilled water. The following measuring steps were the same as those described in making calibration curve.

Calculation of the concentration of caffeine in sample

$$C_{caffeine} = C \times \frac{50}{25} \times \frac{100}{V} \text{ (mg ml}^{-1}\text{)} \qquad (9.2)$$

where C is the concentration of caffeine from the standard curve, V is the volume used for measurement (10 ml).

9.11 Synthetic membrane preparation technique

The most important techniques for preparing synthetic membranes are sintering, stretching, track-etching, phase inversion and coating. (Mulder, 1996)

1. Sintering

In this method, a powder made form either organic or inorganic materials is pressed and sintered at elevated temperature. The interface between the contacting particles of a given sizes contained in the powder disappears during sintering, resulting in the formation of membrane. The pore size of membranes obtained from this technique arranges from 0.1 to 10 μm. Therefore, only microfiltration membranes can be prepared via this method.

2. Stretching

This method involves the stretching of an extruded film or foil perpendicular to the direction of the extrusion and small ruptures as mechanical stress applies. The resulting porous membranes have pore sizes of 0.1 μm to 3 μm. The required materials must be (semi) crystalline polymeric materials.

3. Track-etching

In this method, high energy particle radiation is applied perpendicularly to a film or foil. The polymer matrix is damaged by these particles and tracks are therefore form on the film. The subsequent immersion of the film into an acid (or alkaline) bath leads to the formation of uniform cylindrical pores as the polymeric material is etched away along the tracks. This technique allows pore sizes of 0.02 to 10 μm to be obtained.

4. Template leaching

In this technique, one of the components is leached out from a film. The porous membrane is therefore prepared.

5. Phase inversion

Most commercially available membranes are prepared by phase inversion. This process involves the solidification of a polymer in a controlled manner. The resulting membrane morphology depends on the control of the initial stage of phase transition. Either porous or nonporous membranes can be obtained by phase inversion. This versatile technique includes solvent evaporation, precipitation by controlled evaporation, thermal precipitation, precipitation from the vapour phase and immersion precipitation. Among them, immersion precipitation is the most commonly used method where precipitation takes place when a polymer solution casted on a support is immersed in a coagulation bath containing a non-solvent.

6. Coating

Coating is a method used for preparing composite membranes which consist of two different materials. A thin layer of membrane material is deposited on a porous sublayer in this method. The membrane selectivity is mainly controlled by the top layer, while the sublayer serves mainly as a support.